

**Western Australian School of Mines  
Department of Applied Geology**

**Holocene Reef Accretion of the Inshore Kimberley Bioregion and  
Response to Sea-level Changes**

**Tubagus Solihuddin**

**This thesis is presented for the Degree of  
Doctor of Philosophy  
of  
Curtin University**

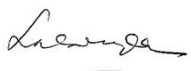
**May 2016**

## **Declaration**

To the best of my knowledge and belief this thesis contains no material previously published by any other person except where due acknowledgement has been made.

This thesis contains no material which has been accepted for the award of any other degree or diploma in any university.

Name : Tubagus Solihuddin

Signature : 

Date : May 2016

## Abstract

The Kimberley Bioregion is one of the most remote and isolated areas in Northwest Australia and is poorly known and studied. The region is considered one of the world's last great pristine marine environments and requires protection because of potential development. The Kimberley Marine Research Program (KMRP) of the Western Australia Marine Science Institution (WAMSI) is a program of marine research aimed to provide a scientific based foundation for planning and managing the proposed marine parks in the Kimberley Bioregion. One of the research priorities listed in the KMRP Science Plan is research on ***Holocene reef growth and maintenance***.

This PhD study's central aim is to gain a comprehensive description of reef geomorphology and associated benthic habitats, stratigraphy and palaeoecology, geochronology and accretion history in combination with reef architecture and seismic profile within a macrotidal, low wave energy, frequent cyclones, and high turbidity setting of the Kimberley Bioregion. A combination of remote sensing techniques, ore-pit mapping, multiple reef coring and drilling, and shallow seismic profiling were employed to address the objectives of the study.

The remote sensing of contemporary reef habitats provides a spatial framework for reef facies, geomorphic and ecological research at both regional (between reefs) and local (within reefs) scale. This reconnaissance study provides insight on spatial reef distribution linked to an understanding of reef geomorphology, coastal geology and biodiversity processes.

Reef mapping and transects conducted along the abandoned reef exposures in the Cockatoo mine pit provide the first information on Holocene reef accretion for an inshore reef of the Kimberley Bioregion. Subsidence since the Last Interglacial has provided accommodation for ~15 – 20 m of Holocene reef accretion upon an older, probably Last Interglacial, reef. Here, the reef initiated at ~9,000 cal yr BP and accreted in a catch-up mode reaching sea-level at ~3000 cal yr BP. The catch-up interpretation is supported by the predominance of branching *Acropora* throughout the Holocene section and the absence of contemporary intertidal indicators such as *Porites cylindrica* and *Millepora intricata*.

The systematic drilling program conducted in the selected inshore reefs of the Buccaneer Archipelago, including Tallon, Sunday and Irvine/Bathurst Islands extends previous work on Cockatoo Island. The study provides more details on the internal architectures of the reefs and allows comparisons between the investigated islands. The internal architecture of all cored reefs is broadly similar, constituting well-preserved detrital coral fragments, predominantly branching *Acropora*, in a poorly-sorted sandy mud matrix. However, once the reefs reach sea-level, they diverge into two types: low intertidal reefs that maintain their detrital character, with horizontal or gently sloping reef flats at approximately mean low water spring (MLWS), and high intertidal reefs that develop broad coralline algal-dominated reef flats at elevations between mean low water neap (MLWN) and mean high water neap (MHWN). Both reef types are ultimately constrained by sea-level but differ in elevation by 3 to 4 m. Due to the limitations of the coring equipment and the thickness of the Holocene reefs, the oldest/lowermost reef sections were not sampled. However, the position of the Holocene/pre-Holocene contact of several boreholes was inferred from, and supported by, earlier work at Cockatoo Island where the Holocene/Last Interglacial reef boundary was directly traced in the mine pit cross-section.

The shallow percussion coring conducted at Adele Reef on the mid-continental shelf may bridge the biogeographic knowledge gap on Holocene reef development between the inshore Cockatoo Island and oceanic Scott Reef. Shallow subsurface facies of Adele Reef consist predominantly of transported domal corals in a sandy matrix, which contrasts with the *in situ* branching *Acropora*-rich muddy facies of the inshore reefs and frame-dominated structures of branching and domal corals (including *Porites*) of the oceanic reefs. Further, the study supports the hypothesis of subsidence with tilting and is suggestive of hinge subsidence for the Kimberley coast and adjacent shelf, with progressively greater subsidence across the shelf.



## **Acknowledgements**

This thesis is dedicated to the memory of my former supervisor, the late Professor Lindsay Collins, for his guidance, patience, availability and inspiring ideas. He was not only an academic supervisor for me but also acting as my father who looked after his child with full compassion.

I would like to thank my new supervisor panel Dr. Mehrooz Aspandiar, Dr. Michael J. O’Leary, Dr. Moyra Wilson and thesis committee chairperson Dr. Gretchen Benedix-bland, who have assisted me in the research and study completion. Without their support, completing this thesis would not have been easy. I would also like to thank Alexandra Steven for the editing and improvement of the accuracy and clarity of this thesis.

I would like to thank my colleagues who provided a lot of support with my study and research, especially for Moataz Kordi and Giada Bufarale were valued members of the research team at Curtin University. Thanks to my fellow PhD students, including Hamed Arosi, Khalid Alhmoud, and Therese Morris who gave me lots of help and comfort to my study and research.

I would like to thank all the staff members of the Department of Applied Geology for the support, hospitality and togetherness throughout my PhD research with special thanks to Mrs. Annette Labrooy for administrative help. It was great to be part of the big family of Department of Applied Geology, Curtin University.

I would like to thank Western Australian State Government and partners of the Western Australian Marine Science Institution (WAMSI) who have funded this research project under the Kimberley Reef Geomorphology Project 1.3.1. I am grateful for the sponsorship of Australian Award Scholarship (AAS) who gave me a great chance to undertake PhD in Australia, with special grateful thanks going to Julie Craig, the manager and AAS Student Contact Officer at Curtin University, for the tremendous assistance and support.

I would like to thank my employer, Research Centre for Marine and Coastal Resources, Ministry of Marine Affairs and Fisheries, the Republic of Indonesia for the support throughout my PhD research.

I would also thank the Dambimangari, Bardi Jawi and Mayala people for their advice and consent to access their traditional lands. Pluton Resources

(particularly Jeremy Bower and Anson Griffith) are thanked for providing access to parts of their Cockatoo Island Mining Tenement and for logistic support during the study. The Cygnet Bay Marine Research Station provided vessel support for marine operations and access to research facilities at Cygnet Bay. James Brown assisted in the planning stage of the project, and Erin McGinty capably managed marine operations. MScience is thanked for providing access to marine video of the reef.

Special thanks to my wife Dewi Kartika Sari for the care and encouragement and to my little girls Ratu Nawal Mumtaz and Ratu Adiva Najihah for understanding the rare occasion together and the short sharing time available.

Finally, my very special thank you goes to my mother Fikriyah and my late father Tubagus Ahmad Turmudzi who have taught me to be tough and having a challenging spirit and strong belief in doing right things.

Indeed, in the creation of the heavens and earth, and the alternation of the night and the day, and the [great] ships which sail through the sea with that which benefits people, and what Allah has sent down from the heavens of rain, giving life thereby to the earth after its lifelessness and dispersing therein every [kind of] moving creature, and [His] directing of the winds and the clouds controlled between the heaven and the earth are signs for a people who use reason.

(Qur'an 2:164)

Kimberley, Western Australia — the world's pristine area; from cockroach to sea-crocs (Tubagus Solihuddin)

To my beloved  
Dewi Kartika Sari  
Ratu Nawal Mumtaz  
Ratu Adiva Najihah  
Ratu Syifa Aufia

This thesis is a hybrid thesis that compiles a collection of research papers that were either published or under review. The objectives and significance of the various papers are described in the introductory chapter. The final chapter is a concluding thesis chapter, summarising main findings, and suggestions for future work.

The research papers presented in this thesis are as follow:

**Solihuddin T.**, Collins L. B., Blakeway D., O’Leary M. J. (2015). Holocene coral reef accretion and sea-level in a macrotidal, high turbidity setting: Cockatoo Island, Kimberley Bioregion, northwest Australia. *Marine Geology*, 359: 50–60 (published).

**Solihuddin T.**, O’Leary M. J., Blakeway D., Kordi M., Parnum I., Collins L. B. (2016). Holocene reef evolution in a macrotidal setting: Buccaneer Archipelago, Kimberley Bioregion, Northwest Australia. *Coral Reefs*. 35:783-794 (published).

**Solihuddin T.**, Bufarale G., O’Leary M. J., Blakeway D. (2016). Geomorphology and Holocene accretion history of a mid-shelf platform reef: Adele Reef, Kimberley Bioregion, Northwest Australia. *Geo-Marine Letters*. doi: 10.1007/s00367-016-0465-3 (published).

List of relevant publications and conference abstracts:

**Solihuddin T.**, Collins L. B., Blakeway D., O’Leary M. J. (2014). Geomorphology and Holocene Accretion History of the Cockatoo Island Fringing Reefs, Kimberley Bioregion, Northwest Australia. Centenary postgraduate symposium, Perth, Western Australia.

Bufarale G., Collins L. B., O’Leary M. J., Steven A. M., Kordi M., **Solihuddin T.** (2014). Subbottom profiling and accretion patterns of Kimberley coral reefs, North West Australia. Centenary postgraduate symposium, Perth, Western Australia.

**Solihuddin T.**, Collins L. B., Blakeway D., O’Leary M. J. (2014). Reef Geomorphology and Holocene Accretion History of Cockatoo Island, Inshore Kimberley Bioregion, Northwest Australia. Coast to Coast Conference, Mandurah, Western Australia.

Collins L. B., O’Leary M. J., Stevens A. M., Bugarale G., Kordi M., **Solihuddin T.** (2015). Geomorphic patterns, internal architecture and reef accretion in a macrotidal, high-turbidity setting of coral reefs from the Kimberley Bioregion. *AJMOA*, 7:1, 12-22.

**Solihuddin T.**, Collins L. B., Blakeway D., O’Leary M. J. (2015). The variety of records of sea-level during Holocene environmental changes from Kimberley Bioregion, Northwest Australia. INQUA Congress, Nagoya, Japan.

**Solihuddin T.**, Collins L. B., O’Leary M. J., Blakeway D. (2015). Records of sea-level variation during Holocene environmental changes from the Kimberley Bioregion, Northwest Australia. CUPSA conference, Perth, Western Australia.

Bugarale, G., Collins, L.B., O’Leary, M.J., Stevens, A.M., Kordi, M., **Solihuddin, T.** (2016). Quaternary onset and evolution of Kimberley coral reefs (Northwest Australia) revealed by high-resolution seismic imaging. *Continental Shelf Research*, 123:80-88.

**Statement of the contribution of others:**


This thesis was supported by the Western Australian Marine Science Institution (WAMSI) and Curtin University. A collaborative research work was conducted with the Department of Environment and Agriculture - Curtin University, Fathom 5 Marine Research, Centre for Marine Science and Technology (CMST) - Curtin University, the Dambimangari, Bardi Jawi and Mayala indigenous people, Pluton Resources and the Cygnet Bay Marine Research Station (CRMS). The results of such collaborative research work comprise part of the thesis and are included in articles and publications as co-authors, data-access provider, logistic support, advice and assistance. However, as an author of this thesis, I am responsible for the interpretation, research and development of the scientific context and content of the published papers. Written statement of co-authors contribution is provided in the Appendix.

Student : Tubagus Solihuddin

Signature : 

Date : May 2016

Supervisor : Dr. Mehrooz Aspandiar

Signature : 

Date : May 2016

Co-Supervisor : Dr. Michael J. O'Leary

Signature : 

Date : May 2016

## Table of Contents

Abstract .....	iii
Acknowledgements .....	v
Table of Contents .....	xi
List of Figures .....	xv
List of Tables.....	xxi
Chapter 1 Introduction .....	1
1.1    Rationale.....	1
1.2    Regional Oceanography .....	4
1.3    Onshore Geological Elements .....	7
1.4    Reefs Bioregions of the Northwest Shelf .....	9
1.4.1    Reefs of the isolated Oceanic Shoals (OSS) Bioregion .....	9
1.4.2    Reefs of the nearshore Kimberley (KIM) Bioregion .....	11
1.5    Objectives .....	12
1.6    Thesis Structures .....	13
Chapter 2 Reef geomorphology and distribution patterns of modern coral communities from selected islands in the Buccaneer Archipelago, Kimberley Bioregion, Northwest Australia .....	18
2.1    Introduction .....	18
2.1.1    Field Settings.....	19
2.2    Methods .....	21
2.2.1    Satellite images .....	21
2.2.2    Image processing and analysis .....	21
2.3    Results .....	22
2.3.1    Tallon Island.....	22
2.3.2    Sunday Island .....	26
2.3.3    Irvine/Bathurst Islands .....	31
2.4    Discussion .....	35
2.4.1    Challenges of using remote sensing for coral reef mapping .....	35
2.4.2    Reef characteristics of the Buccaneer Archipelago .....	36

2.4.3	Specialised nature of reefs in the Buccaneer Archipelago .....	38
2.5	Conclusions .....	39
Chapter 3 Holocene coral reef accretion and sea-level in a macrotidal, high turbidity setting: Cockatoo Island, Kimberley Bioregion, Northwest Australia .....		44
3.1	Introduction .....	45
3.1.1	Oceanography of the Kimberley Region .....	46
3.2	Location and Methodology .....	47
3.2.1	Geophysical Surveys .....	47
3.2.2	Reef Mapping .....	48
3.2.3	Ore Pit Mapping .....	49
3.2.4	Geochronology .....	49
3.3	Results .....	50
3.3.1	Living coral community zonation .....	50
3.3.2	Stratigraphy and palaeoecology .....	52
3.3.3	Reef Geochronology and Accretion History .....	55
3.3.4	Reef Architecture and Seismic Structure .....	60
3.4	Discussion .....	61
3.4.1	Evidence of neotectonic subsidence along the Kimberley Coast and offshore shelf .....	61
3.4.2	Holocene reef accretion .....	62
3.4.3	Comparisons with other Holocene Reef Systems .....	64
3.5	Conclusions .....	69
Chapter 4 Holocene reef evolution in a macrotidal setting: Buccaneer Archipelago, Kimberley Bioregion, Northwest Australia .....		76
4.1	Introduction .....	77
4.2	Regional setting .....	78
4.2.1	Geology .....	78
4.2.2	Tides .....	79
4.2.3	Oceanography .....	80
4.3	Material and methods .....	80
4.3.1	Multibeam .....	80
4.3.2	Reef coring .....	80
4.3.3	Core logging and sampling .....	81



4.3.4	Radiocarbon dating .....	81
4.4	Results .....	82
4.4.1	Tallon Island.....	82
4.4.2	Sunday Island .....	84
4.4.3	Irvine/Bathurst Islands .....	86
4.5	Discussion .....	90
4.5.1	Reef geomorphology .....	90
4.5.2	Chronology of Holocene reef build-up .....	95
4.5.3	Reef facies and accretionary style.....	96
4.6	Conclusions .....	97
Chapter 5 Geomorphology and Late Holocene accretion history of Adele Reef: a Northwest Australian mid-shelf platform reef .....		102
5.1	Introduction .....	103
5.2	Methods .....	105
5.2.1	Remote sensing of reef habitats using Landsat 8 imagery .....	105
5.2.2	Seismic interpretation.....	106
5.2.3	Reef coring, logging and sampling .....	106
5.2.4	Radiocarbon dating .....	107
5.3	Results .....	107
5.3.1	Contemporary reef biogeomorphic zones .....	107
5.3.2	Reef architecture and seismic structure.....	110
5.3.3	Reef stratigraphy and geochronology .....	115
5.4	Discussion .....	119
5.4.1	Reef stratigraphy and sea-level changes .....	119
5.4.2	Mode of Holocene growth .....	120
5.4.3	Comparison with other reef systems .....	121
5.4.4	Cross shelf profile of Holocene reef accretion.....	122
5.5	Conclusions .....	123
Chapter 6 Reconstruction of Holocene sea-level and reef accretion history .....		128
6.1	Holocene sea-level and reef accretion history .....	128
6.2	Drowning Kimberley Shelf model .....	130

Chapter 7 General Conclusions.....	137
Chapter 8 References and Bibliography .....	140

## List of Figures

Figure 1.1	Map of research location – Kimberley Bioregion. Topographic data (250 m x 250 m resolution) provided by Geoscience Australia. The map also shows the bioregions of the Northwest Australian Shelf modified from the Interim Marine and Coastal Regionalisation of Australia (IMCRA).....	3
Figure 1.2	Surface current in the northwest marine region (from DEWHA, 2008).	4
Figure 1.3	Tidal ranges around the Australian shelf and classification of the shelf into microtidal, mesotidal and macrotidal zones (after Haris et al., 1991). .....	6
Figure 1.4	Paleoproterozoic geology of the Kimberley region. The inset shows the location of the Kimberley Craton (KC), King Leopold-Halls Creek Orogen and North Australian Craton (NAC) (from Griffin and Grey, 1990). .....	8
Figure 2.1	Map of study locations and adjacent areas. The map is produced from a colour composite image from Landsat 5 TM 17 July 2006 bands 321.	20
Figure 2.2	Map of Tallon Reef geomorphology and associated habitats with ground-truth points, derived from Landsat5 TM 17 July 2006. ....	24
Figure 2.3	Contemporary reef habitats of Tallon Island with the spot locations of the photographs shown on the high-resolution aerial photo. ....	25
Figure 2.4	Map of Sunday Reef geomorphology and associated habitats with groundtruth points, derived from Landsat 5 TM 17 July 2006.....	28
Figure 2.5a	Contemporary interisland reef habitats of Sunday Island with the spot locations of the photographs shown on the high-resolution aerial photo. ....	29
Figure 2.5b	Contemporary reef habitats of Hancock Reef with the spot locations of the photographs shown on the high-resolution aerial photo. ....	30
Figure 2.6	Map of Irvine/Bathurst Reef geomorphology and associated habitat with groundtruth points, derived from Landsat 5 TM 17 July 2006.....	33

Figure 2.7	Contemporary reef habitats of Irvine/Bathurst Islands with the spot locations of the photographs shown on the high-resolution aerial photo. ....	34
Figure 3.1	Map showing Bioregions modified from the Integrated Marine and Coastal Regionalisation of Australia (IMCRA) and geology of the Kimberley Region (After Griffin and Grey, 1990). ....	48
Figure 3.2	Map showing Cockatoo Island geomorphic and substrate classification, based on aerial photography interpretation (RGB 321). Numbers in legend correlate with habitats identified by on ground and towed video observation: (1) intertidal beach and boulder zone, (2) inner sand flat and reef platform, (3) outer reef platform. The narrow and steep forereef slope is not mappable here. The inset map (A) shows sub-bottom profile (white line) and towed camera (yellow line) transects and (B) location of the mine-pit measured sections. ....	50
Figure 3.3	Living coral communities on the SW Cockatoo Island fringing reefs. (A) The extensive shallow pools on reef flat at low tide showing small thickets of the branching hydroid <i>Millepora</i> and the branching coral <i>Porites cylindrica</i> . B) <i>Turbinaria</i> and branching <i>Porites</i> in the outer reef flat. (C) High coral cover of branching <i>Acropora</i> on the forereef slope. ....	52
Figure 3.4	Lithostratigraphic and chronostratigraphic summary of measured sections of Cockatoo mine-pit. ....	54
Figure 3.5	Idealised stratigraphic column of Cockatoo mine-pit section (S2_P1). Photo (A) showing the domal coral framestone with a muddy matrix, photo (B) showing the prevailing branching coral and coral rubble, photo (C) showing the contact between Holocene reef and Last Interglacial reef with a hematitic breccia as pre-transgressive deposits, and photo (D) showing the calcretized Last Interglacial reef exposure. Note 14C ages and % carbonate in matrix fraction are also shown. ....	55
Figure 3.6	Holocene vertical reef accretion and accretion history curve for Cockatoo Island sections S2_P1, S2_P2, and S3_P2. ....	58

- Figure 3.7 Composite accretion history records for Kimberley region and GBR derived from coral sections at Cockatoo Island (this study), coral in core from Middle Reef GBR (Perry et al., 2012), coral in core from North Scott Reef (Collins et al., 2011), cemented coral shingle pavement from Abrolhos reefs (Collins et al., 2006), and corals in core from Morley Island Abrolhos (Eisenhauer et al., 1993). Microtidal Abrolhos reefs from SW Australia lack subsidence since the LIG, in contrast with macrotidal Kimberley reefs with post-LIG subsidence. This is reflected in presence or absence of a Late Holocene highstand in the contrasting SL records. Abrolhos data for a keep-up reef; Kimberley data for catch-up reefs..... 59
- Figure 3.8 Southwest Cockatoo Island SBP cross section showing two stages of reef development; Holocene and Last Interglacial, with a clear correlation to the measured island sections. Unconformities are coloured. (Blue = top Proterozoic; Green = top Last Interglacial Reflector). ..... 60
- Figure 3.9 SBP line with superimposed core log from adjacent mine pit, showing correlation between SBP units and lithological units in the subsurface. .... 61
- Figure 4.1 Map of the study area in the Buccaneer Archipelago. The green shading indicates reef habitat. Locations of the three study sites and surrounding islands are indicated by arrows. .... 79
- Figure 4.2 Cross section of the Tallon Island reefs with isochrons and summary of Holocene reef facies. The dominant facies was branching coral floatstone with mud to sand matrix, overlaid by a thin layer of unconsolidated carbonate sand. .... 83
- Figure 4.3 Cross section of the North (a) and South (b) Pool of Sunday Island with isochrons and summary of Holocene reef facies. Facies in the North Pool comprised a domal coral floatstone at the base of the cores and a branching coral floatstone at the top. Facies in the South Pool are medium to coarse-grained carbonate sands with corallgal fragments. .. 85

Figure 4.4	Cross section of the interisland fringing reef of Irvine/Bathurts Islands with isochrons and summary of Holocene reef facies. The dominant facies was a branching coral floatstone, especially in the cores around the deep tidal pools. Note the exaggerated scale in the upper 5 m of the reef section. ....	88
Figure 4.5	Probability density curves of reef elevations measured by multibeam echo-sounder surveys. ....	94
Figure 5.1	Map of the study area in the Kimberley Bioregion showing the bathymetry contour derived from 250-m resolution digital elevation model (DEM) sourced from Geoscience Australia (note: there is some uncertainty in the depths due to the coarse nature of the Bathymetric grid). The light blue shading indicates reef habitat. ....	104
Figure 5.2	Map of Adele platform geomorphology and associated habitats, derived from Landsat 8, 23 May 2015. ....	109
Figure 5.3	Contemporary reef habitats of the Adele Reef platform with ground-truth locations. (AR1) Crustose coralline algae with platy <i>Acropora</i> , <i>Favia</i> , <i>Goniastrea</i> , and macroalgae ( <i>Sargassum</i> ), (AR2) crustose coralline algae with branching <i>Porites</i> , <i>Goniastrea</i> , and <i>Sargassum</i> , (AR3) the extensive shallow pool on reef flat colonised by <i>Sargassum</i> , <i>Favia</i> , and crustose coralline algae, (AR4) rhodolith banks exposed on low spring tides form low-relief reef crest on the SE reef flat, (AR5) coral rubble and <i>Sargassum</i> on the SE outer reef flat, (AR6) <i>Sargassum</i> on coral rubble and carbonate sand substrates, (AR7) branching <i>Acropora</i> and <i>Lobophyllia</i> on the SE outer reef flat, and (AR8) robust branching coral near the narrow drainage channel of Fraser Inlet. ....	110
Figure 5.4	Characteristics of the acoustic features identified in the seismic profiles of Adele Reef (after Bufarale et al., 2016). ....	112
Figure 5.5	Cross-sections showing multiple stages of reef buildup (MIS 1, 5, 7, 9 or 11 respectively). A) Profile 1, oriented W – E, intersects the northern portion of Adele Reef; Modified after Collins et al., 2015. B) Profile 3 runs longitudinally through Fraser Inlet and Profile 2 cuts the southern	

	branch of the Inlet. Holocene reef is 25-35 m thick, with drowned pinnacle reefs on the western forereef slope. Along Fraser Inlet, a series of pinnacle reefs are buried within muddy sediments (left insert). The location of the profiles is shown in insert B at lower right. ....	113
Figure 5.6	Bathymetric and seismic profile across Adele Reef and adjacent platforms (see inset for location). Bathymetry data were sourced from Geoscience Australia's 250-m DEM. Note repeated deep incisions between the platforms, probably by palaeorivers during sea level lowstands. Reef building events are vertically stacked within the platforms as repeated platform growth has occurred during SL highstands (MIS 1, 5, 7, 9 or 11), as interpolated from seismic data. Dashed lines are inferred. ....	114
Figure 5.7	Core photograph of Adele Reef showing representative Adele Reef facies where the cores were collected. ....	116
Figure 5.8	Lithostratigraphic and chronostratigraphic summary of Holocene reef facies for Adele Reef. The dominant facies was domal coral but the sections also contain fragments and colonies of branching coral. ....	117
Figure 5.9	Diagrammatic cross-shelf profile of Holocene reef growth from Cockatoo Island in the inner-shelf to Adele Island in the mid-shelf and Scott Reefs in the outer-shelf, showing estimated post-LIG subsidence rates of 0.12 mm/yr at Cockatoo Island, 0.2 mm/yr at Adele Island, and 0.2 mm/yr at Scott Reef. ....	123
Figure 6.1	Composite Holocene reef accretion history for the Kimberley Shelf with a modified Houtman Abrolhos sea-level curve from the past 10,000 years BP derived from coral exposure in the Cockatoo Island mine pit (Solihuddin et al., 2015), coral and crustose coralline algae in cores from Tallon Island, Sunday Island, Bathurst/Irvine Islands (Solihuddin et al., 2016), coral in cores from Adele Reef (Solihuddin et al., 2016), coral in cores from Scott Reef (Collins et al., 2011), cemented coral shingle pavement from the Abrolhos Reefs (Collins et al., 2006), and corals in core from Morley Island, Abrolhos (Eisenhauer et al., 1993). ....	129

Figure 6.2	Kimberley shelf exposure at Last Glacial Maximum, ~19,000 yr BP with channel dissections on a coastal plain; sea-level is estimated at 125 mbsl. Scott Reefs and Rowley Shoals were exposed as remnants from LIG reef building. ....	131
Figure 6.3	Kimberley shelf exposure at ~14,000 yr BP (MWP 1A) with channel dissections separating limestone hills of pre-existing LIG reefs at Adele complex (circled); sea-level is estimated 80 mbsl. ....	132
Figure 6.4	Kimberley shelf exposure at ~11,000 yr BP (MWP 1B) with LIG Reef remnants at Adele complex were isolated from mainland; sea-level is estimated at 40 m mbsl. ....	133
Figure 6.5	Kimberley shelf exposure at ~9,000 yr BP. Montgomery Reef and Cockatoo Reef were initiated and accumulated as sea-level rose considerably to approx. 20 mbsl. ....	134



## **List of Tables**

Table 3.1	Radiocarbon dates from selected samples across Cockatoo mine-pit transects.....	57
Table 3.2	Summary of characteristics of turbid reefs from the GBR (after Browne et al., 2012) and the Cockatoo fringing reef (this study).....	67
Table 4.1	Radiocarbon ages from selected samples across Tallon, Sunday, and Irvine/Bathurst Reefs.....	89
Table 5.1	AMS Radiocarbon dates from selected samples across Adele Reef.....	118

## Chapter 1

### Introduction

#### 1.1 Rationale

The Kimberley Bioregion is one of the most isolated and sparsely populated sections of the Australian coastline, extending from approximately 12°S to 18°S and from 118°E to 126°E (Fig. 1.1). This region is considered one of the world's last great pristine marine environments (Chin et al., 2008), consisting of over 13,000 km of highly dissected coastline and over 2,500 mapped islands (DEWHA, 2008; Kordi et al., 2016). Its geological and geomorphic development has been driven mainly by tectonic and sedimentary events during the Cenozoic (last 66 million years) and orbitally driven changes in sea-level during the Quaternary (Wilson, 2013). The region is also recognised for its complex coastal geomorphology, diverse habitats and high species diversity, and has been described as a “biodiversity hotspot” (Wilson, 2013).

Compared to the well-studied Great Barrier Reef on the northeast coast of Australia (Hopley et al., 2007), reefs in the Kimberley Bioregion are, by comparison, poorly understood. Studies into the Kimberley reefs are limited to Teichert and Fairbridge (1948), and Fairbridge (1950), who utilised aerial photograph interpretation to define distribution and characterise Kimberley reef geomorphology. They noted the presence of fringing reefs and their structures around the margin of a number of the islands in the Kimberley Bioregion. They also developed the hypothesis of northwest continental shelf subsidence (tilted westward) through diagrammatic sections of Adele Island on the mid-shelf, Cartier Island on the outermost continental shelf, and Browse Island in an intermediate position (Teichert and Fairbridge, 1948). Unpublished reports by Brooke (1995, 1996, and 1997) provide valuable reconnaissance information on coastal characteristics, landforms, and reefs for the northern (from Montgomery to Cape Londonderry) and southern (Buccaneer Archipelago and Yampi Peninsula) Kimberley Bioregion. He noted two principal fringing reef types; those characterised by terraced intertidal reef flat and those characterised by a sloping ramp. He also estimated the maximum Holocene reef thickness of reefs in the central part of the Kimberley Bioregion, along with their

accretion rates through direct measurement of forereef slope using a depth sounder and/or SCUBA diving. Blakeway (1997), on the other hand, provides hypothetical reef framework cross-sections. He made some general comments on reef communities and noted the abundance of large colonies of *Goniastrea* on the outer reef flats. He also noticed that turbidity appears to significantly influence coral depth zonation. The coral cover was estimated >10% at a depth of about 23 m with an estimated visibility of about 10 m, while in the more turbid water, where visibility can be less than 2 m, there were only little scleractinian corals growth below 12 m deep. Further descriptions have been published (Wilson et al., 2011; Wilson and Blake, 2011) inferring significant accumulations of coral framework in Montgomery Reef and Talbot Bay. Their studies focused on reef geomorphology, processes and ecological zonation, attesting to specialised coral-algal communities with varied but high sediment loads in reefs with extreme tidal fluctuations. The more recent studies conducted by Collins (2011) and Collins et al. (2011) described detailed reef morphology, internal architecture, and accretion history of Scott Reef and the Rowley Shoals located in the Oceanic Shoals Bioregion. These reefs and associated carbonate platforms such as Ashmore Reef, Cartier Reef, and Seringapatam Reefs were formed along an old Miocene continental margin, and the reefs have maintained their development despite rapid (0.29-0.45 m/ky) subsidence of the shelf edge since the mid-Miocene (Collins et al., 2011). A combination of coring, U-series dating and seismic methods were applied to document the morphology and growth history of Scott Reefs and Rowley Shoals. The studies have identified the Holocene sea-level rise rates, types of reef communities and the resilience and longevity of the offshore reefs. However, knowledge of the development of reef framework, palaeoecological communities, geomorphology, and the Holocene evolution of the inshore Kimberley reefs are still very limited and virtually unknown.

The remoteness, rugged terrain and large tides of the Kimberley coast have kept the area relatively undeveloped. However, development is expected to increase significantly due to the area's potential for tourism, aquaculture, and extraction of natural resources including oil, gas, and iron ore (DEC, 2011). Recognising the need for comprehensive scientific studies of the Kimberley marine areas, including its coast and islands, the Western Australian Government established the Kimberley Marine Research Program (KMRP) within the Western Australian Marine Science

Institution (WAMSI). The Program's central aim is to provide a scientific basis for planning and managing the proposed marine parks in the Kimberley Bioregion (Simpson, 2011). One of the priorities in the KMRP Science Plan is research on Holocene reef growth and maintenance, which aims to gain a regional understanding of the geomorphology of the Kimberley coral reefs, including their interaction with different substrates, morphological patterns, distribution and relative exposure to terrestrial and other impacts.

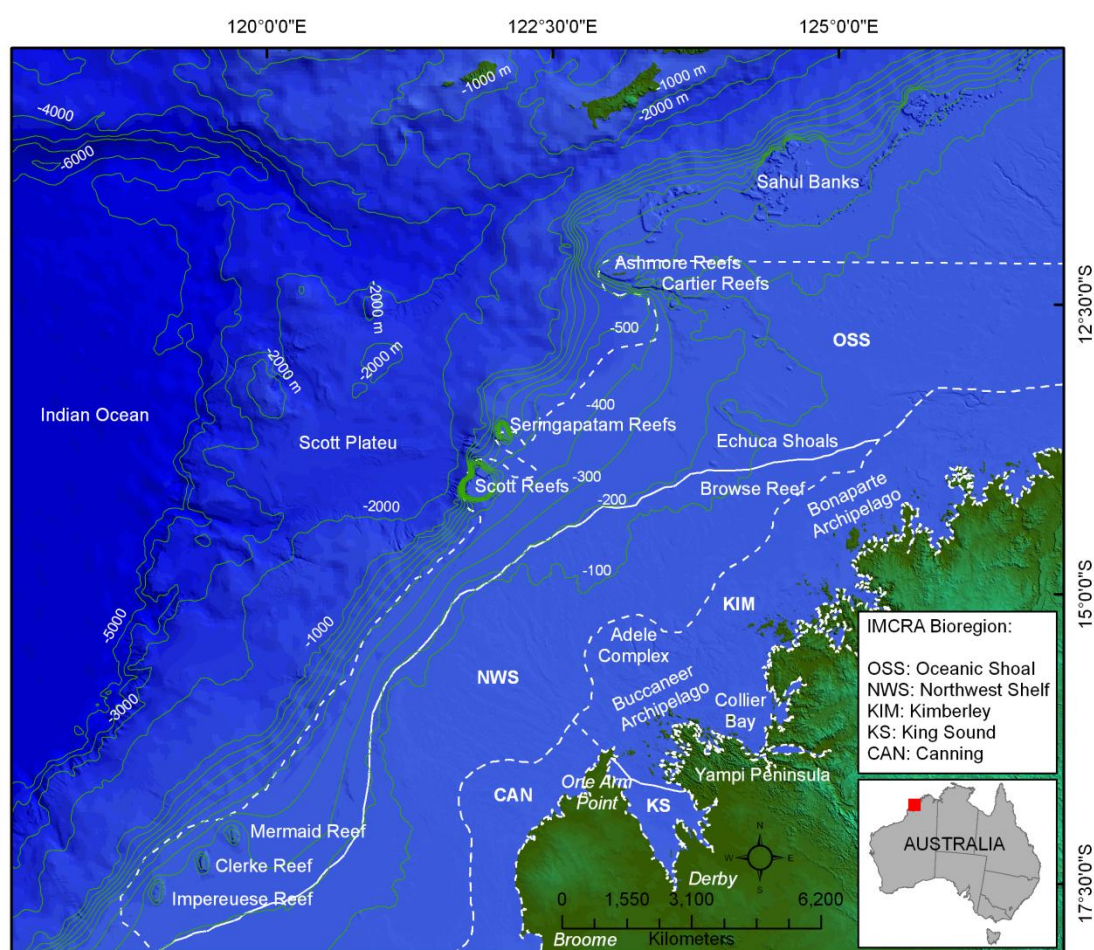


Figure 1.1 Map of research location – Kimberley Bioregion. Topographic data (250 m x 250 m resolution) provided by Geoscience Australia. The map also shows the bioregions of the Northwest Australian Shelf modified from the Interim Marine and Coastal Regionalisation of Australia (IMCRA).

This particular research project was designed to address the information gaps which exist in relation to the overall project, including 1) Regional distribution and

geomorphology of reefs of the Kimberley Bioregion, linked to an understanding of geomorphology and coastal geology, 2) Patterns of Holocene growth and response to sea-level changes.

## 1.2 Regional Oceanography

The regional oceanography of the Kimberley Bioregion in the northwest of Australia is significantly influenced by the south equatorial current, the ITF (Indonesian Throughflow), the Leeuwin current, and the eastern Gyral current (DEWHA, 2008) (Fig. 1.2). The prominent feature of this large-scale regional circulation is the Leeuwin Current which flows southward, moving off the equator, transporting warm, low salinity and low nutrient waters to the Western Australian coast (Pearce and Griffiths, 1991).

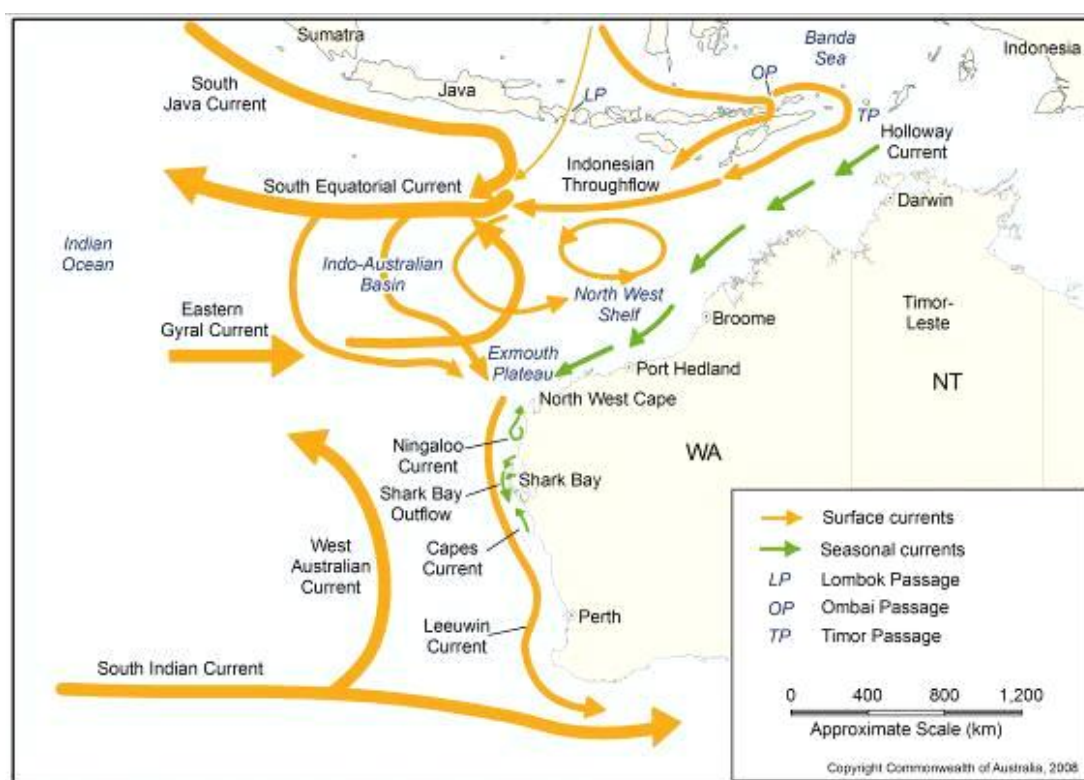


Figure 1.2 Surface current in the northwest marine region (from DEWHA, 2008).

The Holloway current is a seasonal and localised current in the region which is thought to occupy the upper surface water layers over almost the entire marine

realm of northwest Australia (DEWHA, 2008). This current flows strongly from April to September and is closely associated with the SE monsoon, a south-easterly wind blowing offshore, releasing surface water mass over the shelf from around Darwin to as far south as Ningaloo Reef (DEWHA, 2008). During the NW monsoon (December to March), the Indonesian Throughflow is deflected eastward, releasing a weak Holloway current along the inner-shelf of the Kimberley. Along with *in situ* planktonic production, the Holloway current is believed contribute to reef development along the Western Australian coast due to its role in delivering larvae and nutrients through the mechanism of upwelling (Pearce and Griffiths, 1991; Hatcher, 1991; Fang and Morrow, 2003).

In a tropical region, the Northwest Shelf of Australia has annual average sea surface temperatures ranging from 22 to 28°C nearshore and between 17 and 27°C offshore, whilst sea surface salinity ranges from a low of 34.5 to a high 35.7 PSU (Pearce and Griffiths, 1991). This region is also subject to frequent cyclones; with approximately 3 cyclones per year during the wet season from January to March (Lough, 1998).

The Northwest Shelf is also characterised by macrotidal conditions in some areas with a tidal range varying from a maximum spring of 12.5 m at Collier Bay and in King Sound to a minimum of 1.7 m at Exmouth (Harris et al., 1991) (Fig. 1.3). The King Sound/Collier Bay tidal range is the highest in Australia and the second highest tide in the world after the Bay of Fundy in Canada (Wolanski and Spagnol, 2003; Purcell, 2002). The only coastline in Australian waters which is also macrotidal is Broad Sound in eastern Queensland with a tidal range of up to 8.2 m (Harris et al., 1991). The macrotides generate an extensive intertidal zone and strong tidal currents in the nearshore Kimberley Bioregion, which in turn causes significant resuspension of sediment, resulting in high turbidity waters along the coast as well as areas with high volumes of river run-off (Brooke, 1997).

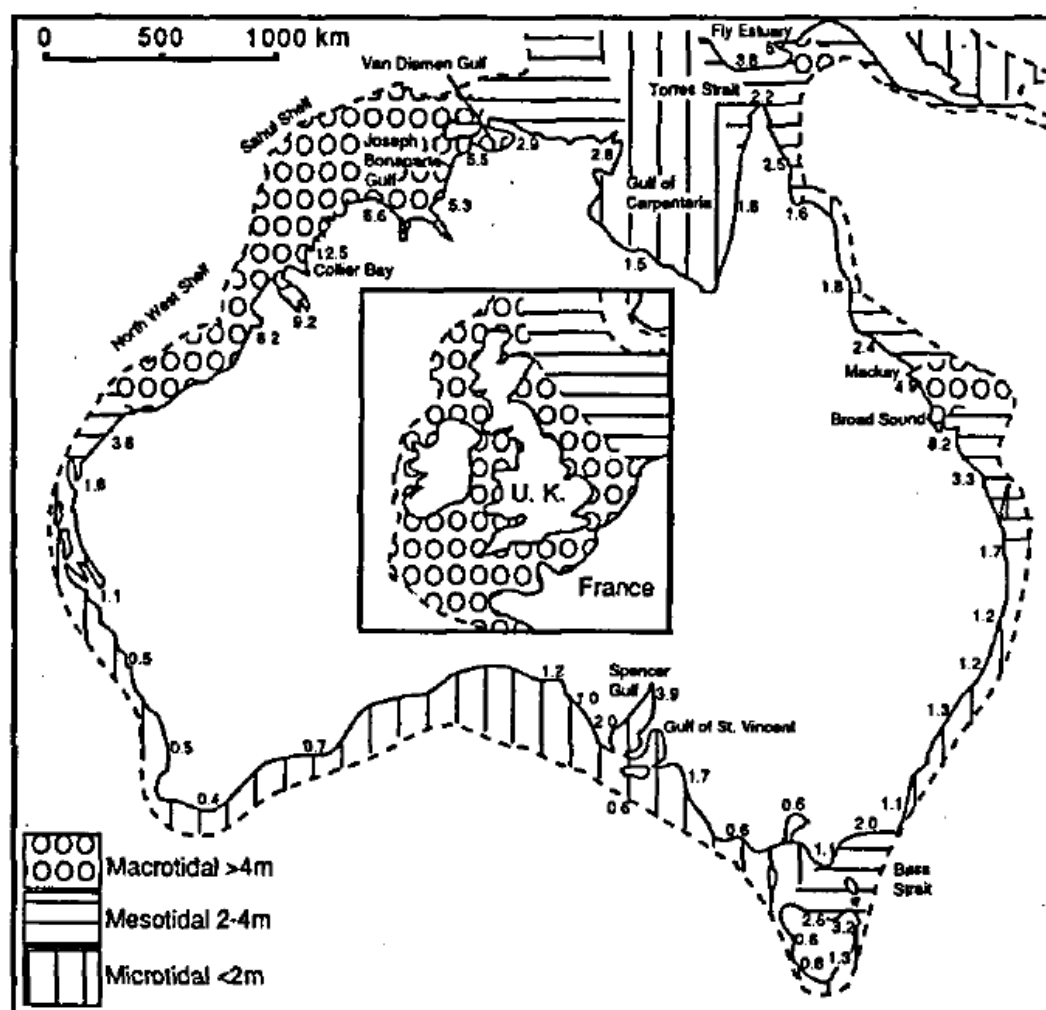


Figure 1.3 Tidal ranges around the Australian shelf and classification of the shelf into microtidal, mesotidal and macrotidal zones (after Haris et al., 1991).

The bathymetry of the Region is relatively shallow representing of less than 200 m water depths over more than 40 per cent of its area and less than 500 m for more than 50 per cent of the region, which typical of the continental shelf and continental slope (Baker et al. 2008). However, high-resolution contemporary bathymetric data over vast areas of the region are limited or not available and many areas remain uncharted. Geoscience Australia (GA) has a broad-scale data for the region with a ground resolution of 250 m (see Fig. 1.1), whilst the Australian Hydrographic Office (AHO) is currently processing data from contemporary surveys in the northern Kimberley.

### 1.3 Onshore Geological Elements

The hinterland of Kimberley bioregion comprises a massive of two-Precambrian blocks i.e. Kimberley Basin and King Leopold-Halls Creek Orogen (Griffin and Grey, 1990) (Fig. 1.4)

The Kimberley Basin is mainly composed of Proterozoic rocks of the Kimberley Group, including undeformed-metamorphosed sandstone and siltstone, volcanic and intrusive basalts. Locally, extensive sheet like bodies (sills) of the Hart Dolerite are conspicuous. The very ancient erosion of the flat-lying rocks of Kimberley Basin occupies the contemporary terrestrial surface of the basin forming a plateau geomorphic feature. This complex basin is dominant in the Kimberley region both inland and along the coast extending seaward with approximately 50 km off of the current coastline. The islands around the inner shelf are remnants of the terrestrial inundation during the Holocene transgression with a dissected coast and irregular bathymetry over the Proterozoic basement.

The King Leopold-Hals Creek Orogen is a semi-circumferential belt of highly deformed Archaeozoic and Proterozoic folded and faulted rocks consists of granites and other intrusive igneous rocks, gneisses, porphyries, metamorphic rocks, metasedimentary rocks, and volcanic rocks, with locally infolded sedimentary rocks of the Kimberley Basin. These narrow and mobile belts of deformed rocks (King Leopold Orogen to the southwest and Hall Creek Orogen to the southeast) border the margin of the Kimberley Basin and form the rocky ria coast of the Yampi Peninsula and the adjacent islands of the Buccaneer Archipelago in the western end of the orogen. A detailed description of the King Leopold-Halls Creek Orogen is described in the maps and explanatory notes of the geological series Yampi, Western Australia, sheet SE 51-3 (Griffin and Grey, 1990).



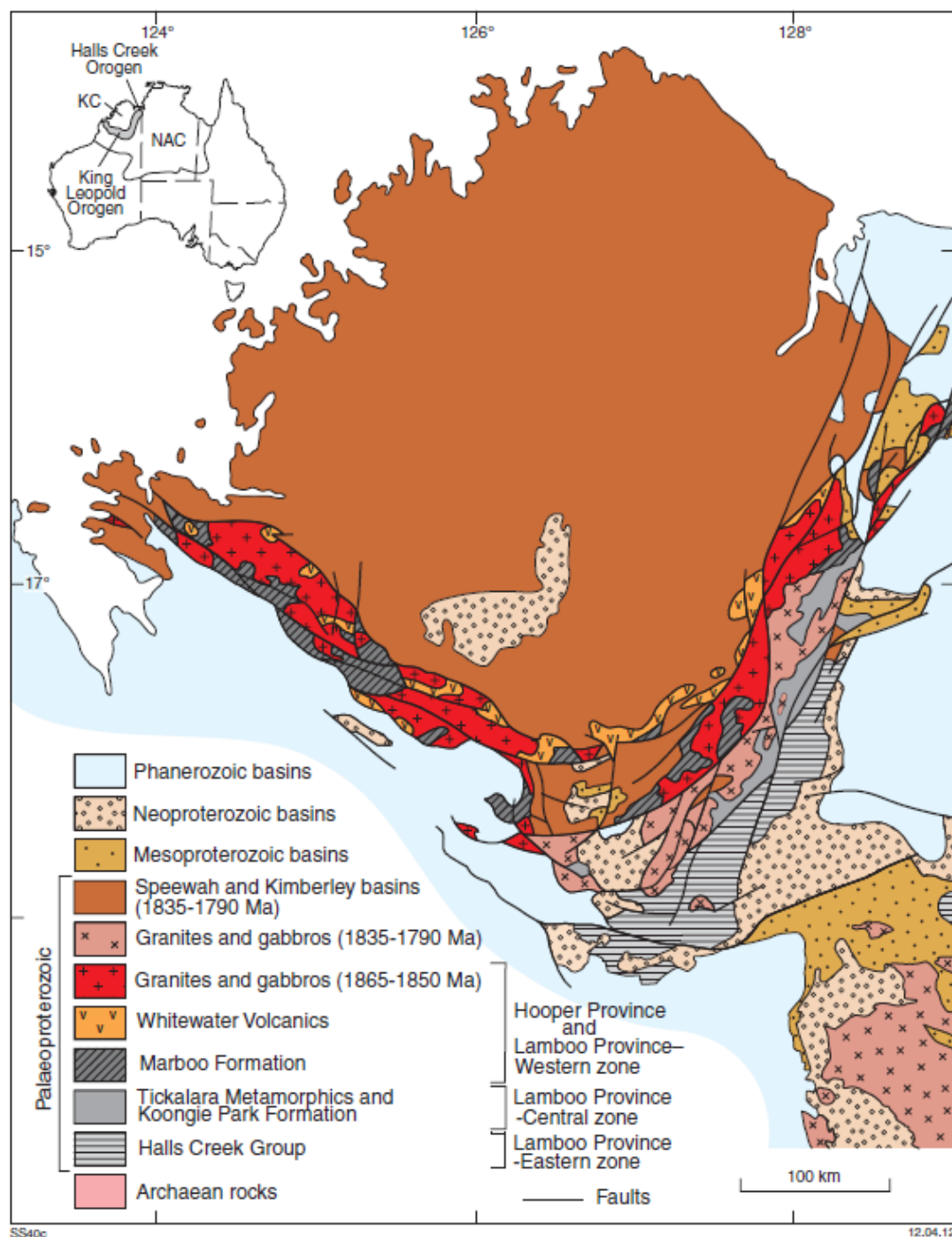


Figure 1.4 Paleoproterozoic geology of the Kimberley region. The inset shows the location of the Kimberley Craton (KC), King Leopold-Halls Creek Orogen and North Australian Craton (NAC) (from Griffin and Grey, 1990).

## 1.4 Reefs Bioregions of the Northwest Shelf

Coral reefs of the Northwest Shelf of Australia are divided between those in the isolated Oceanic Shoals (OSS) and in the nearshore Kimberley (KIM) Bioregions (see Fig. 1.1). The isolated Oceanic Shoals Bioregion occupies the shelf-edge and continental slope of the northern and central part of the Northwest Shelf, forming a string of banks within the outermost continental margin (Levering, 1993). The reefs in the nearshore Kimberley Bioregion are widespread along the Kimberley coast, forming a major geomorphic feature in a macrotidal, turbid, coastal environment (Collins, 2011).

### 1.4.1 Reefs of the isolated Oceanic Shoals (OSS) Bioregion

The isolated offshore reefs of the OSS Bioregion occur between 12°S and 18°S and approximately 400 km from the Northwest Australian coast. These reefs have evolved under low nutrient oligotrophic conditions and lack of sediment input from the mainland. The region has also experienced high rates of continental margin subsidence predicted to be on the order of 15-20 m/ky since the beginning of collision between the Australian and Eurasian plate in the Miocene (Sandiford, 2007). The combination of subsidence along with Pleistocene sea-level fluctuations has influenced the Quaternary development and evolution of the reefs in the OSS Bioregion (Collins et al., 2011). Here, the reefs are rising steeply from the edge of the continental shelf at depths of 200-400 m and consist of multiple stages of Pleistocene and Holocene reef growth (Collins et al., 2011).

There are two coral reef provinces in the region, separated based on biotic assemblages (Wilson, 2013): Sahul and Rowley Provinces. Sahul Province includes Ashmore Reef, Hibernia Reef, Cartier Reef, and Sahul Banks. Rowley Province encompasses Seringapatam Reef, Scott Reef, Rowley Shoals, Browse Reef, and Heywood and Echuca Shoals. Based on characteristics and origins (Wilson, 2013), the reefs are sub-classified into slope atolls, platform reefs, and banks. An overview of the different reef types in the OSS Bioregion are provided below.

Slope atolls refer to an exclusively morphologic feature, that is, a ring-shaped ribbon or circular reef enclosing a central lagoon (Fairbridge, 1950). There seems to be no marked difference in appearance between an “annular reef” rising from an

oceanic cone or platform and one rising from the continental shelf (Fairbridge, 1950). Reefs of the OSS Bioregion that are included in this category are the Rowley Shoals, Scott Reef, and Seringapatam Reef. The Rowley Shoals comprise a group of three offshore isolated reefs including Mermaid, Clerke and Imperieuse. The three shoals are almost circular and rise steeply from the outer shelf at a depth of 440 m, 390 m, and 230 m respectively. These reefs have similarities in terms of dimensions, shape, orientation, and distance apart, making them the most perfect morphological examples of the Northwest Shelf (Fairbridge, 1950). Scott Reef has an area of 800 km<sup>2</sup> and consists of two atolls (North and South) separated by a deep channel of ~400 m. North Scott Reef is annular pear-shaped reef with a shallow lagoon of ~20 m), while South Scott is a crescent-shaped reef and open to the north with deeper lagoon of ~60 m (Collins et al., 2011). Seringapatam Reef, on the other hand, is a rare example of a completely enclosed atoll with a moderately deep (~30 m) central lagoon and rises from the edge of continental shelf in water depth of ~400 m (Teichert and Fairbridge, 1948).

Platform reefs are islandless reefs built from the accumulated carbonate skeletal remains of marine organisms (Fairbridge, 1950). Ashmore Reef, Hibernia Reef, Cartier Reef, and Browse Reef are representative of platform reefs on the shelf margin of the OSS Bioregion. Ashmore Reef is a large ovoid platform reef with two lagoons separated by a calcareous rise, intertidal reef flat, and a precipitous reef front (Collins et al., 2011). Its long axis extends approximately 26 km long by 14 km wide with an approximate area of 239 km<sup>2</sup>. The two lagoons open to the leeward side, while the windward reef flat is 2–6 km wide. There is a 5-degree sloping forereef, about 150 m wide, with a strong spur and groove system (Wilson, 2013). Hibernia Reef is a coral-rich intertidal platform with shallow lagoon atop a pinnacle (Collins and Testa, 2010). Cartier Reef is an elongate-ovate shape platform reef, relatively small (~4.5 km wide), rising from the outer shelf—slightly beyond the ~180 m water depth, with a central sand cay surrounded by a 10.85 km<sup>2</sup> reef platform (Teichert and Fairbridge, 1948; Wilson, 2013). Browse Reef, in addition, is a small platform reef, rising steeply from ~150 m water depth with a small (274 m wide and 457 m long) vegetated sand islet in the centre surrounded by a wide intertidal reef platform with no lagoon (Teichert and Fairbridge, 1948).

Banks are submerged reefs built largely from accumulations of skeletal remains of calcareous algae *Halimeda* (Wilson, 2013). Sahul Banks and Heywood and Echuca Shoals are typical banks in the OSS Bioregion. Sahul Banks are composed of 13 isolated submerged carbonate banks and shoals including Big Bank, Happy, Snow White, Grumpy, Udang, Kepiting, Tiram, Kepah, Sneezy, Wicked, South Bank, etc. They emerge from water depths of 200–300 m and rise steeply from the seabed to within 16–30 m below the water surface. Heywood and Echuca Shoals are submerged carbonate banks and shoals with abundant coral debris and dead coral bombies, suggesting that these shoals may be a failed (drowned) platform reef rising steeply from the seabed along the shelf edge–continental slope (Wilson, 2013).

#### **1.4.2 Reefs of the nearshore Kimberley (KIM) Bioregion**

The majority of reefs in the nearshore Kimberley Bioregion are located in the inner to mid-shelf, water depths throughout the bioregion are shallow, ranging between 0–100 m (Baker et al., 2008). These reefs accreted during Holocene time and overlie the pre-existing Proterozoic basement rocks (Brooke, 1997). Unlike the reef development of the Abrolhos and Ningaloo reefs in Southwest Australia (Collins et al., 1993; 2003), Pleistocene coral reefs do not outcrop above sea-level in the Kimberley Bioregion (Brooke, 1997). This lack of Pleistocene reef exposures is the result of Quaternary subsidence rather than the absence of reef development during previous interglacial periods (Brooke, 1997).

There are a number of geomorphic reef types characterised primarily on reef exposure relative to tidal datum i.e. high intertidal, low intertidal and subtidal reef (Kordi et al., 2016). High intertidal reefs are defined as reefs which are situated above mean low water neap (MLWN). Examples of these reefs include East Tallon Reef, Irvine-Bathurst Reef, and Sunday Reef in the Buccaneer Archipelago. Low intertidal reefs lie slightly below the MLWN, but are exposed during low tide. West Tallon Reef, South Cockatoo Reef and East Bathurst Reef in the Buccaneer Archipelago are typical of low intertidal reef. Subtidal reefs are situated below the mean low water spring (MLWS) and are always below sea level. Such reef types are the most common type in the nearshore Kimberley Bioregion especially reefs in the Bonaparte Archipelago (Kordi et al., 2016).

## 1.5 Objectives

The main objective of this study is to develop and acquire knowledge of the geomorphology and Holocene accretion history of selected reefs in the Kimberley Bioregion and their responses to sea-level changes. These investigated reefs were selected due to: 1) proximity to the Kimberley Marine Research Station (KMRS), 2) easiness to reach as collecting data in such environment is challenging, 3) availability of workable reef exposure such as in Cockatoo Island, and 4) spatially representative of inner and mid shelf reefs. The following research aims have been developed in order to address this overall research goal.

1. Establish the regional distribution of Kimberley coral reefs and examine how reef geomorphology influences associated habitats.
2. Use Cockatoo Island (which has a full Holocene reef section exposed within an iron ore pit) as an exemplar to investigate the contemporary reef habitats, reef stratigraphy and palaeoecology, reef accretion history, and reef antecedent platform.
3. Investigate how the unique Kimberley environments including, the up to 11-m macrotidal range, have influenced reef development across the Buccaneer Archipelago, which is located along the inner shelf of the southern Kimberley.
4. Compare the Holocene evolutionary history of the mid-shelf Adele complex of platform reefs with the inner-shelf fringing reefs of the Buccaneer Archipelago and Scott Reefs located on the shelf-edge.

Based on the above research aims, the detailed objectives of the study are:

1. To map the contemporary geomorphology and associated habitats of selected reefs in the Buccaneer Archipelago using remote sensing techniques supported by groundtruth observations.
2. To document the exposed Holocene reef of the Cockatoo Island open-cut mine pit, examining the antecedent substrate, facies framework, and coral community composition.
3. To establish a record of Holocene reef evolution of selected islands in the Buccaneer Archipelago including reef stratigraphy, geochronology, accretion

rates, facies, and composition, through multiple coring surveys as an extension work of the previous study at Cockatoo Island.

4. To describe the geomorphology and Holocene accretion history of Adele platform reef in the mid-shelf Kimberley Bioregion and to fill the knowledge gap of reef development between reefs in the inshore Buccaneer Archipelago and Scott Reefs in the Oceanic Shoals.

## 1.6 Thesis Structures

**Chapter 1** presents the rationale, an overview of the reefs in the Kimberley Bioregion, oceanographic settings, aims and objectives of the study. This thesis is structured under the “hybrid” thesis model, and so each chapter has its own literature review, and therefore there is no need for a standalone extended literature review chapter.

**Chapter 2** presents the geomorphology and distribution patterns of modern reef communities from selected islands in the Buccaneer Archipelago. It involved using remote sensing techniques and groundtruth observations to produce a Landsat-derived reef geomorphology and associated habitats map of Tallon, Sunday, and Irvine/Bathurst Reefs.

**Chapter 3** presents the Holocene coral reef growth and sea-level changes in a macrotidal, high turbidity setting of Cockatoo Island. Reef transects were established to log the Holocene reef section in the Cockatoo mine-pit and four evenly spaced transects were selected along the workable exposure. The results of transect investigation are interpreted and discussed in the context of Holocene coral reef growth and sea-level changes.

**Chapter 4** presents the Holocene reef evolution in a macrotidal setting of the Buccaneer Archipelago. A drilling program of selected inshore reefs in the Buccaneer Archipelago including Tallon, Sunday, and Irvine/Bathurst Reefs was conducted to obtain a timing of Holocene reef initiation, chronology, accretion rates, reef facies and composition.

**Chapter 5** presents a reef geomorphology and Holocene accretion history of Adele Reef in the mid-shelf Kimberley Bioregion. Through multiple coring surveys, this

study attempts to address the biogeographic knowledge gap on Holocene reef development between the inshore Cockatoo Reef and oceanic Scott Reef. The study also presents the first calculation of quantitative subsidence rates in the mid-shelf Kimberley Bioregion.

**Chapter 6** presents a brief chapter presenting palaeogeographical reconstructions linked to the coral records presented in earlier part of the thesis, provide a fairly uncontentious interpretation of long-term landform change.

**Chapter 7** presents a general conclusion, combining and synthesising a Holocene coral reef accretion and growth history presented in earlier chapters including suggestions for future work.

## References

- Baker, C., Potter, A., Tran, M., Heap, A. D. (2008), *Sedimentology and Geomorphology of the North West Marine Region of Australia*, Geoscience Australia, Canberra.
- Blakeway, D. (1997). Scleractinian corals and reef development, part 9. In: Walker, D. (ed.), *Marine biological survey of the central Kimberley coast, Western Australia*. Perth: University of Western Australia. Unpublished report, W. A. Museum Library No. UR377, pp. 77–85.
- Brooke, B. (1995). *Geomorphology*, part 4. In: Wells, F. E., Hanley, J. R., Walker, D. (ed.), *Survey of the marine biota of the southern Kimberley islands*. Unpublished report No. UR286, Western Australian Museum, Perth, pp. 67–80.
- Brooke, B. (1996). *Geomorphology of the north Kimberley coast*. In: Walker, D. (ed.), *Marine biological survey of the eastern Kimberley, Western Australia*. Unpublished report No. UR353, Western Australian Museum, Perth.
- Brooke, B. (1997). *Geomorphology of the north Kimberley coast*, part 9. In: Walker, D. (ed.), *Marine biological survey of the central Kimberley coast. Western Australia*. University of Western Australia, Perth, unpublished report, W.A. Museum Library No. UR377, pp. 13–39.

- Chin, A., Sweatman, H., Forbes, S., Perks, H., Walker, R., Jones, G., Williamson, D., Evans, R., Hartley, F., Armstrong, S., Malcolm, H., Edgar, G. (2008). Status of the Coral Reefs in Australia and Papua New Guinea. In: Wilkinson, C. (ed), *Status of Coral Reefs of the World. Global Coral Reef Monitoring Network. Reef and Rainforest Research Centre*, 159–176.
- Collins, L. B. (2011). Geological setting, marine geomorphology, sediment and oceanic shoals, growth history of the Kimberley Region. *Journal of the Royal Society of Western Australia*, 94(2), 89-105.
- Collins, L. B., Testa, V. (2010). Quaternary development of resilient reefs on the subsiding Kimberley continental margin, northwest Australia. *Brazilian Journal of Oceanography*, 58, 1-13.
- Collins, L. B., Testa, V., Zhao, J., Qu, D. (2011). Holocene growth history and evolution of the Scott Reef carbonate platform and coral reef. *Journal of the Royal Society of Western Australia*, 94(2), 239–250.
- Collins, L. B., Zhu, Z. R., Wyrwoll, K. H., Eisenhauer, A. (2003). Late Quaternary structure and development of the northern Ningaloo Reef, Australia. *Sedimentary Geology*, 159(1-2), 81-94.
- Collins, L. B., Zhu, Z. R., Wyrwoll, K. H., Hatcher, B. G., Playford, P. E., Eisenhauer, A., Chen, J. H., Wasserburg, G. J., Bonani, G. (1993). Holocene growth history of a reef complex on a cool-water carbonate margin: Easter Group of the Houtman Abrolhos, Eastern Indian Ocean. *Marine Geology*, 115(1-2), 29–46.
- Department of the Environment, Water, Heritage and the Arts, DEWHA (2008). A Characterisation of the Marine Environment of the North-west Marine Region: Perth Workshop Report, A Summary of an Expert Workshop Convened in Perth, Western Australia, 5-6 September 2007, Commonwealth of Australia, Hobart.
- Department of Environment and Conservation. (2011). Kimberley science and conservation strategy. DEC, Perth. Accessed 16/03/2012 <http://www.dec.wa.gov.au/content/view/5180/2191>.



- Fairbridge, R. W. (1950). Recent and Pleistocene coral reefs of Australia. *The Journal of Geology*, 58(4), 330-401.
- Fang, F., Morrow, R. (2003). Evolution, movement and decay of warm-core Leeuwin Current eddies. *Deep Sea Research Part II: Topical Studies in Oceanography*, 50(12-13), 2245-2261.
- Griffin, T. J., Grey, K. (1990). Kimberley Basin, in: Memoir 3, Geology and Mineral Resources of Western Australia. Perth, Geological Survey of Western Australia, 293–304.
- Harris, P. T., Baker, E. K., Cole, A. R. (1991). Physical sedimentology of the Australian continental shelf, with emphasis on Late Quaternary deposits in major shipping channels, port approaches and choke points. Ocean Science Institute, Report 51, University of Sydney.
- Hatcher, B. G. (1991). Coral reefs in the Leeuwin Current: an ecological perspective. *Journal of the Royal Society of Western Australia*, 74, 115-127.
- Hopley, D., Smithers, S., Parnell, K. (2007). The Geomorphology of the Great Barrier Reef: Development, diversity, change: Cambridge, UK, Cambridge University Press, pp. 532.
- Kordi, M., Collins, L. B., O'Leary, M., Stevens, A. (2016). ReefKIM: An integrated geodatabase for sustainable management of the Kimberley Reefs, North West Australia. *Ocean & Coastal Management* 119, 234-243.
- Lavering, I. H. (1993). Quaternary and modern environments of the Van Diemen Rise, Timor Sea, and potential effects of additional petroleum exploration activity. *Journal of Australian Geology and Geophysics*, 13, 281-292.
- Lough, J. M. (1998). Coastal climate of northwest Australia and comparisons with the Great Barrier Reef: 1960 to 1992. *Coral Reefs*, 17(4), 351-367.
- Pearce, A. F., Griffiths, R. W. (1991). The Mesoscale Structure of the Leeuwin Current: A Comparison of Laboratory Models and Satellite Imagery. *J. Geophys. Res.*, 96(C9), 16739-16757.
- Purcell, S. P. (2002). Intertidal reefs under extreme tidal flux in Buccaneer Archipelago, Western Australia. *Coral Reefs*, 21(2), 191-192.

- Sandiford, M. (2007). The tilting continent: A new constraint on the dynamic topographic field from Australia. *Earth and Planetary Science Letters*, 261(1-2), 152–163.
- Simpson, C. J. (2011). Kimberley Marine Research Program Science Plan. Report to the WAMSI Board and Strategic Program Committee.
- Teichert, C., Fairbridge, R. W. (1948). Some coral reefs of the Sahul Shelf. *Geographical Review*, 38(2), 222-249.
- Wilson, B. R. (2013). The Biogeography of the Australian North West Shelf: Environmental Change and life's response. Elsevier, Burlington MA, USA.
- Wilson, B. R., Blake, S., 2011. Notes on the origin and biogeomorphology of Montgomery Reef, Kimberley, Western Australia. *Journal of the Royal Society of Western Australia*, 94(2), 107–119.
- Wilson, B. R., Blake, S., Ryan, D., Hacker, J. (2011). Reconnaissance of species-rich coral reefs in a muddy, macro-tidal, enclosed embayment, Talbot Bay, Kimberley, Western Australia. *Journal of the Royal Society of Western Australia*, 94(2), 251–265.
- Wolanski, E., Spagnol, S. (2003). Dynamics of the turbidity maximum in King Sound, tropical Western Australia. *Estuarine Coastal and Shelf Science*, 56(5-6), 877-890.

## Chapter 2

### Reef geomorphology and distribution patterns of modern coral communities from selected islands in the Buccaneer Archipelago, Kimberley Bioregion, Northwest Australia

#### 2.1 Introduction

The geomorphology of coral reefs is determined by an interaction of hydrodynamic, geomorphic, and ecological processes (Harris, 2010; Kaczmarek et al., 2010; Madden et al., 2013). Geomorphic features can be recognised by *in situ* field surveys and/or remote sensing techniques. Since it is usually very time-consuming and prohibitively expensive to conduct on ground observations over a large area, the application of time-series/multi-temporal data acquisition of remote sensing technology (Mumby et al., 1998) offers the most rapid and cost-effective approach to observe and characterise an entire region of reefs without relying on sampling and extrapolation, depending on scale of the features, area mapped and data availability (Andrefouet et al., 2006).

Prior to the use of satellite-based remote sensing imagery in the 1970's, the reconnaissance of coral reef systems mainly relied on aerial photography interpretation as originally conducted by Teichert and Fairbridge (1948) and Fairbridge (1950) who described the geomorphic features of coral reefs in Northwest Australia, including Adele Island, Browse Island, Cartier Island, and Seringapatam Atoll. The aerial photos used by Teichert and Fairbridge (1948) were taken by the Netherlands East Indies Squadron RAAF for military purposes during World War Two. More recently spaceborne remote sensing imagery provides researchers with the opportunity to map broad-scale areas of coral reefs with reliable and acceptable accuracy (Andrefouet et al., 2001; Maedar et al., 2002; Rankey, 2002; Purkis et al., 2005; Harris, 2010; Kaczmarek et al., 2010; Madden et al., 2013).

Reef geomorphology and associated habitats are closely related to depth distribution and benthic community structures which are mappable and measurable by both passive (e.g. satellite) and active (e.g. radar) sensors (Mumby and Harborne, 2006). Since reef build-up generally flourishes in clear and optically shallow water (<30 m deep), these environmental conditions are ideal for passive remote sensors

(e.g. Landsat, SPOT, ASTER, IKONOS, Quickbird) which measure the electromagnetic radiance from the sun reflected off submerged coral reefs. Landsat imagery has been the most commonly used remotely sensed data for large-scale mapping purposes of coral reef geomorphology and associated habitats (Andrefouet et al., 2001; Maeder et al., 2002; Capolsini et al., 2003) as it is freely available and its spatial, temporal and spectral resolutions suit the coral reef study purposes. Spatial resolution refers to a measure of the smallest discrete identifiable area of an image resulted in the dimensions of ground-resolution cell, commonly known as picture element or pixel of the image (Jensen, 2007). Spectral resolution is one of sensor characteristics that determines the capability of coral reef discrimination in the certain electromagnetic spectrum i.e. blue (0.45 – 0.52  $\mu\text{m}$ ), green (0.52 – 0.60  $\mu\text{m}$ ) and red (0.63 – 0.69  $\mu\text{m}$ ).

Mapping of reef geomorphology has also proven to be one of Landsat's most successful applications from its earliest days (Smith et al., 1975) through to the present (Kordi et al., 2016). The study reported in this chapter, therefore, explores the utility of multispectral bands of Landsat imagery to delineate reef geomorphology and associated habitats of selected islands in the inner-shelf of the Buccaneer Archipelago, including Tallon, Sunday, and Irvine/Bathurst Islands, supported by groundtruth checking.

### **2.1.1 Field Settings**

The Buccaneer Archipelago is a series of islands which are interpreted as a seaward extension of the deformed sedimentary and volcanic rocks of the Yampi Peninsula (Fig. 2.1). The rocks are strongly folded and faulted in a general northwest–southeast direction and these fracture systems are cut by northeast-trending Late Jurassic to Early Cretaceous fault systems (Griffin and Grey, 1990). The tectonic history of the area has significantly caused the shoreline change over geological time. Evidence of this is clearly seen in the present Buccaneer Islands' morphology, showing the seaward extension of the folded, faulted, eroded of the Yampi Peninsula (Wilson, 2013). The region comprises over 700 islands (Kordi et al., 2016), many of which are uninhabited and unnamed.

Holocene sea-level rise has inundated the valleys and peneplains, generating the complex coastal morphology seen today as a function of variations in structure and lithology. Sandy pocket beaches are formed at the entrance of many of the flooded valleys along with mangrove fringes, supratidal flats and peneplains of colluvial and alluvial Cainozoic soils behind them (Brooke, 1997). The morphology of these drowned landscapes has undoubtedly been a strong control on Holocene reef development as they provided different substrates and foundation types for reef accretion in addition to the Quaternary regional subsidence (Wilson, 2013).

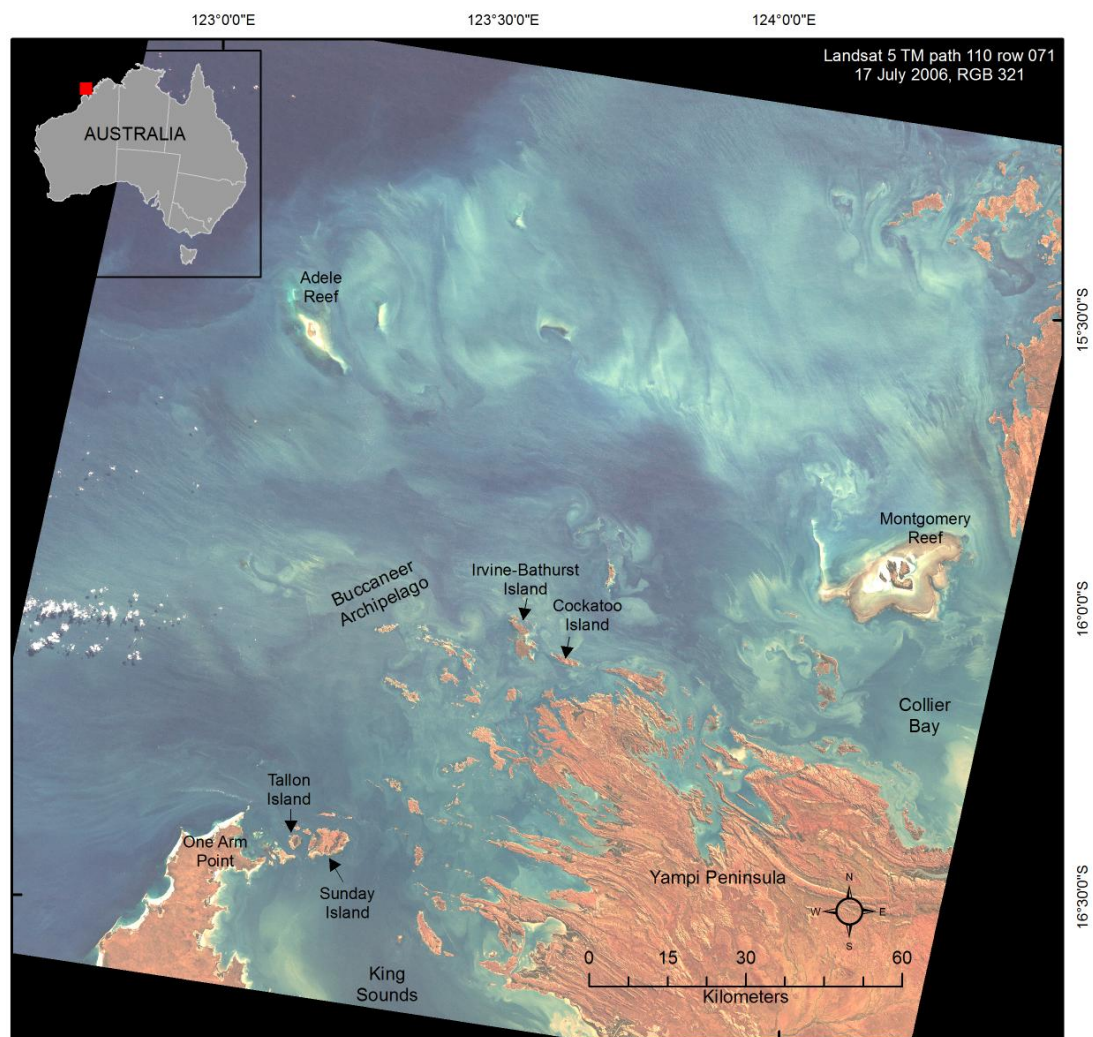


Figure 2.1 Map of study locations and adjacent areas. The map is produced from a colour composite image from Landsat 5 TM 17 July 2006 bands 321.

## 2.2 Methods

### 2.2.1 Satellite images

The fundamental data used in this study is multispectral satellite imagery from Landsat 5 TM 17 July 2006 (path 110, row 071) acquired over seven spectral (thematic) bands with a spatial resolution of 30 m. (bands 1 to 5 and band 7 have a spatial resolution of 30 m whereas band 6 has a spatial resolution of 120 m). Image scenes with low cloud cover and low water turbidity were chosen and downloaded from the United State Geological Survey (USGS) Earth Resources Observation and Science Data Centre ([www.earthexplorer.usgs](http://www.earthexplorer.usgs); downloaded in 2012).

The three visible bands of Landsat TM, i.e. band 1 (0.45 – 0.52  $\mu\text{m}$ ), band 2 (0.52 – 0.60  $\mu\text{m}$ ), and band 3 (0.63 – 0.69  $\mu\text{m}$ ) were selected because of their water penetration characteristics. Jupp et al. (1985) reported that the depths of penetration are about 30 m, 18 m and 5 m for band 1, 2 and 3, respectively. Band 4 (0.76 – 0.90  $\mu\text{m}$ ) is used to the differentiate land from water in the land-masking workflow.

A single multispectral colour composite image resulting from a combination of individual spectral bands was produced in the software package (ERDAS) ER Mapper toolkit. The image was then corrected geometrically using Universal Transverse Mercator (UTM) zone 51 and WGS 84 as the coordinate system and reference datum respectively. For the purpose of a two-dimensional layout, the classified Landsat raster image was converted to vector data and presented within ESRI's ArcGIS 10.0 software.

### 2.2.2 Image processing and analysis

Landsat-derived reef geomorphology and associated habitat maps were produced by integrating Landsat multispectral data, unsupervised classification, and ground-truth observations following the simplified workflow of Kaczmarek et al. (2010). Ground-truth and sample locations were photographed and recorded with a camera with a built-in GPS. Visual assessment and description were the first stage of obtaining preliminary habitat descriptions for each geomorphic zone and digital photos were then undertaken to document and assist the interpretation. Due to the

difficulty in producing accurate species level determinations, living coral communities were compared at the genus level.

Several distinct habitats identified from ground-truth observations were linked to a group of pixels within the classified image, produced by the (ERDAS) ER Mapper unsupervised classification utility, to assign the habitat zone. For pixel groups with no corresponding groundtruth point, habitat determinations were assisted by high-resolution aerial photo interpretation, location of nearby or adjacent investigated habitats and expert and local knowledge.

After enhancement (filtering, smoothing and land-masking) and classification, reef habitats are identified, assigned, and saved as vector files. Polygons from each study area are imported as shapefiles into ESRI's ArcGIS. Where present, overlap between polygons is removed and polygons are merged and corrected. The reef geomorphic and associated habitat map was created and attributes such as perimeter and area were directly measured.

## 2.3 Results

The results of digital classification image produced by the (ERDAS) ER Mapper toolkit and supported by on ground observations from the selected islands studied: Tallon Island, Sunday Island and Irvine/Bathurst Islands are provided below.

### 2.3.1 Tallon Island

The Landsat-derived reef geomorphology and associated habitat map (Fig. 2.2), supported by ground-truth observations (Fig. 2.3), allowed delineation of six characteristic reef biogeomorphic zones, including (1) intertidal beach and rubble zone (0.12 km<sup>2</sup>), (2) coralgall pavement (1.05 km<sup>2</sup>), (3) mangrove (0.35 km<sup>2</sup>), (4) shallow lagoon of seagrass and carbonate sand (1.52 km<sup>2</sup>), (5) crustose coralline algal terraces (0.96 km<sup>2</sup>), and (6) steep-sided coralline algae.

*Intertidal beach:* the intertidal beach is generally short ( $\pm 50$  m) and narrow ( $\pm 15$  m) and developed in the embayment sections on the west side of Tallon Island. The beach consists of coarse terrigenous sand and various detrital elements derived from reef communities such as coral fragments, shells, and foraminifera.

*Boulder rubble zones:* the boulder rubble zones stretch along the base of rocky cliff sections of the west side of Tallon Island and consist mainly of hematite-rich sandstone.

*Coralgal pavement:* the coralgal pavement mainly occurs on the west side of Tallon Island and consists of coralline algae and intertidal coral such as live tabular *Acropora*, *Goniastrea aspera*, and other faviids (Fig. 2.3 – WT3; WT4; WT5). The pavement occupies almost the entire 0.9 km wide, gently sloping-seaward reef flat. Macroalgal-covered coral rubble and carbonate sand substrates are also found every  $\pm 10$ -15 m on the reef flat (Fig. 2.3 – WT2).

*Mangrove:* the mangrove habitat, approximately 200–500 m wide, fringes the embayment sections of Tallon Island especially on the eastern side. The mangrove, mainly from the genera of *Rhizophora* and *Avicennia*, occurs at the landward margin of the reef flat, backed by cliff rock, and rests on silty sand substrates.

*Shallow lagoon of seagrass and carbonate sand:* the shallow lagoon of seagrass and carbonate sand, approximately 30-50 cm deep at low tide, is widely distributed on the east side of Tallon Island and associated with coral rubble and coralline algal fragments. The lagoon is retained by a series of low relief (10–20 cm) coralline algal terraces (Fig. 2.3 – ET2; ET7) during low tide. The seagrass is mainly *Thalassia* and covers the carbonate sand substrates (Fig. 2.3 – ET9; ET10).

*Crustose coralline algal terraces:* the crustose coralline algae terraces occur on the seaward-sloping reef on the east side of Tallon Island and are exposed at low spring tides, forming a broad and extensive (about 2.5 km long and 0.5 wide) reef crest. The water impounded by the terraces remains as shallow ( $\pm 30$  cm deep) tidal pools, providing habitats for soft algae, gastropods, lamellibranchs, echinoderms, starfishes, short seagrass, and small colonies of coral (Fig. 2.3 – ET3; ET4; ET5). The series of terraced reef crests are a striking geomorphic feature on the east side of Tallon Island, impounding a 30-50 cm deep lagoon and forming a spectacular series of waterfalls on an ebbing tide (Fig. 2.3 – ET6).

*Steep-sided coralline algae:* the steep-sided coralline algae colonises the forereef slope especially on the east side of Tallon Island. The forereef slope drops down steeply, sometimes almost vertically, resembling an undercut wall in the upper few metres of the slope (Fig. 2.3 – ET8).



## Tallon Reef geomorphology and associated habitats

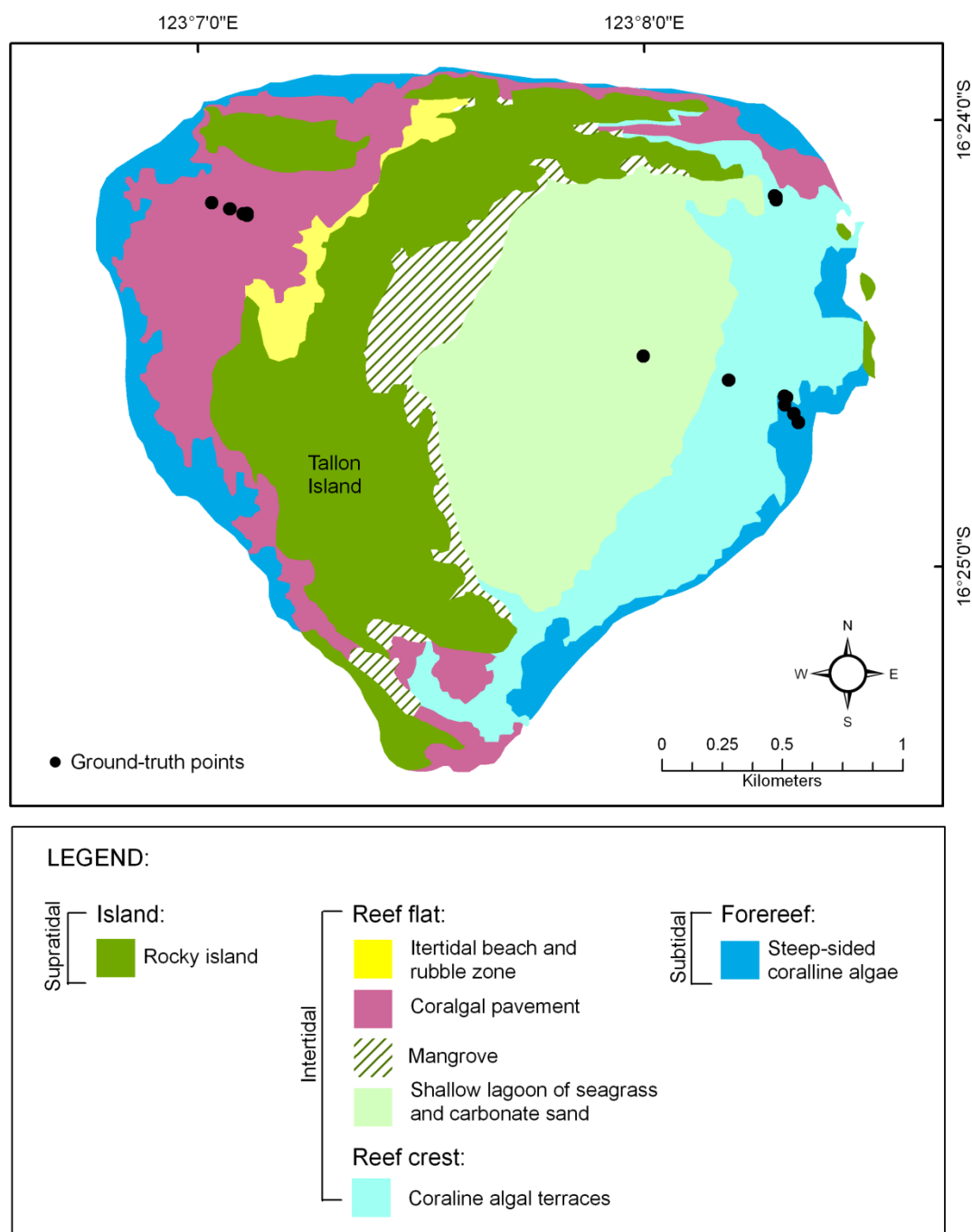


Figure 2.2 Map of Tallon Reef geomorphology and associated habitats with ground-truth points, derived from Landsat5 TM 17 July 2006.

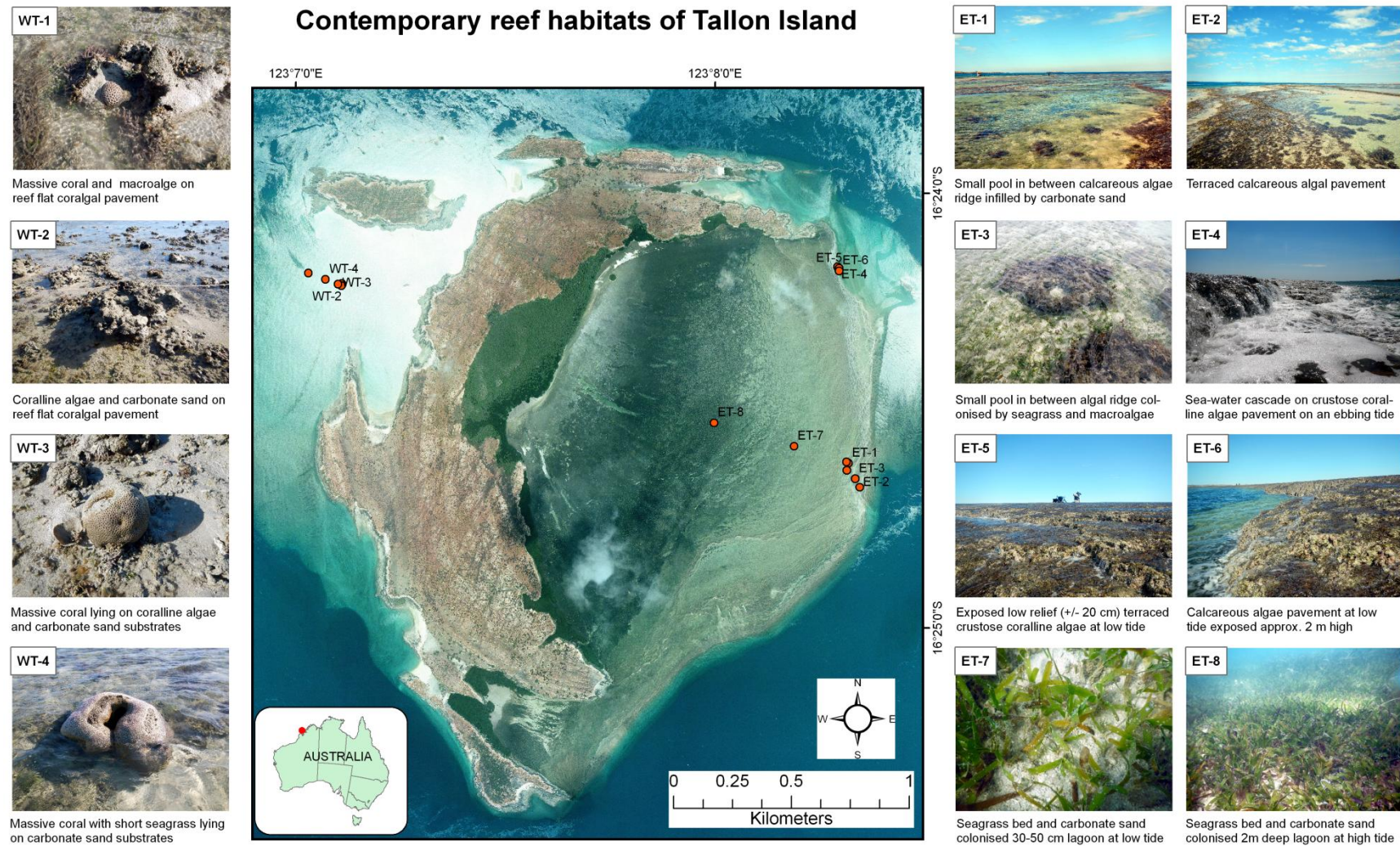


Figure 2.3 Contemporary reef habitats of Tallon Island with the spot locations of the photographs shown on the high-resolution aerial photo.

### 2.3.2 Sunday Island

The Landsat-derived reef geomorphology and associated habitat map (Fig. 2.4), supported by groundtruth observations (Fig. 2.5), delineates six characteristic reef biogeomorphic zones, including (1) mangrove (4.06 km<sup>2</sup>), (2) intertidal sand flats (1.12 km<sup>2</sup>), (3) coralg al pavement (8.82 km<sup>2</sup>), (4) seagrass beds (0.73 km<sup>2</sup>), (5) coralline algal terraces (0.97 km<sup>2</sup>), and (6) encrusting and massive corals (2.26 km<sup>2</sup>).

*Mangrove:* the mangrove habitat (*Avicennia*) is found in the more sheltered embayed sections of Sunday and Allora Islands where tributaries drain off fresh water from the island. The mangrove habitat occupies the most landward area in the intertidal zone and rests on silty sand substrates.

*Intertidal sand flats:* the intertidal sand flats contain coralline algae fragments, coral debris, shells, and gastropods. The sand flats are distributed on the sheltered embayment beaches across the island and intermittently deposited adjacent to/in front of mangrove habitat (Fig. 2.5a – NP16).

*Coralgal pavement:* an extensive coralg al pavement is widely distributed on the interisland reef platform (also known as the ‘Pool’) with abundant small colonies (< 0.5 m in diameter) of *Goniastrea aspera* and many other coral genera including *Acropora*, *Montipora*, and *Porites*. The Pool occupies an area in between Sunday and Allora Island which is interpreted to be coalescing together forming broad and terraced reef flats. There is no reef crest recorded in the Pool as the reef flat is gently sloping seaward. Coralg al pavement on the northern Pool mainly consists of coralline algal-coated branching coral fragments (Fig. 2.5a – NP1; NP4), whilst on the southern Pool, the pavement comprises coralline algae with low relief rhodolith terraces (5–10 cm high), occurring where seawater streams off the elevated reef at low tide. Shallow ( $\pm$  30 cm deep) tidal pools formed by a series of terraces provide habitats for soft algae, invertebrates, fishes, turtles, short seagrass, and small colonies of coral. Unlike on the northern Pool, here colonies of living coral and coral rubble are found very rare (approximately every 50-100 m) and soft coral and rhodoliths ( $\pm$  5-8 cm in diameter) are abundant on the reef flat, indicating high energy hydrodynamic environments including tidal streams.

*Seagrass beds:* the seagrass beds, mainly *Thalassia*, are abundant over the carbonate sand substrates adjacent to the intertidal sand flats (Fig. 2.5b – SS4-SS6). They

widely occur on the south side of Sunday Island (also known as the ‘Hancock’ Reef). Microatoll colonies from the genera *Porites* (up to 1 m diameter) are also frequently found on the Hancock reef flat (Fig. 2.5b – SS8).

*Coralline algal terraces*: the coralline algal terraces along with low-relief rhodolith banks occur on the seaward sloping reef of the ‘Hancock’ Reef, forming a broad and extensive (about 2.5 km long and 150 m wide) reef crest at the edge of the reef platform (Fig. 2.5b – SS4).

*Encrusting and massive corals*: the encrusting and massive corals occur on the steep (>30 degree) forereef slope at depths to about 15 m. The encrusting coral is mainly *Montipora*, while the massive corals are *Lobophyllia* and faviids. Branching *Acropora* and macroalgae (mainly *Sargassum*) are also found on the sheltered forereef slope of Sunday Island.

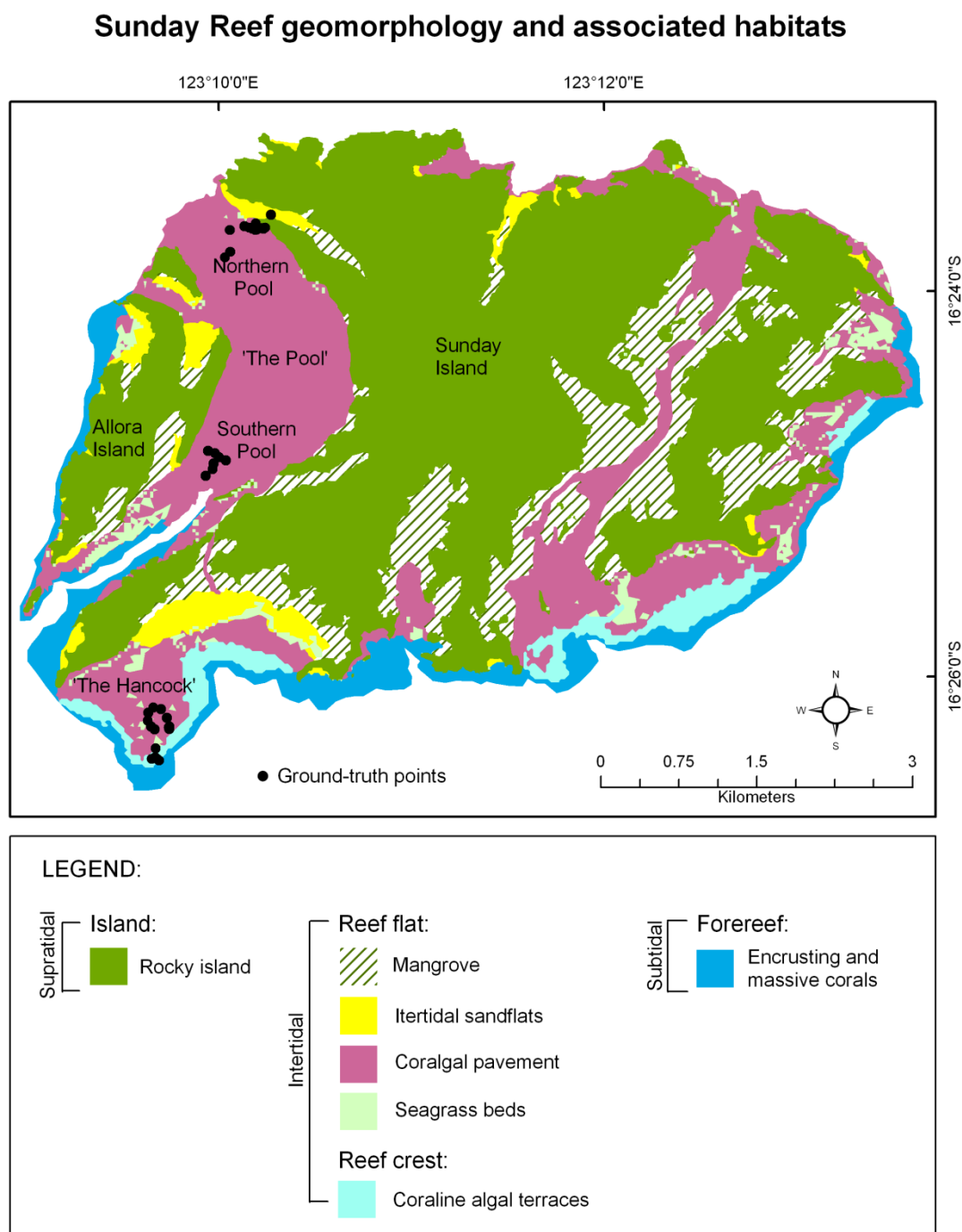


Figure 2.4 Map of Sunday Reef geomorphology and associated habitats with groundtruth points, derived from Landsat 5 TM 17 July 2006.



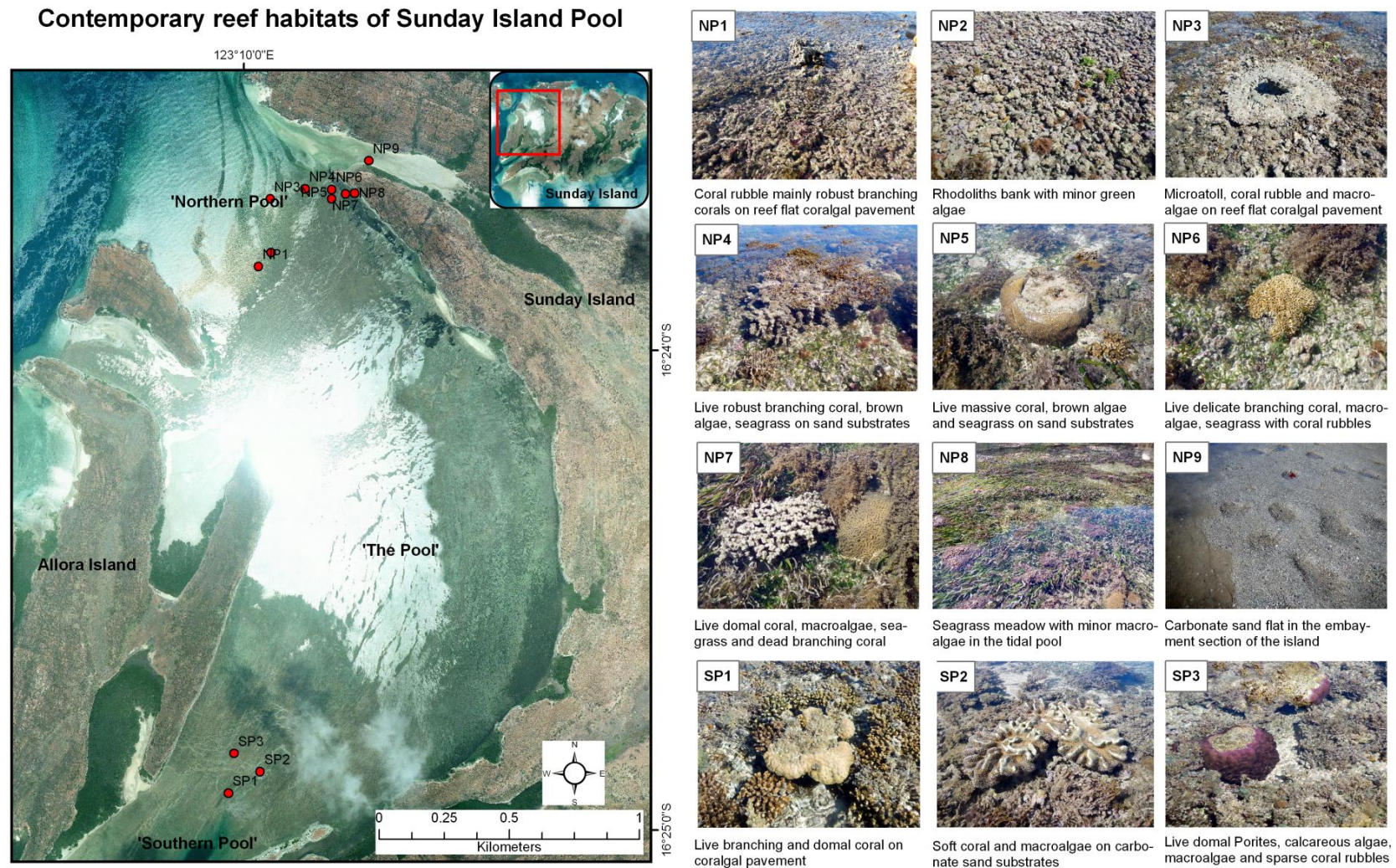


Figure 2.5a Contemporary interisland reef habitats of Sunday Island with the spot locations of the photographs shown on the high-resolution aerial photo.



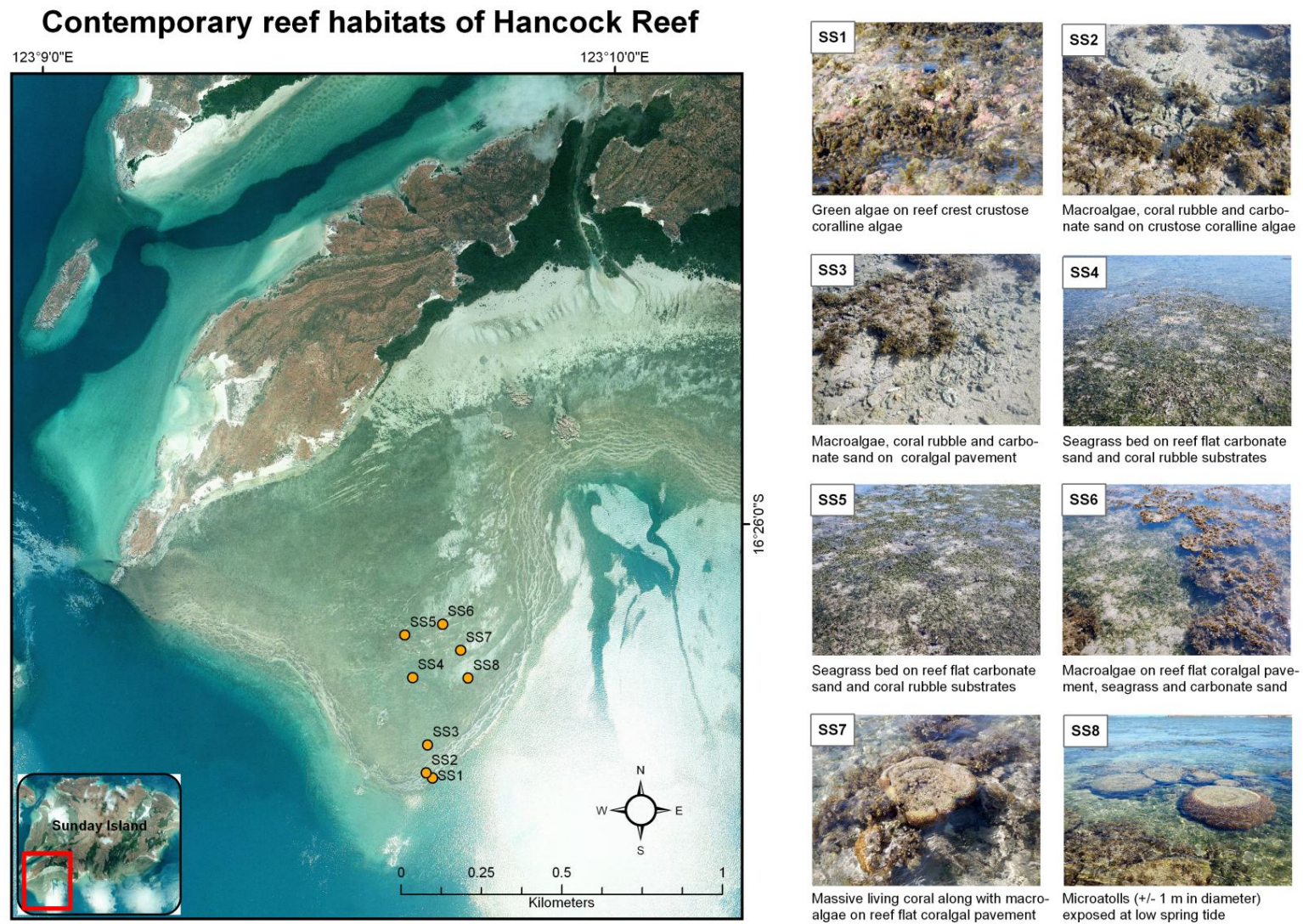


Figure 2.5b Contemporary reef habitats of Hancock Reef with the spot locations of the photographs shown on the high-resolution aerial photo.

### 2.3.3 Irvine/Bathurst Islands

The Landsat-derived reef geomorphology and associated habitat map (Fig 2.6), supported by groundtruth observations (Fig. 2.7), allowed delineation of five characteristic reef biogeomorphic zones, including (1) mangrove (0.39 km<sup>2</sup>), (2) intertidal sand flat (4.98 km<sup>2</sup>), (3) deep tidal pool (0.31 km<sup>2</sup>), (4) coralg al pavement (10.2 km<sup>2</sup>), and (5) coralline algal terraces (1.86 km<sup>2</sup>).

*Mangrove:* the mangrove habitat, mainly *Rhizophora*, is moderately broad (approximately 50 – 400 m wide), fringing the island, especially in the more sheltered bays on the northeast side of Irvine Island and on the southern side of Bathurst Island (Fig. 2.7 – B20). The mangrove is backed by rocky cliffs and rests on sand substrates.

*Intertidal sand flats:* the intertidal sand flats derived mainly from bioclastic components, often with gravely sandstone and coral rubble, occupy almost the entire embayed sections of the islands. The sand flats are also deposited as banks on the inner reef flat consisting of *in situ* or broken corals, especially *Acropora* at the front of the mangrove habitat. The sediments are also found within the deeper south and east-facing bays of Irvine Island with occasionally patchy corals resting on them.

*Deep tidal pools:* the deep enclosed tidal pools (up to 35 m deep) are spaces left by coalescing reef accretion in between Irvine and Bathurst Islands. The pools are steep-sided, coral-lined within the reef flat. The vertical or overhanging walls of the pools are colonised mainly by fast-growing branching *Acropora* and *Montipora*.

*Coralgal pavement:* an extensive coralg al pavement occurs on the interisland reef platform and is composed of coralline algae, massive and robust branching corals. *Platygyra*, *Goniastrea* and *Favites* were the most abundant faviid genera encountered on the reef flat which included many other genera: *Porites*, *Goniopora*, *Acropora*, *Astreopora*, *Montipora*, *Acanthastrea*, *Lobophyllia*, and *Turbinaria*. Microatolls were also found on the reef flat, particularly in the pools where water is retained at low tide. They are individual sub-circular coral colonies mainly from the genera of *Porites* sp (<1 m in width; Fig. 2.7 – B1). Also, *in situ* clams (*Tridacna maxima* and *T. derasa*) were found on the reef flat every 3-5 m (Fig. 2.7 – B04). Seagrass beds of *Thalassia* and macroalgae (*Sargassum*) were sparsely distributed over the reef flat and found occasionally in small tidal pools.



*Coralline algal terraces*: the coralline algal terraces occur on the seaward-sloping reefs of the west side of interisland reef platform. The terraces are less developed than those on Tallon and Sunday Islands. The forereef slope is not well-defined and is not presented on map.

### Irvine/Bathurst Reef geomorphology and associated habitats

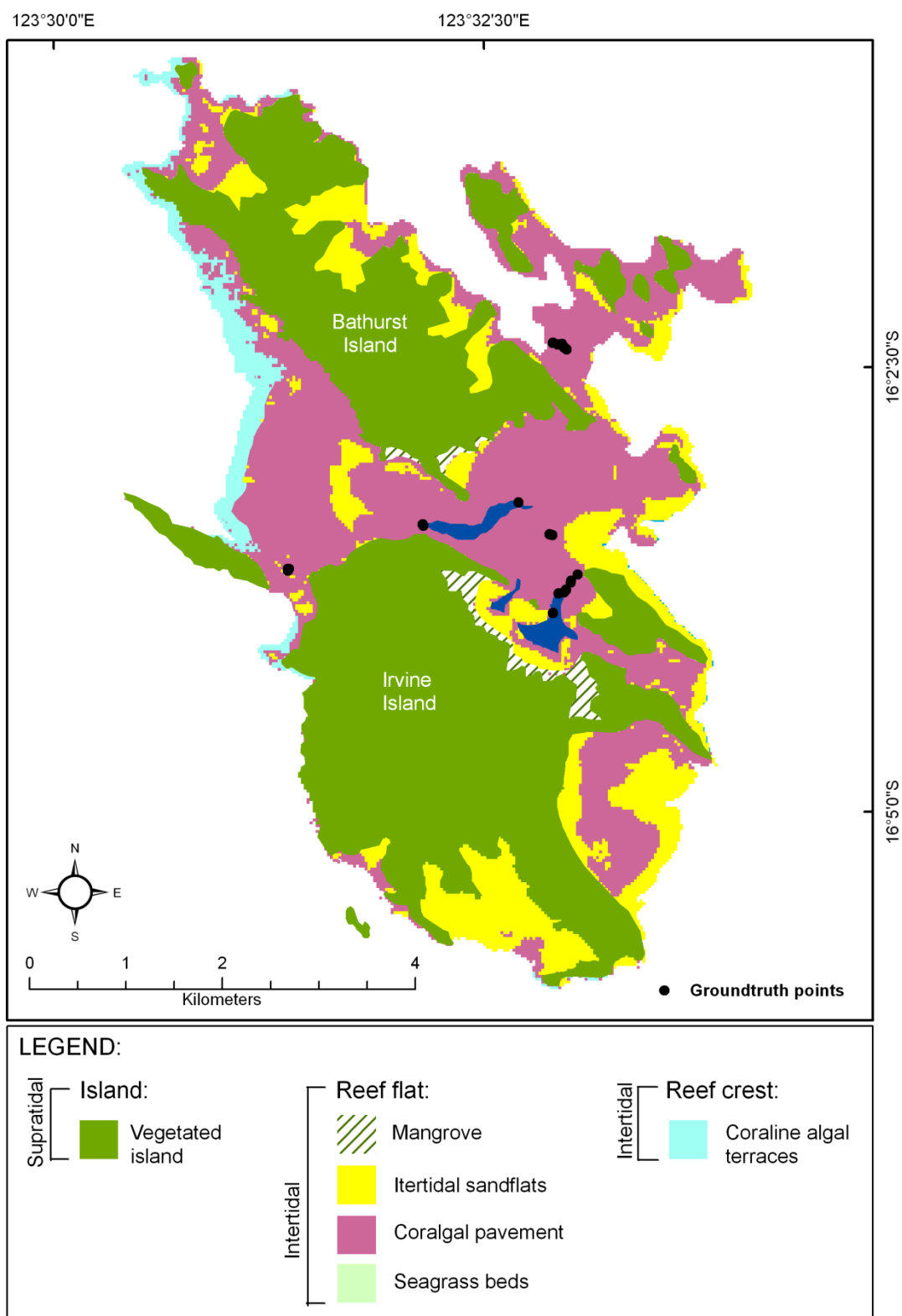


Figure 2.6 Map of Irvine/Bathurst Reef geomorphology and associated habitat with groundtruth points, derived from Landsat 5 TM 17 July 2006.

## Contemporary reef habitat of Irvine/Bathurst Island

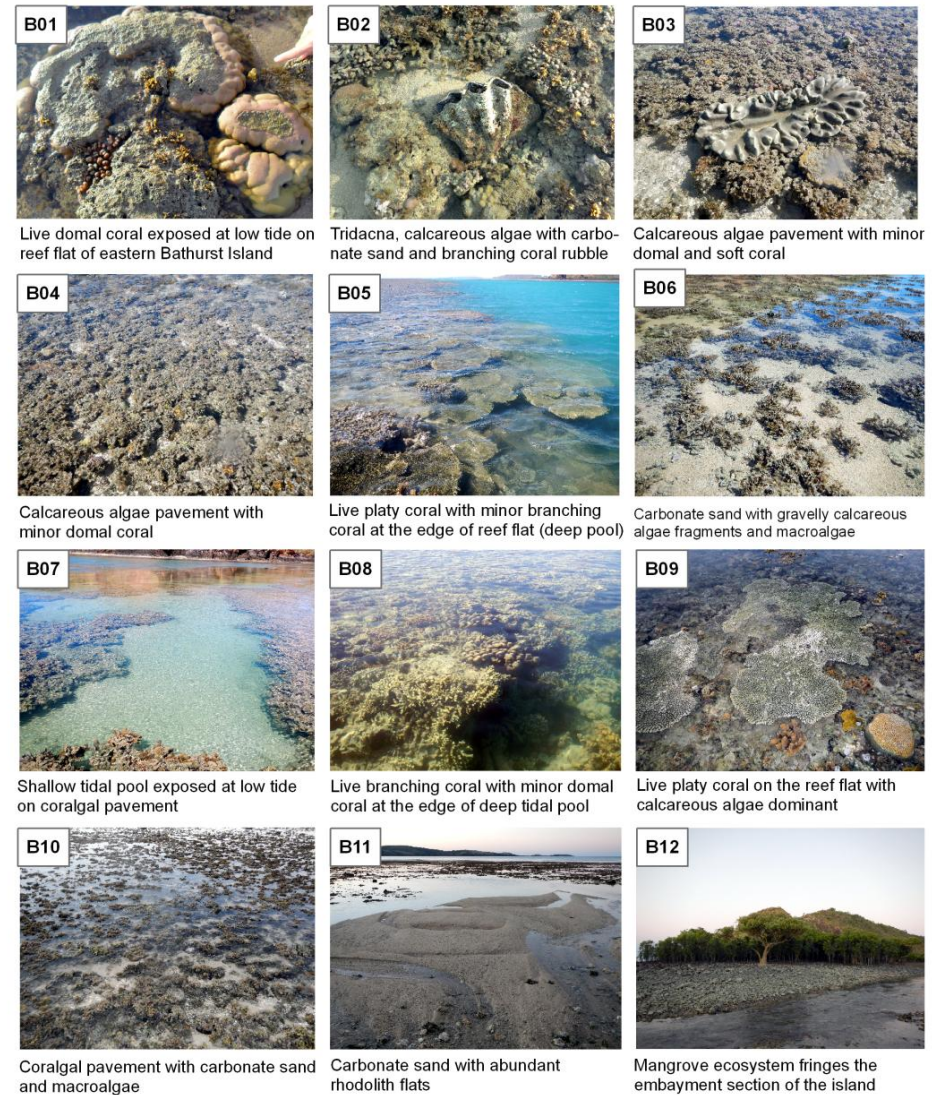
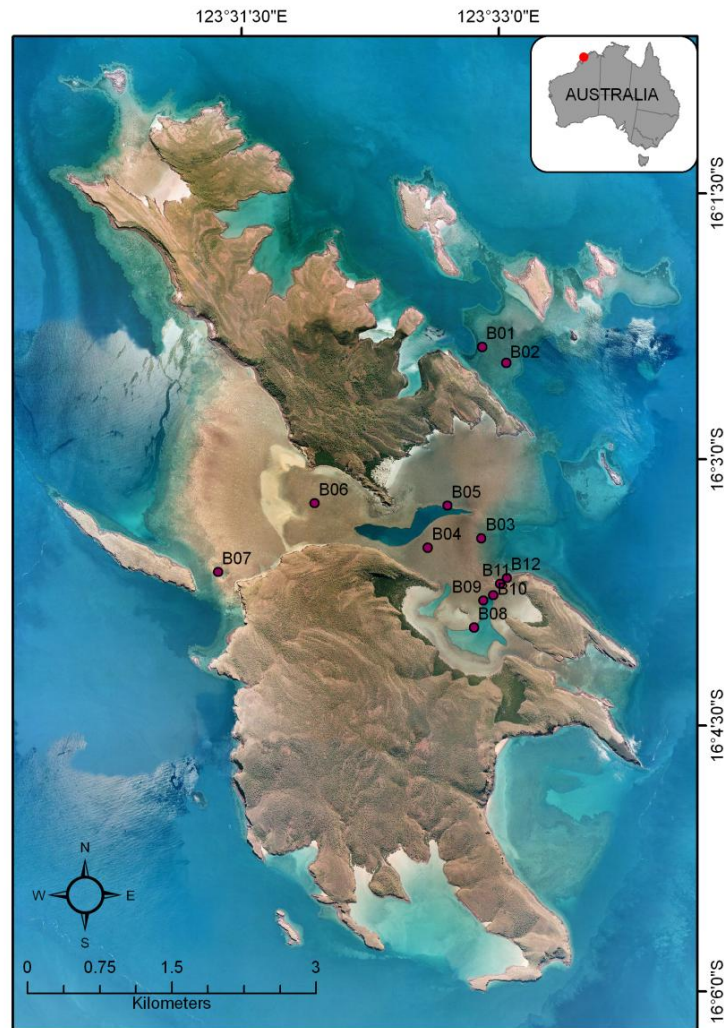


Figure 2.7 Contemporary reef habitats of Irvine/Bathurst Islands with the spot locations of the photographs shown on the high-resolution aerial photo.

## 2.4 Discussion

### 2.4.1 Challenges of using remote sensing for coral reef mapping

Despite the fact that remote sensing techniques offer the most rapid and cost-effective approach to observe and characterise a large area of reef environments, the complexity and spatial variability of the Kimberley Reefs limit the transferability and accuracy of detailed coral reef mapping accomplished via Landsat imagery in this region. During image processing, there were, at least, four challenges encountered in the workflow, including:

- a) The investigated area had limited research and is poorly studied, leading to a lack of preliminary information that is useful to assist interpretation;
- b) The high turbidity of the water column covers the coral reef platforms, resulting in misclassification of coral reef training-areas due to mixed-up spectral reflectance;
- c) The spatial resolution of a Landsat image is of relatively low-moderate resolution (30 m), constraining the mapping of small reefs (< 30 m wide), and;
- d) The difficulty of matching the spatial resolution of Landsat image with available bathymetric data sourced from Geoscience Australia with a ground resolution of 250 m may result in inaccurate water depth identification.

As preliminary information in the study area was lacking, the photo-transects taken from groundtruth observations were used to assign reef habitats by linking individual pixels corresponding to sample locations. The high-resolution aerial photography was then used to verify the interpretation and to cross-check the classification results.

The inherent absorption, scattering and attenuation of radiance by the water column as captured by the sensor leads to a major error in the spectral reflectance of the objects which in turn may result in inappropriate classifications (Green et al., 2000). The empirical method from Lyzenga (1981) has been widely recommended to improve coral habitat zone classifications (Green et al., 2000). However, experiments using Lyzenga's formula reported by Mumby et al. (1998) and Nurlidiasari (2004) on their work using ICAS and Quickbird satellite imagery showed improvement by only 13% and 20% respectively, indicating that applying Lyzenga's method in a turbid water environment would not show significant improvement in classification

accuracy. Consequently, the number of classes is principally constrained by the spectral and spatial resolution of the sensor utilised (Zainal et al., 1993).

The difficulty in distinguishing the reef crest and reef slope environments is related to the narrow width of the reef crests and slope dimension (<30 m), and the absence of a well-defined, highly reflective forereef slope. Each pixel of a Landsat image represents approximately 900 m<sup>2</sup> in the field, thus, any land feature less than such area is not mappable. A high-resolution image (1-10 m ground resolution) has been widely suggested by Joyce and Phinn (2001) and Andréfouët et al. (2003) to optimally map coral reef environments. However, hand digitising techniques are reliable to correct these misclassified pixels as applied in this study.

As it was not possible to source bathymetric data that matched the resolution of the Landsat imagery, corrections for variability in water depth were not employed in this study. The only bathymetric map available for the study area is a DEM sourced from Geoscience Australia (GA) with a ground resolution of 250 m.

The maps produced in this study represent a preliminary reef classification which aimed to recognise the general patterns and characteristics of the distribution of coral reefs in the Kimberley, hence, a simple and straightforward approach was applied.

#### **2.4.2 Reef characteristics of the Buccaneer Archipelago**

Reefs formed and developed in the Buccaneer Archipelago in the form of either fringing or platform reefs have a high abundance and diversity of corals (Wells et al., 1995; Purcell, 2002). The reef geomorphology formations observed on the selected islands are typical examples, demonstrating several characteristic morphological features described elsewhere in the Kimberley Bioregion (Teichert and Fairbridge, 1948; Brooke, 1995; Purcell, 2002), including:

1. Two different types of fringing reefs, including terraced reef flats and seaward-sloping reefs. They are well-developed on rocky shores of the islands of the bioregion. The terraced fringing reefs are best developed in the Buccaneer Archipelago (e.g. east Tallon and south Sunday Islands), but also occur in the northern part of the Kimberley coast. The seaward-sloping fringing reefs appear

to be more typical of fringing reefs worldwide and can be found on west Tallon and east Irvine/Bathurst Islands.

2. Narrower reef flat on the windward side (exposed reefs) than that on the leeward side (sheltered reefs). The exposed reefs have a steep side where there is a raised reef front ramp and a steep drop-off in the forereef zone (e.g. east Tallon and south Sunday Islands), while the sheltered reefs gently slope, though often irregularly, into the subtidal zone without a raised reef edge such as at west Tallon, north Sunday and east Irvine/Bathurst Islands.
3. Forereef slopes drop quickly at the reef front, forming steep-sloping reefs beyond the crest of the reef flat at approximately 5 m depth and tend to end at depths around 20 m where the coral gives way to a seabed of silty sand.

Likewise, the benthic habitats/facies of the Buccaneer Archipelago appear typical of fringing reefs characterised elsewhere in the Kimberley Bioregion (Blakeway, 1997; Purcell 2002; Wilson et al., 2011), including:

- 1) The sediment comprising the sandy pocket beaches is mainly derived by erosion of the hinterland but may include some bioclastic material, including carbonate fragments from intertidal and subtidal reef development and organic material from the mangrove.
- 2) Mangrove ecosystem, mainly *Rhizophora* and *Avicennia*, fringes the landward margin of reef flats, backed by rock cliffs on the more sheltered embayment beaches.
- 3) Tidal sand flats are generally small on the shores of the coastal islands and developed as part of fringing reef and platform reef ecosystem.
- 4) Corals are common in the intertidal zone of the reef platform throughout the bioregion, in spite of the turbid water conditions.
- 5) Large colonies of *Goniastrea aspera* are abundant on the contemporary reef flats along with *Porites cylindrica*, branching *Acropora*, and massive *Porites*.
- 6) Seagrass beds are mainly *Thalassia*, while macroalgae are predominantly *Sargassum*.
- 7) Forereef slopes that descend into the subtidal zone have substantial coral growth with very high percentage cover of live coral including encrusting coral (e.g. *Montipora*) and branching coral (e.g. *Acropora*).



### 2.4.3 Specialised nature of reefs in the Buccaneer Archipelago

A special reef type found in the Buccaneer Archipelago is high intertidal reef (HIR) in addition to low intertidal reef (LIR). The HIR is rare worldwide, while the LIR is more common, including in the Kimberley Bioregion (Solihuddin et al., 2016). High intertidal reef is defined as a reef situated above mean low water neap (MLWN), such as the reef on the east side of Tallon Island (0.5 m above MSL) and Irvine/Bathurst Islands (0.25 m above MSL). The cause of this is not well-understood, but is likely related to the macrotidal conditions as the tidal range in the Buccaneer Archipelago is more than 9 m (Kordi et al., 2016). In a geomorphic feature, the HIR is characterised by the greater width (up to 1.5 km) of the reef flat than those on the LIR. While the reef flat habitats are dominated by coralline algae versus coral and sediment on the LIR (Solihuddin et al., 2016). This suggests that some or a combination of macrotidal conditions, reef flat width, and coralline algae, interact together to produce HIR (Solihuddin et al., 2016; discussed in more detail in Chapter 4).

The enclosed deep tidal pools (up to 35 m deep) found in the Irvine/Bathurst Islands reef are prominent morphological features in the region as remnants of the coalescence of fringing reefs in between Irvine and Bathurst Islands. These deep tidal pools are not well-developed on other reef systems in the Buccaneer Archipelago or elsewhere in the Kimberley Bioregion. The presence of extensive coralline algal terraces on the seaward-sloping reefs at Tallon and Sunday Islands is unusual in nature as the crustose coralline algae in the Buccaneer Archipelago has developed in a low-energy setting (Richard and O’Leary, 2015). The terraces impound water up-slope on an ebbing tide, creating a sea-water cascade on the reef platform margin. This crustose coralline algae group plays a major role in reef framework construction by binding together reef communities such as corals, coralline red algae, vermetid gastropods, encrusting foraminifera, molluscs, and cemented sediment.

## 2.5 Conclusions

A Landsat-derived reef geomorphology and associated habitats analysis provides significant information relevant to the biodiversity present as physical structures that can be indications of coral communities and benthic habitats. However, on ground observations, high-resolution aerial photography and expert knowledge are essential in assisting accurate interpretation, especially for the benthic habitats mapping. This reconnaissance study provides a spatial framework for reef facies, geomorphic and ecological research at both regional (between reefs) and local (within reefs) scale, providing guidance for field sampling strategies.

The distinctive pattern of reef geomorphic zones and associated habitats shows the interaction between reef development processes and the physical oceanic environment. For example, branching and plate corals are sparse in the intertidal zone but are abundant in the subtidal zone. Conversely, coralline red algae (rhodoliths) and small robust corals tend to develop in the shallow and more energetic water as reefs became intertidal at their surface.

The HIR appears to be a special type of reef found in the Buccaneer Archipelago in addition to terraced reef flat structures. This reef type is well-developed in the Buccaneer Archipelago where tidal ranges can exceed 9 m. The most striking geomorphological feature in the region is the presence of extensive crustose coralline algae on the eastern Tallon Reef and Hancock Reef which have developed in an unusual low-energy setting for a crustose coralline algae environment, but the tidal current energy would be high given the tidal streams and the tropical cyclones episodically strike the area.

## References

- Andréfouët, S., Muller-Karger, F. (2006). Global assessment of modern coral reef extent and diversity for regional science and management applications: a view from space. *Proceedings of 10th International Coral Reef Symposium*, Okinawa, Japan, 28 June-3rd July 2004, Japanese Coral Reef Society.



- Andréfouët, S., Pagès, J. P. (2001). Water renewal time for classification of atoll lagoons in the Tuamotu Archipelago (French Polynesia). *Coral Reefs*, 20(4), 399-408.
- Andréfouët, S., Kramer, P., Torres-Pulliza, D., Joyce, K.E., Hochberg, E.J., Garza-Pérez, R., Mumby, P.J., Riegl, B., Yamano, H., White, W.H., Zubia, M., Brock, J.C., Phinn, S.R., Naseer, A., Hatcher, B.G., Muller-Karger, F.E. (2003). Multi-site evaluation of IKONOS data for classification of tropical coral reef environments. *Remote Sensing of Environment*, 88, 128–143.
- Blakeway, D. (1997). Scleractinian corals and reef development, part 9. In: Walker, D. (ed.), Marine biological survey of the central Kimberley coast, Western Australia. Perth: University of Western Australia. Unpublished report, W.A. Museum Library No. UR377, pp. 77–85.
- Brooke, B. (1995). Geomorphology, part 4. In: Wells, F. E., Hanley, J. R., Walker, D. (ed.), Survey of the marine biota of the southern Kimberley islands. Unpublished report No. UR286, Western Australian Museum, Perth, pp. 67–80.
- Capolsini, P., Andréfouët, S., Rion, C. Payri, C. (2003). A comparison of Landsat ETM+, SPOT HRV, Ikonos, ASTER, and airborne MASTER data for coral reef habitat mapping in South Pacific islands. *Canadian Journal of Remote Sensing*, 29(2), 187–200.
- Fairbridge, R.W. 1950. Recent and Pleistocene coral reefs of Australia. *The Journal of Geology*, 58(4), 330-401.
- Green, E. P., Mumby, P. J., Edwards, A. J. (2000). Remote Sensing Handbook for Tropical Coastal Management Sourcebooks, 3. UNESCO, Paris (316 pp. and plates).
- Griffin, T. J., Grey, K. (1990). Kimberley Basin, in: Memoir 3, Geology and Mineral Resources of Western Australia. Perth, Geological Survey of Western Australia, 293–304.

- Harris, P.M. (2010). Delineating and quantifying depositional facies patterns in carbonate reservoirs: insight from modern analogs. *American Association of Petroleum Geologists Bulletin* 94, 61–86.
- Jensen, J.R. (2007). Remote sensing of the environment: an earth resource perspective/ John R. Jensen. Pearson Prentice Hall, Upper Saddle River, N.J.
- Joyce, K. E., Phinn, S. R. (2001). Optimal spatial resolution for coral reef mapping. *Proceedings of the International Geoscience and Remote Sensing Symposium*, 2, 619–621.
- Jupp, D. L., Mayo, K. K., Kuchler, D. A. (1985). Remote sensing for planning and managing the Great Barrier Reef of Australia. *Photogrammetria*, 41, 21–42.
- Kaczmarek, S. E., Hicks, M. K., Fullmer, S. M., Steffen, K. L., Bachtel, S. L. (2010). Mapping facies distributions on modern carbonate platforms through integration of multispectral Landsat data, statistics-based unsupervised classifications, and surface sediment data. *American Association of Petroleum Geologists Bulletin*, 94, 1581–1606.
- Kordi, M., Collins, L. B., O'Leary, M., Stevens, A. (2016). ReefKIM: An integrated geodatabase for sustainable management of the Kimberley Reefs, North West Australia. *Ocean & Coastal Management*, 119, 234–243.
- Lyzenga, D. R. (1981). Remote sensing of bottom reflectance and water attenuation parameters in shallow water using aircraft and Landsat data. *International Journal of Remote Sensing*, 2, 71–82.
- Madden, R.H.C., Wilson, M.E.J., O'Shea, M. (2013). Modern fringing reef carbonates from equatorial SE Asia: An integrated environmental, sediment and satellite characterisation study, *Marine Geology*. doi: 10.1016/j.margeo.2013.07.001.
- Maedar, J., Narumalani, S., Rundquist, D. C., Perk, R. L., Schalles, J., Hutchins, K., Keck, J. (2002). Classifying and mapping general coral-reef structure using IKONOS data. *Photogrammetric Engineering and Remote Sensing*, 68, 1297–1305.

- Mumby, P.J. and Harborne, A.R., 2006. A seascape-level perspective of coral reef ecosystem. In: I.M. Cote and J.D. Reynolds (Editors), *Coral reef conservation*. Cambridge University Press, New York, pp. 568.
- Mumby, P. J., Green, E. P., Clark, C. D., Edwards, A. J. (1998). Digital analysis of multispectral airborne imagery of coral reefs. *Coral Reefs*, 17, 59–69.
- Mumby, P. J., Skirving, W., Strong A. E., Hardy, J. T., LeDrew, E. F., Hochberg, E. J., Stumpf, R. P., David, L. T. (2004). Remote sensing of coral reefs and their physical environment. *Marine Pollutan Bulletin*, 48, 219-228.
- Nurlidiasari, M. (2004). The application of Quickbird and Multi-temporal Landsat TM data for coral reef habitat mapping. Case Study: Derawan Island, East Kalimantan, Indonesia, International Institute for Geo-Information Science and Earth Observation, Enschede, The Netherlands.
- Purkis, S.J., Riegl, B.M., Andréfouët, S. (2005). Remote sensing of geomorphology and facies on a modern carbonate ramp (Arabian Gulf, Dubai, U.A.E.). *Journal of Sedimentary Research* 75, 861–876.
- Purcell, S. P. (2002). Intertidal reefs under extreme tidal flux in Buccaneer Archipelago, Western Australia. *Coral Reefs*, 21(2), 191-192.
- Richards, Z. T., O’Leary, M. J. (2015). The Coralline Algal Cascades of Tallon Island (Jalan) Fringing Reef, NW Australia. *Coral Reefs*, 34(2), 595.
- Smith, S. V., Jokkel, P. L. (1975). Water composition and biogeochemical gradients in the Canton atoll lagoon. *Atoll Research Bulletin*, 221, 15-45.
- Solihuddin, T., O’Leary, M.J., Blakeway, D., Parnum I., Kordi, M., Collins, L. B. (2016). Holocene reef evolution in a macrotidal setting: Buccaneer Archipelago, Kimberley Bioregion, Northwest Australia. *Coral Reefs*. 35:783-794.
- Stoddard, D. R. (1969). The shape of atolls. Ecology and morphology of recent coral reefs. *Biological Reviews*, 44(4), 433–498.
- Teichert, C., Fairbridge, R.W. (1948). Some coral reefs of the Sahul Shelf. *Geographical Review*, 38(2), 222-249.

- Wells, F. E., Hanley, R., Walker, D. I. (1995). Marine Biological survey of the southern Kimberley, Western Australia. Western Australia Museum, Perth, WA.
- Wilson, B. R. (2013). The Biogeography of the Australian North West Shelf: Environmental Change and life's response. Elsevier, Burlington MA, USA.
- Wilson, B. R., Blake, S., Ryan, D., Hacker, J. (2011). Reconnaissance of species-rich coral reefs in a muddy, macro-tidal, enclosed embayment, Talbot Bay, Kimberley, Western Australia. *Journal of the Royal Society of Western Australia*, 94(2), 251–265.
- Zainal, A. J. M., Dalby, D. H., Robinson, I. S., 1993, Monitoring marine ecological changes on the east coast of Bahrain with Landsat TM. *Photogrammetric Engineering and Remote Sensing*, 59, 415–421.

### Chapter 3

#### **Holocene coral reef accretion and sea-level in a macrotidal, high turbidity**

**setting: Cockatoo Island, Kimberley Bioregion, Northwest Australia**

Tubagus Solihuddin<sup>1,4,\*</sup>, Lindsay. B. Collins<sup>1,4</sup>, David Blakeway<sup>2</sup>, Michael J. O' Leary<sup>3,4</sup>

<sup>1</sup>Department of Applied Geology, Curtin University, Bentley, WA 6102, Australia

<sup>2</sup>Fathom 5 Marine Research, 17 Staines Street, Lathlain, WA 6100, Australia

<sup>3</sup>Department of Environment and Agriculture, Curtin University, Bentley, WA 6102, Australia

<sup>4</sup>The Western Australian Marine Science Institution, Floreat, WA 6014, Australia

#### **Abstract**

The inshore Kimberley Bioregion of northwest Australia is a macrotidal, low wave energy, frequent cyclones, and high turbidity setting with abundant fringing coral reefs. Here we describe the Holocene development of a sheltered fringing reef at Cockatoo Island in the Kimberley, using data from reef cross-sections subaerially exposed in an iron ore mining pit, seismic profiles across the adjacent contemporary reef, and GIS and ground truth mapping of contemporary reef habitats. Subsidence since the Last Interglacial has provided accommodation for ~15 – 20 m of Holocene reef accretion upon an older, probably Last Interglacial, reef. In the pit cross-sections, the reef initiated at ~9,000 cal yr BP and accreted in a catch-up mode, reaching sea-level at ~3000 cal yr BP, and reef accretion rates varied from 26.8 mm/yr to 0.8 mm/yr, averaging ~2 mm/yr. The catch-up interpretation is supported by the predominance of branching *Acropora* throughout the Holocene section and the absence of contemporary intertidal indicators such as *Porites cylindrica* and *Millepora intricata*. This pattern differs from the otherwise similar mud-rich but mostly microtidal inshore fringing reefs of the Great Barrier Reef, which initiated in the late Holocene on shallow substrates under a stable sea-level. The study provides the first Holocene reef accretion history for an inshore Kimberley reef within a biodiversity “hotspot”.

Keywords: *Acropora*, *Porites*, Reef Geomorphology, Holocene Reef Accretion, Sea-level Change, Accretion Rate.

\* Corresponding author at: Department of Applied Geology, Curtin University, Bentley, WA 6102, Australia. Tel.: +61 8 9266 3710.

E-mail address: [tubagus.solihuddin@postgrad.curtin.edu.au](mailto:tubagus.solihuddin@postgrad.curtin.edu.au) (T. Solihuddin)

### 3.1 Introduction

The Kimberley coast is a remote sparsely populated and poorly studied region located in the NW of Western Australia. However, the discovery of a major hydrocarbon province in the offshore Browse Basin, and an increase in petroleum exploration in the region, has led to a heightened awareness of the region's rich biodiversity (Collins, 2002; Chin et al., 2008; Collins et al., 2011). While the presence of coral reefs have been broadly documented, occurring as fringing reefs in coastal settings, platform reefs in mid-ramp settings and atoll-like reefs along the shelf margin (Wilson et al., 2011), there have been few investigations into their biogeography, diversity and developmental history.

Coral reefs are particularly ubiquitous to the complex drowned landscape of the Kimberley coast, which provides abundant Proterozoic deformed rocky substrate for fringing reef development. These inshore fringing reefs occur in sheltered and exposed settings and endure in seemingly extreme environment conditions including; high turbidity and sediment input, elevated water temperatures (av. 28.5°C), a 10-m macrotidal range, significant subaerial exposure during low tides, and frequent cyclones. Despite these extreme conditions, the coral biodiversity in the Kimberley is far richer than that of the inner GBR fringing reefs and a little richer than those of the Pilbara to the south (Wilson, 2013).

Critically, our understanding of the development of the Kimberley reefs still remains a gap in our knowledge. For example it is not known whether reefs are thin veneers over rock platforms or significant long-lived accretionary structures. Additionally, the linkages between present reef geomorphology, Holocene sea-level rise, reef accretion history, and coastal processes have been recognized (e.g. Wilson, 2013) but are yet to be explored in any detail. Despite this lack of knowledge,

Kimberley reefs have been identified as having international significance and are in need of comprehensive study (Chin et al., 2008; Wilson, 2013).

This study will for the first time investigate the Holocene development and evolution of an inshore Kimberley coral reef located at Cockatoo Island (Fig. 3.1). Cockatoo is unique in that iron ore mining on the Island has exposed a complete vertical section of the inner part of a Holocene fringing reef. This has allowed for detailed stratigraphic, palaeoecological and geochronological analysis spanning the entire reef accretion history, thus enabling an investigation into how these reefs were able to persist under extreme environmental conditions as well as respond to Holocene sea-level change. The addition of seismic reconnaissance data has allowed for the broader reef architecture and structure to be assessed. Lastly, this study develops a Holocene reef accretion rate curve for the Kimberley, so that the shelf drowning history can be reconstructed. The initiative to protect these marine areas through the Kimberley Science and Conservation Strategy (Government of Western Australia, 2011) also requires a fundamental baseline understanding of how the environment formed for effective long term protection.

### **3.1.1 Oceanography of the Kimberley Region**

The region is tidally dominated, with coastal mean spring range of 9.2 m in King Sound (see Fig. 3.1; Harris et al., 1991), the highest tide range in Australia (Short, 2011) and the second highest tide in the world after the Bay of Fundy in Canada (Purcell, 2002; Wolanski and Spagnol, 2003). This macrotidal system generates an extensive intertidal zone and strong tidal currents, which in turn cause high turbidity in coastal waters (Brooke, 1997). The region lies in the monsoonal belt with prevailing westerly or northwesterly rain-bearing winds from November to March, and dry southeasterly or easterly trade winds from May to September. It is cyclone-influenced (average 3 per year, Lough, 1998) and has southwest prevailing swell.

The local oceanography of the inshore Kimberley Bioregion is influenced by the Holloway current, which is driven by the Indonesian Throughflow waters through a southward flow over the shallow Timor Shelf (DEWHA, 2008). This current flows seasonally from March to July and is closely associated with the

northwest monsoon by which a southwesterly flow of surface water mass is released along the shelf margin. During the summer months (December to March), the Throughflow is deflected eastward, releasing a weak Holloway current along the inner shelf of the Kimberley. The upwelling generated by the Holloway current along with *in situ* planktonic production are believed to be contributing to the reef development in this region due to their roles in delivering nutrients where measures of N (0.05/12.8  $\mu\text{M}$ ), P (0.11/0.85  $\mu\text{M}$ ) and carrying planktic biota including planktotrophic larvae and reef animals (Wilson, 2013). Nutrient concentrations in the nearshore coastal Kimberley waters are relatively high here, influenced by riverine inputs from the adjacent terrestrial, high runoff environment (Wilson, 2013).

### 3.2 Location and Methodology

Cockatoo Island (Fig. 3.1) is located in the Buccaneer Archipelago (123.6°E; -16.1°S), approximately 7 km north of Yampi Peninsula. The geomorphology of the Buccaneer Archipelago and Yampi Peninsula are structurally controlled, reflecting the deformation geometry of the King Leopold Orogen (Wright, 1964). Cockatoo is an elongate island approximately 6 km long and 1.5 km wide and oriented along a NW/SE axis; with the NE side exposed to higher wave energies while the SW side is largely sheltered.

#### 3.2.1 Geophysical Surveys

Sub-bottom profiling was performed using an Applied Acoustics Boomer SBP system CSP-P300; with SBP Sound Source, AA201 Boomer Plate, mounted on a CAT100 surface tow catamaran. The receiver streamer had 8 element hydrophones, and A/D Interface Box from NI (National Instruments) Device Monitor V5.3.1. Data acquisition was made using Chesapeake Technology Inc SonarWiz 5 software. Position acquisition was made using a Fugro Seastar 8200XP/HP DGPS receiver. Survey lines were run across the modern reef flat up to a retaining seawall, which runs the length of the mining pit. Two survey lines were also run along the length of the reef flat, parallel to the seawall and close to sections measured onshore.



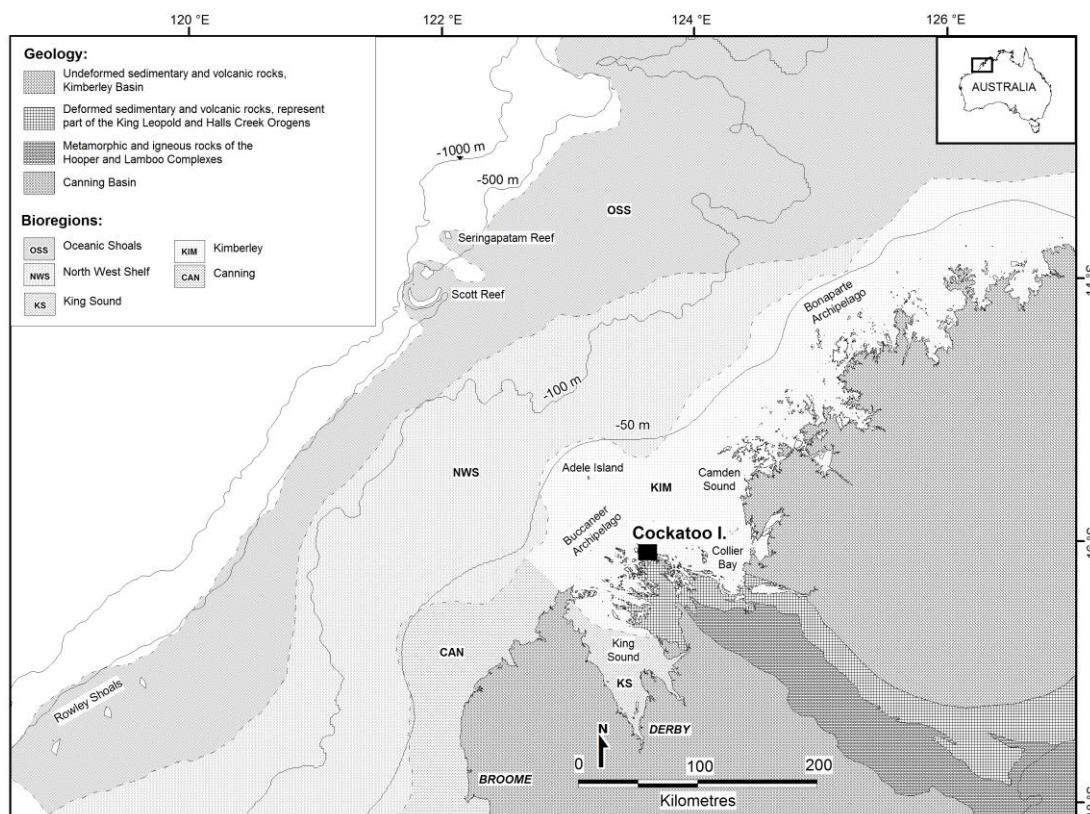


Figure 3.1 Map showing Bioregions modified from the Integrated Marine and Coastal Regionalisation of Australia (IMCRA) and geology of the Kimberley Region (After Griffin and Grey, 1990).

### 3.2.2 Reef Mapping

The distribution of living coral and associated substrates was based on aerial photography acquired on 5 May 2010. The image was corrected geometrically using a geographic coordinate system and WGS 84 ellipsoid reference. The three bands of aerial photography (RGB 321), along with groundtruth information, were employed to extract reef facies information. Discrimination of substrates into distinct classes was recognized from reflectance spectra grouped using unsupervised classification digital processing in ArcMap's Image Analysis toolkit. The spectral signature of each pixel in the aerial photography was determined based on a grouping of the spectra of each individual band. The habitat classifications were groundtruthed using towed camera transects over the reef flat and direct observations of the reef flat made on foot during spring low tides.

### 3.2.3 Ore Pit Mapping

Excavation of a 50-m deep, 750 m long open cut pit on Cockatoo Island has exposed a complete vertical section through the Holocene reef. Four stratigraphic sections were established along the face of the pit to log the reef exposures. At each site a vertical 0.7 m wide section from the base of the sequence to the top was logged, sampled and photographed. Information recorded includes: (i) the ratio of reef framework to matrix (following Embry and Klovan 1971); (ii) sediment textural characteristics (using the Udden-Wentworth nomenclature, as well as a visual assessment of sediment composition); and (iii) coral generic identification. Overlapping photographs (0.7 m x 0.5 m) were also taken up each profile. Reef framework analysis and facies descriptions followed the terminology suggested by Montaggioni (2005), which highlights the accretion forms of the dominant coral reef builders and environmental indicators. The carbonate content of matrix sediment was determined by carbonate bombe (weight % loss after treatment with 50% HCL) following guidelines from Müller & Gastner (1971). Position fixing was by DGPS tied to mine site datum. Elevations from each transect were plotted relative to the Australian Height Datum (AHD), which is 3.987 m below the Cockatoo mine grid datum (mine survey data).

### 3.2.4 Geochronology

*In situ* corals were collected from levels along each vertical section for accelerator mass spectrometry (AMS) radiocarbon dating in order to establish a geochronologic record of reef accretion. Radiocarbon dates were recalibrated using CALIB Version 5.0.2 and calibration curve Marine04 (<http://calib.qub.ac.uk/marine>; accessed November 2012). A weighted mean Delta-R ( $\Delta R$ ) value of +58 (average calculation from 3 nearest points) was used as the best current estimate of variance in the local open water marine reservoir effect for Cockatoo Island and adjacent areas. Dates discussed in the text are calibrated in years Before Present (cal yr BP) with the 68.2% ( $2\sigma$ ) probability range for all dated samples.

### 3.3 Results

#### 3.3.1 Living coral community zonation

A map of reef habitats and substrates around Cockatoo Island, based on aerial photographic interpretation (Fig. 3.2) provides a broad characterisation of the reef flat and its coral and macroalgal cover. Aerial photographic mapping linked to on ground observations and video transects delineates four gradational intertidal habitat zones. From landward to seaward these are the (1) intertidal beach and boulder rubble zone (2) inner sand flat and reef platform, (3) outer reef platform, and (4) forereef slope.

The upper intertidal zone consisting of steep sloping beaches of coarse, well-sorted siliciclastic sand is found in more embayed sections of the island. Along sections of the island consisting of steep plunging cliffs, hematite-rich, sandstone boulder rubble deposits dominate the upper intertidal and supratidal zones.

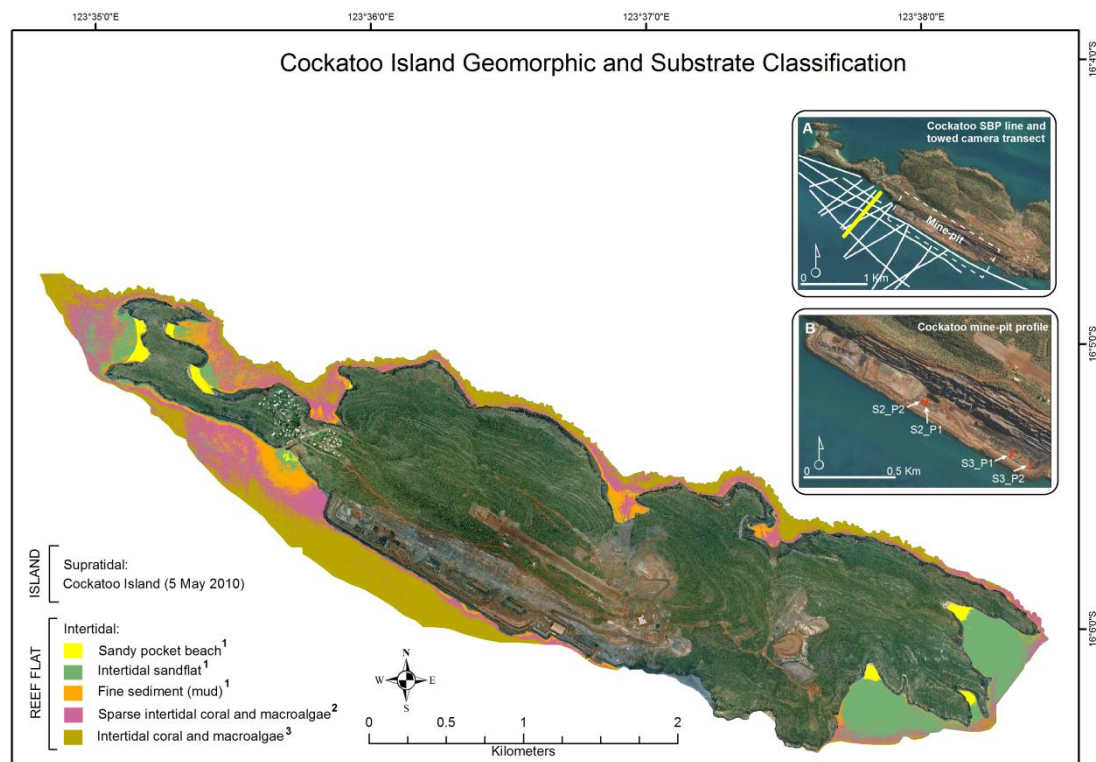


Figure 3.2 Map showing Cockatoo Island geomorphic and substrate classification, based on aerial photography interpretation (RGB 321). Numbers in legend correlate with habitats identified by on ground and towed video

observation: (1) intertidal beach and boulder zone, (2) inner sand flat and reef platform, (3) outer reef platform. The narrow and steep forereef slope is not mappable here. The inset map (A) shows sub-bottom profile (white line) and towed camera (yellow line) transects and (B) location of the mine-pit measured sections.

The lower intertidal zone consists of sand flats of poorly sorted, predominantly calcareous, sand with a matrix of pale grey-green calcareous mud. This transitions into the inner reef platform that includes sparsely distributed small coral colonies, mainly *Porites* and faviids but including many other genera. Macroalgae, predominantly *Sargassum*, are seasonally abundant on coral rubble substrate in this zone. Small thickets of the branching hydroid *Millepora* and the branching coral *Porites cylindrica* are common on the mid reef flat about 50–150 m from shore, occurring within extensive shallow pools (Fig. 3.3A).

The outer reef platform zone occurs seaward of these pools where the reef flat rises slightly, and is emergent for several hours on extreme spring low tides. Corals here occur as numerous close-packed colonies. *Porites* predominates but an extensive range of other genera occur, including, in estimated order of abundance: *Turbinaria* (Fig. 3.3B), *Favia*, *Favites*, *Goniopora*, *Lobophyllia*, *Astreopora*, *Montipora*, *Merulina*, *Pectinia*, *Goniastrea*, *Cyphastrea*, *Galaxea* and *Acropora* (tabular and fine aborescent forms) *P. cylindrica* is the most common *Porites* but massive species are also common, usually as relatively small (< 0.5 m) colonies, often with microatoll architecture due to low tide exposure.

The forereef slope is well defined and slopes seaward at approximately 30°, however, there is no raised reef crest along the reef edge. Video observations on the reef slope show a high cover (50 – 100%) of live branching *Acropora* (Fig. 3.3C) and, occasionally, *Seriatopora*, generally as large colonies, from the reef edge to approximately 10 m below AHD. Downslope, dead coral branches are sparsely colonised by encrusting *Montipora*, encrusting to plating pectiniid corals and small fine branching *Acropora* colonies to approximately 20 m below AHD. The lower slope consists of coral rubble, colonised by gorgonians and sponges, in a mud matrix.



The base of the lower slope grades gently into burrowed mud at approximately 30m below AHD.

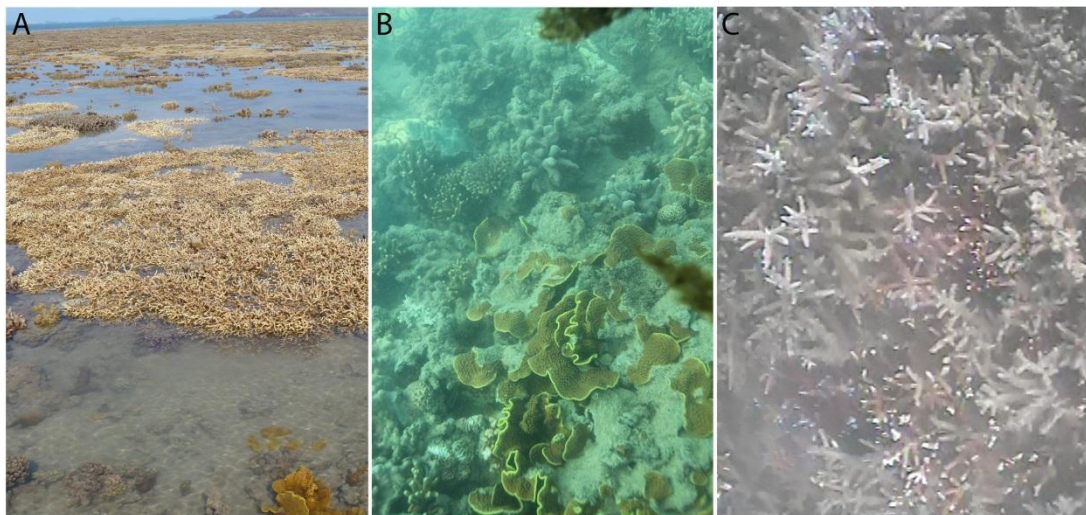


Figure 3.3 Living coral communities on the SW Cockatoo Island fringing reefs. (A) The extensive shallow pools on reef flat at low tide showing small thickets of the branching hydroid *Millepora* and the branching coral *Porites cylindrica*. B) *Turbinaria* and branching *Porites* in the outer reef flat. (C) High coral cover of branching *Acropora* on the forereef slope.

### 3.3.2 Stratigraphy and palaeoecology

Stratigraphic and palaeoecological data from the Cockatoo Island fringing reef is shown in Fig. 3.4. Each of the four measured reef sections are located approximately 50 m seaward of the original steep rocky shoreline, and represent the inner reef platform environment.

The basement is the Proterozoic Elgee Siltstone. Overlying the Elgee Siltstone is a 1 to 2 m thick sedimentary talus breccia containing subangular haematite boulders. Above the breccia is a 3 to 5 m thick pale yellow coral-rich mudstone with occasional weakly-bedded sand horizons and a calcretised, iron-stained upper surface. Corals in this unit are mainly domal, with a few encrusting and branching forms. Colonies are generally small (<30 cm diameter) and invariably recrystallised. Faviids are predominant, including *Favia*, *Goniastrea*, *Cyphastrea* and *Platygyra*. Overlying this unit is a second 0.3 to 1 m thick haematite boulder breccia,

followed by the Holocene reef, which is 8.4 to 12.7 m thick in the measured profiles. This is a minimum thickness because the upper contact is partly obscured by the rock overburden of the overlying seawall, and because there may have been some compaction of the Holocene by the seawall, a 13 m high structure comprising a clay core and rock armour.

All stratigraphic sections are dominated by single coral rudstone reef facies dominated by fragmented *Acropora* (typical diameter approximately 10 – 15 mm and length up to 150 mm) but also containing fragments and whole colonies of many other coral genera as well as abundant and diverse molluscan fauna. Additionally, the preservation of fine surface skeletal detail on most of the coral fragments indicates that they have undergone little transport; many appear to have collapsed where they grew. All interstices in the reef are completely filled with a poorly sorted grey-green calcareous mud containing sand to gravel-sized calcareous fragments and foraminifera tests. Coralline algae are rare throughout the sequence and there is virtually no inorganic cementation.

There are several non-acroporid dominant coral horizons in some sections but they do not appear to be laterally continuous. *Porites* is the most abundant genus but is not dominant to the extent that it is on the modern reef flat, and only occurs as massive forms, *P. cylindrica* is conspicuously absent from the Holocene. Additional taxonomic differences between the Holocene and the living reef are the absence of branching *Millepora* from the Holocene and the relative scarcity of *Turbinaria* and tabular *Acropora* in the Holocene (Fig. 3.5).

Analysis of matrix sediments (Fig. 3.4) showed carbonate content increased up section from 4 – 18% carbonate in the basal 2 – 3 m of the measured sections to 43 – 49% for the uppermost 2 m of the sections. The non-carbonate components include terrigenous clays and minor organics.

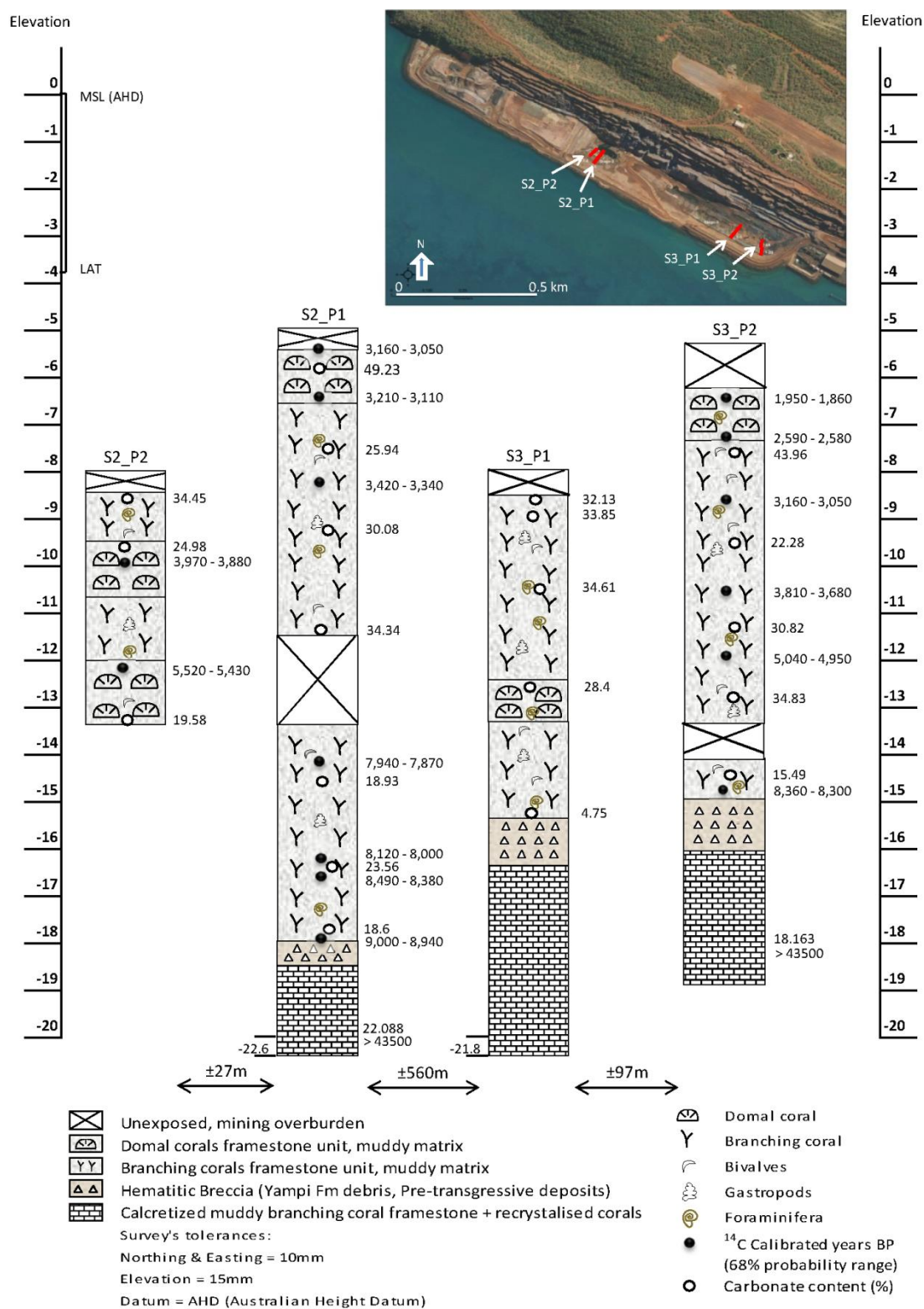


Figure 3.4 Lithostratigraphic and chronostratigraphic summary of measured sections of Cockatoo mine-pit.

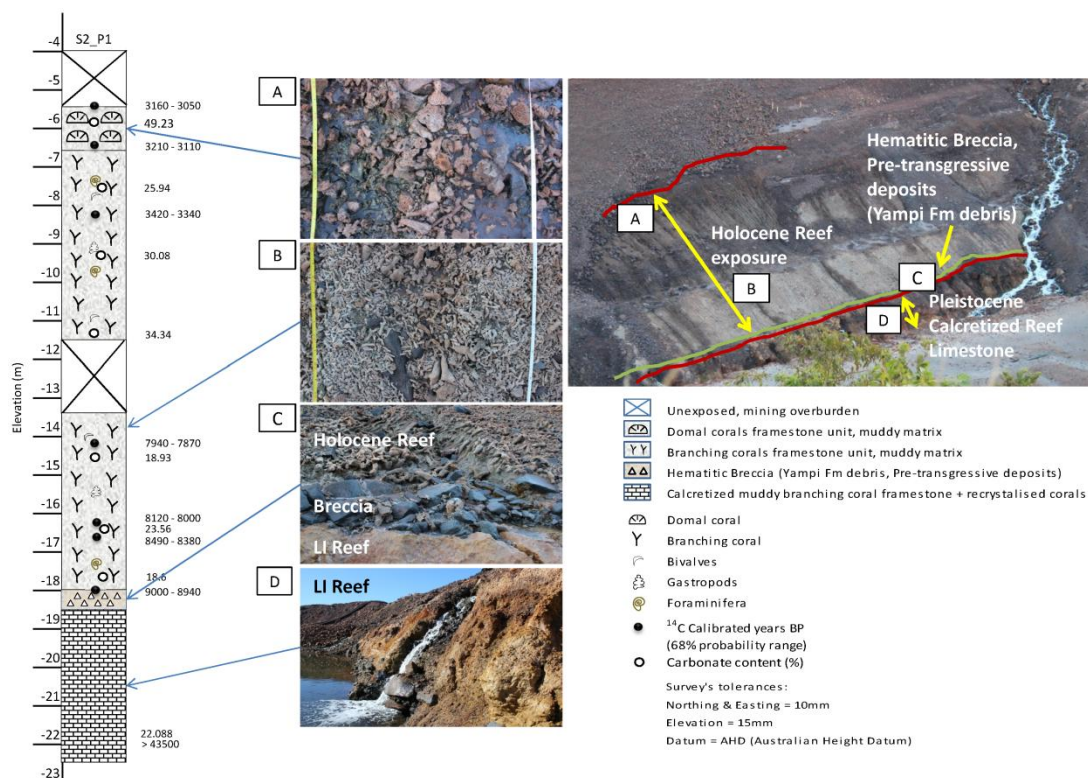


Figure 3.5 Idealised stratigraphic column of Cockatoo mine-pit section (S2\_P1).

Photo (A) showing the domal coral framestone with a muddy matrix, photo (B) showing the prevailing branching coral and coral rubble, photo (C) showing the contact between Holocene reef and Last Interglacial reef with a hematitic breccia as pre-transgressive deposits, and photo (D) showing the calcretized Last Interglacial reef exposure. Note  $^{14}\text{C}$  ages and % carbonate in matrix fraction are also shown.

### 3.3.3 Reef Geochronology and Accretion History

Sixteen radiometric dates were made on coral clasts collected from reef sections (NW and SE) exposed along the seaward mine-pit wall. All colonies were interpreted as *in situ* on taphonomic and orientation criteria. Results indicate earliest Holocene reef accretion initiated directly on the underlying pre-transgressive hematitic breccias along the NW reef section (S2) at a depth of 18.1 m below AHD (MSL) by ~8,970 cal yr BP. While the upper 1 m of reef surface is obscured by the sea wall, it would appear the reef flat had reached the approximate level of mean low water (~5.5 m below present AHD) in the NW reef section (S2) as early as ~3,105



cal yr BP, while the SE reef section (S3) reached mean low water level at around ~1,905 cal yr BP (Table 3.1).

Vertical accretion rates varied across NW and SW reef sites (Fig. 3.6). The NW section shows initial rapid vertical reef aggradation on the order of 3.8 mm/yr between 9 and 8k yr BP, which occurred at some time post the initial flooding. There was an abrupt slowing after 7.9k yr BP to around 1.2 mm/yr until around 5.5k yr BP, where the reef showed gradual but sustained increase in accretion rates of up to 27 mm/yr as the reef flat reached near sea-level with increasing light and energy. The SE section, unlike the NW section, did not show an initial rapid accretion but instead exhibited a more uniform accretion across its entire accretion history. Unlike the NW section the SE section exhibited a slight reduction in vertical accretion after about 4k cal yr BP from 3.6 mm/yr to 2.0 mm/yr. The study was not able to establish the exact timing of when the SE section reached base level due to the top of the section being covered by mine waste.

Table 3.1 Radiocarbon dates from selected samples across Cockatoo mine-pit transects

SAMPLE NUMBER/ ELEVATION (m)	LAB. CODE	MATERIAL	MEASURED AGE	$^{13}\text{C}/^{12}\text{C}$	CONVENTIONAL AGE	CALIBRATED (68% Probability) cal yr BP	CALIBRATED (95% Probability) cal yr BP
S3_P2-31/-14.794	Beta-364241	<i>Goniastrea</i>	7490 $\pm$ 30 BP	+1.3 ‰	7920 $\pm$ 30 BP	8360 - 8300	8390 - 8270
S3_P2-28/-6.387	Beta-361585	<i>Galaxea</i>	1980 $\pm$ 30 BP	-1.7 ‰	2360 $\pm$ 30 BP	1950 - 1860	1990 - 1820
S3_P2-27/-7.337	Beta-361584	<i>Porites</i>	2430 $\pm$ 30 BP	-0.6 ‰	2830 $\pm$ 30 BP	2590 - 2580	2660 - 2340
S3_P2-26/-8.757	Beta-361583	<i>Porites</i>	2920 $\pm$ 30 BP	+0.2 ‰	3330 $\pm$ 30 BP	3160 - 3050	3210 - 2980
S3_P225/-10.667	Beta-361582	<i>Porites</i>	3490 $\pm$ 30 BP	-2.4 ‰	3860 $\pm$ 30 BP	3810 - 3680	3840 - 3630
S3_P2-24/-12.177	Beta-361581	<i>Porites</i>	4430 $\pm$ 30 BP	-1.5 ‰	4820 $\pm$ 30 BP	5040 - 4950	5190 - 5140
S2_P1-13/-5.737	Beta-361580	<i>Porites</i>	2530 $\pm$ 30 BP	-0.7 ‰	2930 $\pm$ 30 BP	2700 - 2640	2720 - 2510
S2_P1-12/-5.377	Beta-361579	<i>Porites</i>	2920 $\pm$ 30 BP	-0.1 ‰	3330 $\pm$ 30 BP	3160 - 3050	3210 - 2980
S2_P1-11/-6.447	Beta-361578	<i>Montastrea</i>	2980 $\pm$ 30 BP	-1.2 ‰	3370 $\pm$ 30 BP	3210 - 3110	3260 - 3050
S2_P1-10/-8.357	Beta-361577	<i>Cyphastrea</i>	3170 $\pm$ 30 BP	-1.4 ‰	3560 $\pm$ 30 BP	3420 - 3340	3450 - 3310
S2_P2-09/-9.956	Beta-364239	<i>Porites</i>	4780 $\pm$ 30 BP	-1.0 ‰	4010 $\pm$ 30 BP	3970 - 3880	4060 - 3830
S2_P2-08/-12.23	Beta-364238	<i>Porites</i>	3172 $\pm$ 30 BP	-1.9 ‰	5160 $\pm$ 30 BP	5520 - 5430	5560 - 5320
S2_P1-07/-14.257	Beta-361576	<i>Porites</i>	7150 $\pm$ 30 BP	-3.1 ‰	7510 $\pm$ 30 BP	7940 - 7870	7970 - 7830
S2_P1-06/-16.087	Beta-361575	<i>Porites</i>	7320 $\pm$ 30 BP	-3.4 ‰	7670 $\pm$ 30 BP	8120 - 8000	8150 - 7970
S2_P1-05/-16.617	Beta-361574	<i>Lepastrea</i>	7650 $\pm$ 40 BP	-1.0 ‰	8040 $\pm$ 40 BP	8490 - 8380	8540 - 8350
S2_P1-04/-18.087	Beta-361573	<i>Goniastrea</i>	8040 $\pm$ 50 BP	-1.1 ‰	8430 $\pm$ 50 BP	9000 - 8940	9070 - 8840
S2_P1-03/-22.088	Beta-385986	<i>Coral</i>	> 43500 BP	-4.4 ‰			
S3_P2-30/-18.163	Beta-385987	<i>Coral</i>	> 43500 BP	-4.9 ‰			

All samples were dated at the Beta Analytic Inc. Miami, Florida USA

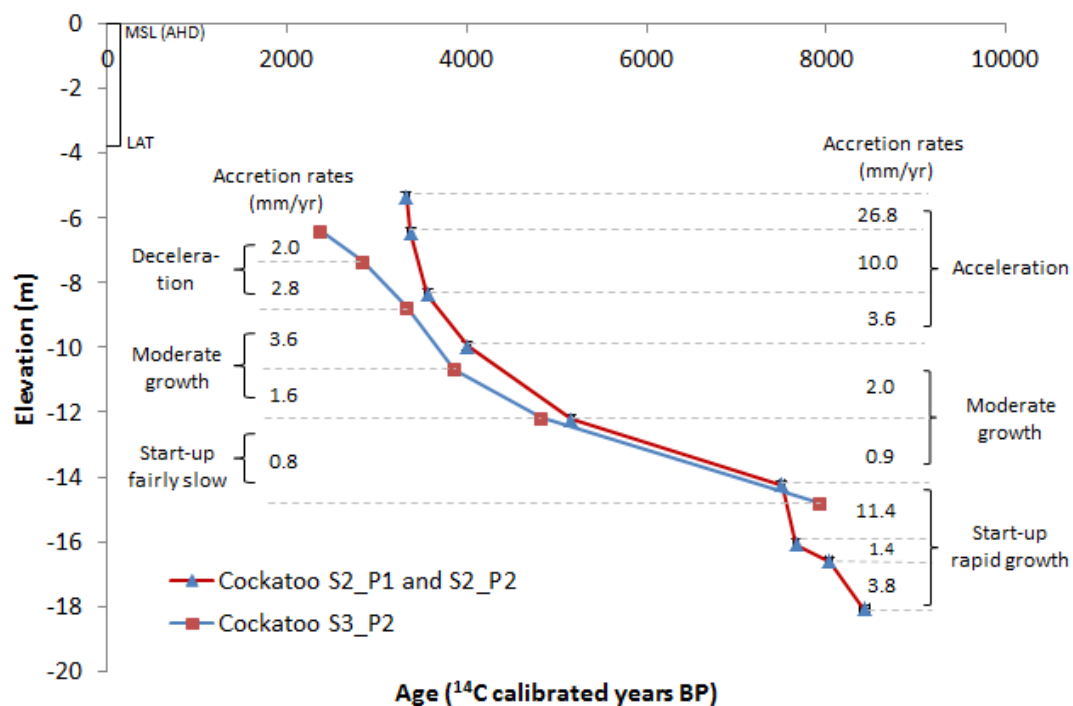


Figure 3.6 Holocene vertical reef accretion and accretion history curve for Cockatoo Island sections S2\_P1, S2\_P2, and S3\_P2.

Reef accretion records from the Abrolhos, Scott Reef, Middle Reef (GBR) and now Cockatoo Island are shown in Fig. 3.7. While the Abrolhos record exhibits a keep-up accretion history closely following sea-level, reef accretion data from Cockatoo suggest it grew in a catch-up phase for most of its accretion history. A lack of subsidence since the LIG and presence of a late Holocene highstand in SW Australian reefs (below 22 degrees south) contrasts with the Kimberley where no late Holocene highstand has been recorded to date, whilst there has been significant post-LIG subsidence at Cockatoo and Scott Reefs (Collins et al., 2011).

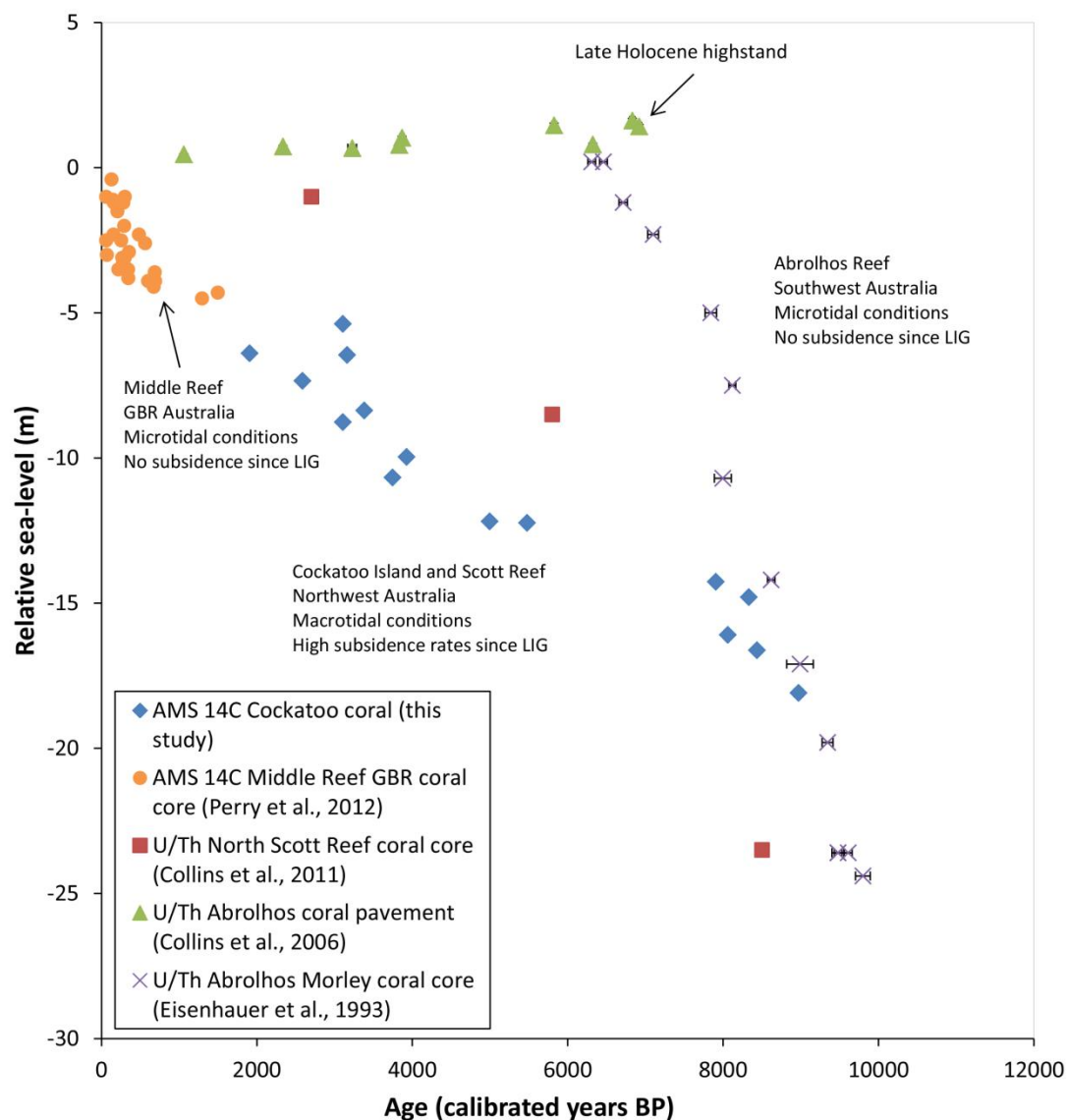


Figure 3.7 Composite accretion history records for Kimberley region and GBR derived from coral sections at Cockatoo Island (this study), coral in core from Middle Reef GBR (Perry et al., 2012), coral in core from North Scott Reef (Collins et al., 2011), cemented coral shingle pavement from Abrolhos reefs (Collins et al., 2006), and corals in core from Morley Island Abrolhos (Eisenhauer et al., 1993). Microtidal Abrolhos reefs from SW Australia lack subsidence since the LIG, in contrast with macrotidal Kimberley reefs with post-LIG subsidence. This is reflected in presence or absence of a Late Holocene highstand in the contrasting SL records. Abrolhos data for a keep-up reef; Kimberley data for catch-up reefs.

### 3.3.4 Reef Architecture and Seismic Structure

Boomer profiles immediately seaward of the logged pit profiles show the modern reef flat surface terminating in a steep ( $\pm 30^\circ$ ) forereef slope with a 20 m thick-bedded sediment mound to seaward (Fig. 3.8). Three subsurface units are apparent, separated by reflectors at 37 m below sea-level (bsl) and 40–45 m bsl.

Based on correlation with the logged sections, the seismic units correspond to the Holocene reef, the LIG reef and the Proterozoic bedrock. The Holocene reef is 15–20 m thick, with a flat upper surface at 8 m bsl, shallowing slightly to landward. The surface of the underlying LIG reef is irregular and has a distinct reef crest at 30 – 40 m (Fig. 3.9). A deeper unconformity with an average depth of 40 – 50 m marks the position of the Proterozoic rock foundation.

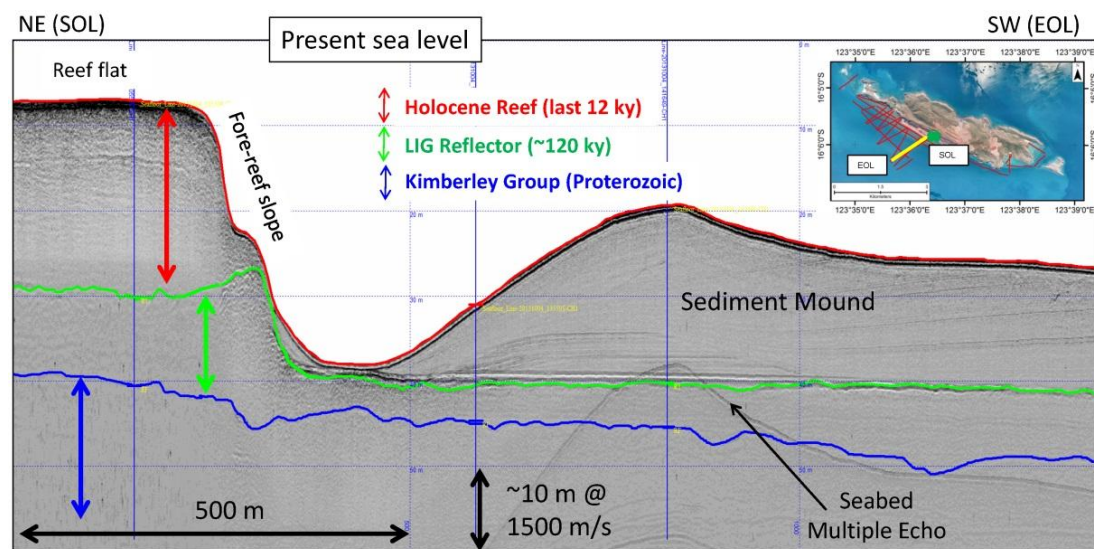


Figure 3.8 Southwest Cockatoo Island SBP cross section showing two stages of reef development; Holocene and Last Interglacial, with a clear correlation to the measured island sections. Unconformities are coloured. (Blue = top Proterozoic; Green = top Last Interglacial Reflector).

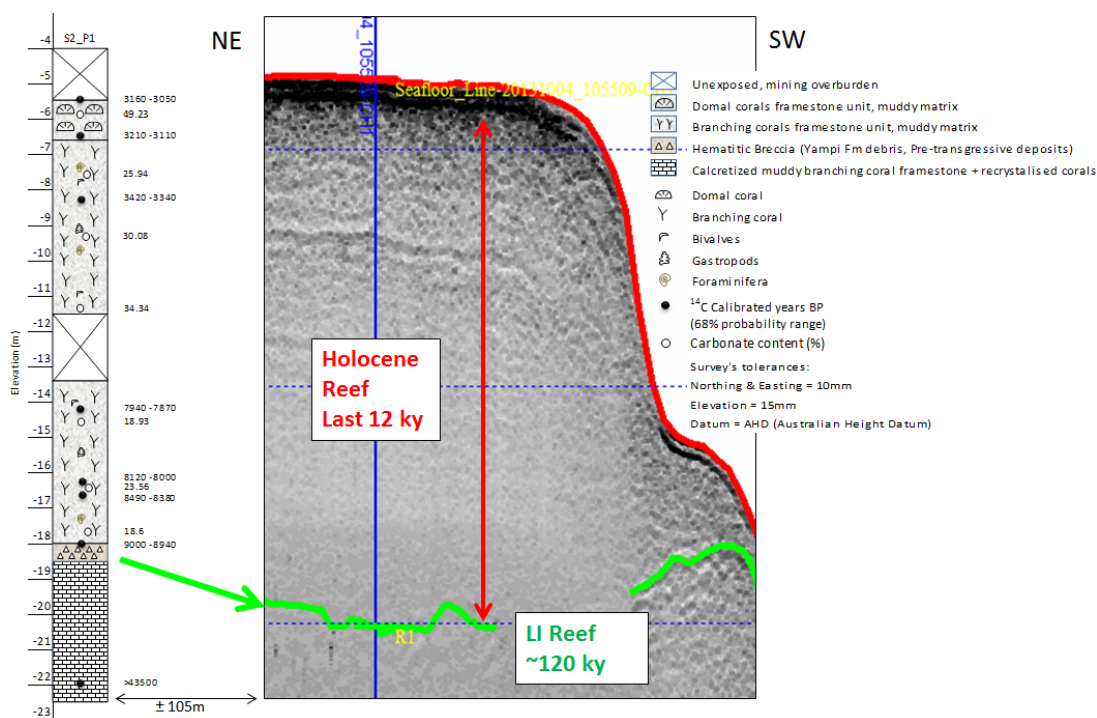


Figure 3.9 SBP line with superimposed core log from adjacent mine pit, showing correlation between SBP units and lithological units in the subsurface.

### 3.4 Discussion

#### 3.4.1 Evidence of neotectonic subsidence along the Kimberley Coast and offshore shelf

As a trailing, intraplate continental margin, coastal WA should be relatively tectonically stable. However, recent studies have identified seismic activity, and structural and geomorphological features consistent with ongoing crustal deformation (Sandiford 2003; Quigley et al., 2006, 2007). On the continental scale Sandiford (2007) and DeCaprio et al. (2009) have identified tilting of the Australian plate driven by changes in mantle convection, whereby eastern and northwestern Australia is experiencing subsidence and southern and southwestern Australia is experiencing uplift.

Evidence supporting this theory can be found in the relative elevation of LIG shorelines along the WA coast. Presently LIG reefs outcrop intermittently above present sea-level along a stretch of coast from Foul Bay (34°S) to Cape Keraudran (20° S) (O'Leary et al., 2008; 2013 and Collins et al., 1996). North of this line the

only occurrence of LIG reefs that has been observed is in bore holes from the shelf edge Scott Reef at an elevation of 36 to 60 m below AHD (Collins et al., 2011). Here we are able to provide the first evidence of a LIG reef from the Kimberley region, which outcrops at an elevation of 15 m below AHD. Although U-series analysis has not been carried out on this basal reef unit, the fact that corals exhibit a high degree of diagenetic alteration in contrast to the Holocene reef, and the Holocene and LIG reef are separated by a hematite breccia layer supports this interpretation.

Stratigraphic data from Cockatoo transects confirm that the LIG reef surface underlies the Holocene reef more broadly and exhibits reef terrace morphology. Assuming the LIG reef terrace reached base level the elevation would suggest a linear subsidence rate of around 0.12 m/ky since the LIG, this compares to a recent study which estimated subsidence rates at South and North Scott Reef on the Rowley Shelf margin as 0.45 m/ky and 0.29 m/ky respectively (Collins et al., 2011), where the shallowest LIG reef is at 36 m below AHD. Based on the proximal Cockatoo and distal Scott Reef subsidence data a subsidence with tilting offshore appears likely for the Kimberley coast and adjacent shelf.

### 3.4.2 Holocene reef accretion

Reef accretion on Cockatoo Island initiated around 9k cal yr BP at -18 m below AHD as evidenced from the radiocarbon ages from the basal Holocene corals. The timing of this event would suggest that corals became established not long after flooding of the antecedent substrate had occurred with sea-level transgressing the -20 m elevation at around 10k cal yr BP (Lambeck et al., 2010). Accretion curves plotted in Fig. 3.6 indicate the reef initially grew in a Keep-Up phase as shown by the high vertical accretion rates for this period. A reduction in reef accretion rate after 7.5k cal yr BP and a shift from Keep-Up to Catch-Up accretion phase likely resulted from the rapid deepening of the reef which became submerged to >10 m below AHD by ~7k cal yr BP before eventually reaching MLW (~4 m below AHD) at ~3,000 cal yr BP.

Palaeoecological and sedimentological evidence for a Catch-Up reef accretion includes the abundance of branching *Acropora* throughout the sequence and the predominance of a sandy mud matrix that becomes dominated by sand at the top, only becoming sandy at the top of the sequence. The absence of present-day

intertidal indicators such as *Porites cylindrica*, branching *Millepora*, tabular *Acropora* and coral micro atolls can also be considered to support a subtidal characterisation of the reef facies. However these indicators are also absent from the top of the logged profiles, when the reef had reached the intertidal zone. We conclude either that environmental or ecological conditions at the time did not suit the modern intertidal taxa, or that the modern coral community and zonation have only developed after prolonged intertidal exposure, and may therefore be restricted to a thin zone at the very top of the logged profiles which may not always show up in cross-section, or which we may have missed due to the seawall overburden.

As we currently lack any cross-reef age isochrons, we can only propose a reef accretion style, based on field observations supported by seismic profiles. The interpretation outlined above—of the reef initiating as a blanket and growing upward—is one possibility; another is that the reef initiated close to shore and prograded seaward. These alternatives correspond to models A and B respectively in Kennedy and Woodroffe's (2002) review of fringing reef accretion and morphology. We consider Kennedy and Woodroffe's more complex models C to F to be less likely analogs, due mainly to the apparently uniform internal structure of the Cockatoo reef in seismic profiles.

While we believe the vertical accretion model best represents our logged profiles, the reef further seaward may have become submerged too deeply to allow significant vertical accretion. On the modern reef, live coral cover is sharply reduced below about 10 m AHD and virtually absent below 20 m AHD, probably due to rapid light attenuation in the turbid water (Blakeway, 1997; Wilson et al., 2011). If this depth limit applied throughout the Holocene, only those areas submerged to less than ~10–15 m AHD are likely to have accreted vertically to sea-level, while deeper areas may have drowned before eventually being prograded over by the shallow reef (c.f. Hopley and Partain, 1986). Live coral cover on the shallow reef was probably relatively high throughout the vertical accretion phase. The baffling effect of the coral framework would have trapped suspended sediment, depositing the grey-green interstitial mud seen in cross-section. Tropical cyclones must have intermittently affected the reef, and are perhaps the main agent responsible for its detrital reef fabric (c.f. Braithwaite et al., 2000). When the reef reached sea-level, which probably first occurred at or near the rocky shore, surface sediments would have become



coarser due to wave winnowing, the zone of high coral density would have retracted seaward, and the characteristic community makeup of the current intertidal reef flat would have begun to develop. Eventually the reef attained its present state, with vertical accretion essentially ceased but progradation continuing through *in situ* accretion of branching *Acropora* colonies on the upper slope and deposition of *Acropora* fragments on the lower slope.

The typical sub-bottom profile of the reef shows a steep forereef slope unconformably overlying the LIG reef surface at 37 m. A further unconformity marks the boundaries between LIG reef and Proterozoic rock foundation underneath at a depth of 40 – 50 m. A 15 – 20 m Holocene reef build-up overlies consistently LIG reef at 37 – 40 m. This is in accordance with the stratigraphy examined at the adjacent mine-pit with the exception that the Holocene reef is thicker to seaward.

### 3.4.3 Comparisons with other Holocene Reef Systems

The Cockatoo Island reef conforms reasonably well to the ‘arborescent coral facies’ description in Montaggioni’s (2005) Indo-Pacific reef classification scheme. It differs from the typical arborescent coral reef in a couple of respects which probably reflect the reef’s environmental setting, particularly the high turbidity and high terrigenous input. Firstly, the mud matrix is more pervasive at Cockatoo Island than in most arborescent coral reefs. As mentioned earlier we attribute this to high suspended sediment loads being baffled by the coral framework. Secondly, live branching coral (virtually all *Acropora*) on the modern Cockatoo Island reef occurs solely on the upper fore-reef between 4 and 10 m below AHD, whereas on other Indo-Pacific reefs it typically occurs on mid and lower fore-reef slopes to approximately 20 m, and also on shallow inner reef flats and back-reef slopes (Montaggioni, 2005; Hopley et al., 2007). The compressed shallow subtidal distribution of branching *Acropora* at Cockatoo Island is probably a function of a) the low hydrodynamic energy, which allows it to grow undamaged in shallow water (at least during fair-weather conditions), b) the high turbidity, which sets the lower depth limit through light attenuation and possibly also sedimentation stress, and c) their low tolerance to subaerial exposure, which excludes them from the reef flat. Within their optimal 4 to 10 m depth range at Cockatoo Island, branching corals are

prolific and seem able to competitively exclude (i.e. outgrow) all other coral types. The restriction of *Porites cylindrica* and branching *Millepora* to the intertidal zone may be a consequence of this competitive exclusion, as both would normally extend into subtidal habitat (Veron, 2000; Glynn and de Weerd, 1991).

The Cockatoo fringing reef shares several similarities with the nearshore turbid zone reefs of the GBR. Browne et al. (2012) describe reefs within 20 km of the Queensland coast influenced by episodic terrigenous sediment input, and fluctuating salinities (24–36 ppt). Table 3.2 compares the inshore GBR systems with the Cockatoo fringing reef. With the exception of the greater tidal range at Cockatoo, both have a similar oceanographic setting with significant sediment influx, sediment-tolerant corals, high coral cover, a significant proportion of *in situ* coral framework, and a mud-dominated matrix (coarsening at the top of the sequence). Differences include the hard foundation of the Cockatoo fringing reef versus the sand and gravel substrates of the GBR reefs, the greater age and thickness of the Cockatoo fringing reef, the higher proportion of detrital branching *Acropora* in the Cockatoo reef, and an apparently more sharply-defined coral depth zonation on the modern Cockatoo Island reef.

The overall mean accretion rate of the Cockatoo Island reef is ~2 mm/yr, significantly lower than most turbid zone GBR reefs. However, the mean rate at Cockatoo Island includes approximately 2,000 years of slow accretion when we infer the reef was deeply submerged. Accretion rates in the lowermost and uppermost few metres of the Cockatoo section, when the reef was probably submerged to the depth at which the GBR reefs have developed ( $\leq 5$  m), are approximately equivalent to the mean rate of 8.4 mm/yr recorded at Middle Reef, the fastest-growing of the cored turbid zone GBR reefs. These accretion rates are high in a global context and are only exceeded by a handful of reefs, generally within the aborescent or detrital categories (Perry et al., 2012; Montaggioni, 2005). Perry et al. (2012) attribute Middle Reef's rapid accretion to the deposition of fine-grained terrigenous sediments that are suspended from the surrounding seafloor or introduced during major floods. The fine-grained sediment infills the open reef fabric and inhibits post depositional skeletal destruction, thus aiding primary framework preservation and reef accretion. The Cockatoo fringing reef appears to have developed in a very similar way, with

only a few deviations from Perry et al.'s model, including the predominance of detrital fabric instead of *in situ* framework.

There are strong contrasts between the nearshore Cockatoo reef and the offshore reefs of the Oceanic Shoals Biozone located ~300 km to the northwest including Scott Reef (Fig. 3.1) which rise from depths of 400 m, in cyclone and swell wave exposed and clear water settings. These reefs are atoll like, dominated by coral framework with sandy calcareous intercalations, with earlier Holocene reef onset ages (e.g. 11.5 ka for Scott Reef; Collins et al., 2011) and higher subsidence rates.

Table 3.2 Summary of characteristics of turbid reefs from the GBR (after Browne et al., 2012) and the Cockatoo fringing reef (this study).

Environmental controls	Inshore turbid reefs on the GBR (Browne et al., 2012)		Inshore turbid reefs at Cockatoo Island (this study)	
	Typical condition	Description	Typical condition	Description
Oceanography	Locally wind driven waves	Lack of coralline algae and robust <i>Acropora</i> communities, lack of oceanic swell	Strong tidal currents generated by high tidal range Low swell waves	Domal and robust-branching coral, coral rubble coralline algae exist on the contemporary reef surface
Fine-grained sediment load	High levels of sedimentation and turbidity	Sedimentation rate > 10mg/cm <sup>2</sup> /day and turbidity levels from <10 mg/L to >50 mg/L	Intermittent high turbidity	Background turbidity is 1-2 NTU, and high turbidity is event-related
Reef initiation	Holocene	6000 - 1000 yBP	Holocene	9,000 yBP
Substrate availability	mixed	Sediment deposits on shallow coastal embayment are the most common substrates for reef accretion	Lithified pre-existing reef, or Proterozoic metasediments are common substrates.	Most reefs develop on the LI reef with/without pre-transgressive deposits
Average rate of reef accretion	Variable	2-7 mm/yr	Variable	2.16 - 7.4 mm/yr
Mode of accretion	Mixed	Reefal foundations, terrigenous sand and rubble	Mixed	Reefal foundations, sand/silt matrix, coral rubble
Surrounding bathymetry	Shallow water (<15 m)	Reef accretion restricted by shallow, turbid waters	Shallow water (<20-40 m)	Reefs occur down to 15 m depth with a sharp foreereef slope and sand/silt sediment mound to seaward
Sea-level		Strongly influence high level wind driven suspended sediment, substrate availability and reef morphology	Rising Holocene sea-levels have influenced reef accretion	Plays a major role in reef development

Composition	Variable to low coral diversity	100-150 species Many inshore reefs have diverse coral communities, but many are also dominated by physiologically robust corals which may be more tolerant to change	Moderate biodiversity	17 coral genera are identified with the most common community and facies association being of branching corals (especially of the genera <i>Acropora</i> ) and domal corals including <i>Porites</i>
Community age structure	Low coralline algae cover  Mixed to older     Low recruitment and survival rates	<1% cover on the GBR  Many inshore reef characterised by large, older coral colonies which are capable of tolerating high sediment loads  Less suitable substrate availability due to high sediment cover and high level of algal competition. High sediment loads can affect the survival of coral juveniles	Low coralline algae cover	Specialised fauna capable of tolerating high sediment loads

### 3.5 Conclusions

This study provides the first information on Holocene reef accretion for a nearshore reef of the Kimberley Biozone.

- The Cockatoo fringing reef initiated on lithified Pleistocene substrates at approximately 9,000 cal yr BP and accreted in a catch-up mode, first reaching sea-level at approximately 3,000 cal yr BP. The predominance of fast-growing branching *Acropora*, and the high rate of mud deposition, produced very rapid reef accretion in the upper and lower few metres of the sequence, when the reef surface was probably  $\leq 5$  m deep.
- A knowledge of the reef's foundations also leads to a calculated subsidence rate of the coastal Kimberley since Last Interglacial time of 0.12 m/ky.
- Like Scott Reef of the Oceanic Shoals Biozone to seaward, the Holocene reef at Cockatoo Island lacks evidence of the Late Holocene highstand that characterises coral reefs of the tectonically stable microtidal southwest Australian coast. Macrotidal conditions and coastal subsidence may have obscured such records, although further data from the Kimberley are needed to evaluate this conclusion.

Whilst accretion rates of the Cockatoo reef fall into the Montaggioni (2005) “fast to moderate growing reef” category of Indo-Pacific reefs, a direct comparison with turbid reefs of the GBR is more appropriate given both systems are muddy in character, and similar accretion rates are recorded for the two systems which contrast with the mainly clear water reefs studied by Montaggioni.

- Whilst the GBR and Cockatoo turbid reefs show broad similarities, one contrast is between palaeoecological and contemporary reef communities, which are similar in the GBR but distinctly different at Cockatoo Island. A likely explanation is that the modern Cockatoo community needs to adapt to manage the extreme conditions of currents, mud from slack water suspension fallout, and prolonged exposure due to macrotidal conditions, in contrast to more stable reef accretion in catch up mode earlier in the Holocene.
- A potential analogue for the Holocene palaeoenvironment of muddy branching *Acropora* is provided by the contemporary shallow subtidal reef slope, which is the only habitat where live branching *Acropora* occur at

present. The contemporary intertidal environment is characterised by abundant *Porites cylindrica* and *Millepora intricata*, both absent from the Holocene.

- The muddy framework facies recorded at Cockatoo Island are in keeping with the turbid macrotidal conditions, whilst contrasting with the off shore sand Kimberley reefs.

The Cockatoo reef accretion pattern suggests that the Kimberley near-shore reefs may be more resilient to periodic disturbance and the effects from terrestrial runoff than reefs elsewhere. Further, the study shows that reef response to climate is resilience through time. As such the information presented here should be taken into consideration when planning and siting Marine Parks.

### Acknowledgements

The Kimberley Reef Geomorphology Project 1.3.1 is funded by the Western Australian State Government and partners of the Western Australian Marine Science Institution. This research was assisted by the Dambimangari people through their advice and consent to access their traditional lands. Pluton Resources (particularly Jeremy Bower and Anson Griffith) are thanked for providing access to parts of their Cockatoo Island Mining Tenement and for logistic support during the study. The Cygnet Bay Marine Research Station provided vessel support for marine operations and access to research facilities at Cygnet Bay. James Brown assisted in the planning stage of the project, and Erin McGinty capably managed marine operations. MScience is thanked for providing access to marine video of the reef. Giada Bufarale (seismic data acquisition), Moataz Kordi (remote sensing) and Alexandra Stevens (editing and improvement of drafts) at Curtin University were valued members of the research team. Finally, it must be noted that this research was completed in an area where the Traditional Owners have a rich cultural history of climate, land and environment based on thousands of years of habitation. It is important to consider that broad understanding alongside the modern science completed here.

## References

- Blakeway, D. (1997). Scleractinian corals and reef development, part 9. In: Walker, D. (ed.), Marine biological survey of the central Kimberley coast, Western Australia. Perth: University of Western Australia. Unpublished report, W.A. Museum Library No. UR377, 77–85.
- Braithwaite, C. J. R., Montaggioni, L. F., Camoin, G. F., Dalmaso, H., Dullo, W. C., Mangini, A. (2000). Origins and development of Holocene coral reefs: a revisited model based on reef boreholes in the Seychelles. *Indian Ocean. International Journal of Earth Science*, 89, 431–445.
- Brooke, B. (1997). Geomorphology of the north Kimberley coast, part 9. In: Walker, D. (ed.), Marine biological survey of the central Kimberley coast. Western Australia. University of Western Australia, Perth, unpublished report, W.A. Museum Library No. UR377, pp. 13–39.
- Browne, N. K., Smithers, S. G. (2012). Coral reefs of the turbid inner-shelf of the Great Barrier Reef, Australia: An environmental and geomorphic perspective on their occurrence, composition and accretion. *Earth Science Reviews*, 115(1–2), 1–20.
- Chin, A., Sweatman, H., Forbes, S., Perks, H., Walker, R., Jones, G., Williamson, D., Evans, R., Hartley, F., Armstrong, S., Malcolm, H., Edgar, G. (2008). Status of the Coral Reefs in Australia and Papua New Guinea. In: Wilkinson, C. (ed), *Status of Coral Reefs of the World*. Global Coral Reef Monitoring Network. Reef and Rainforest Research Centre, pp. 159–176.
- Collins, L. B. (2002). Tertiary Foundation and Quaternary Evolution of Coral Reef Systems of Australia's North West Shelf. In: Keep, M., Moss, S. J. (ed), *Proceeding of the Petroleum Exploration Society of Australia Symposium*, Perth, WA, pp. 129–152.
- Collins, L. B., Zhao, J. X., Freeman, H. (2006). A high-precision record of mid–late Holocene sea-level events from emergent coral pavements in the Houtman Abrolhos Islands, southwest Australia. *Quaternary International*, 145–146(0), 78–85.



- Collins, L. B., Zhu, Z. R., Wyrwoll, K. H. (1996). The structure of the Easter Platform, Houtman Abrolhos reefs: Pleistocene foundations and Holocene reef accretion. *Marine Geology*, 135(1–4), 1–13.
- Collins, L. B., Testa, V., Zhao, J., Qu, D. (2011). Holocene accretion history and evolution of the Scott Reef carbonate platform and coral reef. *Journal of the Royal Society of Western Australia*, 94(2), 239–250.
- DeCaprio, L., Gurnis, M., Mueller, R. D. (2009). Long-wavelength tilting of the Australian continent since the Late Cretaceous. *Earth and Planetary Science Letters*, 278(3–4), 175–185.
- Department of the Environment, Water, Heritage and the Arts, DEWHA (2008). A Characterisation of the Marine Environment of the North-west Marine Region: Perth Workshop Report, A Summary of an Expert Workshop Convened in Perth, Western Australia, 5–6 September 2007, Commonwealth of Australia, Hobart.
- Embry, A. F., Klovan, J. E. (1971). A late Devonian reef tract on northeastern Banks Island, N.W.T. *Bulletin of Canadian Petroleum Geology*, 19(4), 730–781.
- Eisenhauer, Wasserburg, A. G. J., Eisenhauer, A., Chen, J.H., Bonani, G., Collins, L.B., Zhu, Z. R., Wyrwoll, K. H. (1993). Holocene sea-level determination relative to the Australian continent: U/Th (TIMS) and <sup>14</sup>C (AMS) dating of coral cores from the Abrolhos Islands. *Earth and Planetary Science Letters*, 114(4), 529–547.
- Government of Western Australia (2011). Kimberley Science and Conservation Strategy. Department of Environment and Conservation, Kensington, Perth.
- Glynn, P., de Weerd, W. H. (1991). Elimination of two reef building hydrocorals following the 1982–83 El Niño warming event. *Science*, 253, 69–71.
- Griffin, T. J., Grey, K. (1990). Kimberley Basin. In: Memoir 3, Geology and Mineral Resources of Western Australia. Perth, Geological Survey of Western Australia, 293–304.

- Harris, P. J., Baker, E. K., Cole, A. R. (1991). Physical sedimentology of the Australian continental shelf with emphasis on Late Quaternary deposits in major shipping channels, port approaches and choke points. University of Sydney, Ocean Sciences Institute, Report 51.
- Hopley, D., Partain, B. (1986). The structure and development of fringing reefs of the Great Barrier Reef Province, in: Baldwin, C. L. (ed.), *Fringing Reef Workshop: Science, Industry and Management*. Great Barrier Reef Marine Park Authority, Townsville, 13–33.
- Hopley, D., Smithers, S., Parnell, K. (2007). *The Geomorphology of the Great Barrier Reef: Development, diversity, change*. Cambridge University Press, Cambridge, UK.
- Kennedy, D. M., Woodroffe, C. D. (2002). Fringing reef accretion and morphology: a review. *Earth Science Review*, 57, 255–277.
- Lough, J. M. (1998). Coastal climate of northwest Australia and comparisons with the Great Barrier Reef: 1960 to 1992. *Coral Reefs*, 17(4), 351–367.
- Lambeck, K., Woodroffe, C. D., Antonioli, F., Anzidei, M., Gehrels, W.R., Laborel, J., Wright, A. J. (2010). Paleoenvironmental records, geophysical modelling, and reconstruction of sea-level trends and variability on centennial and longer timescales, in: Church, J.A., Woodworth, P.L., Aarup, T., Wilson, W.S. (ed.), *Understanding Sea-level Rise and Variability*. Blackwell Publishing Ltd, 61–121.
- Montaggioni, L. F. (2005). History of Indo-Pacific coral reef systems since the last glaciation: Development patterns and controlling factors. *Earth-Science Reviews*, 71(1-2), 1–75.
- Müller, G., Gastner, M. (1971). The 'Karbonat-Bombe', a simple device for the determination of carbonate content in sediment, soils, and other materials. *Neues Jahrbuch für Mineralogie-Monatshefte* 10, 466–469.
- O’Leary, M. J., Hearty, P. J., McCulloch, M. T. (2008). U-series evidence for widespread reef development in Shark Bay during the last interglacial. *Palaeogeography, Palaeoclimatology, Palaeoecology*, 259, 424.

- O'Leary, M., Hearty, P. J., Thompson, W. G., Raymo, M. E., Mitrovica, J. X., Webster, J. M. (2013). Ice sheet collapse following a prolonged period of stable sea-level during the last interglacial. *Nature Geoscience*, 6(9), 796–800.
- Perry, C. T., Smithers, S. G., Gulliver, P., Browne, N. K. (2012). Evidence of very rapid reef accretion and reef accretion under high turbidity and terrigenous sedimentation. *Geology*, 40(8), 719–722.
- Purcell, S. P. (2002). Intertidal reefs under extreme tidal flux in Buccaneer Archipelago, Western Australia. *Coral Reefs*, 21(2), 191–192.
- Quigley, M. C., Cupper, M. L., Sandiford, M. (2006). Quaternary faults of south-central Australia: Palaeoseismicity, slip rates and origin. *Australian Journal of Earth Sciences*, 53(2), 285–301.
- Quigley, M. C., Sandiford, M., Cupper, M. L. (2007). Distinguishing tectonic from climatic controls on range-front sedimentation. *Basin Research*, 19(4), 491–505.
- Sandiford, M. (2003). Neotectonics of southeastern Australia: linking the Quaternary faulting record with seismicity and in situ stress. In: Hillis, R. R., Muller, D. (ed.), *Evolution and Dynamics of the Australian Plate*. Geological Society of Australia Special Publication, 22, 101–113.
- Sandiford, M. (2007). The tilting continent: A new constraint on the dynamic topographic field from Australia. *Earth and Planetary Science Letters*, 261(1-2), 152–163.
- Short, A. D. (2011). Kimberley beach and barrier systems: An overview. *Journal of the Royal Society of Western Australia*, 94(2), 121–132.
- Veron, J. E. N. (2000). Corals of the world. Australian Institute of Marine Science 1-3, 1,382 pp.
- Wilson, B. R. (2013). The Biogeography of the Australian North West Shelf: Environmental Change and life's response. Elsevier, Burlington MA, USA.
- Wilson, B. R., Blake, S., Ryan, D., Hacker, J. (2011). Reconnaissance of species-rich coral reefs in a muddy, macro-tidal, enclosed embayment, Talbot Bay,

- Kimberley, Western Australia. *Journal of the Royal Society of Western Australia*, 94(2), 251–265.
- Wolanski, E., Spagnol, S., 2003. Dynamics of the turbidity maximum in King Sound, tropical Western Australia. *Estuarine, Coastal and Shelf Science*, 56(5–6), 877–890.
- Wright, R. L., 1964. Geomorphology of the West Kimberley Area. CSIRO Land Research, Series 9, 103–118.

## Chapter 4

### **Holocene reef evolution in a macrotidal setting: Buccaneer Archipelago, Kimberley Bioregion, Northwest Australia**

Tubagus Solihuddin<sup>1,2,\*</sup>, Michael J. O' Leary<sup>2,3</sup>, David Blakeway<sup>4</sup>, Iain Parnum<sup>5</sup>,  
Moataz Kordi<sup>1,2</sup>, Lindsay B. Collins<sup>1,2</sup>

<sup>1</sup> Department of Applied Geology, Curtin University, Bentley, WA 6102

<sup>2</sup> The Western Australian Marine Science Institution, Floreat, Australia, 6014

<sup>3</sup> Department of Environment and Agriculture, Curtin University, Bentley, WA 6102

<sup>4</sup> Fathom 5 Marine Research, 17 Staines Street, Lathlain, WA 6100

<sup>5</sup> [Centre for Marine Science and Technology](#), Curtin University, Bentley, WA 6102

#### **Abstract**

This study uses information derived from cores to describe the Holocene accretion history of coral reefs in the macrotidal (up to 11 m tidal range) Buccaneer Archipelago of the southern Kimberley coast, Western Australia. The internal architecture of all cored reefs is broadly similar, constituting well-preserved detrital coral fragments, predominantly branching *Acropora*, in a poorly sorted sandy mud matrix. However, once the reefs reach sea-level, they diverge into two types: low intertidal reefs that maintain their detrital character and develop relatively narrow, horizontal or gently sloping reef flats at approximately mean low water spring (MLWS), and high intertidal reefs that develop broad coralline algal-dominated reef flats at elevations between mean low water neap (MLWN) and mean high water neap (MHWN). The high intertidal reefs develop where strong, ebb dominated, tidal asymmetry retains seawater over the low tide and allows continued accretion. Both reef types are ultimately constrained by sea-level but differ in elevation by 3 to 4 m.

**Keywords:** Reef geomorphology, Holocene reef accretion, Sea-level, Rhodoliths, Coralline algal reefs

\*Corresponding author: e-mail at: Department of Applied Geology, Curtin University, Bentley, WA 6102, Australia. Tel.: +61 8 9266 3710.

E-mail address: [tubagus.solihuddin@postgrad.curtin.edu.au](mailto:tubagus.solihuddin@postgrad.curtin.edu.au) (T. Solihuddin)

## 4.1 Introduction

Advances in our understanding of the post-glacial evolution of coral reefs throughout the Indo-Pacific and Caribbean regions have come mainly through knowledge gained by reef coring, beginning with Ladd et al. (1953) whose drilling on Eniwetok Atoll encountered basalt basement at a depth of 1.4 km, lending support to Darwin's (1842) theory of atoll island evolution. A number of more recent review papers and books (e.g., Kennedy and Woodroffe, 2002; Montaggioni, 2005; Hopley et al., 2007) have described particular reef development patterns based on the timing of Holocene reef initiation, rates and modes of reef accretion, and reef facies associations. These same reviews also highlighted a number of factors controlling reef accretion, including sea-level, tectonics, antecedent topography, sea surface temperatures and salinities, nutrient, light and turbidity levels, aragonite saturation, hydrodynamic energy and substrate availability. Despite the number of factors controlling reef accretion, most reefs exist within a fairly narrow range of physiochemical parameters and can, therefore, be classified and categorized according to a small range of sedimentary facies, accretionary styles, and geomorphic typologies. Here, we investigate reef development and evolution within a region where one environmental variable, tidal range, significantly exceeds that of typical reefs.

The Buccaneer Archipelago located on Western Australia's Kimberley coast experiences a macrotidal tidal range of up to 11 m, which is the largest recorded in any tropical region. In addition to the extreme tidal range, the Buccaneer Archipelago is subject to strong currents, frequent cyclones and elevated turbidity. Despite these seemingly challenging environmental conditions, the region is known for its extensive and diverse coral reefs. Teichert and Fairbridge (1948) discuss the profusion of reefs in the Kimberley region, Brooke (1997) and Blakeway (1997) depict substantial (hypothetical) reef framework cross-sections, and Wilson et al. (2011) infer significant accumulations of coral framework in Talbot Bay. However,

the true extent of reef framework development in the Kimberley was unknown until Solihuddin et al. (2015) described the Holocene development of a sheltered fringing reef at Cockatoo Island in the Kimberley. An open cut iron ore pit on the southwestern side of the island has exposed a complete 15–20 m thick Holocene reef sequence resting atop an older Pleistocene reef surface. Radiocarbon dating showed that reef initiation at Cockatoo Island occurred around 9,000 calibrated years before present (cal yr BP), soon after the post-glacial flooding of the antecedent substrate, and accreted in catch-up mode (*sensu* Neumann and Macintyre, 1985), reaching sea-level by approximately 3,000 cal yr BP.

The presence of a thick reef framework at Cockatoo Island raises broader questions around Holocene reef development in the Kimberley including: 1) what was the timing of reef “turn on” (*sensu* Buddemeier and Hopley, 1988) and does this vary regionally; 2) what was the accretionary style and how does this compare to other reef systems; and 3) how do coral reef facies reflect changing accretionary patterns or environmental stressors?

To address these questions, we conducted a systematic coring program from selected inshore reefs in the Buccaneer Archipelago, including Tallon Island, Sunday Island, and Irvine/Bathurst Islands, and performed sedimentary, palaeoecological and chronostratigraphic analyses on recovered cores.

## **4.2 Regional setting**

### **4.2.1 Geology**

The Buccaneer Archipelago is located between latitudes 16.0°S and 16.4°S in the southern Kimberley region of northwestern Australia (Fig. 4.1). The archipelago is the seaward extension of the King Leopold Orogen, which consists of highly metamorphosed, strongly folded, faulted, and eroded Proterozoic rocks of the Kimberley Group (Bruschweiler, 1957; Griffin and Grey, 1990). A strong regional-scale northwest–southeast foliation has resulted in a deeply incised ria coast with more than 700 inshore islands, almost all of which are uninhabited and many unnamed. These islands represent the drowned remnants of a broad, structurally controlled peneplain (Wilson, 2013).

### 4.2.2 Tides

The Buccaneer Archipelago has a semidiurnal macrotidal regime with spring tides ranging between 8 and 11 m. The complex bathymetry, embayed coast and numerous islands result in very strong and turbulent tidal flows, in some areas scouring the seabed and producing high levels of turbidity. Narrow passages between islands and inlets give rise to waterfall effects whereby water piles up on one side of an inlet as the tide falls faster than the water can drain through the pass (e.g., Horizontal Falls, Talbot Bay). The rapidly falling tide also results in impounding of water on raised reef flats which then cascades over the forereef crest and slope (Richards and O’Leary, 2015; Lowe and Falter, 2015).

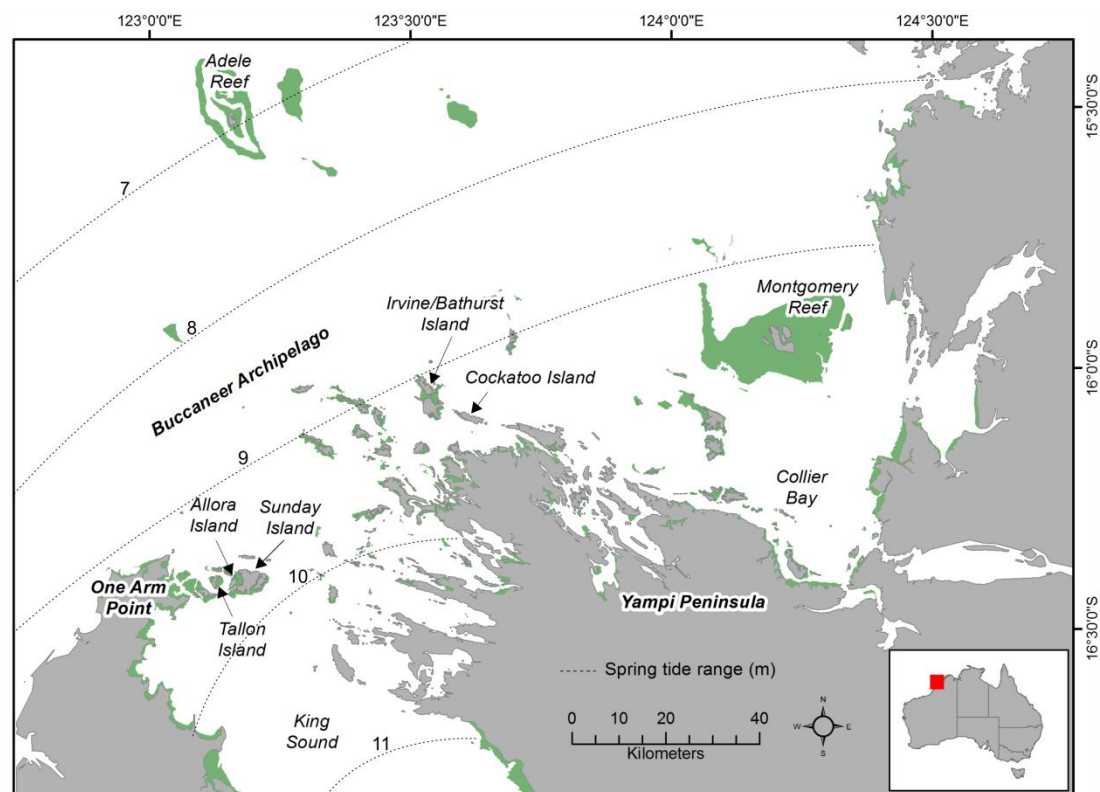


Figure 4.1 Map of the study area in the Buccaneer Archipelago. The green shading indicates reef habitat. Locations of the three study sites and surrounding islands are indicated by arrows.



### 4.2.3 Oceanography

Sea surface temperatures reach 22 to 28°C inshore and 17 to 27°C offshore (Pearce and Griffiths, 1991). The climate is semi-arid monsoonal, with pronounced ‘wet’ summers and ‘dry’ winters. Tropical monsoonal storms between November and April produce intense rainfall with an annual average from approximately 800 mm in the west to 1500 mm in the central and east Kimberley, whereas the dry season from May to September brings warm temperatures and low humidity (DEWHA, 2008). Nutrient concentrations in the inshore Kimberley waters are relatively high, influenced by riverine inputs from the adjacent terrestrial, high runoff catchments (Wilson, 2013). The region is prone to cyclones, experiencing approximately three per year (Lough, 1998) and has a prevailing southwest swell (Pearce and Griffiths, 1991).

## 4.3 Material and methods

### 4.3.1 Multibeam

Reef elevation was measured through a multibeam echo-sounder survey. The depth below the vessel was measured using an Odom ES3 multibeam echo-sounder, which was combined with a Valeport sound velocimeter, a TSS 355B motion sensor and an iX Blue Octans gyro compass, and elevation was measured using Trimble Net R9 using RTX satellite subscription ( $\pm 2$  cm). Data were acquired and processed using QPS QINSy software (ver 8.10). Longitude and latitude were calculated relative to the Geocentric Datum of Australia 1994 (GDA 94) and elevation relative to the Australian Height Datum (*AUSGeoid09*). The processed data were gridded to either 0.5 or 1 m<sup>2</sup> and imported into MATLAB (ver 2013B) where a probability distribution was derived empirically for each site using the ‘ksdensity’ function.

### 4.3.2 Reef coring

A total of forty-two reef cores were collected from Tallon Island, Sunday Island, and Irvine/Bathurst Islands (Fig. 4.1). Coring sites were selected to support the interpretation of previously surveyed sub-bottom profile survey data (Collins et al., 2015) and to ensure a spatially representative record of reef accretion. Cores were

obtained by percussion coring and rotary drilling. Percussion coring was used where reef flats consisted of open framework and unconsolidated reef sediments. A 6.5-m long, 80-mm wide aluminium tube with 3 mm wall thickness was hammered into the reef using either a manual slide hammer or hydraulic powered post driver. Coralline algal reef was sampled by rotary coring, using a handheld hydraulic core drill to drive a 50-cm long and 80-mm diameter diamond core with a 1 m extension rod. Core site positions were fixed by GPS and elevations were derived from multibeam data, corrected to mean sea-level (MSL).

### **4.3.3 Core logging and sampling**

Core logging and sampling documented characteristics including (1) the ratio of reef framework to matrix (after Embry and Klovan, 1971); (2) sediment textural characteristics (using the Udden–Wentworth nomenclature, as well as a visual assessment of sediment composition); and (3) generic coral identification. Reef framework analysis and facies descriptions follow the terminology of Montaggioni (2005), highlighting the accretion forms of the dominant reef builders and environmental indicators. Matrix sediments were collected for carbonate content analysis determined by the carbonate bombe technique (weight % loss after treatment with 50% HCL) following guidelines from Müller and Gastner (1971). All core log elevations were corrected and plotted relative to MSL.

### **4.3.4 Radiocarbon dating**

Coral specimens from distinct facies in each core were selected for accelerator mass spectrometry and radiometric carbon dating to establish a geochronological record of reef accretion. All specimens were in situ, based on orientation and skeletal condition, and free of boring, encrustation, and submarine cementation. Radiocarbon ages were recalibrated using CALIB Version 7.0.4 and the Marine13 calibration curve (<http://calib.qub.ac.uk/marine>). A weighted mean Delta-R ( $\Delta R$ ) value of  $58 \pm 21$  (average calculation from three nearest points) was used as the best current estimate of variance in the local open water marine reservoir effect

for the Buccaneer Archipelago and adjacent areas. Ages discussed in the text are in calibrated years before present (cal yr BP) with a 68.2% ( $2\sigma$ ) probability range.

## 4.4 Results

Below we summarise the geomorphology, contemporary benthic habitat, Holocene facies and accretion history of the three study sites. Due to the limitations of the coring equipment and the thickness of the Holocene reefs, the oldest/lowermost reef sections were not sampled. However, the position of the Holocene/pre-Holocene contact of several boreholes was supported by earlier work at Cockatoo Island (Solihuddin et al., 2015) where the inferred seismic boundary was traced directly to the Holocene/Last Interglacial reef contact in the mine pit cross-section.

### 4.4.1 Tallon Island

Tallon Island is an arc-shaped outcrop of Precambrian quartzite, rising to a maximum elevation of 10 m above MSL based on shuttle radar topography mission (SRTM) data (<http://dds.cr.usgs.gov/srtm/>). The island is flanked to the west and east by Holocene fringing reefs. Reefs on the west and east sides of Tallon Island differ significantly in elevation, geomorphology and contemporary benthic habitats (Fig. 4.2). The western reef flat is 0.9 km wide and dips gently seaward with an inner elevation of 2.7 m below MSL dropping to 3.5 m below MSL at the reef flat edge. The modern reef flat habitats consist of sand and macroalgae-covered coral rubble with sparse live tabular *Acropora* and small colonies of *Goniastrea aspera* and other faviids. The eastern reef flat is 1.3 km wide and exhibits a near horizontal surface at an elevation of between 0.25 to 0.5 m above MSL. It shows zonation from nearshore mangroves to a shallow lagoon of seagrass and carbonate sand rimmed by a series of low relief (10–20 cm) coralline algal terraces (Fig. 4.2).

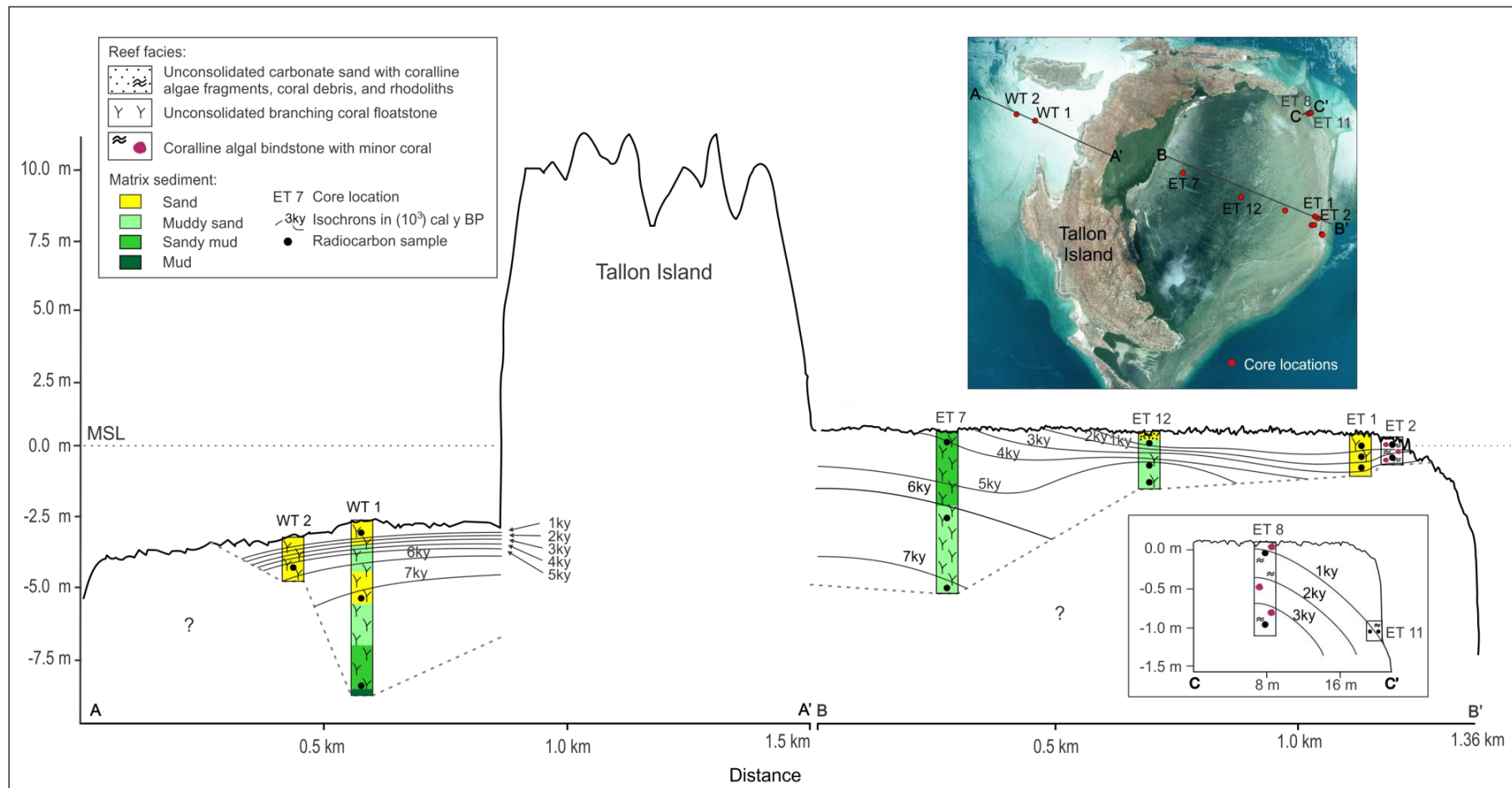


Figure 4.2 Cross section of the Tallon Island reefs with isochrons and summary of Holocene reef facies. The dominant facies was branching coral floatstone with mud to sand matrix, overlaid by a thin layer of unconsolidated carbonate sand.

Reef cores penetrated to a maximum depth of 6.3 m. The dominant facies was a delicate branching coral floatstone with mud to sand matrix, poorly sorted, overlaid by a thin layer of unconsolidated carbonate sand with carbonate content increasing up section from 55 % (ET7) to 89% (ET1). A series of anastomosing coralline algal terraces occur along the outer margin of the eastern reef flat, coalescing into a 3-m high wall on the reef's northeast corner. Rotary coring of the wall recovered a coralline algal bindstone with a minimum vertical thickness of 1.1 m (the capacity of the equipment).

Nineteen radiometric ages were obtained from corals collected from eight cores (four percussions and four rotary) at Tallon Island. The oldest age, 7,790–7,645 cal yr BP, was obtained from the base of core WT1, 8.4 m below MSL on the west side of the island (Fig. 4.2). A similar age of 7,305–7,165 cal yr BP was recorded from the base of core ET7, 5.2 m below MSL on the east side of Tallon Island. The western core WT1 shows rapid vertical reef accretion until 6,000 cal yr BP with a compressed section of 5,000 yr in the upper 1.3 m. This is in contrast to core ET7 which shows continual rapid accretion and reached MSL elevation by 4,000 cal yr BP. The coralline algal bindstone on the outer margin of the eastern reef flat accreted at approximately 0.5 mm/yr for at least 3,000 years. Core from the coralline algal wall (ET 11) indicates that it is no longer accreting vertically, but continues to prograde laterally at 0.6 mm/yr.

#### **4.4.2 Sunday Island**

The Sunday Island reef (also known as “The Pool”) is a 0.5–1-km wide interisland reef platform between Sunday Island and Allora Island (Fig. 4.3). The reef surface is situated approximately 0.5 m below MSL but deepens to approximately 1.5 m below MSL at the core sites to the north and south. Modern habitats at these sites are composed of coarse carbonate sediments with abundant coralline algal-coated branching coral fragments and occasional small colonies of live massive coral. Low-relief rhodolith terraces, approximately 5–10 cm high, occur where seawater streams off the elevated reef at low tide. Immediately southeast of the southern core sites is a long (1.5 km), narrow (<100 m) and deep (30 m) channel flanked by a fringing reef (Fig. 4.3).

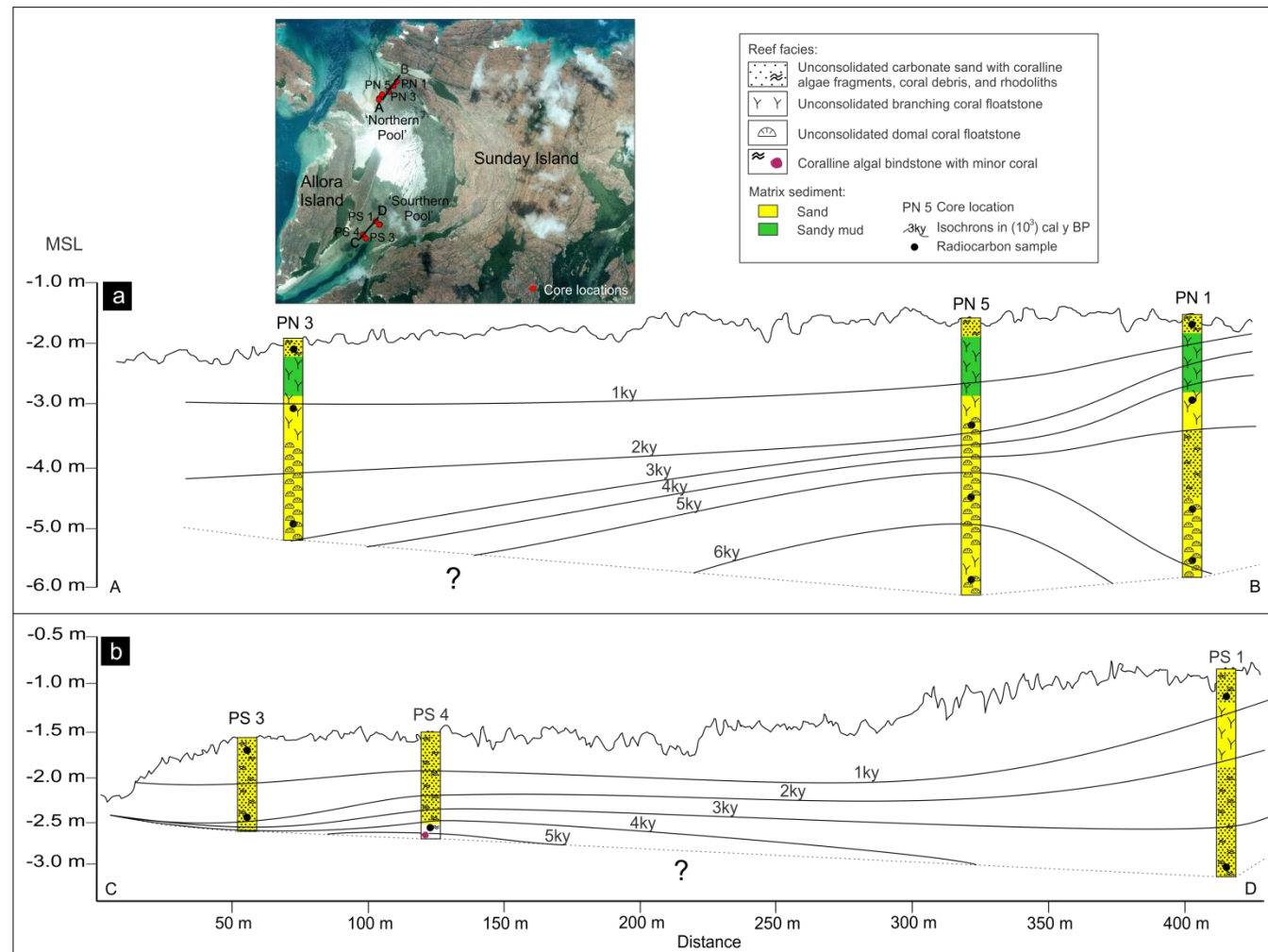


Figure 4.3 Cross section of the North (a) and South (b) Pool of Sunday Island with isochrons and summary of Holocene reef facies. Facies in the North Pool comprised a domal coral floatstone at the base of the cores and a branching coral floatstone at the top. Facies in the South Pool are medium to coarse-grained carbonate sands with corallal fragments.

Reef cores penetrated to a maximum depth of 4.5 m below MSL at the northern side of the interisland reef platform and 2 m below MSL at the southern side. Facies in the northern side include a domal coral floatstone at the base of the cores and a branching coral floatstone at the top. The matrix is sand with abundant corallgal and shell fragments, fining to sandy mud in the uppermost 1 m and overlaid by coarse carbonate sand containing abundant coralline algal fragments and rhodoliths. Analysis of matrix sediments showed carbonate content ranged from 74% (PN5) to 86% (PS2). Facies in the southern side are medium to coarse-grained carbonate sands with corallgal fragments. A coralline algal bindstone was encountered at 1.8 m below MSL in core PS1.

Fifteen radiometric ages were obtained from six cores at Sunday Island (five percussion and one rotary). The oldest age, 6,780–6,625 cal yr BP, was from a *Porites* at 5.8 m below MSL in core PN5 on the northern side of the interisland reef platform (Fig. 4.3). The transition from domal facies to branching *Acropora* upcore occurred at approximately 3 m below MSL and 2,500–5,000 cal yr BP. Shallow subsurface coral samples from cores PN1 and PN3 had modern ages of 240–0 cal yr BP and 120–0 cal yr BP respectively. Reef accretion was relatively uniform throughout the recorded sequence, averaging approximately 1 mm yr<sup>-1</sup>. The coralline algal bindstone at the base of core PS1 had an age of 3,070–2,870 cal yr BP. Shallow subsurface samples throughout the interisland reef platform were modern or near-modern (Table 4.1).

#### 4.4.3 Irvine/Bathurst Islands

Irvine/Bathurst Islands are approximately 60 km northeast of Tallon and Sunday Island and 5 km northwest of Cockatoo Island (Fig. 4.1). Both islands consist of tightly folded Palaeoproterozoic sandstones. The islands are surrounded by fringing reefs which express a range of morphologies, with mangroves lining the more sheltered bays. An interisland fringing reef between the islands rises to a maximum height of approximately 0.25 m above MSL, comparable to the maximum elevation of the Tallon (~0.5 m above MSL) and Sunday Island (~0.5 m below MSL) reef flats but significantly higher than the neighbouring Cockatoo Island reef flat (~4.5 m below MSL; Solihuddin et al., 2015). Modern reef habitats include patchy

coral and sand within the deeper south- and east-facing bays of Irvine Island, extensive coralgall pavement and rhodolith flats of the interisland reef platform, and steep-sided coral-lined pools within the reef flat. Coralline algal terraces occur on the seaward-sloping reef margins but are less developed than those of Tallon and Sunday Islands.

Cores penetrated to a maximum depth of 6.3 m below MSL. The dominant facies at Irvine/Bathurst Islands was a branching coral floatstone, which is especially abundant in the cores around the deep tidal pools. A domal coral floatstone was abundant in some sections, especially in the B04 and B05 cores (Fig. 4.4). Both coral units occurred in a muddy to sandy matrix with carbonate content ranging from a minimum of 46 % (B05) to a maximum of 88% (B15). Surface facies were either coarse carbonate sand or coralline algal bindstone, both up to 30 cm thick.

Six cores were collected along an east-west transect between the islands (Fig. 4.4). The oldest reef encountered was ~3,500–3,345 cal yr BP at 2.7 m below MSL in core B15. This domal coral unit grew upward to 0.4 m below MSL at ~2,000 cal yr BP before being covered by 0.3 m of carbonate sand. A similar domal coral unit occurs at ~5 m below MSL in cores B04 and B05 which dates to ~2,395–2,900 cal yr BP. In core B05 the domal coral unit is underlain by ~2 m of branching coral framestone with an age of ~3,350–3,165 cal yr BP. Thick sequences of branching *Acropora* framework were present in cores from the western margin of the reef flat and around the deep reef pool shown in Fig 4.4. Near-surface samples from all cores except B15 returned modern or near-modern dates.



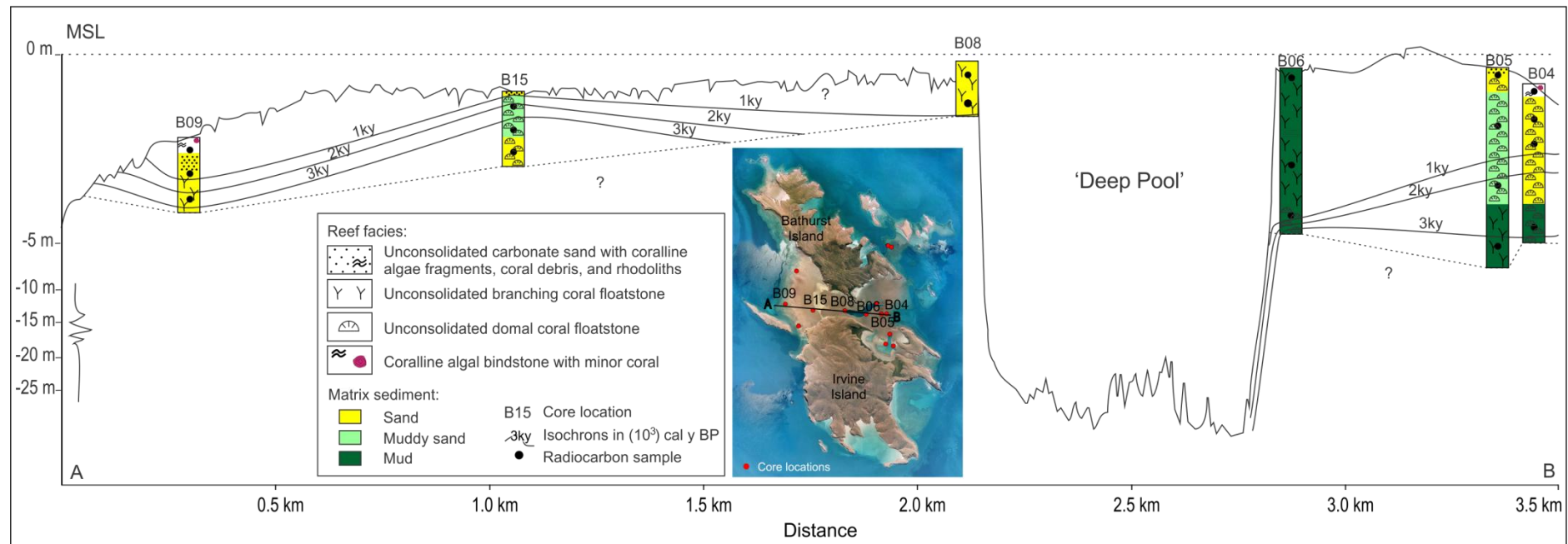


Figure 4.4 Cross section of the interisland fringing reef of Irvine/Bathursts Islands with isochrons and summary of Holocene reef facies. The dominant facies was a branching coral floatstone, especially in the cores around the deep tidal pools. Note the exaggerated scale in the upper 5 m of the reef section.

Table 4.1 Radiocarbon ages from selected samples across Tallon, Sunday, and Irvine/Bathurst Reefs.

Location	Sample Code	Depth (m)	Lab. Code	Material	Method	Measured Age	$^{13}\text{C}/^{12}\text{C}$	Conventional Age (BP)	Calibrated (68% Probability) cal yr BP	Accretion (mm/yr)
Tallon Is.	ET7-30	-0.6	Beta-385991	<i>Acropora</i>	AMS	3610 ± 30	+0.4 ‰	4030 ± 30	4075 - 3870	
	ET7-313	-2.6	Beta-385992	<i>Seriatophora</i>	AMS	5730 ± 30	-0.3 ‰	6140 ± 30	6605 - 6410	0.8
	ET7-573	-5.2	Beta-385993	<i>Porites Cylindrica</i>	AMS	6360 ± 30	+0.0 ‰	6770 ± 30	7305 - 7165	3.6
	ET1-24.5	0.0	Beta-385988	<i>Acropora</i>	AMS	170 ± 30	+0.5 ‰	590 ± 30	265 - 55	
	ET1-74	-0.5	Beta-385989	<i>Porites Cylindrica</i>	AMS	1840 ± 30	-0.4 ‰	2240 ± 30	1865 - 1690	0.3
	ET1-123	-1.0	Beta-385990	Coralline algae	AMS	2630 ± 30	+1.0 ‰	3060 ± 30	2840 - 2715	0.5
	ET12-23	0.2	Beta-389407	Coral	AMS	370 ± 30	0.0 ‰	780 ± 30	450 - 285	
	ET12-132	-0.1	Beta-389408	Coral	AMS	4470 ± 30	+0.7 ‰	4890 ± 30	5265 - 5005	0.1
	ET12-202	-1.6	Beta-389409	Coral	AMS	4760 ± 30	-0.3 ‰	5170 ± 30	5570 - 5420	4.2
	ET2-8	0.2	Beta-391788	Coralline algae	AMS	650 ± 30	+1.8 ‰	1090 ± 30	660 - 540	
	ET2-100	-0.7	Beta-391789	Coral	AMS	2460 ± 30	-0.1 ‰	2870 ± 30	2690 - 2440	0.5
	WT1-30	-3.0	Beta-389404	<i>Acropora</i>	AMS	140 ± 30	-1.3 ‰	530 ± 30	230 - post 0	
	WT1-294	-5.6	Beta-389405	Coral	AMS	6410 ± 30	+1.0 ‰	6840 ± 30	7395 - 7245	0.4
	WT1-573	-8.4	Beta-389406	Coral	AMS	6890 ± 30	+0.9 ‰	7310 ± 30	7790 - 7645	7.0
	WT2-87	-4.3	Beta-389469	<i>Porites Cylindrica</i>	Radiometric	4790 ± 30	+0.5 ‰	5210 ± 30	5805 - 5445	2.0
	ET8-12	-0.2	Beta-397764	Rhodoliths	AMS	1300 ± 30	-3.2 ‰	1660 ± 30	1250 - 1070	
	ET8-115	-1.2	Beta-397765	Coralline algae	AMS	2880 ± 30	+1.0 ‰	3310 ± 30	3175 - 2960	0.5
	ET11-10	-1.1	Beta-397766	Coralline algae	AMS	100.4 ± 0.4 pMC	+0.4 ‰	390 ± 30	Post 0	
	ET11-90	-1.9	Beta-397767	Coralline algae	AMS	1330 ± 30	+1.8 ‰	1770 ± 30	1320 - 1220	0.6
Sunday Is.	PN3-13	-2.0	Beta-389410	<i>Acropora</i>	AMS	130 ± 30	+0.3 ‰	540 ± 30	240 - post 0	
	PN3-120	-3.1	Beta-385994	<i>Acropora</i>	AMS	1670 ± 30	+0.3 ‰	2080 ± 30	1685 - 1515	0.7
	PN3-319	-5.1	Beta-385995	<i>Platygra</i>	AMS	2710 ± 30	-3.0 ‰	3070 ± 30	2850 - 2725	1.7
	PN1-25	-1.8	Beta-389470	<i>Acropora</i>	Radiometric	90 ± 30	-1.2 ‰	480 ± 30	120 - post 0	
	PN1-122	-2.8	Beta-389471	<i>Pavia</i>	Radiometric	3220 ± 30	+1.3 ‰	3650 ± 30	3570 - 3395	0.3
	PN1-308	-4.7	Beta-389472	Coral	Radiometric	4040 ± 30	-2.9 ‰	4400 ± 30	4565 - 4395	1.9
	PN1-388	-5.5	Beta-389473	Rhodoliths	Radiometric	4300 ± 30	-2.1 ‰	4680 ± 30	4905 - 4795	2.2
	PN5-169	-3.4	Beta-389474	<i>Porites</i>	Radiometric	1630 ± 30	-1.1 ‰	2020 ± 30	1595 - 1415	
	PN5-271	-4.5	Beta-389475	<i>Galaxea</i>	Radiometric	4420 ± 30	-1.2 ‰	4810 ± 30	5115 - 4865	0.3
	PN5-410	-5.8	Beta-389476	<i>Porites</i>	Radiometric	5900 ± 30	-0.2 ‰	6310 ± 30	6780 - 6625	0.8
	PS1-20	-1.2	Beta-385996	Coral	AMS	540 ± 30	-0.1 ‰	950 ± 30	545 - 465	
	PS1-184	-2.8	Beta-385997	Coralline algae	AMS	2800 ± 30	+1.7 ‰	3240 ± 30	3070 - 2870	0.6
	PS3-9	-1.8	Beta-389411	<i>Acropora</i>	AMS	80 ± 30	-0.7 ‰	480 ± 30	120 - post 0	
	PS3-90	-2.6	Beta-391787	<i>Acropora</i>	AMS	1570 ± 30	+1.0 ‰	2000 ± 30	1565 - 1400	0.4
	PS4-100	-2.6	Beta-385998	Coral	AMS	4160 ± 30	+1.3 ‰	4590 ± 30	4825 - 4625	
Irvine/Bathurst Is.	B04-30	-0.8	Beta-389477	Coralline algae	Radiometric	140 ± 30	+1.1 ‰	570 ± 30	255 - post 0	
	B04-50	-1.0	Beta-389478	<i>Porites</i>	Radiometric	160 ± 30	+0.5 ‰	580 ± 30	260 - post 0	80.0
	B04-130	-1.8	Beta-389479	<i>Favia</i>	Radiometric	490 ± 30	-1.0 ‰	880 ± 30	505 - 415	2.4
	B04-427	-4.8	Beta-389480	<i>Porites</i>	Radiometric	2370 ± 30	+4.4 ‰	2850 ± 30	2680 - 2395	1.4
	B05-16	-0.3	Beta-389413	<i>Galaxea</i>	AMS	160 ± 30	-2.2 ‰	530 ± 30	230 - post 0	
	B05-160	-1.7	Beta-389414	<i>Galaxea</i>	AMS	740 ± 30	-1.0 ‰	1130 ± 30	680 - 565	2.8
	B05-385	-3.9	Beta-389415	<i>Galaxea</i>	AMS	2690 ± 30	+0.5 ‰	3110 ± 30	2900 - 2740	1.0

B05-600	-6.1	Beta-389416	<i>Porites Cylindrica</i>	AMS	3070 ± 30	-1.7 ‰	3450 ± 30	3350 - 3165	5.0
B08-12	-0.5	Beta-389417	<i>Acropora</i>	AMS	140 ± 30	-0.3 ‰	550 ± 30	245 - post 0	
B08-81	-1.2	Beta-389418	Coralline algae	AMS	270 ± 30	+0.5 ‰	690 ± 30	320-240	4.4
B08b-35	-0.7	Beta-389481	Coralline algae	Radiometric	360 ± 30	-1.7 ‰	740 ± 30	420-265	
B08b-64	-1.0	Beta-389482	Coralline algae	Radiometric	390 ± 30	+2.2 ‰	840 ± 30	490-325	4.6
B09-12	-2.2	Beta-389483	<i>Porites</i>	Radiometric	70 ± 30	+0.3 ‰	480 ± 30	120 - post 0	
B09-30	-2.4	Beta-389484	Coralline algae	Radiometric	580 ± 30	+0.4 ‰	1000 ± 30	615-415	0.4
B09-114	-3.2	Beta-389485	<i>Porites</i>	Radiometric	2270 ± 30	+0.4 ‰	2690 ± 30	2365 - 2275	0.4
B12-35	-0.7	Beta-389419	<i>Acropora</i>	AMS	90 ± 30	-0.5 ‰	490 ± 30	130 - post 0	
B12-238	-2.8	Beta-389420	<i>Acropora</i>	AMS	220 ± 30	-0.2 ‰	630 ± 30	285 - 120	15.3
B12-367	-4.1	Beta-389421	<i>Acropora</i>	AMS	360 ± 30	-1.0 ‰	750 ± 30	425 - 270	9.0
B12-571	-6.1	Beta-389422	Coral	AMS	430 ± 30	-2.1 ‰	810 ± 30	470 - 300	53.3
B14-16	-0.7	Beta-389423	<i>Favia</i>	AMS	110 ± 30	+2.6 ‰	560 ± 30	250 - post 0	
B14-154	-2.0	Beta-389424	Coral	AMS	280 ± 30	-1.0 ‰	670 ± 30	305 - 190	10.8
B14-325	-3.7	Beta-389425	Coral	AMS	340 ± 30	+1.4 ‰	770 ± 30	440 - 280	14.8
B14-554	-6.0	Beta-389426	Coral	AMS	500 ± 30	-1.1 ‰	890 ± 30	510 - 420	21.9
B15-54	-1.3	Beta-391046	Coral	AMS	2060 ± 30	+3.3 ‰	2520 ± 30	2200 - 2005	
B15-101	-1.8	Beta-391047	Coral	AMS	2830 ± 30	-0.7 ‰	3230 ± 30	3060 - 2860	0.6
B15-189	-2.7	Beta-391048	Coral	Radiometric	3190 ± 30	-0.4 ‰	3590 ± 30	3500 - 3345	1.9
B13-18	-0.7	Beta-391043	Coral	AMS	120 ± 30	-2.5 ‰	490 ± 30	130 - post 0	
B13-321	-3.6	Beta-391044	Coral	AMS	560 ± 30	-3.4 ‰	910 ± 30	520 - 435	7.0
B13-597	-6.4	Beta-391045	Coral	AMS	700 ± 30	-1.5 ‰	1090 ± 30	660 - 540	22.9
B07-32	-0.5	Beta-391040	Coral	AMS	110 ± 30	-1.8 ‰	490 ± 30	130 - post 0	
B07-316	-3.4	Beta-391041	Coral	AMS	520 ± 30	-0.2 ‰	930 ± 30	530 - 450	6.8
B07-620	-6.4	Beta-391042	Coral	AMS	1100 ± 30	-1.1 ‰	1490 ± 30	1050 - 910	6.1
B06-43	-0.7	Beta-391037	Coral	AMS	80 ± 30	-1.6 ‰	460 ± 30	75 - post 0	
B06-294	-3.2	Beta-391038	Coral	AMS	640 ± 30	-0.8 ‰	1040 ± 30	635 - 510	4.7
B06-434	-4.6	Beta-391039	Coral	Radiometric	880 ± 30	-0.6 ‰	1280 ± 30	855 - 680	7.2

*All samples were dated at Beta Analytic Inc, Miami, Florida USA*

## 4.5 Discussion

### 4.5.1 Reef geomorphology

The surveyed fringing reefs can be classified into two geomorphic groups based on reef flat elevation: ‘low intertidal reefs’ (LIR) in which reef flat elevation is approximately mean low water spring (MLWS), and ‘high intertidal reefs’ (HIR) in which reef flat elevation clusters between mean low water neap (MLWN) and mean high water neap (MHWN) (Fig. 4.5). The two reef types can occur in close proximity as shown by the Tallon Island cross-section (Fig. 4.2). While low intertidal elevations are typical of fringing reef flats worldwide, elevated reef flats are rare; the only documented example we are aware of occurs at Atol das Rocas off Brazil, where Gherardi and Bosence (2001, 2005) reported reef elevations up to 1.5 m above

MSL (see Fig. 4.2). Google Earth imagery indicates there may be several additional undocumented HIR—the platform reefs of Nova Viçosa, for example, 1,500 km south of Atol das Rocas, appear morphologically similar to both Atol das Rocas and the Kimberley HIR. Like the Kimberley examples, the Brazilian HIR occurs in a tide-dominated environment (defined by mean tidal range exceeding mean significant wave height; Lowe and Falter, 2015). It is likely that many more HIR exist in tide-dominated environments worldwide, although the Kimberley probably holds the ultimate examples, given its extreme tidal range.

The apparent absence of reef flat elevations between MLWS and MLWN in the Kimberley (Fig. 4.5) suggests that both the HIR and LIR may be constrained at their present elevations. The question then arises as to how the HIR attain their elevation while LIR remain at the more typical MLWS level. The HIR versus LIR dichotomy is best represented at Tallon Island, where the western (LIR) and eastern (HIR) reefs differ markedly in elevation (Fig. 4.2) despite occurring in similar, relatively sheltered settings. The main differences between these reefs, apart from their elevation, are the greater width of the HIR and the predominance of coralline algae on the HIR versus coral and sediment on the LIR. These features appear to be consistent throughout the Kimberley (e.g., Blakeway, 1997; Purcell, 2002). Similarly, the Brazilian HIRs are also characterised by extensive reef flats and coralline algal terraces (Gherardi and Bosence, 2001; Fonseca et al., 2012). These consistencies suggest that some or all of the three factors of tidal range, reef flat width and coralline algae, interact to produce HIR. A recent hydrodynamic study of the Tallon Island HIR by Lowe et al. (2015) indicates how the process may occur. Lowe et al. (2015) recorded a dramatic tidal asymmetry, with the reef flat rapidly inundated over 2–3 hours but draining very slowly over 9–10 hours. Consequently, the reef flat never entirely dries, and reef flat organisms are able to survive and grow despite their elevation. Field measurements and modelling indicate that the ponding effect depends primarily on reef flat width and bottom friction; water residence times are greater on wide and ‘rough’ reefs, with roughness determined by benthic composition and biota (Lowe et al., 2015). This is perhaps the essential difference between the eastern HIR and the western LIR of Tallon Island. The wide and microtopographically complex eastern reef flat (Fig. 4.2) retains a film of seawater throughout the low tide cycle, effectively creating its own pseudo-accommodation

space. Reef flat accretion here has an element of positive feedback; in that vertical reef accretion will pond seawater at a greater elevation, allowing further accretion. In contrast, the narrower, inclined, and somewhat less complex (Fig. 4.2) western reef flat sheds seawater and therefore remains at MLWS. Based on Lowe et al.'s (2015) findings, we suggest that this division may apply throughout the Kimberley: reef flats that are wide enough to retain seawater over the low tide cycle become HIR and those that do not remain as LIR at MLWS. We interpret the apparent absence of intermediate elevations to indicate that, during the Holocene highstand, all reefs with the potential to become HIR have done so, whereas other reefs have remained at MLWS.

In addition to reef flat width, several other factors may also influence water retention at low tide, but are perhaps secondary (e.g., reef aspect, reef flat slope, reef porosity, the presence or absence of tidal creeks and mangroves that may store and release seawater, and surrounding bathymetry that may restrict or enhance ebb tide runoff). Another factor that could promote water retention is a continuous marginal rim, i.e., a 'bucket' structure. However, our subsurface information suggests that raised rims have been absent or only very weakly developed through the Holocene and that the reefs have accreted more as 'banks' than 'buckets' (e.g., Fig. 4.2). Although coralline algal-terraced margins are a consistent feature of Kimberley HIRs (Blakeway, 1997; Brooke, 1997; Purcell, 2002; Wilson and Blake, 2011; Lowe et al., 2015; Richards and O'Leary, 2015), we interpret these as relatively late-stage surface features that develop as the reefs accrete beyond MLWS. Although coralline algal-terraced margins are a consistent feature of Kimberley HIRs (Blakeway, 1997; Brooke, 1997; Purcell, 2002; Wilson and Blake, 2011; Lowe et al., 2015; Richards and O'Leary, 2015), we interpret these as relatively late-stage surface features that develop in areas subject to low-tide runoff as the reefs accrete beyond MLWS. The predominance of coralline algae in these macrotidal but relatively sheltered habitats contrasts with their occurrence in exposed wave-dominated habitats on reefs elsewhere (e.g. Wells, 1957; Adey, 1975; Blanchon, 2011). However, these contrasting habitats provide essentially similar physical conditions, both being relatively fast-flowing, turbulent, well-oxygenated and well-illuminated—ideal conditions for coralline algae.

We interpret the hydraulic analysis by Lowe et al. (2015) to indicate that the critical reef flat width initiating HIR development may be around 1 km for fringing reefs. The potential for any particular reef to attain this critical width may be determined largely by local factors, bathymetry perhaps being the most influential. Other factors being equal, wide reef flats are most likely to develop on broad shallow banks or where the fringing reefs of adjacent islands suture or coalesce together, whereas narrow reef flats are most likely to develop on narrow banks or against isolated steep-sided islands. At the sites we examined, the underlying structure appears to be a major determinant of bathymetry, and hence of modern reef configuration. The HIR of Tallon Island is a possible example of structural control, because it appears to lie within a synclinal basin (Brunschweiler, 1957) which, when flooded by sea-level rise, may have become a sheltered, semi-enclosed habitat, perhaps more conducive to reef accretion than adjacent habitats outside the basin. Similarly, the relatively narrow (300 m) LIR at Cockatoo Island is limited primarily by the underlying structure. Because the bedrock there dips steeply seaward, the reef is prograding into relatively deep water ( $> 30$  m; Solihuddin et al., 2015) and can only widen very slowly despite its high coral cover. The Cockatoo Island reef flat will therefore likely remain at its current MLWS elevation. This limitation may also apply to the LIR reef on the western side of Tallon Island (Fig. 4.2). Such HIR apparently occur in macrotidal tropical environments worldwide but remain relatively understudied. Further research on HIR in the Kimberley and elsewhere would clarify the applicability and generality of our interpretations, and may provide significant insights into Holocene reef accretion and development in macrotidal settings.

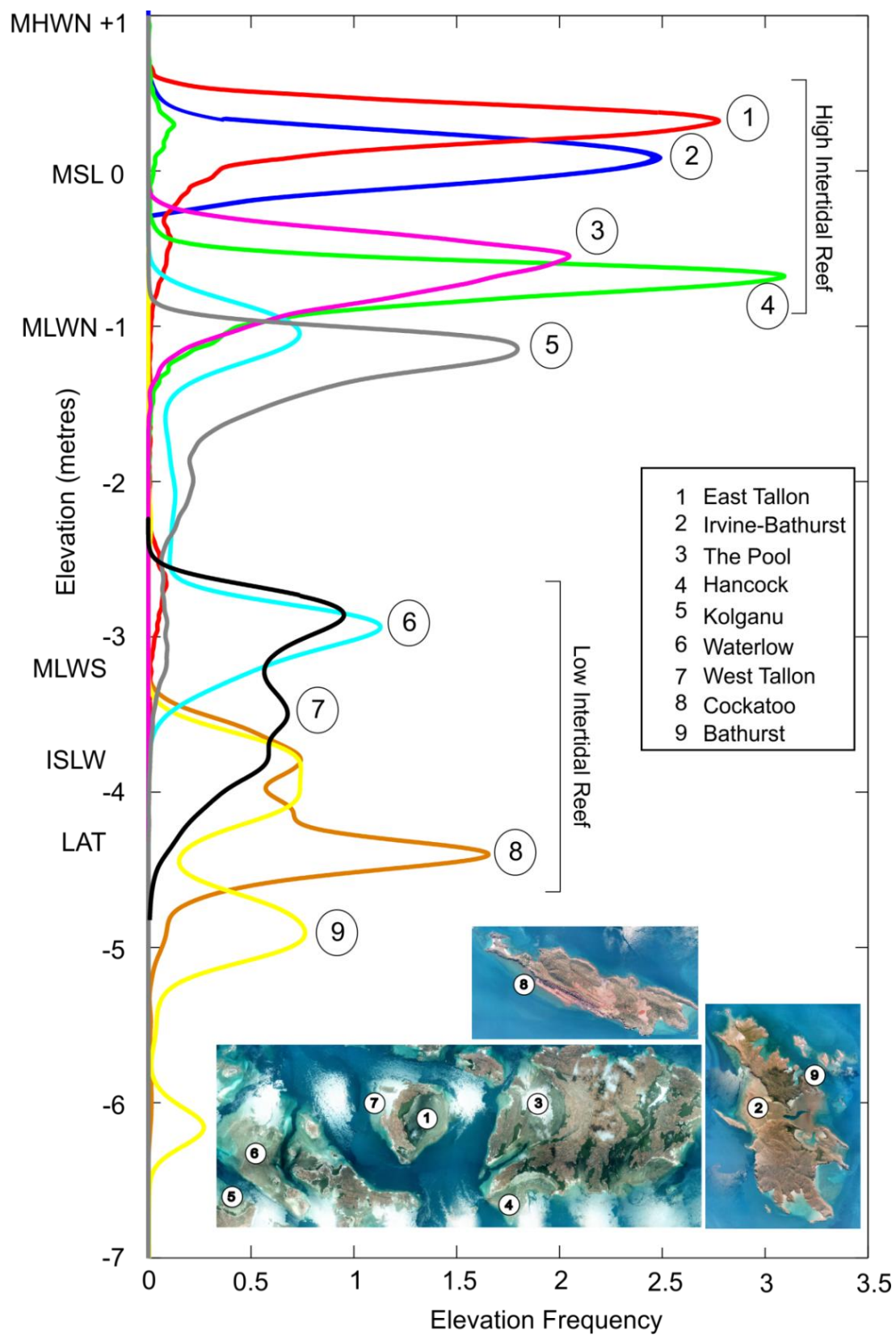


Figure 4.5 Probability density curves of reef elevations measured by multibeam echo-sounder surveys.

### **4.5.2 Chronology of Holocene reef build-up**

Radiometric coral ages from reef cores suggest that reef accretion initiated soon after Holocene sea-level rise flooded the antecedent surface [based on the sea-level curve of Lambeck et al. (2014)]. The oldest dates recorded were 7,305–7,165 and 7,790–7,645 cal yr BP at 5.2 m below MSL from core ET7 on East Tallon Island and at 8.7 m below MSL in core WT1 on West Tallon Island respectively. The latter age supports chronological data from Cockatoo Island in the Buccaneer Archipelago (Solihuddin et al., 2015), which showed reef initiation beginning at around 18 m below MSL as early as 9,000–8,940 cal yr BP, and more broadly suggests that the early Holocene environmental and oceanographic conditions in the southern Kimberley were favourable for the recruitment of corals and the development of coral reefs.

Isochrons for Tallon Island show that by 7,000 cal yr BP, fringing reefs on both the eastern and western side of the island had reached an elevation of ~5.0 m below MSL, which is ~1.8 m below present MLWS. Subsequently, the high intertidal fringing reef on the eastern side of Tallon continued to accrete vertically, reaching a maximum elevation of 0.5 m above MSL by around 4,000 cal yr BP, whereas the low intertidal fringing reef on the western side of Tallon Island ceased vertical accretion at an elevation of 2.5 m below MSL (0.7 m above MLWS) at around 5,000 cal yr BP (Fig. 4.2).

Reef cores were recovered from the northern and southern entrances of “The Pool” which forms a high intertidal fringing reef between Sunday and Allora islands to capture the transition zone between the HIR and LIR reef morphologies (Fig. 4.3). The oldest coral collected from 5.8 m below MSL in core PN5 at the North Pool site returned a calibrated radiocarbon age of 6,780–6,675 cal yr BP, while the oldest coral collected from 2.6 m below MSL in core PS4 had an age of 4,825–4,625 cal yr BP at the South Pool site. The age isochrons in the North Pool indicate accretion in a quasi progradational accretion direction which may indicate the reefs prograded seaward from the islands rather than having aggraded from depth. This may suggest that a deeper channel may have run the length of The Pool only to be sutured closed as the two prograding reefs from Allora and Sunday islands joined. A remnant of this



passage is evident in the southern portion of The Pool where age isochrons suggest it is ‘zipping’ closed in a north–south direction (Fig. 4.3).

A high intertidal interisland fringing reef joins Irvine/Bathurst islands and is characterised by a central 30-m deep pool (Fig. 4.4) rather than a narrow channel opening to the sea, as is the case on the interisland reef joining Sunday and Allora islands. A 5 m long core (B06) taken from the edge of the deep pool had a core top age of 75 to post 0 and a core bottom age of 855 to 680 cal yr BP. This suggests that accretion is dominantly progradational, and like the interisland reef joining Sunday and Allora islands, likely formed by the suturing of two fringing reefs prograding from each island (Fig. 4.4).

The oldest coral sample recovered at Irvine/Bathurst was 3,500–3,345 cal yr BP from core B15 at 2.7 m below MSL. The absence of older coral ages from Irvine/Bathurst is likely due to limited core penetration rather than late initiation, given that the neighbouring Cockatoo Island Reef initiated at 9,000 cal yr BP (Solihuddin et al., 2015).

Core top ages for the Irvine/Bathurst islands of less than 1,000 cal yr BP suggests the reef flat has only recently reached its current elevation of 0.25 m above MSL, possibly indicating that the reef could still be aggrading and has not yet reached its maximum elevation. Low intertidal reefs are evident on the southern and southeastern sides of Irvine Island which are similar in elevation to the west Tallon LIR. However, no cores were retrieved at those locations so it is not possible to determine whether these low intertidal reefs are actively aggrading or have reached their maximum elevation, as interpreted for the west Tallon Reef.

#### 4.5.3 Reef facies and accretionary style

The internal composition of the sampled reefs was largely comprised of coral fragments (predominantly delicate branching *Acropora*) in a poorly sorted sandy mud matrix. This suggests that relatively sheltered depositional environments have prevailed throughout the Holocene, in keeping with the low wave energy environment of the sample sites. Most of the coral fragments appear to be *in situ*, based on skeletal preservation. Occasional horizons dominated by robust domal coral

colonies are intercalated with the detrital units, and many of these colonies also appear to be *in situ*, based on orientation and preservation. We interpret the reefs to have been low-energy subtidal *Acropora*-dominated meadows that most likely had a relatively high live cover, and moderate diversity and structural complexity. The reef structure would have baffled the tidal currents and trapped fine sediment within the reef interstices similar to the nearby Cockatoo Island reef (Solihuddin et al., 2015). Based on these interpretations, the facies of the sampled Kimberley Reefs conform closely to those described by Perry et al. (2012) at Middle Reef, a turbid nearshore reef within the mesotidal range (3.6 m) located in the central Great Barrier Reef (GBR). Both have high coral cover, sediment-tolerant corals, and a mud-dominated matrix (Solihuddin et al., 2015).

The distribution of runoff from impounded seawater is probably responsible for the marked divergence between low and high intertidal reefs once they reach sea-level (as discussed in ‘Reef geomorphology’). LIR usually maintain their general facies characteristics which are composed of coral fragments and colonies in a muddy to sandy matrix, although the coral species often change (i.e., *Goniastrea aspera*, *Favia*, and *Montipora digitata* are observed to increase in abundance in some cores) and entirely different communities may arise in some localised areas (e.g., the inshore seagrass beds of East Tallon). In contrast, the HIR undergo a radical facies change and become dominated by coralline algae as they rise above MLWS and begin to form terraces.

## 4.6 Conclusions

This study extends previous work at Cockatoo Island (Solihuddin et al., 2015) to three additional sites in the southern Kimberley. The emerging picture is that southern Kimberley reefs are extensive, thick three-dimensional structures that initiated shortly after inundation and accreted relatively rapidly, such that most reefs are now vertically constrained and are enlarging by progradation. Holocene reef communities were dominated by branching *Acropora*, which accumulated as broad banks of *in situ* framework, infilled with poorly-sorted carbonate and siliciclastic sediments, predominantly mud-sized.

The massive Kimberley tides are a dominant influence on reef geomorphology, particularly on reef flat elevation. Reefs that dry at low tide remain coral-dominated and are constrained at MLWS, whereas reefs that retain seawater over the low tide cycle become coralline algal-dominated and accrete to between MLWN and MHWN, up to ~4 m above MLWS. Such ‘high intertidal reefs’ may be widespread in macrotidal tropical environments but remain relatively understudied.

### Acknowledgements

The Kimberley Reef Geomorphology Project 1.3.1 was funded by the Western Australian State Government and partners of the Western Australian Marine Science Institution. This research was assisted by the Bardi Jawi and Mayala people through their advice and consent to access their traditional lands. The Kimberley Marine Research Station at Cygnet Bay provided vessel support and access to research facilities. Thanks to Giada Bufarale for assistance with subsurface interpretations and to Alexandra Stevens for improvement of the manuscript.

### References

- Adey, W. H. (1975). The algal ridges and coral reefs of St. Croix, their structure and Holocene development. *Reef Research Bulletin*, 187, 1-66.
- Blakeway, D. (1997). Scleractinian corals and reef development, part 9. In: Walker, D. (ed.), Marine biological survey of the central Kimberley coast, Western Australia. Perth: University of Western Australia. Unpublished report, W.A. Museum Library No. UR377, 77–85.
- Blanchon, P. (2011). Geomorphic zonation. In: Hopley, D. (ed.), *Encyclopedia of modern coral reefs: structure, form and process*. Dordrecht: Springer, 469-486.
- Brooke, B. (1997). Geomorphology of the north Kimberley coast, part 9. In: Walker, D. (ed.), Marine biological survey of the central Kimberley coast. Western Australia. University of Western Australia, Perth, unpublished report, W.A. Museum Library No. UR377, 13–39.

- Brunnschweiler, R. O. (1957). The geology of Dampier Peninsula, Western Australia. Department of National Development, Bureau of Mineral Resources, Geology and Geophysics, Canberra.
- Buddemeier, R.W., Hopley, D. (1988). Turn-ons and turn-offs: causes and mechanisms of the initiation and termination of coral reef accretion. *Proc 6th Int Coral Reef Symp*, 1, 253–261.
- Collins, L. B., O’Leary, M. J., Stevens A. M., Bufarale G., Kordi M., Solihuddin T. (2015). Geomorphic patterns, internal architecture and reef accretion in a macrotidal, high-turbidity setting of coral reefs from the Kimberley Bioregion. *AJMOA*, 7, 12-22.
- Darwin, C. R. (1842). The structure and distribution of coral reefs. Being the first part of the geology of the voyage of the ‘Beagle’. London: Smith, Elder and Co.
- Department of the Environment, Water, Heritage and the Arts, DEWHA (2008). A characterisation of the marine environment of the northwest marine region: Perth workshop report, a summary of an expert workshop convened in Perth, Western Australia, 5-6 September 2007, Commonwealth of Australia, Hobart.
- Embry, A. F., Klován J. (1971). A late Devonian reef tract on Northeastern Banks Island, N.W.T. Bull. *Can Petrol Geol*, 19, 730–781.
- Fonseca, A. C., Villaçá, R., Knoppers, B. (2012). Reef Flat Community Structure of Atol das Rocas, Northeast Brazil and Southwest Atlantic. *J Mar Biol*, 2012. doi:10.1155/2012/179128.
- Gherardi, D. F. M., Bosence, D. W. J. (2001). Composition and community structure of the coralline-algal reefs from Atol das Rocas, South Atlantic, Brazil. *Coral Reefs*, 19, 205–219.
- Gherardi, D. F. M., Bosence, D. W. J. (2005). Late Holocene reef accretion and relative sea-level changes in Atol das Rocas, equatorial South Atlantic. *Coral Reefs*, 24, 264–272.

- Griffin, T. J., Grey, K. (1990). Kimberley Basin. In: Memoir 3, Geology and mineral resources of Western Australia. Geological Survey of Western Australia, Perth, 293–304.
- Hopley, D., Smithers, S.G., Parnell, K.E. (2007). The geomorphology of the Great Barrier Reef; Development, diversity and change. Cambridge University Press, New York.
- Kennedy, D. M., Woodroffe, C. D. (2002). Fringing reef accretion and morphology: a review. *Earth-Sci Rev*, 57, 255–277.
- Ladd, H. S., Ingerson, E., Townsend, R.C., Russell, M., Stevenson, H. K. (1953). Drilling on Eniwetok Atoll, Marshall Islands. *AAPG bulletin*, 37, 2257–2280.
- Lambeck, K., Rouby, H., Purcell, A., Sun, Y., Sambridge, M. (2014). Sea-level and global ice volumes from the Last Glacial Maximum to the Holocene. *Proc Natl Acad Sci*, 111(43), 15296–15303.
- Lough, J. M. (1998). Coastal climate of Northwest Australia and comparisons with the Great Barrier Reef: 1960 to 1992. *Coral Reefs*, 17, 351–367.
- Lowe, R. J., Falter, J. L. (2015). Oceanic forcing of coral reefs. In: *Annual Review of Marine Science*, 7, 43–66.
- Lowe, R. J., Leon, A.S., Symonds, G., Falter, J. L., Gruber, R. (2015). The intertidal hydraulics of tide-dominated reef platforms. *J Geophys Res*, 120. doi:10.1002/2015JC010701.
- Montaggioni, L. F. (2005). History of Indo-Pacific coral reef systems since the last glaciation: Development patterns and controlling factors. *Earth-Sci Rev*, 71(1–2), 1–75.
- Müller, G., Gastner M. (1971). The 'Karbonat-Bombe', a simple device for the determination of carbonate content in sediment, soils, and other materials. *Neues Jahrbuch für Mineralogie-Monatshefte*, 10, 466–469.
- Neumann, A. C., Macintyre, I. G. (1985). Reef response to sea-level rise: keep-up, catch-up or give-up. *Proc 5th Int Coral Reef Symp*, 3, 105–110.

- Pearce, A. F., Griffiths, R. W. (1991). The mesoscale structure of the Leeuwin Current: A comparison of laboratory models and satellite imagery. *J Geophys Res*, 96, 16739-16757.
- Perry, C. T., Smithers, S. G., Gulliver, P., Browne, N. K. (2012). Evidence of very rapid reef accretion and reef accretion under high turbidity and terrigenous sedimentation. *Geology*, 40, 719-722.
- Purcell, S. (2002). Intertidal reefs under extreme tidal flux in Buccaneer Archipelago, Western Australia. *Coral Reefs*, 21, 191-192.
- Richards, Z. T., O'Leary, M. J. (2015). The coralline algal cascades of Tallon Island (Jalan) Fringing Reef, NW Australia. *Coral Reefs*, 34, 595.
- Solihuddin, T., Collins, L. B., Blakeway, D., O'Leary, M. J. (2015). Holocene coral reef accretion and sea-level in a macrotidal, high turbidity setting: Cockatoo Island, Kimberley Bioregion, northwest Australia. *Mar Geol*, 359, 50–60.
- Teichert, C., Fairbridge, R. W. (1948). Some coral reefs of the Sahul Shelf. *Geogr Rev*, 28, 222–249.
- Wells, J. W. (1957). Coral Reefs. In: Hedspeth J. W. (ed.), *Treatise on marine ecology and paleoecology*. Geological Society of America Memoir 67, 609-632
- Wilson, B. R. (2013). The biogeography of the Australian North West Shelf: environmental change and life's response. Elsevier, Burlington MA
- Wilson, B. R., Blake, S. (2011). Notes on the origin and biogeomorphology of Montgomery Reef, Kimberley, Western Australia. *J R Soc West Aust*, 94(2), 107–119
- Wilson, B. R., Blake, S., Ryan, D., Hacker, J., 2011. Reconnaissance of species-rich coral reefs in a muddy, macro-tidal, enclosed embayment, Talbot Bay, Kimberley, Western Australia. *J R Soc West Aust*, 94, 251–265.

## Chapter 5

### Geomorphology and Late Holocene accretion history of Adele Reef: a Northwest Australian mid-shelf platform reef

Tubagus Solihuddin<sup>1,2</sup>, Giada Bufarale<sup>1,2</sup>, David Blakeway<sup>3</sup>, Michael J. O' Leary<sup>2,4</sup>

<sup>1</sup>Department of Applied Geology, Curtin University, Bentley, WA 6102

<sup>2</sup>The Western Australian Marine Science Institution, Floreat, Australia, 6014

<sup>3</sup>Fathom 5 Marine Research, 17 Staines Street, Lathlain, WA 6100

<sup>4</sup>Department of Environment and Agriculture, Curtin University, Bentley, WA 6102

#### Abstract

The mid-shelf reefs of the Kimberley Bioregion are one of Australia's more remote tropical reef provinces and such have received little attention from reef researchers. This study describes the geomorphology and late Holocene accretion history of Adele Reef, a mid-shelf platform reef, through remote sensing of contemporary reef habitats, shallow seismic profiling, shallow percussion coring, and radiocarbon dating. Seismic profiling indicates that the Holocene reef sequence is 25 to 35 m thick and overlies at least three earlier stages of reef build-up, interpreted as deposited during Marine Isotope Stages 5, 7, and 9 respectively. The cored shallow subsurface facies of Adele Reef are predominantly detrital, comprising small coral colonies and fragments in a sandy matrix. Reef cores indicate a 'catch-up' growth pattern, with the reef flat being approximately 5-10 deep when sea level stabilised at its present elevation 6,500 years BP. The reef flat is rimmed by a broad low-relief reef crest, only 10-20 cm high, characterised by anastomosing ridges of rhodoliths and coralloliths. The depth of the Holocene/Last Interglacial contact (25-30 m) suggests a subsidence rate for Adele Reef since the Last Interglacial of 0.2 mm/yr. This value, incorporated with subsidence rates from Cockatoo Island (inshore) and Scott Reef (offshore), provides the first quantitative estimate of hinge subsidence for the Kimberley coast and adjacent shelf, with progressively greater subsidence across the shelf.

Keywords: Accretion, Biogeomorphic zonation, Continental shelf, Coral reef, Coralline algae, Kimberley, Reef coring, Remote sensing, Sea level, Shelf subsidence.

\*Corresponding author: e-mail at: Department of Applied Geology, Curtin University, Bentley, WA 6102, Australia. Tel.: +61 8 9266 3710.

E-mail address: [tubagus.solihuddin@postgrad.curtin.edu.au](mailto:tubagus.solihuddin@postgrad.curtin.edu.au) (T. Solihuddin)

## 5.1 Introduction

Adele Reef is a large (200 km<sup>2</sup>) platform reef located 15.5°S 123.5°E on Australia's Northwest shelf, approximately 80 km from the mainland Kimberley coast and 200 km from the shelf edge (Fig. 5.1). Adele Reef is approximately 22 km long and 9 km wide, and is topped by a 4 km<sup>2</sup> vegetated sand cay. Four smaller submerged reefs, Churchill, Albert, Mavis and Beagle Reefs, lie to the east. The surrounding shelf is 70-80 m deep and is incised by channels to approximately 90-100 m depth (Fig. 5.1).

The regional climate is semi-arid and monsoonal, with two seasons: a 'wet' season from November to April and 'dry' season from May to October. Monsoon storms in the wet season bring intense rainfall, averaging 800-1500 mm. The dry season is characterised by warm to hot temperatures and low humidity (DEWHA, 2008). Sea surface temperatures around Adele range from 22° to 28°C (Pearce and Griffiths, 1991). The predominant swell is from the south-west and the predominant winds are westerly to south-westerly. The region is cyclone-influenced (average 3 per year, Lough, 1998) and has semidiurnal tides with a maximum range of 7 m.

Previous research on Adele Reef has described its surface geomorphology (Teichert and Fairbridge, 1948; Brooke, 1997), petroleum potential (Ingram, 1982; Marshall, 1995) and reef flat habitats (Richards et al., 2013). The stratigraphic sequence beneath the northern tip of Adele Island was investigated in a petroleum exploration well drilled in 1982 ('Adele Island 1' Ingram 1982; Marshall, 1995). The first 156 m of the bore-hole intersected multiple stacked sedimentary units, consisting of Holocene and Pleistocene limestone, with abundant shell fragments and



coral remains in the upper 30 m (Ingram, 1982). Palaeogene sandstone was found below 160 m, overlying a Cretaceous and Upper Jurassic sand/silt sequence; Proterozoic basement was intersected at 798 m (Ingram, 1982).

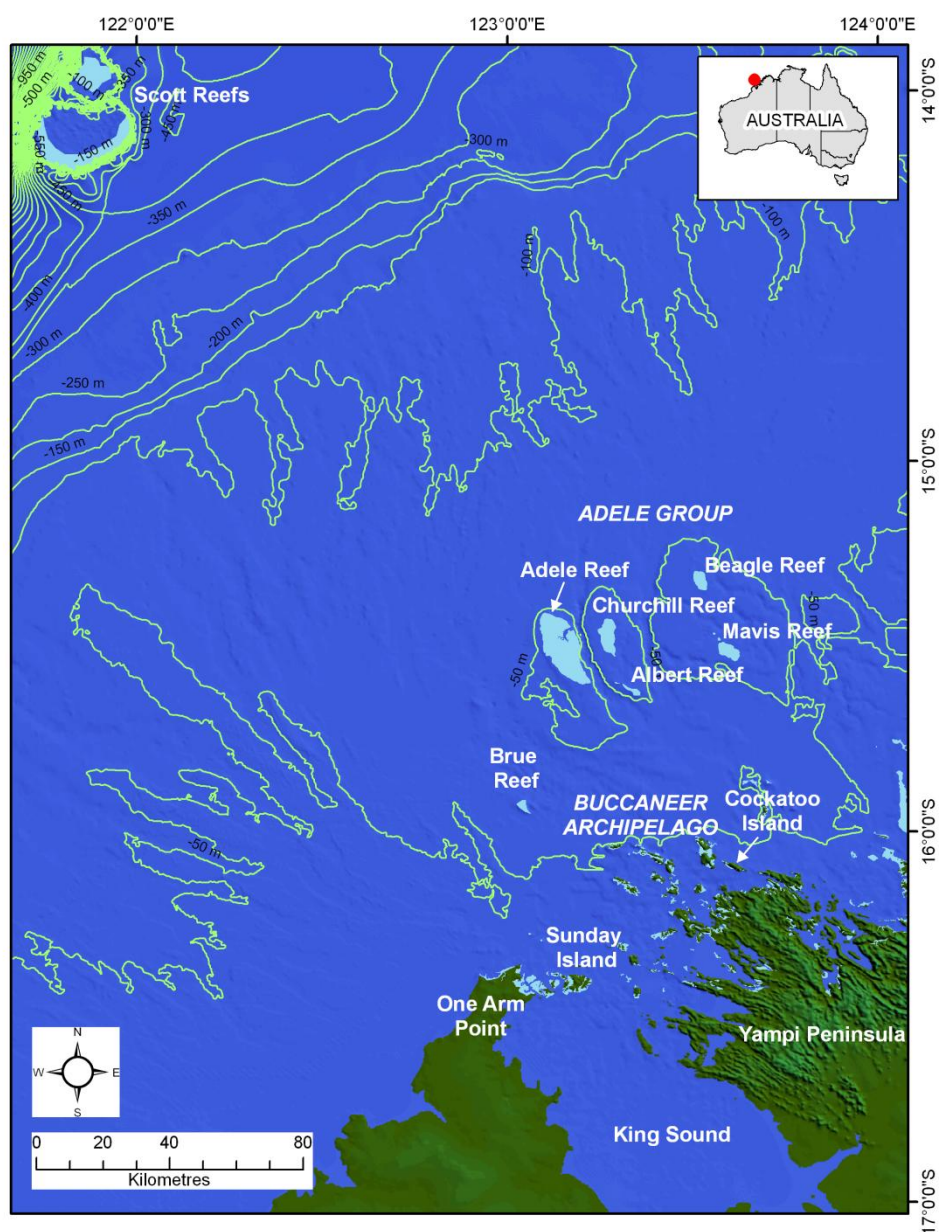


Figure 5.1 Map of the study area in the Kimberley Bioregion showing the bathymetry contour derived from 250-m resolution digital elevation model (DEM) sourced from Geoscience Australia (note: there is some uncertainty in the depths due to the coarse nature of the Bathymetric grid). The light blue shading indicates reef habitat.

In a recent survey by the Western Australian Museum, Richards et al. (2013) reported the discovery of a unique ‘rollolith’ habitat along the southwestern margin of Adele Reef. This includes mobile corals (coralliths) and red crustose coralline algae (rhodoliths) that have coalesced to form low-relief banks on the outer reef flats. This atypical habitat likely formed in response to a combination of wave action and strong surface currents driven by the 7 m macrotidal range (Richards et al., 2013).

Compared to the relatively well-studied oceanic reefs such as Scott Reef and the Rowley Shoals (Collins, 2011), and the inshore reefs of the Buccaneer Archipelago (Collins et al., 2015; Solihuddin et al., 2015, 2016; Bufarale et al., 2016), the Holocene development of the mid-shelf platform reefs of Australia’s northwest shelf remains unknown. The present study attempts to address the information gap by investigating modern habitats, geomorphology and the late Holocene accretion history of Adele Reef through remote sensing, shallow sub-bottom profiling, reef core stratigraphy, and radiocarbon dating.

## **5.2 Methods**

### **5.2.1 Remote sensing of reef habitats using Landsat 8 imagery**

Contemporary reef communities and associated habitats were mapped using a Landsat 8 multispectral satellite image taken on the 23<sup>rd</sup> May 2015 (path 110, row 071). This image was corrected geometrically to the WGS 84 reference datum. A digital unsupervised classification from Erdas’ ER Mapper utility was used to define reef habitat zones based on a grouping of the reflectance spectra of Landsat 8 bands 2 (0.45 – 0.52  $\mu\text{m}$ ; blue), 3 (0.52 – 0.60  $\mu\text{m}$ ; green) and 4 (0.63 – 0.68  $\mu\text{m}$ ; red). Ground-truth observations of reef habitats from the current study and from the Woodside Collection Project (Kimberley): 2008-2011 (<http://www.museum.wa.gov.au/Kimberley/marine-life-kimberley-region>; accessed November 2015) were assigned to the corresponding Landsat 30 x 30 m pixels. All pixels with similar spectral characteristics were then automatically assigned to that ground-truthed habitat.

### 5.2.2 Seismic interpretation

A high-resolution shallow seismic survey of the reef subsurface was undertaken using a boomer/sub-bottom profiler system (AA201 Applied Acoustic Engineering Limited, Great Yarmouth, UK). A Differential Global Positioning System (DGPS, FugroSeastar 8200XP/HP) provided accurate positioning (decimetric differential accuracy, typically  $\pm 20$  cm). Sub-bottom profiling data was digitally acquired, recorded, post-processed and analysed using SonarWiz 5 (Chesapeake Technology Inc., Mountain View, CA). Interpretation of the seismic reflectors depicted in the profiles was performed using a combination of inshore reef seismic data from Bufarale et al. (2016) and petroleum well-log data from Adele Island 1 (Ingram, 1982; Marshall, 1995). Geoscience Australia's 250 m bathymetry dataset was analysed using ESRI's Arc Hydro Tools Terrain Pre-processing toolset to map the position and bathymetry of shelf palaeochannels.

### 5.2.3 Reef coring, logging and sampling

Eight percussion cores were collected from Adele Reef. Coring sites were selected to groundtruth the seismic interpretations and to ensure a spatially representative record of reef accretion. A manual slide hammer or a hydraulic post driver was used to drive lengths of 6 m long, 80 mm diameter aluminium pipe with near-100% core recovery. Compaction was measured onsite and corrected by linear stretching of the core logs. Logs were plotted to local mean sea level (MSL), which is 3.9 m above the lowest astronomical tide (LAT) and referred to metre below sea level (mbsl) in the text. Core locations were recorded by handheld GPS with an accuracy of  $\pm 5$  m.

Core logging and sampling documented sediment characteristics including: (1) the ratio of reef framework to matrix (after Embry and Klovan, 1971); (2) visual assessment of sediment textural characteristics using the Udden-Wentworth nomenclature (Wentworth, 1922); and (3) generic coral identification (after Veron, 2000). Reef framework analysis and facies descriptions followed the terminology proposed by Montaggioni (2005), which highlights the growth forms of the dominant reef builders and environmental indicators. Between 300-500 g samples of matrix sediment were collected for carbonate content analysis using the carbonate bombe

technique (weight % loss after treatment with 50% HCL) following guidelines from Müller & Gastner (1971). A pipe dredge was used to collect subtidal sediment samples and these were analysed using the same methods applied to the core samples.

#### 5.2.4 Radiocarbon dating

Three to five coral specimens from top, middle and base of each core were selected, based on size and preservation, for accelerator mass spectrometry (AMS) radiocarbon dating in order to establish a geochronological record of late Holocene reef accretion. Individual coral specimens were ultrasonically cleaned and cut into pieces with minimum weight of 50 mg. All samples were dated at Beta Analytic Inc USA and recalibrated using the CALIB Version 7.0.4 and the Marine13 calibration curve (<http://calib.qub.ac.uk/marine>; accessed January 2016). A weighted mean Delta-R ( $\Delta R$ ) value of  $58 \pm 21$  (average calculation from 3 nearest points: Cape Leveque NE side, King Sound, Port George) was used as the best current estimate of variance in the local open water marine reservoir effect for Adele Reef and adjacent areas (Reimer et al., 2013). Ages discussed in the text are in calibrated years Before Present (cal years BP) with the 68.2% ( $2\sigma$ ) probability range for all dated samples.

### 5.3 Results

#### 5.3.1 Contemporary reef biogeomorphic zones

The Landsat-derived reef geomorphology and associated habitat map (Fig. 5.2), supported by ground-truth observations, allowed delineation of six distinct biogeomorphic zones: (1) sand cay, (2) coral rubble and carbonate sand, (3) corallgal pavement, (4) mixed assemblage of coralloliths and rhodoliths, (5) crustose coralline algae, and (6) soft and encrusting plate corals. Each of these habitats is described in detail below.

*Sand Cay:* The sand cay forms a NW-SE elongated, 12 km x 3 km unvegetated island consisting of poorly sorted coarse carbonate sand with approximately 30% coral, 30% mixed of shell fragments and foraminifera tests and 40% unidentified sand to silt size grains. Comparing the Landsat image with Teichert and Fairbridge's

(1948) aerial photographs indicates that the intertidal sand is relatively stable in the south, where it encircles Adele Island (the vegetated sand cay), but forms mobile sand waves in the north (Fig. 5.2).

*Coral rubble and carbonate sand:* Coral rubble and coarse carbonate sand is the dominant reef flat sediment facies. This habitat is distributed around the sand cay and on the outer reef flat especially along the north side of the reef platform. The sediments around the sand cay are exposed at every low tide while those on the outer reef flat and especially on the NE side are only exposed below mean low water spring (MLWS).

*Coralgal pavement:* An extensive coralgal pavement is distributed over the intertidal reef flat and forms low-relief ridges on the outer reef flat. The pavement is approximately colonised by 10% macroalgae, primarily *Sargassum*, and 20% coral colonies of the genera *Goniastrea*, *Acropora*, *Porites*, and *Favites* (Fig. 5.3. AR1-AR3). A broad 1–2 km wide intertidal coralgal pavement, completely exposed at MLWS, separates the sand cay from the outer reef flat.

*Crustose coralline algae:* Crustose coralline algae occur in a 100–1000 m wide zone along the outer reef flat, which is broadest on the southern side of the platform, and narrowing on the eastern (leeward) side. This zone forms a broad low-relief reef crest and intergrades with the coralliths and rhodolith assemblage.

*Mixed assemblage of coralliths and rhodoliths:* Coralliths and rhodoliths with a maximum diameter of approximately 8 and 5 cm respectively, accumulate in anastomosing ridges approximately 15–20 cm high toward the outer edge of the reef crest (Fig. 5.3. AR4). They are sub-spherical and mobile, and appear to develop where seawater flows off the elevated reef at low tide.

*Soft and hard corals:* On the SW side of the reef, the forereef slope gently dips seaward to a broad submerged terrace at 25–30 m depth, and then slopes steeply to the surrounding shelf seafloor at 70–90 m depth. The upper few metres of forereef slope are colonised mainly by soft corals, branching *Acropora* and encrusting *Montipora* up to 1 m in diameter.

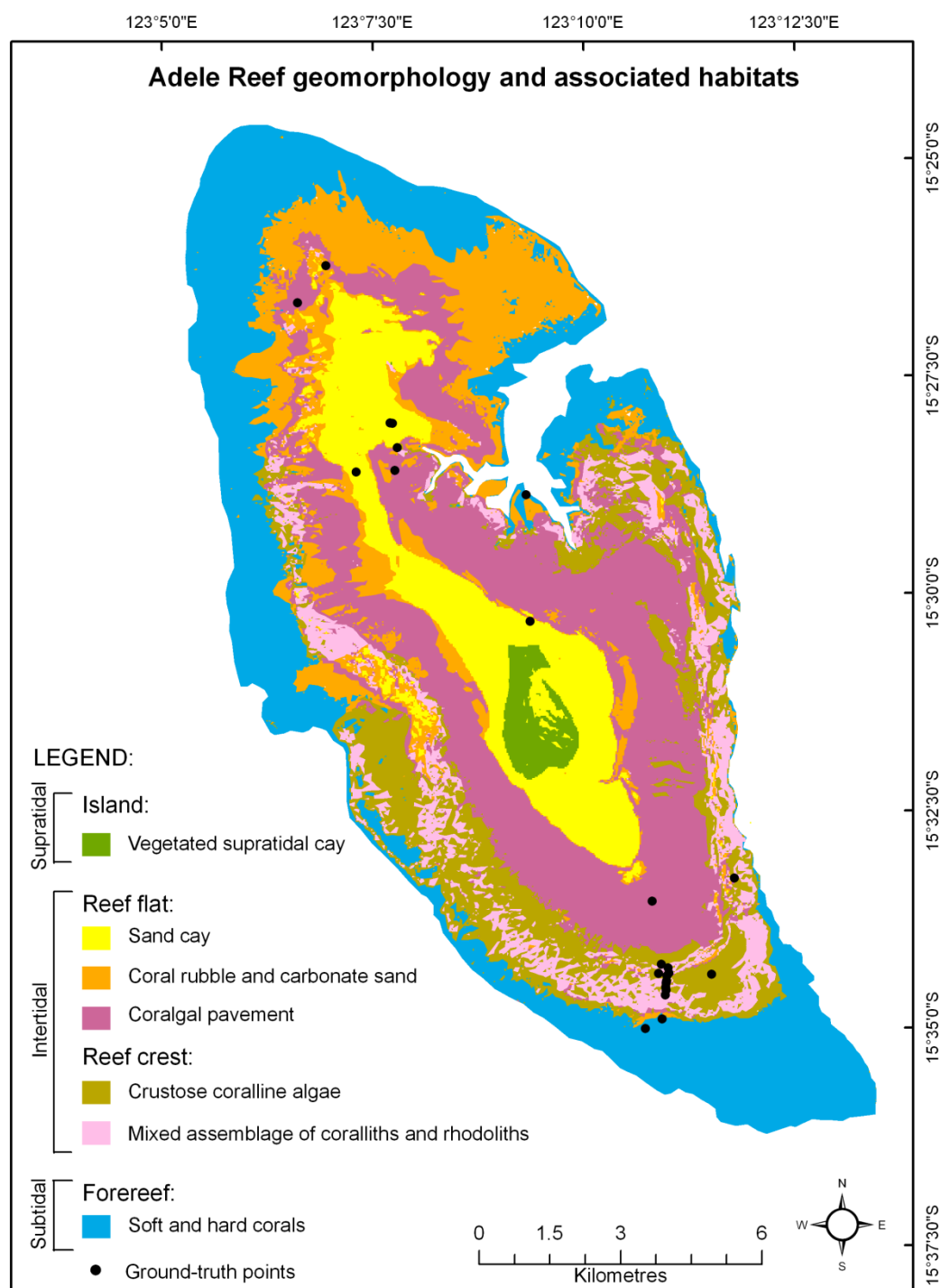


Figure 5.2 Map of Adele platform geomorphology and associated habitats, derived from Landsat 8, 23 May 2015.



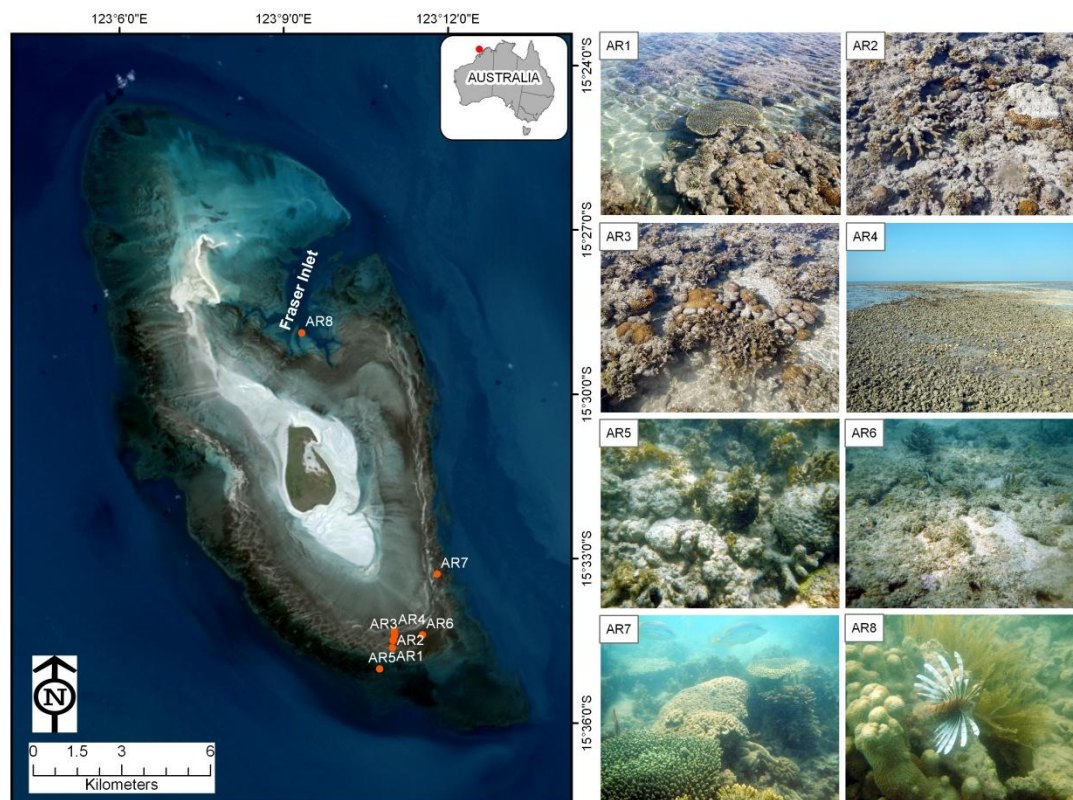


Figure 5.3 Contemporary reef habitats of the Adele Reef platform with ground-truth locations. (AR1) Crustose coralline algae with platy *Acropora*, *Favia*, *Goniastrea*, and macroalgae (*Sargassum*), (AR2) crustose coralline algae with branching *Porites*, *Goniastrea*, and *Sargassum*, (AR3) the extensive shallow pool on reef flat colonised by *Sargassum*, *Favia*, and crustose coralline algae, (AR4) rhodolith banks exposed on low spring tides form low-relief reef crest on the SE reef flat, (AR5) coral rubble and *Sargassum* on the SE outer reef flat, (AR6) *Sargassum* on coral rubble and carbonate sand substrates, (AR7) branching *Acropora* and *Lobophyllia* on the SE outer reef flat, and (AR8) robust branching coral near the narrow drainage channel of Fraser Inlet.

### 5.3.2 Reef architecture and seismic structure

Interpretation of the acoustic horizons across the Adele Reef platform suggests that there are at least three separate stages of reef accretion, bounded by seismic reflectors R1, R2 and R3 (Fig. 5.4).

*R1 Reflector.* R1 (Fig. 5.4; depicted in green in Fig. 5.5) is a high-energy reflector, typically expressed as a horizontal surface that parallels the modern surface morphology between 25 and 35 mbsl. The shallowest reef unit (unit 1, or U1) between R1 and the modern reef surface is up to 30 m thick.

*R2 Reflector.* R2 (Fig. 5.4; depicted in yellow in Fig. 5.5) is a low to medium amplitude reflector and was encountered in the northern portion of Adele Reef, around 40 mbsl. Unit 2 (U2), between R1 (-30 mbsl) and R2 (-40 mbsl), is mostly acoustically transparent and up to 10 m thick.

*R3 Reflector.* This low amplitude reflector R3 (Fig. 5.4; depicted in pink in Fig. 5.5) was detected only within Fraser Inlet, at a depth of about 65 mbsl. Since the bottom of this channel is relatively deep (~ 30 mbsl), the substrate that overlies this reflector is thinner than elsewhere, allowing deeper penetration of the acoustic signal. Seismic unit 3 (U3) is constrained between R2 and R3 and it is at least 20 m thick, with no recognisable internal architecture. Reflector R3 covers a deeper seismic unit, the lower limit of which cannot be detected within the acoustic profiles.



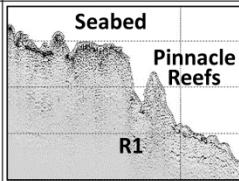
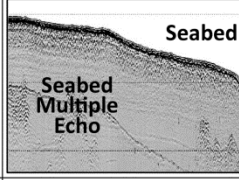
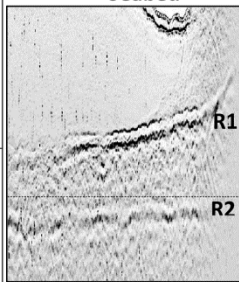
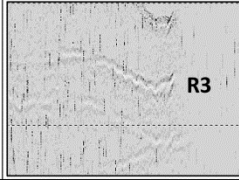
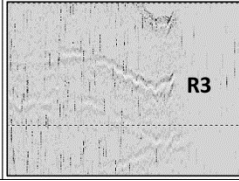
Seismic Unit	Thickness	Limits	Internal Structure	Morphology	Interpretation	Example
U1	Variable: 20-28 m	<b>Top:</b> seabed  <b>Bottom:</b> unconformity R1	Moderate to low amplitude. Local discontinuous and sub-parallel reflectors (H1, H2 and H3)	Reef flat, crest forereef slope. Local pinnacle reefs	Reef facies	
			Well-defined, locally parallel to subparallel, prograding layers. Minor discontinuities	Channel fill. Sediment mounds or drapes	Sediment Bodies	
U2	Variable: 5-10 m	<b>Top:</b> unconformity R1  <b>Bottom:</b> unconformity R2	Weak to moderate amplitude with discontinuous, subparallel minor reflectors	Reef flat, crest, forereef slope. Local pinnacle reef	Reef facies	
U3	~ 22 m	<b>Top:</b> unconformity R2  <b>Bottom:</b> unconformity R3	Low to medium amplitude, mostly acoustically transparent	Reef flat, crest, forereef slope	Reef facies	
U4	NA	<b>Top:</b> unconformity R3  <b>Bottom:</b> NA	Low amplitude	Reef flat	Reef facies	

Figure 5.4 Characteristics of the acoustic features identified in the seismic profiles of Adele Reef (after Bufarale et al., 2016).

The forereef slopes are characterised by irregular topography (Fig. 5.5a) that likely represents pinnacle reefs, or perhaps linear ridges, rimming the reef platform. These features occur at various depths, typically rising from between 27 and 12 mbsl. Most of these structures have an average relief of about 3 m and occur in small groups of three to five pinnacles/ridges. Larger pinnacles/ridges of up to 8 m in height occur in deeper water (> 20 mbsl).

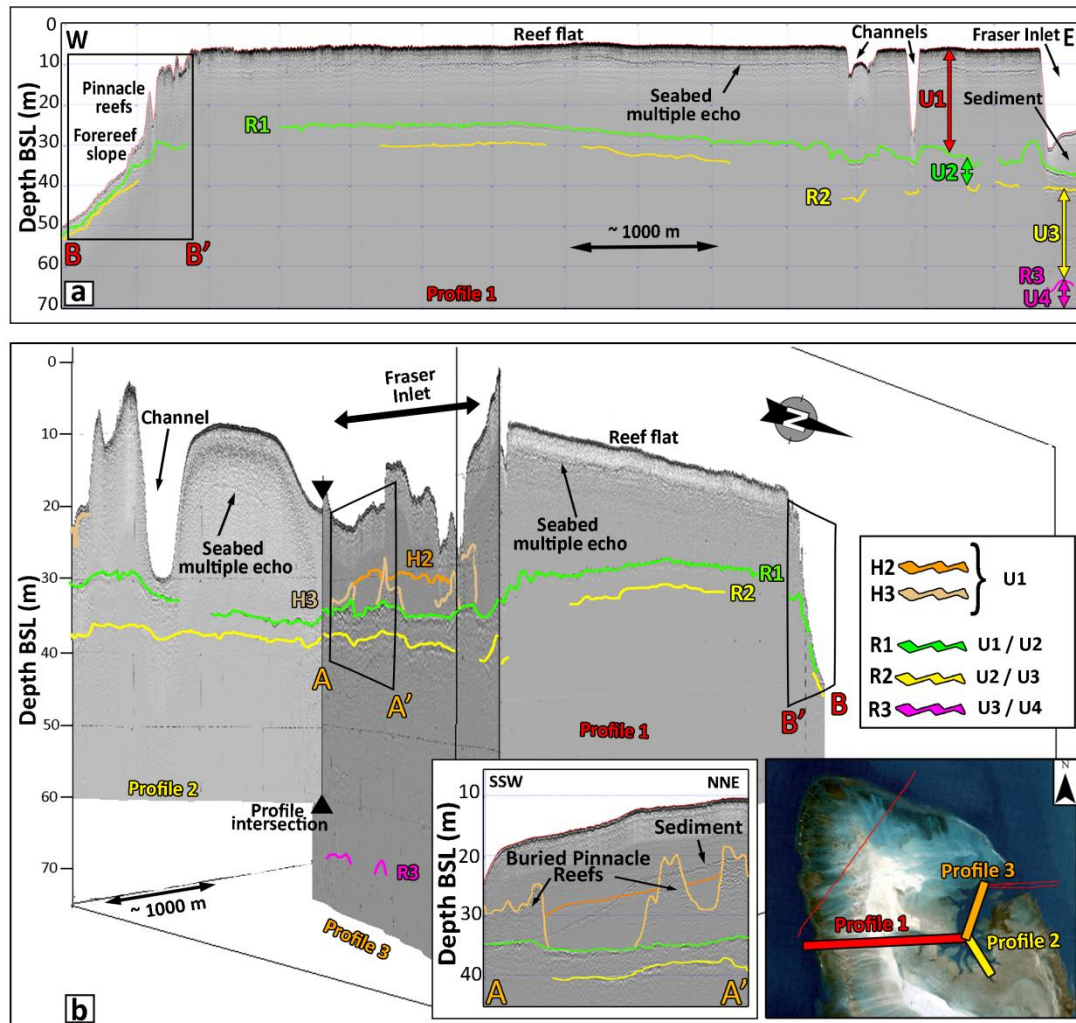


Figure 5.5 Cross-sections showing multiple stages of reef buildup (MIS 1, 5, 7, 9 or 11 respectively). A) Profile 1, oriented W – E, intersects the northern portion of Adele Reef; Modified after Collins et al., 2015. B) Profile 3 runs longitudinally through Fraser Inlet and Profile 2 cuts the southern branch of the Inlet. Holocene reef is 25-35 m thick, with drowned pinnacle reefs on the western forereef slope. Along Fraser Inlet, a series of pinnacle reefs are buried within muddy sediments (left insert). The location of the profiles is shown in insert B at lower right.

Bathymetric and seismic profile across the Adele group of platform reefs reveal a series of deeply incised channels separating the platforms. The channels are relatively broad (between 7 and 30 km) and are oriented in a north-south to northwest-southeast direction, aligning with the river channels along the mainland

coast (Fig. 5.6). The channel separating Adele and Churchill Reef platforms is around 6 km wide and more than 90 m deep. Based on seismic reflection data and the sediments collected with the pipe dredge, the base of this incised channel contains approximately 7 m of thinly bedded fine-grained sediments.

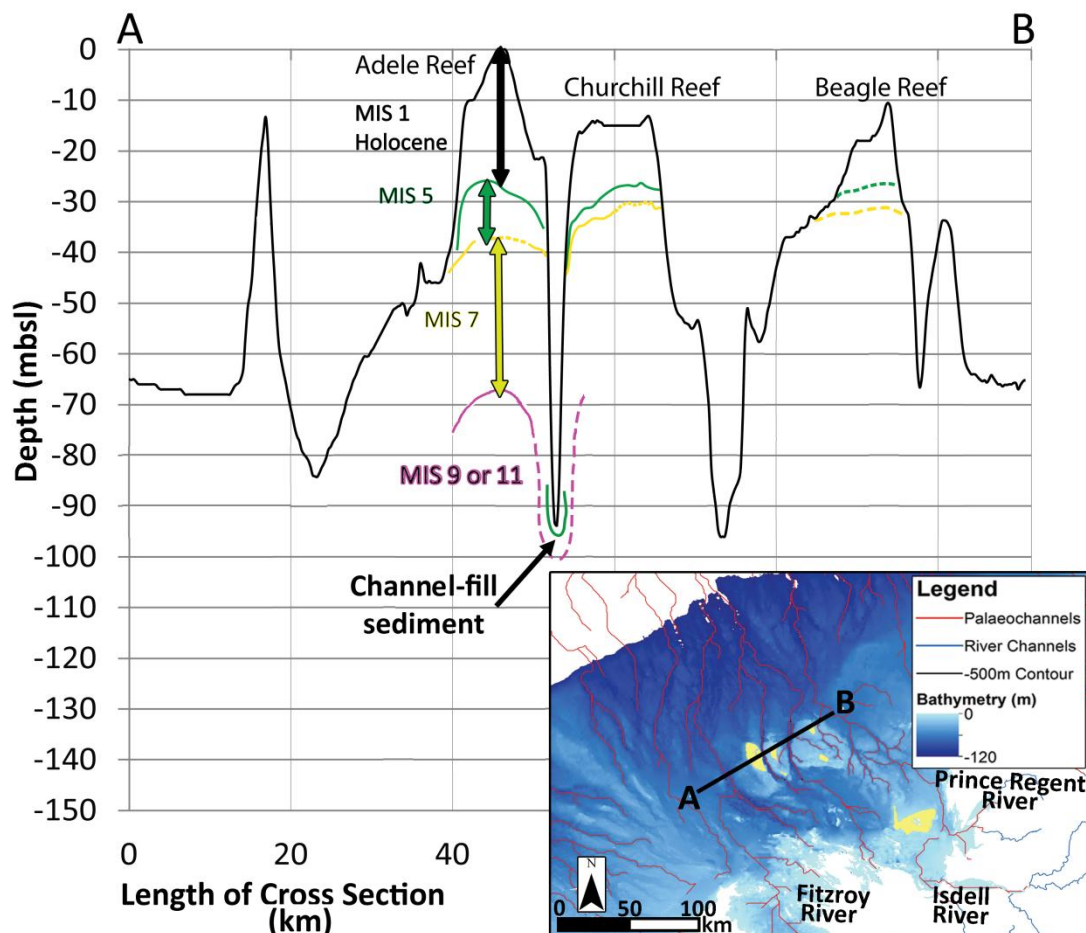


Figure 5.6 Bathymetric and seismic profile across Adele Reef and adjacent platforms (see inset for location). Bathymetry data were sourced from Geoscience Australia's 250-m DEM. Note repeated deep incisions between the platforms, probably by palaeorivers during sea level lowstands. Reef building events are vertically stacked within the platforms as repeated platform growth has occurred during SL highstands (MIS 1, 5, 7, 9 or 11), as interpolated from seismic data. Dashed lines are inferred.

### 5.3.3 Reef stratigraphy and geochronology

Eight percussion cores were collected around Adele Reef: five on the northwest and three on the southeast sides of the platform. Core penetration ranged from 1.84 to 5.06 m. The cored reef facies are primarily detrital; no reef framework was encountered and few colonies were unequivocally in growth position (Fig. 5.7). However the predominance of detrital facies is at least partly due to the selection of coring sites—coralline algal pavement was avoided because it could not be penetrated.

The coarser detrital clasts are predominantly coarse gravel to cobble-sized fragments of domal (dome-shaped) corals, with occasional branching coral fragments. Coral genera recorded include, in estimated order of abundance: *Favia*, *Goniopora*, *Porites*, *Galaxea*, *Acropora*, *Cyphastrea*, *Favites*, *Astreopora*, *Heliopora*, *Lobophyllia*, *Fungia*, and *Pavona*. Matrix sediment is dominated by carbonate sand with an upward coarsening sequence from mud to coarse sand. The carbonate content ranges from 75% (A08) to 91% (A09), and generally increases up section. The non-carbonate materials are terrigenous mud and organics.

Twenty-two coral samples were collected from the cores for radiometric dating (Fig. 5.8, Table 1). Due to the thick Holocene reef build-up (up to 30 m based on seismic data) the shallow reef coring (maximum core penetration of ~5 m) only penetrated the late Holocene. Therefore the timing of reef initiation and the style and rates of reef aggradation over the full growth sequence is unknown. The oldest date, ~5,240–4,960 cal years BP, was obtained from the base of the core A03, 7 mbsl on the NW (seaward) side of the island. The reef sequence on the relatively sheltered SE side of the island is apparently younger; the oldest date there being ~3,155–2,940 cal years BP at 5 mbsl in core A08. At both sites, the reef accreted relatively rapidly (mean 4.2 mm/yr and 3.3 mm/yr respectively) until it attained present LAT level at approximately 4,000 cal years BP in core A03 and 2,000 cal years BP in core A08, and subsequently decelerated to approximately 1.0 and 2.0 mm/yr respectively. Near-surface samples were dated to ~3,225–3,025 cal years BP at 2.9 mbsl in core A04 and ~360–245 cal years BP at 1 mbsl in core A08 (Fig. 5.8, Table 1).



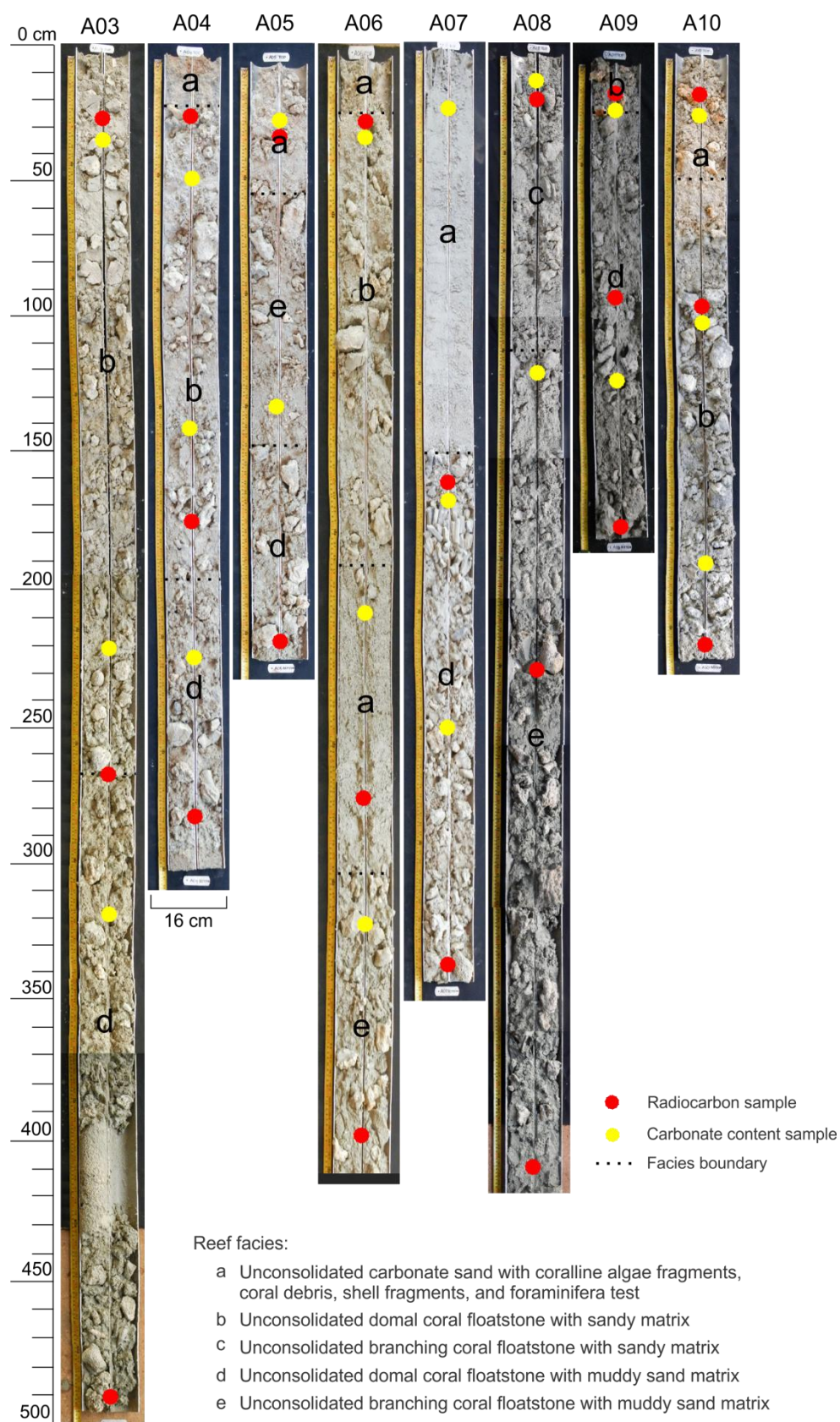


Figure 5.7 Core photograph of Adele Reef showing representative Adele Reef facies where the cores were collected.

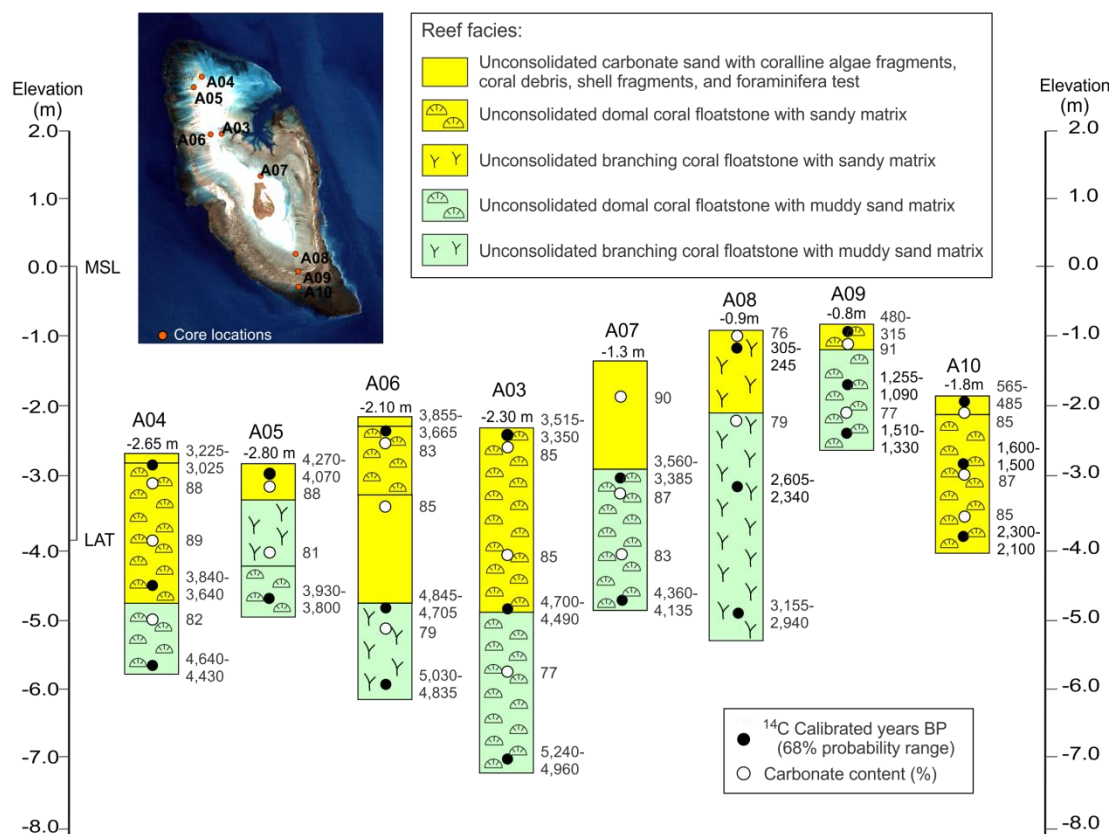


Figure 5.8 Lithostratigraphic and chronostratigraphic summary of Holocene reef facies for Adele Reef. The dominant facies was domal coral but the sections also contain fragments and colonies of branching coral.

Table 5.1 AMS Radiocarbon dates from selected samples across Adele Reef.

Location	Sample Code	Depth (m)	Lab. Code	Material	Method	Measured Age	$^{13}\text{C}/^{12}\text{C}$	Conventional Age (BP)	Calibrated (68% Probability) cal yr BP	Accretion (mm/yr)
Adele I.	A03-43	-2.33	Beta-397758	<i>Favia</i>	AMS	3190 ± 30	+0.3 ‰	3600 ± 30	3515 - 3350	
	A03-269	-4.59	Beta-397759	<i>Goniopora</i>	AMS	4100 ± 30	-2.1 ‰	4480 ± 30	4700 - 4490	1.94
	A03-492	-6.82	Beta-397760	<i>Galaxea</i>	AMS	4500 ± 30	-2.9 ‰	4860 ± 30	5240 - 4960	4.42
	A04-25	-2.75	Beta-425803	<i>Favia</i>	AMS	2930 ± 30	+0.4 ‰	3350 ± 30	3225 - 3025	
	A04-175	-4.25	Beta-425791	<i>Acropora</i>	AMS	3490 ± 30	-2.6 ‰	3860 ± 30	3840 - 3640	0.4
	A04-284	-5.34	Beta-425792	<i>Lobophyllia</i>	AMS	4040 ± 30	-0.2 ‰	4450 ± 30	4640 - 4430	1.3
	A05-29	-2.89	Beta-425793	<i>Acropora</i>	AMS	3780 ± 30	-1.2 ‰	4170 ± 30	4270 - 4070	
	A05-217	-4.77	Beta-425794	<i>Favites</i>	AMS	4270 ± 30	+0.7 ‰	4690 ± 30	4930 - 4800	2.7
	A06-25	-2.25	Beta-425795	<i>Faviid</i>	AMS	3460 ± 30	+0.1 ‰	3870 ± 30	3855 - 3665	
	A06-278	-4.78	Beta-425796	<i>Acropora</i>	AMS	4210 ± 30	+0.4 ‰	4630 ± 30	4845 - 4705	2.5
	A06-400	-6	Beta-425797	<i>Acropora</i>	AMS	4370 ± 30	-1.1 ‰	4760 ± 30	5030 - 4835	7.7
	A07-180	-1.8	Beta-425798	<i>Lobophyllia</i>	AMS	3250 ± 30	-1.0 ‰	3640 ± 30	3560 - 3385	
	A07-341	-3.41	Beta-425799	<i>Favia</i>	AMS	3820 ± 30	-0.5 ‰	4220 ± 30	4360 - 4135	2.1
	A08-18	-1.68	Beta-397761	<i>Favia</i>	AMS	250 ± 30	+2.5 ‰	700 ± 30	360 - 245	
	A08-226	-3.76	Beta-397762	<i>Lobophyllia</i>	AMS	2450 ± 30	-3.8 ‰	2800 ± 30	2605 - 2340	0.9
	A08-416	-5.66	Beta-397763	Coralline algae	AMS	2880 ± 30	-0.3 ‰	3290 ± 30	3155 - 2940	3.3
	A09-26	-2.36	Beta-425800	<i>Chypastrea</i>	AMS	440 ± 30	-1.4 ‰	830 ± 30	480 - 315	
	A09-100	-3.1	Beta-425801	Coralline algae	AMS	1240 ± 30	+1.0 ‰	1670 ± 30	1255 - 1090	0.9
	A09-177	-3.87	Beta-425802	<i>Porites</i>	AMS	1530 ± 30	-0.4 ‰	1930 ± 30	1510 - 1330	3.1
	A10-14	-2.84	Beta-425804	<i>Rhodoliths</i>	AMS	580 ± 30	-0.5 ‰	980 ± 30	565 - 485	
	A10-128	-3.98	Beta-425806	<i>Porites</i>	AMS	1650 ± 30	-0.3 ‰	2060 ± 30	1655 - 1500	1.1
	A10-211	-4.81	Beta-425805	<i>Galaxea</i>	AMS	2190 ± 30	-0.8 ‰	2590 ± 30	2300 - 2110	1.3

## 5.4 Discussion

### 5.4.1 Reef stratigraphy and sea-level changes

Seismic surveys across Adele Reef reveal multiple stacked seismic units that likely represent distinct phases of reef accretion during sea level highstands. The seafloor and seismic reflectors R1, R2, and R3 correspond to the top of each seismic unit. Although it is not possible to establish the age of each seismic unit due to the limitations in core penetration (max depth 5 m), the age can be inferred based on a comparison with seismic, stratigraphic and chronological data from the outer shelf Scott Reef, 200 km NW of Adele Reef (Collins et al., 2011) and the inner shelf Kimberley reefs, 70 km SW of Adele Reef (Solihuddin et al., 2015).

Reflector R1, identified at a depth of 25-35 mbsl on Adele Reef (Fig. 5.5), was also recorded on the inner shelf of Cockatoo Island and the shelf edge Scott Reefs (see Fig. 5.1 for location). On Cockatoo Island an open cut iron ore pit has exposed a complete Holocene section, allowing the R1 reflector to be directly correlated with the logged stratigraphic contact. Solihuddin et al. (2015) found that the depth of the R1 reflector at 15 to 20 mbsl corresponded closely with the Holocene/Last Interglacial (LIG) stratigraphic contact in the mine pit, measured at 15 to 18 mbsl. At Scott Reef, the R1 reflector occurs from 26 mbsl (interpreted as a palaeoreef crest; Collins et al., 2011), a similar depth to Adele, down to 58 mbsl (interpreted as a palaeoreef lagoon; Collins et al., 2011). Shallow bore-holes made by Woodside Energy Ltd in 2006/07, and analysed by Collins et al. (2011), found the Scott Reef Holocene sequence rested unconformably on a karstified LIG reef exposure surface. U-series analysis of corals beneath the R1 reflector at Scott Reef returned ages of 125,000 and 130,000 cal years BP. Therefore we infer that R1 on Adele Reef also marks the LIG unconformity surface and seismic unit U1 is a Holocene reef sequence up to 30 m thick.

Reflector R2 occurs at a depth of 30-40 mbsl on Adele Reef. A similar second reflector was identified Scott Reef at a depth of 58 m, and was interpreted as a Marine Isotope Stage (MIS) 7 exposure surface, based on a U-series age of 208,000 cal years BP (Collins et al., 2011). Based on the Scott Reef observations we interpret R2 at Adele Reef to also represent the MIS 7 exposure surface. R2 was not observed in any of the inner shelf seismic surveys (Bufarale et al., 2016) or in the mine pit



stratigraphic section of Cockatoo Island (Solihuddin et al., 2015), perhaps indicating that this area remained above sea level during MIS 7.

Reflector R3 is the lowermost unconformity at 65 mbsl (Fig. 5.5). R3 was only observed along seismic lines within the 30 m deep Fraser Inlet. Its apparent absence along the main Adele Reef platform may be due to energy loss with increasing depth; i.e R3 may be more extensive, but not detected. The Adele Island 1 stratigraphic log shows limestone to a depth of 160 mbsl so it is likely that R3 is a middle to late Pleistocene unconformity surface. It may correlate to the third stratigraphic unconformity at 90 mbsl in Scott Reef (Collins et al., 2011). A coral sample immediately below this unconformity returned a U-series age of 313,000 cal years BP (Collins et al., 2011), suggesting that the R3 reflector at Scott Reef, and potentially also at Adele Reef, is the MIS 9 exposure surface.

Fraser Inlet presently has a broad flat sandy mud floor, however seismic profiling along and across the axis of the channel reveals a buried complex of pinnacle reefs. The pinnacle reefs are considered to be of early Holocene age as they sit atop the R1 reflector. Sedimentation was probably minimal during the early-middle Holocene catch-up phase, however as the reef platform reached sea level around 3,000 years BP, sediment delivery into Fraser Inlet probably increased, eventually burying the pinnacles.

There is evidence of cross shelf fluvial incision as seen in a series of deep channels that dissect the main platforms of Adele, Churchill, and Beagle Reefs. The channel floors have depths of more than 65 mbsl and likely represent glacial lowstand palaeoriver channels, possibly tributaries of the Fitzroy, Isdell and Prince Regent Rivers (Fig. 5.6).

#### **5.4.2 Mode of Holocene growth**

The early to mid-Holocene history of Adele Reef remains unknown due to the limited core penetration. Holocene sea-level reconstructions (Collins et al., 2006; 2011) suggest that the subaerial LIG surface of Adele Reef would have been transgressed at ~10,000 years BP. Subsequent colonisation and accretion was relatively rapid, as the reef was already up to 20 m thick at the time of the earliest core dates (~5,000 years BP). The internal seismic structure of the Holocene reef appears uniform, consistent with simple vertical aggradation of an extensive low-

relief cover of coral and sediment, as inferred for Cockatoo Island where the complete Holocene section was sampled (Solihuddin et al., 2015). Adele Reef at this time may have resembled the coral-rich submerged banks reported from the Timor Sea by Heyward et al. (1997). The flanks of the platform are topographically complex and appear to be slowly prograding through pinnacle reef growth and platform-derived sedimentation.

The cores indicate a ‘catch-up’ growth pattern in the late Holocene, with the reef surface being approximately 5-10 m deep when sea level stabilised at its present elevation 6,500 years BP (Collins et al., 2006). The ‘catch-up’ pattern on Adele Reef coincides with a ‘catch-up’ phase from 5,500 years BP at Cockatoo Island, after a short initial period of ‘keep-up’ growth followed by deeper submergence (Solihuddin et al., 2015). Accretion slowed as Adele reef reached the intertidal zone, probably due to increasing wave energy and periodic emergence on spring low tides, as inferred for Scott Reef (Collins et al., 2011). The central and northern parts of the platform reached sea level around 3,000 years BP, whereas the southern part of the platform reached sea level only very recently.

### **5.4.3 Comparison with other reef systems**

The Kimberley Bioregion has abundant inner shelf fringing reefs but relatively few mid and outer shelf reefs. This contrasts with the Great Barrier Reef (GBR), which has more mid and outer shelf reefs than inner shelf reefs. The Kimberley and the GBR reefs also differ in that the Kimberley reefs are generally flat-topped platforms (Brooke, 1997; Wilson, 2013; Kordi et al., 2016) whereas most GBR reefs have a raised marginal rim surrounding a deeper lagoon (Maxwell, 1968; Hopley et al., 2007).

Adele Reef differs from the inshore Buccaneer Archipelago in its relatively exposed oceanic setting, smaller tidal range (7 m vs 11 m), deeper surrounding bathymetry, lower freshwater input, and lower turbidity. These contrasts result in obvious differences in the surface features of Adele, including the presence of a sand cay and the absence of mangroves. However there are also similarities between the mid-shelf and inshore reefs, particularly the abundance of coralline algae and the development of coralline algal ridges, although these consist largely of uncemented

rhodoliths on Adele whereas they are often strongly cemented framework structures on the inshore platform (Richards and O'Leary, 2015; Solihuddin et al., 2016).

Subsurface facies of Adele Reef differ from those inshore, consisting predominantly of matrix-supported transported domal coral fragments and sand at Adele versus in-situ branching *Acropora*-rich muddy units inshore (Solihuddin et al., 2015, 2016). This difference is probably due to the greater exposure of Adele to wave action and cyclones. Reef accretion patterns and rates between Adele and the inshore reefs appear broadly similar, with 'catch-up' growth predominating at both sites and accretion rates averaging  $< 5$  mm/yr, although some more rapid intervals (up to 27 mm/yr) were recorded in the intensively-sampled Cockatoo Island sequence (Solihuddin et al., 2015).

#### 5.4.4 Cross shelf profile of Holocene reef accretion

A schematic cross-shelf profile of Holocene reef accretion (Fig. 5.9) was drawn from Cockatoo Island (inner-shelf), to Adele Reef (mid-shelf) and Scott Reefs on the edge of the continental shelf (outer-shelf). Stratigraphic data from Cockatoo Island and other inner-shelf reefs suggest that the LIG reef beneath the Holocene reef is 15 to 20 mbsl, suggesting a maximum subsidence rate of 0.12 mm/yr (Solihuddin et al., 2015). Collins et al. (2011) reported the upper LIG reef surface of 26 m Scott Reefs, estimating the post-LIG subsidence rate of Scott Reefs to be  $\sim 0.2$  mm/yr. Similarly, seismic profiles at Adele Reef indicate that the upper LIG reef surface is 25 mbsl (Fig. 5.5), giving an inferred subsidence rate of  $\sim 0.2$  mm/yr. So while the subsidence of the NW is well documented, particularly in the petroleum well (Ingram, 1982; Marshall, 1995) and seismic data (Bufarale et al., 2016) this study is able to constrain rates based on the elevation of the Holocene/LIG unconformity surface.

This cross shelf dataset of LIG reef elevations provides the first quantitative estimate of neotectonic subsidence rates across the NW shelf of Australia, spanning the last 120,000 years. Interestingly, subsidence appears to change at a relatively uniform rate of 0.2 m across the mid to outer shelf with a lower rate of 0.12 along the inner shelf. This difference may be a function of the underlying structural geology which borders the Proterozoic Kimberley basement rocks and the offshore Browse

Basin sediments on which both the Adele and Scott Reefs are situated. The higher rate of subsidence across the middle and outer shelf relative to the inner shelf has provided additional accommodation space to build thicker Holocene sequences, as has been recorded on the GBR (Browne et al., 2012).

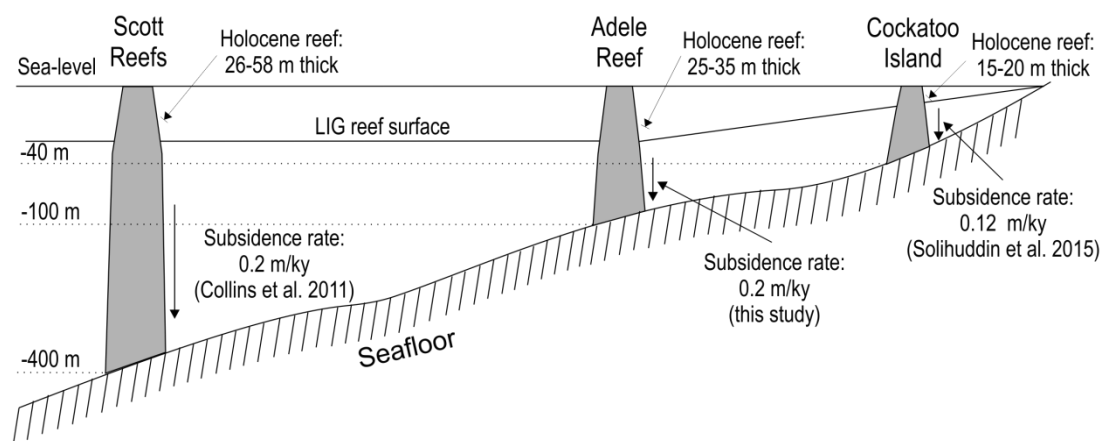


Figure 5.9 Diagrammatic cross-shelf profile of Holocene reef growth from Cockatoo Island in the inner-shelf to Adele Island in the mid-shelf and Scott Reefs in the outer-shelf, showing estimated post-LIG subsidence rates of 0.12 mm/yr at Cockatoo Island, 0.2 mm/yr at Adele Island, and 0.2 mm/yr at Scott Reef.

## 5.5 Conclusions

This study is the first investigation of the Holocene geomorphology and accretion history of a mid-shelf platform reef of the Kimberley Bioregion.

Sub-bottom profiles of Adele Reef show at least three stages of reef accretion bounded by reflectors. The shallowest reflector at 25-35 mbsl is interpreted as the Holocene/LIG (MIS 5) contact. Deeper reflectors are interpreted as boundaries between MIS 5 and MIS 7 at depths of 30-40 mbsl and between MIS 7 and MIS 9 at 65 mbsl.

The Holocene sequence is up to 30 m thick. Cores from the uppermost 5 m of the sequence indicate that the reef accreted in a 'catch-up' mode, with accretion rates decreasing as the reef platform approached sea level. The cores were dominated by detrital domal coral colonies and fragments in a sandy matrix, in contrast with the in-

situ, branching *Acropora* and mud-rich subsurface facies of inshore reefs. These differences likely reflect Adele's higher energy setting and greater exposure to cyclones. Coralline algae is a significant component of the contemporary intertidal and shallow subtidal reef surface but was underrepresented in the cores due to the difficulty of percussion coring in this habitat.

The mean post-LIG subsidence rate of the Adele Reef platform was estimated from seismic records to be 0.2 mm/yr. This supports a hinge subsidence hypothesis for the Kimberley coast and adjacent shelf, with greater subsidence on the outer shelf (Scott Reef) and mid shelf (Adele Reef) than inshore (Cockatoo Island).

### Acknowledgments

The Kimberley Reef Geomorphology Project 1.3.1 was funded by the Western Australian State Government and partners of the Western Australian Marine Science Institution. This paper is dedicated to the memory of our former project leader, the late Professor Lindsay Collins, for his inspiring ideas and contribution to our knowledge of Western Australia's seafloor and coral reefs. The research was assisted by the Kimberley Marine Research Station at Cygnet Bay who provided vessel support and access to research facilities. We would like to thank WA Museum for providing ground truth data through the WA Museum/Woodside Collection Project (Kimberley) 2008-2011. We also thank Geoscience Australia (GA) for providing DEMs data and the United States Geological Survey (USGS) for providing Landsat imagery. Last but not least, special thanks to valued members of the research team at Curtin University: Alexandra Stevens and Moataz Kordi.

Conflict of interest: The authors declare that there is no conflict of interest with third parties.

### References

- Brooke, B. (1997). Geomorphology of the north Kimberley coast, Part 9. In: Walker, D. (ed.), Marine biological survey of the central Kimberley coast. Western Australia. University of Western Australia, Perth, unpublished report, W.A. Museum Library No. UR377, 13–39.

- Browne, N.K., Smithers, S.G, Perry, C.T. (2012). Coral reefs of the turbid inner-shelf of the Great Barrier Reef, Australia: An environmental and geomorphic perspective on their occurrence, composition and accretion. *Earth Science Reviews* 115(1–2): 1–20.
- Bufarale, G., Collins, L.B., O’Leary, M.J., Stevens, A.M., Kordi, M., Solihuddin, T. (2016). Quaternary onset and evolution of Kimberley coral reefs (Northwest Australia) revealed by high-resolution seismic imaging. *Continental Shelf Research*, 123:80-88.
- Collins, L. B. (2011). Geological setting, marine geomorphology, sediment and oceanic shoals growth history of the Kimberley Region. *Journal of the Royal Society of Western Australia*, 94(2), 89-105.
- Collins, L. B., Testa, V., Zhao, J., Qu, D. (2011). Holocene growth history and evolution of the Scott Reef carbonate platform and coral reef. *Journal of the Royal Society of Western Australia*, 94(2) 239–250.
- Collins, L.B., Zhao, J.X., Freeman, H. (2006) A high-precision record of mid–late Holocene sea-level events from emergent coral pavements in the Houtman Abrolhos Islands, southwest Australia. *Quaternary International* 145–146(0): 78–85.
- Collins, L. B, O’Leary, M. J, Stevens, A. M, Bufarale, G., Kordi, M., Solihuddin, T. (2015). Geomorphic patterns, internal architecture and reef growth in a macrotidal, high-turbidity setting of coral reefs from the Kimberley Bioregion. *Australian Journal of Maritime and Ocean Affairs*, 7(1), 12-22.
- Department of the Environment, Water, Heritage and the Arts, DEWHA (2008). A characterisation of the marine environment of the North-west Marine Region: Perth Workshop Report, A Summary of an Expert Workshop Convened in Perth, Western Australia, 5-6 September 2007, Commonwealth of Australia, Hobart.
- Embry, A. F., Klovan, J. E. (1971). A late Devonian reef tract on northeastern Banks Island, N.W.T. *Bulletin of Canadian Petroleum Geology*, 19(4), 730–781.

- Heyward, A.J., Pinceratto, E., Smith, L.D. (1997) Big Bank Shoals of the Timor Sea: an environmental resource atlas. Australian Institute of Marine Science & BHP Petroleum. 115p.
- Hopley, D., Smithers, S., Parnell, K. (2007). The Geomorphology of the Great Barrier Reef: Development, diversity, change. Cambridge University Press, Cambridge, UK.
- Ingram, B. S. (1982). Palynological examination of samples from Adele Island No. 1 from Well Completion Report, Brunswick Oil N. L.
- Kordi, M., Collins, L. B., O'Leary, M., Stevens, A. (2016). ReefKIM: An integrated geodatabase for sustainable management of the Kimberley Reefs, North West Australia. *Ocean & Coastal Management*, 119, 234-243.
- Lough, J.M. (1998) Coastal climate of northwest Australia and comparisons with the Great Barrier Reef: 1960 to 1992. *Coral Reefs* 17(4): 351–367.
- Marshall, N. G. (1995). Adele Island No. 1 Palynological Report. Woodside Offshore Petroleum.
- Maxwell, W.G.H. (1968) Atlas of the Great Barrier Reef. Elsevier. 258pp.
- Montaggioni, L. F. (2005). History of Indo-Pacific coral reef systems since the last glaciation: Development patterns and controlling factors. *Earth-Science Reviews*, 71(1-2), 1–75.
- Müller, G., Gastner, M. (1971). The 'Karbonat-Bombe', a simple device for the determination of carbonate content in sediment, soils, and other materials. *Neues Jahrbuch für Mineralogie-Monatshefte*, 10, 466–469.
- Pearce, A. F., Griffiths, R. W. (1991). The Mesoscale Structure of the Leeuwin Current: A comparison of laboratory models and satellite imagery. *J Geophys Res*, 96(C9), 16739-16757.
- Reimer PJ, Bard E, Bayliss A, Beck JW, Blackwell PG, Bronk Ramsey C, Buck CE, Cheng H, Edwards RL, Friedrich M, Grootes PM, Guilderson TP, Hafliðason H, Hajdas I, Hatté C, Heaton TJ, Hoffmann DL, Hogg AG, Hughen KA, Kaiser KF, Kromer B, Manning SW, Niu M, Reimer RW, Richards DA, Scott EM, Southon JR, Staff RA, Turney CSM, van der

- Plicht J (2013). IntCal13 and Marine13 radiocarbon age calibration curves 0–50,000 years cal BP. *Radiocarbon* 55(4):1869–1887.
- Richards, Z. T., Bryce, M., Bryce, C. (2013). New records of atypical coral reef habitat in the Kimberley, Australia. *Journal of Marine Biology*. doi:10.1155/2013/363894.
- Richards, Z. T., O’Leary, M. J., 2015. The coralline algal cascades of Tallon Island (Jalan) fringing reef, NW Australia. *Coral Reefs*, 34(2), 595.
- Richards, Z.T., Bryce, M., Bryce, C. (2013) New records of atypical coral reef habitat in the Kimberley, Australia. *Journal of Marine Biology*. 2013:1-8.
- Solihuddin, T., Collins, L. B., Blakeway, D., O’Leary, M. J. (2015). Holocene coral reef growth and sea level in a macrotidal, high turbidity setting: Cockatoo Island, Kimberley Bioregion, northwest Australia. *Marine Geology*, 359, 50–60.
- Solihuddin, T., O’Leary, M.J., Blakeway, D., Parnum, I., Kordi, M., Collins, L. B. (2016). Holocene reef evolution in a macrotidal setting: Buccaneer Archipelago, Kimberley Bioregion, Northwest Australia. *Coral Reefs*. 783-794.
- Teichert, C., Fairbridge, R. W. (1948). Some coral reefs of the Sahul Shelf. *Geographical Review*, 28(2), 222–249.
- Veron, J. E. N. (2000). *Corals of the world*. Australian Institute of Marine Science 1-3, 1,382 pp.
- Wentworth, C. K. (1922). A scale of grade and class terms for clastic sediments. *The Journal of Geology*, 30(5), 377-392.
- Wilson, B. R. (2013). *The Biogeography of the Australian North West Shelf: Environmental Change and life’s response*. Elsevier, Burlington MA, USA.



## Chapter 6

### Reconstruction of Holocene sea-level and reef accretion history

#### 6.1 Holocene sea-level and reef accretion history

The Kimberley Bioregion of the Northwest Australian Shelf is considered to have been a relatively tectonically stable continental shelf during the Quaternary (Collins et al., 2006) and is categorised as a ‘far-field’ location, providing a good example for observing sea-level events and palaeo-shoreline reconstruction. In such an environment, the effects of seafloor compaction, subsidence, and hydro-isostatic compensation are negligible during a relatively short time interval of thousands of years (Lambeck et al., 2002; Wong et al., 2003). However, the macrotidal conditions of the Kimberley Bioregion are a complicating factor, as the best place for sea-level studies is in microtidal conditions with corals that are always found in shallow water such as *Acropora palmata* on the Caribbean Reefs (Smithers, 2011). Therefore, all available sea-level proxies in this study are limited by the macrotidal (up to 11 m) conditions, as such; the sea level curves are better described as reef accretion history curves.

Studies on Holocene sea-level and reef accretion history near the Kimberley Shelf have been carried out on reef core data from Morley Island in the Abrolhos which resembles a ‘keep-up’ reef mode (Collins et al., 1993; Eisenhauer et al., 1993), cemented coral shingle pavement from the Abrolhos Reefs (Collins et al., 2006), and reef core data from Scott Reef (Collins et al., 2011). Existing reef records from and adjacent to the Kimberley Bioregion incorporating new data obtained from this study provide a composite Holocene reef accretion history with a modified Houtman Abrolhos sea-level curve (Fig. 6.1).

The radiocarbon ages of each dated core sample are plotted against metres below sea-level (mbsl). The curve indicates that the Holocene sea-level transgression and reef accretion history in the inshore Kimberley Bioregion was initiated at ~10k yr BP when sea-level was estimated at around 20 mbsl. At this time, the rising sea-level drowned the Kimberley Shelf and provided different substrates and foundation types for reef accretion, marking the initiation of reef deposits and accumulation. Late Holocene highstands at ~6k yr BP are recorded in the microtidal Ningaloo Reef

and Abrolhos Reefs, Southwest Australia, where there has been little or no subsidence. Whereas, there is no similar highstand recorded at Scott Reef of the Oceanic Shoals and reefs in the inshore Kimberley such as Cockatoo, Tallon, Sunday, and Irvine/Bathurst Islands with macrotidal conditions and significant post-Last Interglacial (LIG) subsidence. Finally, the sea level fell gradually returning to present-day level at nearly modern time (approx. 1k yr BP) (Fig. 6.1).

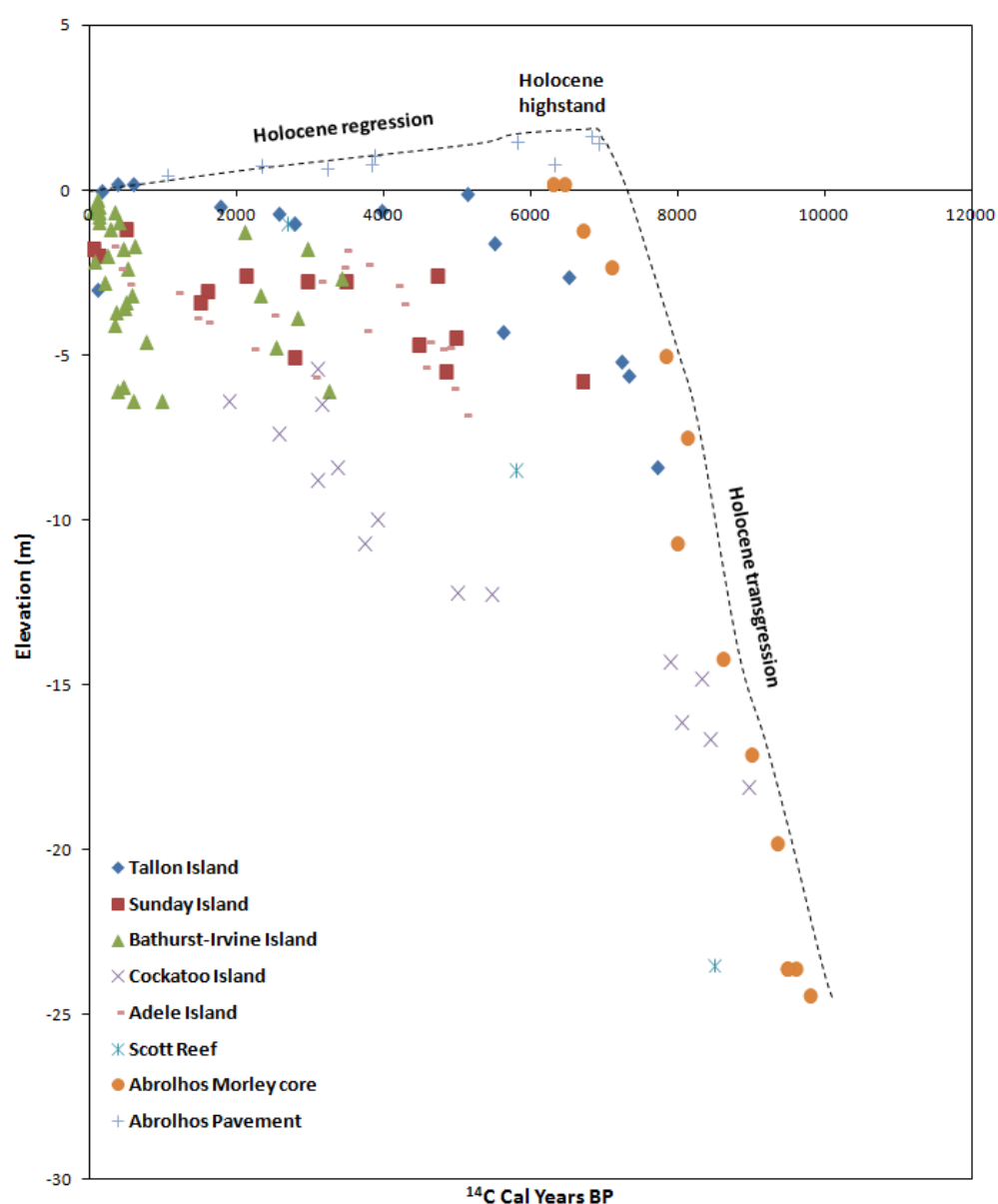


Figure 6.1 Composite Holocene reef accretion history for the Kimberley Shelf with a modified Houtman Abrolhos sea-level curve from the past 10,000 years BP derived from coral exposure in the Cockatoo Island mine pit

(Solihuddin et al., 2015), coral and crustose coralline algae in cores from Tallon Island, Sunday Island, Bathurst/Irvine Islands (Solihuddin et al., 2016), coral in cores from Adele Reef (Solihuddin et al., 2016), coral in cores from Scott Reef (Collins et al., 2011), cemented coral shingle pavement from the Abrolhos Reefs (Collins et al., 2006), and corals in core from Morley Island, Abrolhos (Eisenhauer et al., 1993).

## 6.2 Drowning Kimberley Shelf model

By combining bathymetry and sea-level data derived from reef geochronology, a drowning history can be reconstructed showing key events of coastal and coral reef evolution (Fig. 6.2). Sea-levels are believed to have globally fluctuated by more than 120 m at various times since the LIG (some 125,000 years ago). During this time, sea-level in the west Australian continent was at 0.2 – 1.6 m above that of today enabling reefs to be exposed above the contemporary shoreline, as seen in the Ningaloo and Abrolhos coral pavement. A series of oscillations might have led sea level to fall for a brief period of an extreme low of 125 mbsl at the Last Glacial Maximum (LGM, some 19,000 years ago), resulting in a very large exposure of dissected coastal plain connected to the present-day mainland as wide as approx. 200 km to the shelf margin. The Rowley Shoals and Scott Reef, situated about 110 km and 90 km east of the LGM coastline respectively, were exposed as remnants from LIG reef building (Fig 6.2).

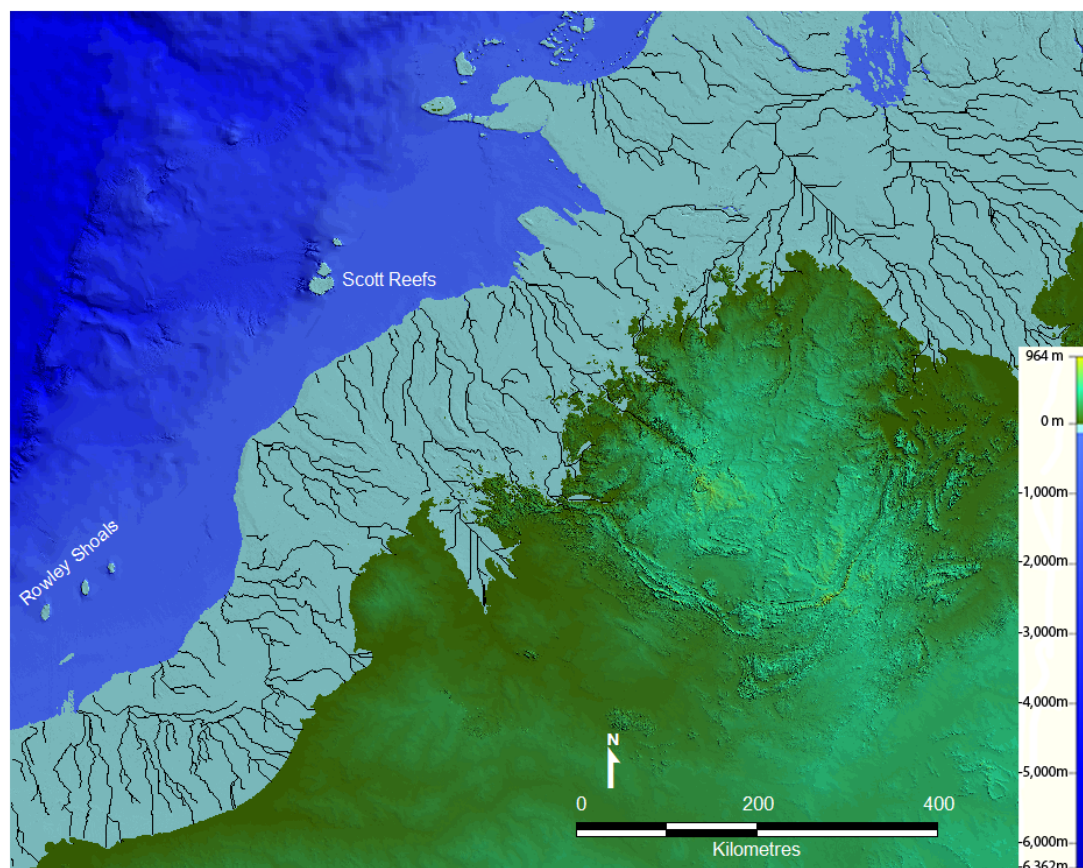


Figure 6.2 Kimberley shelf exposure at Last Glacial Maximum, ~19,000 yr BP with channel dissections on a coastal plain; sea-level is estimated at 125 mbsl. Scott Reefs and Rowley Shoals were exposed as remnants from LIG reef building.

Following the withdrawal of the LIG seas, the Kimberley shelf would have been a coastal plain dissected by rivers until its subsequent drowning during the post-glacial time. The pattern of channel dissection on the shelf led to remnant topographic highs or salients which in turn provided elevated substrates suitable for coral reef colonisation, for example, the Adele Complex of platform reefs to the northwest of Cockatoo Island. During the melt-water pulse (MWP-1A), some ~14,000 yr BP (Fairbanks, 1989), sea-level rose rapidly to 80 mbsl and partly inundated the Kimberley Shelf. However, the present-day inner-shelf reefs of the Adele complex, comprising Adele Reef and its neighbours Churchill, Mavis, Albert, Beagle, and Brue Reefs, were still exposed (as remnants from LIG reef building) and connected to the mainland (Fig 6.3).

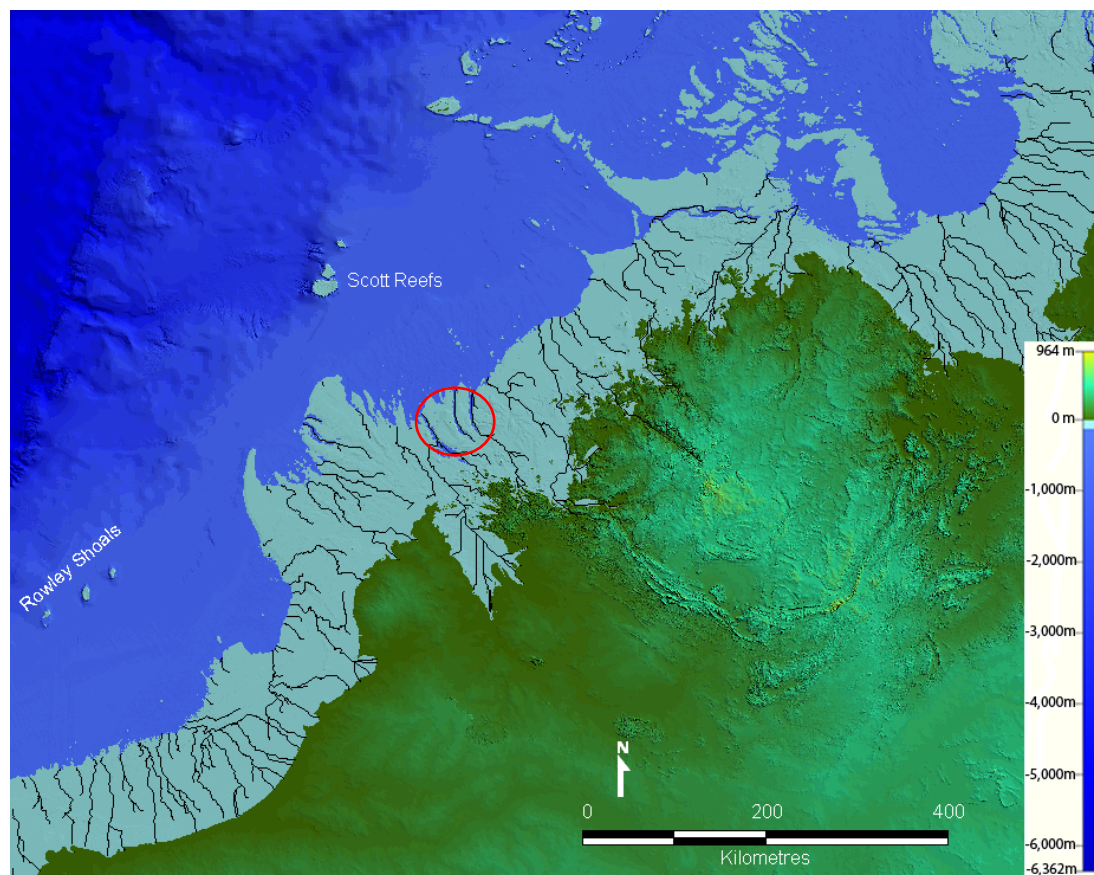


Figure 6.3 Kimberley shelf exposure at ~14,000 yr BP (MWP 1A) with channel dissections separating limestone hills of pre-existing LIG reefs at Adele complex (circled); sea-level is estimated 80 mbsl.

Following that, sea-levels continued to experience a rapid rise and reached around 40 mbsl at about 11,500 yr BP (MWP-1B of Fairbanks, 1989), isolating the Adele complex from the mainland (Fig 6.4).



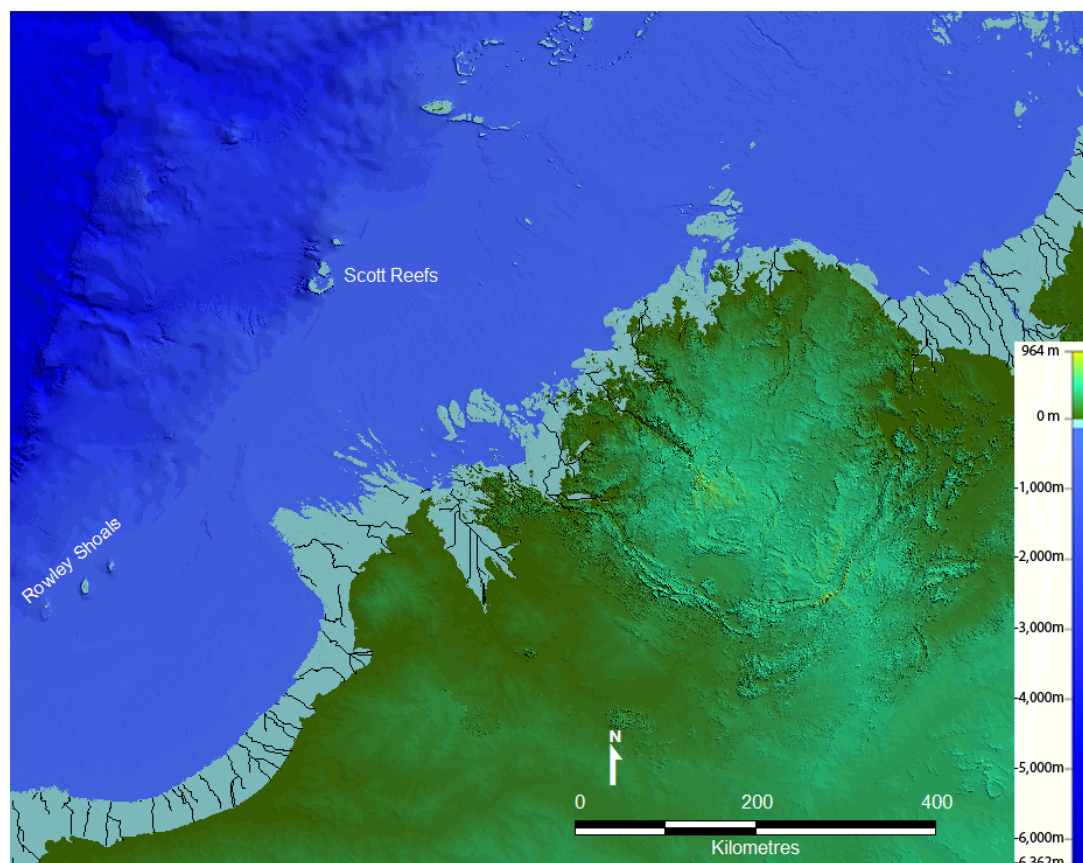


Figure 6.4 Kimberley shelf exposure at ~11,000 yr BP (MWP 1B) with LIG Reef remnants at Adele complex were isolated from mainland; sea-level is estimated at 40 m mbsl.

Subsequently, reefs in the inshore Kimberley Bioregion such as Montgomery Reef in Collier Bay and Cockatoo Island in the Buccaneer Archipelago were initiated and accumulated as sea-level rose considerably to about 20 mbsl at 9,000 yr BP. During the third meltwater pulse, RG3, this rapid sea-level rise inundated the Kimberley Shelf until it reached its present level some ~6,000 years ago, providing accommodation space for reef accretion along the Kimberley Coast (Fig 6.5).

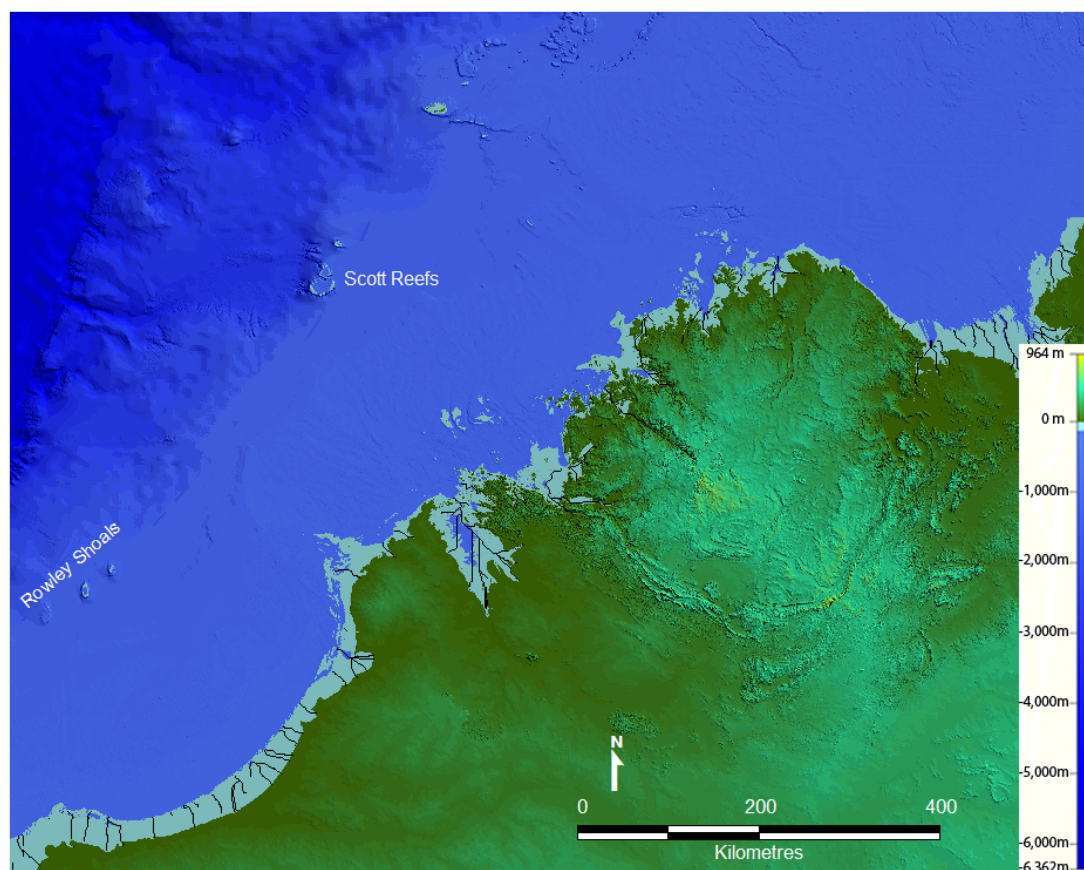


Figure 6.5 Kimberley shelf exposure at ~9,000 yr BP. Montgomery Reef and Cockatoo Reef were initiated and accumulated as sea-level rose considerably to approx. 20 mbsl.

## References

- Collins, L. B., Zhu, Z. R., Wyrwoll, K. H., Hatcher, B. G., Playford, P. E., Eisenhauer, A., Chen, J. H., Wasserburg, G. J., Bonani, G. (1993). Holocene accretion history of a reef complex on a cool-water carbonate margin: Easter Group of the Houtman Abrolhos, Eastern Indian Ocean. *Marine Geology*, 115(1-2), 29–46.
- Collins, L. B., Zhao, J. X., Freeman, H. (2006). A high-precision record of mid–late Holocene sea-level events from emergent coral pavements in the Houtman Abrolhos Islands, southwest Australia. *Quaternary International*, 145–146(0), 78–85.

- Collins, L. B., Testa, V., Zhao, J., Qu, D. (2011). Holocene accretion history and evolution of the Scott Reef carbonate platform and coral reef. *Journal of the Royal Society of Western Australia*, 94(2), 239–250.
- Eisenhauer, Wasserburg, A. G. J., Eisenhauer, A., Chen, J. H., Bonani, G., Collins, L.B., Zhu, Z. R., Wyrwoll, K. H. (1993). Holocene sea-level determination relative to the Australian continent: U/Th (TIMS) and <sup>14</sup>C (AMS) dating of coral cores from the Abrolhos Islands. *Earth and Planetary Science Letters*, 114(4), 529–547
- Lambeck, K., Yokoyama, Y., Purcel, A. (2002). Into and out of the Last Glacial Maximum: sea-level change during Oxygen Isotope Stages 3 and 2. *Quaternary Science Reviews*, 21(1–3), 343–360.
- Smithers, S. G. (2011). Sea-level indicators. In: Hopley, D. (ed), *Encyclopedia of Modern Coral Reefs : structure, form and process*. Encyclopedia of Earth Sciences. Springer, Dordrecht, The Netherlands, 896–902.
- Solihuddin, T., Collins, L. B., Blakeway, D., O’Leary, M. J. (2015). Holocene coral reef accretion and sea-level in a macrotidal, high turbidity setting: Cockatoo Island, Kimberley Bioregion, northwest Australia. *Marine Geology*, 359, 50–60.
- Solihuddin, T., O’Leary, M.J., Blakeway, D., Parnum, I., Kordi, M., Collins, L. B. (2016). Holocene reef evolution in a macrotidal setting: Buccaneer Archipelago, Kimberley Bioregion, Northwest Australia. *Coral Reefs*. 35:783-794.
- Solihuddin, T., Bufarale, G., O’Leary, M. J., Blakeway, D. (2016). Geomorphology and Holocene accretion history of a mid-shelf platform reef: Adele Reef, Kimberley Bioregion, Northwest Australia. *Geo-Marine Letters*. doi: 10.1007/s00367-016-0465-3.
- Wong, H. K., Haft, C., Paulsen, A. M., Lüdmann, T., Hübscher, C., Geng, J. (2003). Late quaternary sedimentation and sea-level fluctuations on the northern Sunda Shelf, southern South China Sea. In: Sidi, F. H., Nummedal, D., Imbert, P., Darman, H., Posamentier, H. W. (ed.), *Tropical Deltas of Southeast Asia – Sedimentology, Stratigraphy, and Petroleum Geology*:



Society Economical Palaeontologists Mineralogists Special Publication  
76: 200–234.

## **Chapter 7**

### **General Conclusions**

The complexity of the Kimberley Bioregion regarding its high biodiversity, geomorphic settings, and oceanographic conditions needs to be understood sufficiently for resources assessment, planning and management purposes. This region, on the other hand, has already been utilised for commercial activities such as marine tourism, fishing, aquaculture, and mining port facilities, besides traditional use by the indigenous people. Based on these facts, strategic studies and conservation are crucial in order to achieve sustainable Kimberley marine and coastal resources. Multi-discipline research and studies have been undertaken for better research-based policy under the Western Australian State Government and partners of the Western Australian Marine Science Institution (WAMSI) programs. This study provides a suitable knowledge base within which assessment can be made of the Kimberley Bioregion along with a basis for analysing shorter-term environmental changes.

A remotely sensed, geo-referenced, GIS-based analysis, Landsat-derived habitat zones, and their derivative products delivered in this study refer back to the specific aim and objective listed in chapter 1 regarding contemporary reef geomorphology and associated habitats mapping. This initial information enables managers to recognise spatial reef distribution linked to an understanding of reef geomorphology, coastal geology, and biodiversity processes and provides a foundation for long-term coral reef studies and management that can be used in several ways both by academia and industry to generate global databases. Further, the study can also be a guidance for future fieldwork and sampling strategies.

Reef mapping and transects conducted in the abandoned reef exposures in the Cockatoo mine pit provide the first information on Holocene reef accretion for an inshore reef of the Kimberley Bioregion, including contemporary intertidal environment, timing of Cockatoo Reef initiation, antecedent reef platform, reef facies units, palaeoecology, reef geochronology and accretion rates. The gap information related to the Holocene coral reef growth in Kimberley Bioregion, which is one of specific aims and objectives listed in this study, is directly addressed by presenting such information. The knowledge of the reef's foundations leads to a calculated

subsidence rate of the coastal Kimberley since LIG time of 0.12 m/ky. The study also suggests that the Kimberley inshore reefs may be more resilient to periodic disturbance and the effects from terrestrial run-off than reefs elsewhere. Further, the study shows that reef response to climate is resilience through time. The long-term quantitative data on Holocene reef growth in combination with sea-level history enables identification of reef response to sea-level changes and is a primary process to reconstruct reef growth over the last thousands of years and beyond.

A systematic drilling program conducted in the selected inshore reefs of the Buccaneer Archipelago including Tallon, Sunday, and Irvine/Bathurst Islands extends previous work at Cockatoo Island. The study provides more detailed information on internal reef architectures and their comparisons among the investigated islands and is directly addressing the attempt to establish a record of Holocene reef evolution in the Buccaneer Archipelago, Kimberley Bioregion. The emerging picture is that the southern Kimberley Reefs are extensive, thick three-dimensional structures that initiated shortly after inundation and accreted relatively rapidly, such that most reefs are now vertically constrained and are enlarging by progradation. The massive Kimberley tides are a dominant influence on reef geomorphology, particularly on reef flat elevation. Reefs that dry at low tide remain coral-dominated and are constrained at MLWS, whereas reefs that retain seawater over the low tide cycle become coralline algal-dominated and accrete to between MLWN and MHWN, up to ~4 m above MLWS.

Through multiple coring surveys at Adele Reef in the mid-shelf Kimberley Bioregion, the study complements the story of Holocene reef accretion of three island coring sites in the Buccaneer Archipelago. The study also attempts to address the biogeographic knowledge gap on Holocene reef development between the inshore Cockatoo and oceanic Scott Reef. The highest Holocene/pre-Holocene reef contact of Adele Reef, as interpreted from seismic data is at ~25 m, estimating the subsidence rate since the LIG to be 0.2 m/ky. When it is correlated with Cockatoo Reef in the innermost shelf and Scott Reef in the outermost shelf, the cross shelf profile is consistent with the hypothesis of subsidence with tilting and is suggestive of a hinge subsidence on the Kimberley coast and adjacent shelf with progressively greater subsidence from inshore Cockatoo to offshore Scott Reef.

The available Holocene reef records obtained from this study incorporated with a modified Houtman Abrolhos sea-level curve enable reconstruction of sea level and drowning history for the Kimberley Shelf, showing key events of coastal and coral reef evolution. However, the complicated factor of this region due to macrotidal conditions constrains the ideal sea-level event reconstruction, as such; the sea-level curves are better described as reef accretion history curves.

Such information presented here should be taken into consideration when planning and siting Marine Parks. Some important management issues can be directed towards the basis of existing knowledge and some will require further work, including scientific research of predicting likely future climate change impacts in collaboration with survey design to inform management options. Furthermore, some records of ecological shifting from palaeo records in the cores against contemporary ecological data would be more challenging and interesting in terms of long-term ecological resilience questions.

## Chapter 8

### References and Bibliography

- Adey, W. H. (1975). The algal ridges and coral reefs of St. Croix, their structure and Holocene development. *Reef Research Bulletin*, 187, 1-66.
- Ahmad, W., Neil, D. T. (1994). An evaluation of Landsat Thematic Mapper (TM) digital data for discriminating coral reef zonation: Heron Reef (GBR). *International Journal of Remote Sensing*, 15(13), 2583-2597.
- Andréfouët, S. A., Pagès, J. P. (2001). Water renewal time for classification of atoll lagoons in the Tuamotu Archipelago (French Polynesia). *Coral Reefs*, 20(4), 399-408.
- Andréfouët, S., Muller-Karger, F. (2006). Global assessment of modern coral reef extent and diversity for regional science and management applications: a view from space. *Proceedings of 10th International Coral Reef Symposium*, Okinawa, Japan, 28 June-32nd July 2004, Japanese Coral Reef Society.
- Andréfouët, S., Kramer, P., Torres-Pulliza, D., Joyce, K. E., Hochberg, E. J., Garza-Pérez, R., Mumby, P. J., Riegl, B., Yamano, H., White, W. H., Zubia, M., Brock, J. C., Phinn, S. R., Naseer, A., Hatcher, B. G., Muller-Karger, F. E. (2003). Multi-site evaluation of IKONOS data for classification of tropical coral reef environments. *Remote Sensing of Environment*, 88, 128–143.
- Baker, C., Potter, A., Tran, M., Heap, A. D. (2008), Sedimentology and Geomorphology of the North West Marine Region of Australia, Geoscience Australia, Canberra.
- Blakeway, D. (1997). Scleractinian corals and reef development, part 9. In: Walker, D. (ed.), Marine biological survey of the central Kimberley coast, Western Australia. Perth: University of Western Australia. Unpublished report, W. A. Museum Library No. UR377, pp. 77–85.

- Blanchon, P. (2011). Geomorphic zonation. In: Hopley, D. (ed.), *Encyclopedia of modern coral reefs: structure, form and process*. Dordrecht: Springer, 469-486.
- Brunnschweiler, R. O. (1957). The geology of Dampier Peninsula, Western Australia. Department of National Development, Bureau of Mineral Resources, Geology and Geophysics, Canberra.
- Buddemeier, R.W., Hopley, D. (1988). Turn-ons and turn-offs: causes and mechanisms of the initiation and termination of coral reef accretion. *Proc 6th Int Coral Reef Symp*, 1, 253–261.
- Braithwaite, C. J. R., Montaggioni, L. F., Camoin, G. F., Dalmasso, H., Dullo, W. C., Mangini, A. (2000). Origins and development of Holocene coral reefs: a revisited model based on reef boreholes in the Seychelles, Indian Ocean. *International Journal of Earth Science*, 89, 431–445.
- Brooke, B. (1995). Geomorphology, part 4. In: Wells, F. E., Hanley, J. R., Walker, D. (ed.), Survey of the marine biota of the southern Kimberley islands. Unpublished report No. UR286, Western Australian Museum, Perth, pp. 67–80.
- Brooke, B. (1996). Geomorphology of the north Kimberley coast. In: Walker, D. (ed.), Marine biological survey of the eastern Kimberley, Western Australia. Unpublished report No. UR353, Western Australian Museum, Perth.
- Brooke, B. (1997). Geomorphology of the north Kimberley coast, part 9. In: Walker, D. (ed.), Marine biological survey of the central Kimberley coast. Western Australia. University of Western Australia, Perth, unpublished report, W.A. Museum Library No. UR377, pp. 13–39.
- Browne, N. K., Smithers, S. G. (2012). Coral reefs of the turbid inner-shelf of the Great Barrier Reef, Australia: An environmental and geomorphic perspective on their occurrence, composition and accretion. *Earth Science Reviews*, 115(1–2), 1–20.
- Bufarale, G., Collins, L. B., O’Leary, M. J., Stevens, A. M., Kordi, M., Solihuddin, T. (2016). Quaternary onset and evolution of Kimberley coral reefs

- (Northwest Australia) revealed by high-resolution seismic imaging. *Continental Shelf Research*, 123:80-88.
- Capolsini, P., Andréfouët, S., Rion, C. Payri, C. (2003). A comparison of Landsat ETM+, SPOT HRV, Ikonos, ASTER, and airborne MASTER data for coral reef habitat mapping in South Pacific islands. *Canadian Journal of Remote Sensing*, 29(2), 187–200.
- Chin, A., Sweatman, H., Forbes, S., Perks, H., Walker, R., Jones, G., Williamson, D., Evans, R., Hartley, F., Armstrong, S., Malcolm, H., Edgar, G. (2008). Status of the Coral Reefs in Australia and Papua New Guinea, in: Wilkinson, C., (ed), Status of Coral Reefs of the World. Global Coral Reef Monitoring Network. *Reef and Rainforest Research Centre*, pp. 159–176.
- Collins, L. B. (2002). Tertiary Foundation and Quaternary Evolution of Coral Reef Systems of Australia's North West Shelf. In: Keep, M., Moss, S. J. (ed), *Proceeding of the Petroleum Exploration Society of Australia Symposium*, Perth, WA, pp. 129–152.
- Collins, L. B. (2011). Geological setting, marine geomorphology, sediment and oceanic shoals growth history of the Kimberley Region. *Journal of the Royal Society of Western Australia*, 94(2), 89-105.
- Collins, L. B., Testa, V. (2010). Quaternary development of resilient reefs on the subsiding Kimberley continental margin, northwest Australia. *Brazilian Journal of Oceanography*, 58, 1-13.
- Collins, L. B., Zhao, J. X., Freeman, H. (2006). A high-precision record of mid-late Holocene sea-level events from emergent coral pavements in the Houtman Abrolhos Islands, southwest Australia. *Quaternary International*, 145–146(0), 78–85.
- Collins, L. B., Zhu, Z. R., Wyrwoll, K. H. (1996). The structure of the Easter Platform, Houtman Abrolhos reefs: Pleistocene foundations and Holocene reef accretion. *Marine Geology*, 135(1–4), 1-13.

- Collins, L. B., Testa, V., Zhao, J., Qu, D. (2011). Holocene growth history and evolution of the Scott Reef carbonate platform and coral reef. *Journal of the Royal Society of Western Australia*, 94(2), 239–250.
- Collins, L. B., Zhu, Z. R., Wyrwoll, K. H., Eisenhauer, A., 2003. Late Quaternary structure and development of the northern Ningaloo Reef, Australia. *Sedimentary Geology*, 159(1-2), 81-94.
- Collins, L. B., O’Leary, M. J., Stevens A. M., Bufarale G., Kordi M., Solihuddin T. (2015). Geomorphic patterns, internal architecture and reef accretion in a macrotidal, high-turbidity setting of coral reefs from the Kimberley Bioregion. *AJMOA*, 7, 12-22.
- Collins, L. B., Zhu, Z. R., Wyrwoll, K. H., Hatcher, B. G., Playford, P. E., Eisenhauer, A., Chen, J. H., Wasserburg, G. J., Bonani, G. (1993). Holocene growth history of a reef complex on a cool-water carbonate margin: Easter Group of the Houtman Abrolhos, Eastern Indian Ocean. *Marine Geology*, 115(1-2), 29–46.
- DeCaprio, L., Gurnis, M., Mueller, R. D. (2009). Long-wavelength tilting of the Australian continent since the Late Cretaceous. *Earth and Planetary Science Letters*, 278(3-4), 175–185.
- Darwin, C. R. (1842). The structure and distribution of coral reefs. Being the first part of the geology of the voyage of the ‘Beagle’. London: Smith, Elder and Co.
- Department of the Environment, Water, Heritage and the Arts, DEWHA (2008). A Characterisation of the Marine Environment of the North-west Marine Region: Perth Workshop Report, A Summary of an Expert Workshop Convened in Perth, Western Australia, 5-6 September 2007, Commonwealth of Australia, Hobart.
- Department of Environment and Conservation, DEC (2011). Kimberley science and conservation strategy. DEC, Perth. Accessed 16/03/2012 <http://www.dec.wa.gov.au/content/view/5180/2191>.



- Embry, A. F., Klovan, J. E. (1971). A late Devonian reef tract on northeastern Banks Island, N.W.T. *Bulletin of Canadian Petroleum Geology*, 19(4), 730–781.
- Eisenhauer, Wasserburg, A. G. J., Eisenhauer, A., Chen, J.H., Bonani, G., Collins, L.B., Zhu, Z. R., Wyrwoll, K. H. (1993). Holocene sea-level determination relative to the Australian continent: U/Th (TIMS) and <sup>14</sup>C (AMS) dating of coral cores from the Abrolhos Islands. *Earth and Planetary Science Letters*, 114(4), 529–547.
- Fairbridge, R. W. (1950). Recent and Pleistocene coral reefs of Australia. *The Journal of Geology*, 58(4), 330–401.
- Fang, F., Morrow, R. (2003). Evolution, movement and decay of warm-core Leeuwin Current eddies. *Deep Sea Research Part II: Topical Studies in Oceanography*, 50(12-13), 2245–2261.
- Fonseca, A. C., Villaçã, R., Knoppers, B. (2012). Reef Flat Community Structure of Atol das Rocas, Northeast Brazil and Southwest Atlantic. *J Mar Biol*, 2012. doi:10.1155/2012/179128.
- Gherardi, D. F. M., Bosence, D. W. J. (2001). Composition and community structure of the coralline-algal reefs from Atol das Rocas, South Atlantic, Brazil. *Coral Reefs*, 19, 205–219.
- Gherardi, D. F. M., Bosence, D. W. J. (2005). Late Holocene reef accretion and relative sea-level changes in Atol das Rocas, equatorial South Atlantic. *Coral Reefs*, 24, 264–272.
- Government of Western Australia (2011). Kimberley Science and Conservation Strategy. Department of Environment and Conservation, Kensington, Perth.
- Glynn, P., de Weerd, W. H. (1991). Elimination of two reef building hydrocorals following the 1982-83 El Niño warming event. *Science*, 253, 69–71.
- Green, E. P., Mumby, P. J., Edwards, A. J. (2000). Remote Sensing Handbook for Tropical Coastal Management Sourcebooks, 3. UNESCO, Paris (316 pp. and plates).

- Griffin, T. J., Grey, K. (1990). Kimberley Basin, in: Memoir 3, Geology and Mineral Resources of Western Australia. Perth, Geological Survey of Western Australia, 293–304.
- Harris, P. T., Baker, E. K., Cole, A. R. (1991). Physical sedimentology of the Australian continental shelf, with emphasis on Late Quaternary deposits in major shipping channels, port approaches and choke points. Ocean Science Institute, Report 51, University of Sydney.
- Hatcher, B. G. (1991). Coral reefs in the Leeuwin Current: an ecological perspective. *J R Soc West Aust*, 74, 115-127.
- Hopley, D., Partain, B. (1986). The structure and development of fringing reefs of the Great Barrier Reef Province, in: Baldwin, C. L. (ed.), *Fringing Reef Workshop: Science, Industry and Management*. Great Barrier Reef Marine Park Authority, Townsville, 13–33.
- Hopley, D., Smithers, S., Parnell, K. (2007). The Geomorphology of the Great Barrier Reef: Development, diversity, change: Cambridge, UK, Cambridge University Press, pp. 532.
- Ingram, B. S. (1982). Palynological examination of samples from Adele Island No. 1 from Well Completion Report, Brunswick Oil N. L.
- Joyce, K. E., Phinn, S. R. (2001). Optimal spatial resolution for coral reef mapping. *Proceedings of the International Geoscience and Remote Sensing Symposium*, 2, 619–621.
- Jupp, D. L., Mayo, K. K., Kuchler, D. A. (1985). Remote sensing for planning and managing the Great Barrier Reef of Australia. *Photogrammetria*, 41, 21-42.
- Kaczmarek, S. E., Hicks, M. K., Fullmer, S. M., Steffen, K. L., Bachtel, S. L. (2010). Mapping facies distributions on modern carbonate platforms through integration of multispectral Landsat data, statistics-based unsupervised classifications, and surface sediment data. *American Association of Petroleum Geologists Bulletin*, 94, 1581–1606.
- Kennedy, D. M., Woodroffe, C. D. (2002). Fringing reef accretion and morphology: a review. *Earth Science Review*, 57, 255–277.

- Kordi, M., Collins, L. B., O'Leary, M., Stevens, A. (2016). ReefKIM: An integrated geodatabase for sustainable management of the Kimberley Reefs, North West Australia. *Ocean & Coastal Management*, 119, 234-243.
- Ladd, H. S., Ingerson, E., Townsend, R. C., Russell, M., Stevenson, H. K. (1953). Drilling on Eniwetok Atoll, Marshall Islands. *AAPG bulletin*, 37, 2257–2280.
- Lambeck, K., Yokoyama, Y., Purcel, A. (2002). Into and out of the Last Glacial Maximum: sea-level change during Oxygen Isotope Stages 3 and 2. *Quaternary Science Reviews*, 21(1–3), 343–360.
- Lambeck, K., Rouby, H., Purcell, A., Sun, Y., Sambridge, M. (2014). Sea-level and global ice volumes from the Last Glacial Maximum to the Holocene. *Proc Natl Acad Sci*, 111(43), 15296-15303.
- Lambeck, K., Woodroffe, C. D., Antonioli, F., Anzidei, M., Gehrels, W.R., Laborel, J., Wright, A. J. (2010). Paleoenvironmental records, geophysical modelling, and reconstruction of sea-level trends and variability on centennial and longer timescales, in: Church, J.A., Woodworth, P.L., Aarup, T., Wilson, W.S. (ed.), *Understanding Sea-level Rise and Variability*. Blackwell Publishing Ltd, 61-121.
- Lavering, I. H. (1993). Quaternary and modern environments of the Van Diemen Rise. Timor Sea, and potential effects of additional petroleum exploration activity. *Jour Austral Geol Geophys*, 13, 281-292.
- Lough, J. M. (1998). Coastal climate of northwest Australia and comparisons with the Great Barrier Reef: 1960 to 1992. *Coral Reefs*, 17(4), 351-367.
- Lowe, R. J., Falter, J. L. (2015). Oceanic forcing of coral reefs. In: Annual Review of *Marine Science*, 7, 43-66.
- Lowe, R. J., Leon, A.S., Symonds, G., Falter, J. L., Gruber, R. (2015). The intertidal hydraulics of tide-dominated reef platforms. *J Geophys Res*, 120. doi:10.1002/2015JC010701.
- Lyzenga, D. R. (1981). Remote sensing of bottom reflectance and water attenuation parameters in shallow water using aircraft and Landsat data. *International Journal of Remote Sensing*, 2, 71–82.

- Maedar, J., Narumalani, S., Rundquist, D. C., Perk, R. L., Schalles, J., Hutchins, K., Keck, J. (2002). Classifying and mapping general coral-reef structure using IKONOS data. *Photogrammetric Engineering and Remote Sensing*, 68, 1297–1305.
- Marshall, N. G. (1995). Adele Island No. 1 Palynological Report. Woodside Offshore Petroleum.
- Montaggioni, L. F. (2005). History of Indo-Pacific coral reef systems since the last glaciation: Development patterns and controlling factors. *Earth-Science Reviews*, 71(1-2), 1–75.
- Müller, G., Gastner, M. (1971). The 'Karbonat-Bombe', a simple device for the determination of carbonate content in sediment, soils, and other materials. *Neues Jahrbuch für Mineralogie-Monatshefte*, 10, 466–469.
- Mumby, P. J., Green, E. P., Clark, C. D., Edwards, A. J. (1998). Digital analysis of multispectral airborne imagery of coral reefs. *Coral Reefs*, 17, 59–69.
- Mumby, P. J., Skirving, W., Strong A. E., Hardy, J. T., LeDrew, E. F., Hochberg, E. J., Stumpf, R. P., David, L. T. (2004). Remote sensing of coral reefs and their physical environment. *Marine Pollutan Bulletin*, 48, 219-228.
- Neumann, A. C., Macintyre, I. G. (1985). Reef response to sea-level rise: keep-up, catch-up or give-up. *Proc 5th Int Coral Reef Symp*, 3, 105-110.
- Nurlidiasari, M. (2004). The application of Quickbird and Multi-temporal Landsat TM data for coral reef habitat mapping. Case Study: Derawan Island, East Kalimantan, Indonesia, International Institute for Geo-Information Science and Earth Observation, Enschede, The Netherlands.
- O’Leary, M. J., Hearty, P. J., McCulloch, M. T. (2008). U-series evidence for widespread reef development in Shark Bay during the last interglacial. *Palaeogeography, Palaeoclimatology, Palaeoecology*, 259, 424.
- O’Leary, M., Hearty, P. J., Thompson, W. G., Raymo, M. E., Mitrovica, J. X., Webster, J. M. (2013). Ice sheet collapse following a prolonged period of stable sea-level during the last interglacial. *Nature Geoscience*, 6(9), 796–800.

- Pearce, A. F., Griffiths, R. W. (1991). The Mesoscale Structure of the Leeuwin Current: A Comparison of Laboratory Models and Satellite Imagery. *J Geophys Res*, 96(C9), 16739-16757.
- Perry, C. T., Smithers, S. G., Gulliver, P., Browne, N. K. (2012). Evidence of very rapid reef accretion and reef accretion under high turbidity and terrigenous sedimentation. *Geology*, 40(8), 719–722.
- Purcell, S. P. (2002). Intertidal reefs under extreme tidal flux in Buccaneer Archipelago, Western Australia. *Coral Reefs*, 21(2), 191-192.
- Quigley, M. C., Cupper, M. L., Sandiford, M. (2006). Quaternary faults of south-central Australia: Palaeoseismicity, slip rates and origin. *Australian Journal of Earth Sciences*, 53(2), 285–301.
- Quigley, M. C., Sandiford, M., Cupper, M. L. (2007). Distinguishing tectonic from climatic controls on range-front sedimentation. *Basin Research*, 19(4), 491–505.
- Richards, Z. T., O’Leary, M. J. (2015). The Coralline Algal Cascades of Tallon Island (Jalan) Fringing Reef, NW Australia. *Coral Reefs*, 34(2), 595.
- Richards, Z. T., Bryce, M., Bryce, C. (2013). New records of atypical coral reef habitat in the Kimberley, Australia. *Journal of Marine Biology*. doi: 10.1155/2013/363894.
- Sandiford, M. (2003). Neotectonics of southeastern Australia: linking the Quaternary faulting record with seismicity and in situ stress. In: Hillis, R.R., Muller, D. (ed.), *Evolution and Dynamics of the Australian Plate*. Geological Society of Australia Special Publication 22, 101–113.
- Sandiford, M. (2007). The tilting continent: A new constraint on the dynamic topographic field from Australia. *Earth and Planetary Science Letters*, 261(1-2), 152–163.
- Short, A. D. (2011). Kimberley beach and barrier systems: An overview. *Journal of the Royal Society of Western Australia*, 94(2), 121–132.
- Simpson, C. J. (2011). Kimberley Marine Research Program Science Plan. Report to the WAMSI Board and Strategic Program Committee.

- Smith, S. V., Jokkel, P. L. (1975). Water composition and biogeochemical gradients in the Canton atoll lagoon. *Atoll Research Bulletin*, 221, 15-45.
- Smithers, S. G. (2011). Sea-level indicators. In: Hopley, D. (ed), *Encyclopedia of Modern Coral Reefs : structure, form and process*. Encyclopedia of Earth Sciences. Springer, Dordrecht, The Netherlands, 896–902.
- Solihuddin, T., Collins, L. B., Blakeway, D., O’Leary, M. J. (2015). Holocene coral reef accretion and sea-level in a macrotidal, high turbidity setting: Cockatoo Island, Kimberley Bioregion, northwest Australia. *Marine Geology*, 359, 50–60.
- Solihuddin, T., O’Leary, M. J., Blakeway, D., Parnum, I., Kordi, M., Collins, L. B. (2016). Holocene reef evolution in a macrotidal setting: Buccaneer Archipelago, Kimberley Bioregion, Northwest Australia. *Coral Reefs*, 35:783-794.
- Solihuddin, T., Bufarale, G., O’Leary, M. J., Blakeway, D. (2016). Geomorphology and Holocene accretion history of a mid-shelf platform reef: Adele Reef, Kimberley Bioregion, Northwest Australia. *Geo-Marine Letters*, doi: 10.1007/s00367-016-0465-3.
- Stoddard, D. R. (1969). The shape of atolls. Ecology and morphology of recent coral reefs. *Biological Reviews*, 44(4), 433–498.
- Teichert, C., Fairbridge, R. W. (1948). Some coral reefs of the Sahul Shelf. *Geographical Review*, 38(2), 222-249.
- Veron, J. E. N. (2000). Corals of the world. Australian Institute of Marine Science 1-3, 1,382 pp.
- Wells, F. E., Hanley, R., Walker, D. I. (1995). Marine Biological survey of the southern Kimberley, Western Australia. Western Australia Museum, Perth, WA.
- Wells, J. W. (1957). Coral Reefs. In: Hedspeth J. W. (ed.), *Treatise on marine ecology and paleoecology*. Geological Society of America Memoir 67, 609-632.
- Wentworth, C. K. (1922). A scale of grade and class terms for clastic sediments. *The Journal of Geology*, 30(5), 377-392.

- Wilson, B. R. (2013). *The Biogeography of the Australian North West Shelf: Environmental Change and life's response*. Elsevier, Burlington MA, USA.
- Wilson, B. R., Blake, S. (2011). Notes on the origin and biogeomorphology of Montgomery Reef, Kimberley, Western Australia. *Journal of the Royal Society of Western Australia*, 94(2), 107–119.
- Wilson, B. R., Blake, S., Ryan, D., Hacker, J. (2011). Reconnaissance of species-rich coral reefs in a muddy, macro-tidal, enclosed embayment, Talbot Bay, Kimberley, Western Australia. *Journal of the Royal Society of Western Australia*, 94(2), 251–265.
- Wolanski, E., Spagnol, S. (2003). Dynamics of the turbidity maximum in King Sound, tropical Western Australia. *Estuarine Coastal and Shelf Science*, 56(5-6), 877-890.
- Wong, H. K., Haft, C., Paulsen, A. M., Lüdmann, T., Hübscher, C., Geng, J. (2003). Late quaternary sedimentation and sea-level fluctuations on the northern Sunda Shelf, southern South China Sea. In: Sidi, F. H., Nummedal, D., Imbert, P., Darman, H., Posamentier, H. W. (ed.), *Tropical Deltas of Southeast Asia – Sedimentology, Stratigraphy, and Petroleum Geology*: Society Economical Palaeontologists Mineralogists Special Publication 76, 200–234.
- Wright, R. L. (1964). Geomorphology of the West Kimberley Area. *CSIRO Land Research*, 9, 103–118.
- Zainal, A. J. M., Dalby, D. H., Robinson, I. S. (1993). Monitoring marine ecological changes on the east coast of Bahrain with Landsat TM. *Photogrammetric Engineering and Remote Sensing*, 59, 415–421.

*Every reasonable effort has been made to acknowledge the owners of copyright material. I would be pleased to hear from any copyright owner who has been omitted or incorrectly acknowledged.*

## List of core collected

No	Core ID	Date collected	Location	GPS position		Method	Core Length (cm)	Compaction (cm)	Penetration (cm)
				Long	Lat				
1	PN3	3/07/2014	N. Passage Sunday I.	123° 10' 3.432"	16° 23' 47.658"	Percussion core	248	114	362
2	PN4	3/07/2014	N. Passage Sunday I.	123° 10' 1.908"	16° 23' 49.614"	Percussion core	87	66	153
3	PN4B	3/07/2014	N. Passage Sunday I.	123° 10' 1.800"	16° 23' 50.244"	Percussion core	120	43	163
4	PN2	3/07/2014	N. Passage Sunday I.	123° 10' 6.918"	16° 23' 46.290"	Percussion core	102	74	176
5	PN1	6/07/2014	N. Passage Sunday I.	123° 10' 11.046"	16° 23' 41.25"	Percussion core	278	130	408
6	PN5	6/07/2014	N. Passage Sunday I.	123° 10' 9.356"	16° 23' 43.476"	Percussion core	247	193	440
7	PS1	4/07/2014	S. Passage Sunday I.	123° 10' 0.246"	16° 24' 50.844"	Percussion core	129	59	188
8	PS2	4/07/2014	S. Passage Sunday I.	123° 10' 2.292"	16° 24' 52.476"	Percussion core	52	14	66
9	PS2B	4/07/2014	S. Passage Sunday I.	123° 10' 2.160"	16° 24' 52.62"	Percussion core	34	7	41
10	PS3	6/07/2014	S. Passage Sunday I.	123° 9' 55.11"	16° 24' 59.417"	Percussion core	80	21	101
11	PS4	6/07/2014	S. Passage Sunday I.	123° 9' 53.652"	16° 24' 57.522"	Drilling core	112	N/A	112
12	ET1	7/07/2014	East Tallon Island	123° 8' 18.906"	16° 24' 36.57"	Percussion core	92	34	126
13	ET2	7/07/2014	East Tallon Island	123° 8' 18.042"	16° 24' 38.706"	Drilling core	100	N/A	100
14	ET3	7/07/2014	East Tallon Island	123° 8' 18.828"	16° 24' 38.664"	Drilling core	68	N/A	68
15	ET4	7/07/2014	East Tallon Island	123° 8' 20.766"	16° 24' 40.602"	Drilling core	88	N/A	88
16	ET5	7/07/2014	East Tallon Island	123° 8' 20.658"	16° 24' 41.076"	Drilling core	100	N/A	100
17	ET6	7/07/2014	East Tallon Island	123° 8' 19.752"	16° 24' 37.02"	Drilling core	22	N/A	22
18	ET7	8/07/2014	East Tallon Island	123° 7' 44.82"	16° 24' 25.668"	Percussion core	380	200	580
19	ET8	8/07/2014	East Tallon Island	123° 8' 17.646"	16° 24' 10.872"	Drilling core	121	N/A	121
20	ET9	8/07/2014	East Tallon Island	123° 8' 17.538"	16° 24' 10.938"	Drilling core	105	N/A	105
21	ET10	8/07/2014	East Tallon Island	123° 8' 17.784"	16° 24' 10.35"	Drilling core	66	N/A	66
22	ET11	8/07/2014	East Tallon Island	123° 8' 18.108"	16° 24' 10.638"	Drilling core	90	N/A	90
23	ET12	9/07/2014	East Tallon Island	123° 7' 59.88"	16° 24' 31.722"	Percussion core	159	56	215
24	ET13	9/07/2014	East Tallon Island	123° 8' 11.238"	16° 24' 31.094"	Percussion core	25	N/A	25
25	WT1	1/08/2014	West Tallon Island	123° 7' 6.672"	-16° 24' 12.75"	Percussion core	410	216	626
26	WT2	1/08/2014	West Tallon Island	123° 7' 1.89"	-16° 24' 11.13"	Percussion core	107	28	135
27	B01	3/08/2014	West Bathurst Island	123° 32' 54.096"	-16° 2' 17.742"	Percussion core	59	1	60
28	B02	3/08/2014	West Bathurst Island	123° 32' 54.359"	-16° 2' 17.886"	Percussion core	99	35	134
29	B03	3/08/2014	West Bathurst Island	123° 32' 57.864"	-16° 2' 19.344"	Percussion core	70	10	80
30	B04	4/08/2014	Inter-Island Bath-Irv	123° 32' 52.926"	-16° 3' 26.232"	Drilling/percussion	275	172	447
31	B05	4/08/2014	Inter-Island Bath-Irv	123° 32' 47.64"	-16° 3' 26.292"	Drilling/percussion	470	162	632
32	B06	5/08/2014	S. Inter-Island Pool	123° 32' 31.71"	-16° 3' 26.55"	Percussion core	315	143	458
33	B07	5/08/2014	N. Inter-Island Pool	123° 32' 42.57"	-16° 3' 15.864"	Percussion core	492	130	622
34	B08	5/08/2014	W. Inter-Island Pool	123° 32' 9.738"	-16° 3' 23.238"	Percussion core	85	14	99
35	B08-b	5/08/2014	W. Inter-Island Pool	123° 32' 9.864"	-16° 3' 23.244"	Drilling core	70	N/A	70
36	B09	6/08/2014	W. Inter-Island Reef	123° 31' 18.148"	-16° 3' 16.662"	Drilling/percussion	103	22	125
37	B10	6/08/2014	NW. Inter-Island Reef	123° 31' 19.608"	-16° 2' 43.548"	Drilling/percussion	80	58	138
38	B11	7/08/2014	SW. Inter-Island Reef	123° 31' 21.888"	-16° 3' 38.586"	Drilling/percussion	214	172	386
39	B12	8/08/2014	Irvine I. Pool	123° 32' 52.182"	-16° 3' 56.454"	Percussion core	525	100	625
40	B13	8/08/2014	Irvine I. Pool	123° 32' 56.346"	-16° 3' 46.5"	Percussion core	426	178	604
41	B14	8/08/2014	Irvine I. Pool	123.55001	-16.06621	Percussion core	455	118	573
42	B15	9/08/2014	Sandbank	123° 31' 36.714"	-16° 3' 22.752"	Percussion core	164	157	221
43	A03	18/10/2014	Sand cay	15° 28' 36.084"	123° 7' 46.05"	Percussion core	350	156	506
44	A04	17/10/2014	North Adele Island	15° 26' 14.862"	123° 6' 56.982"	Percussion core	215	95	310
45	A05	17/10/2014	North Adele Island	15° 26' 40.608"	123° 6' 36.732"	Percussion core	160	67	227
46	A06	17/10/2014	Sand cay	15° 28' 37.344"	123° 7' 18.522"	Percussion core	311	103	414
47	A07	17/10/2014	Sand cay (near island)	15° 30' 20.244"	123° 9' 22.65"	Percussion core	250	97	347
48	A08	18/10/2014	South Adele Island	15° 33' 33.03"	123° 10' 49.5"	Percussion core	340	87	427
49	A09	18/10/2014	South Adele Island	15° 34' 16.692"	123° 10' 56.202"	Percussion core	137	47	184
50	A10	18/10/2014	South Adele Island	15° 34' 54.474"	123° 10' 56.712"	Percussion core	192	33	225
51	Sun01	21/10/2014	South Sunday Island	16° 26' 25.65"	123° 9' 40.644"	Drilling core	35	N/A	35
52	Sun02	21/10/2014	South Sunday Island	16° 26' 19.662"	123° 9' 41.166"	Percussion core	130	35	165
53	Sun03	21/10/2014	South Sunday Island	16° 26' 5.904"	123° 9' 38.232"	Percussion core	140	54	194

Explanation:

PN = North Passage of Sunday Island

PS = South Passage of Sunday Island

ET = East Tallon Island

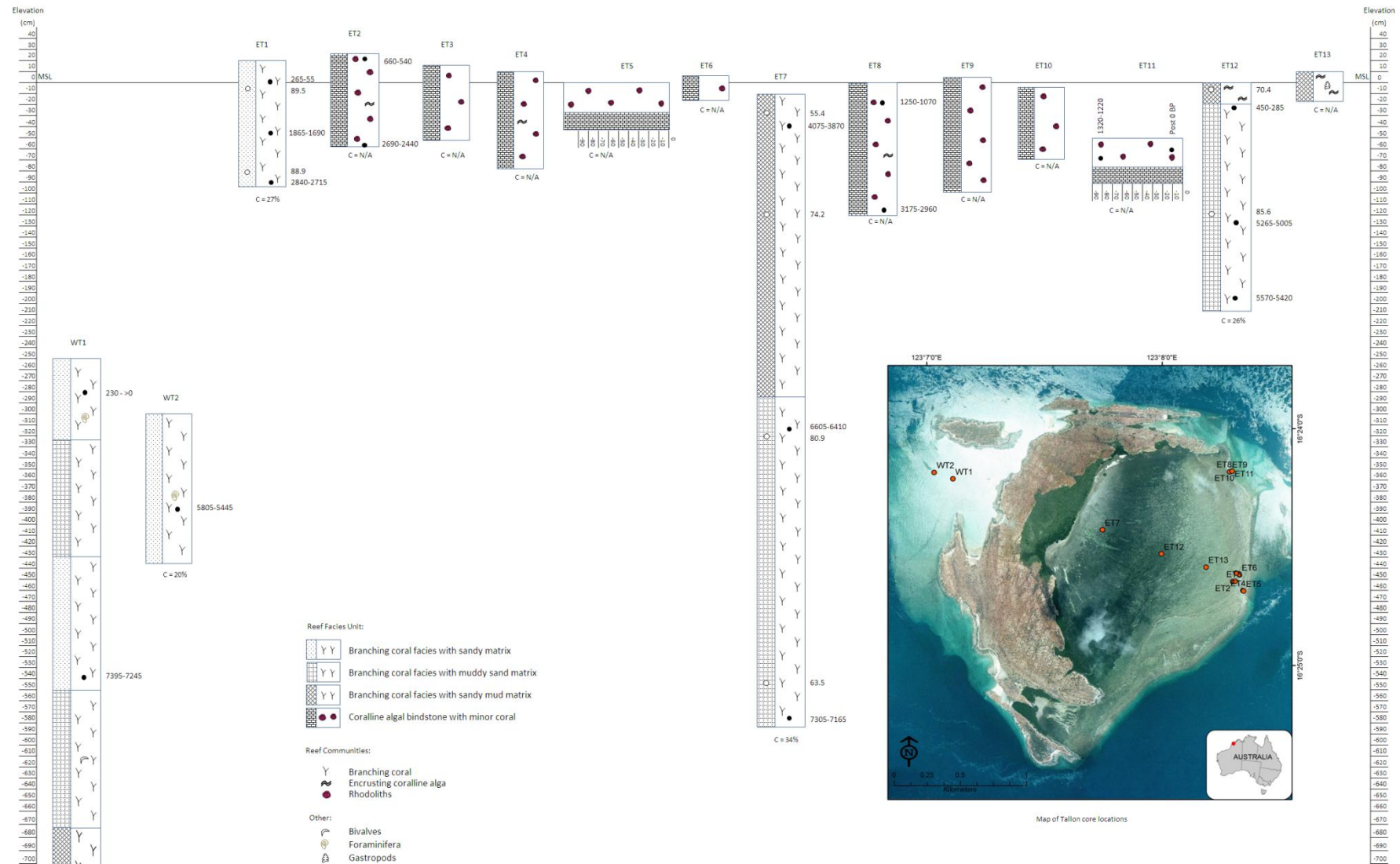
WT = West Tallon Island

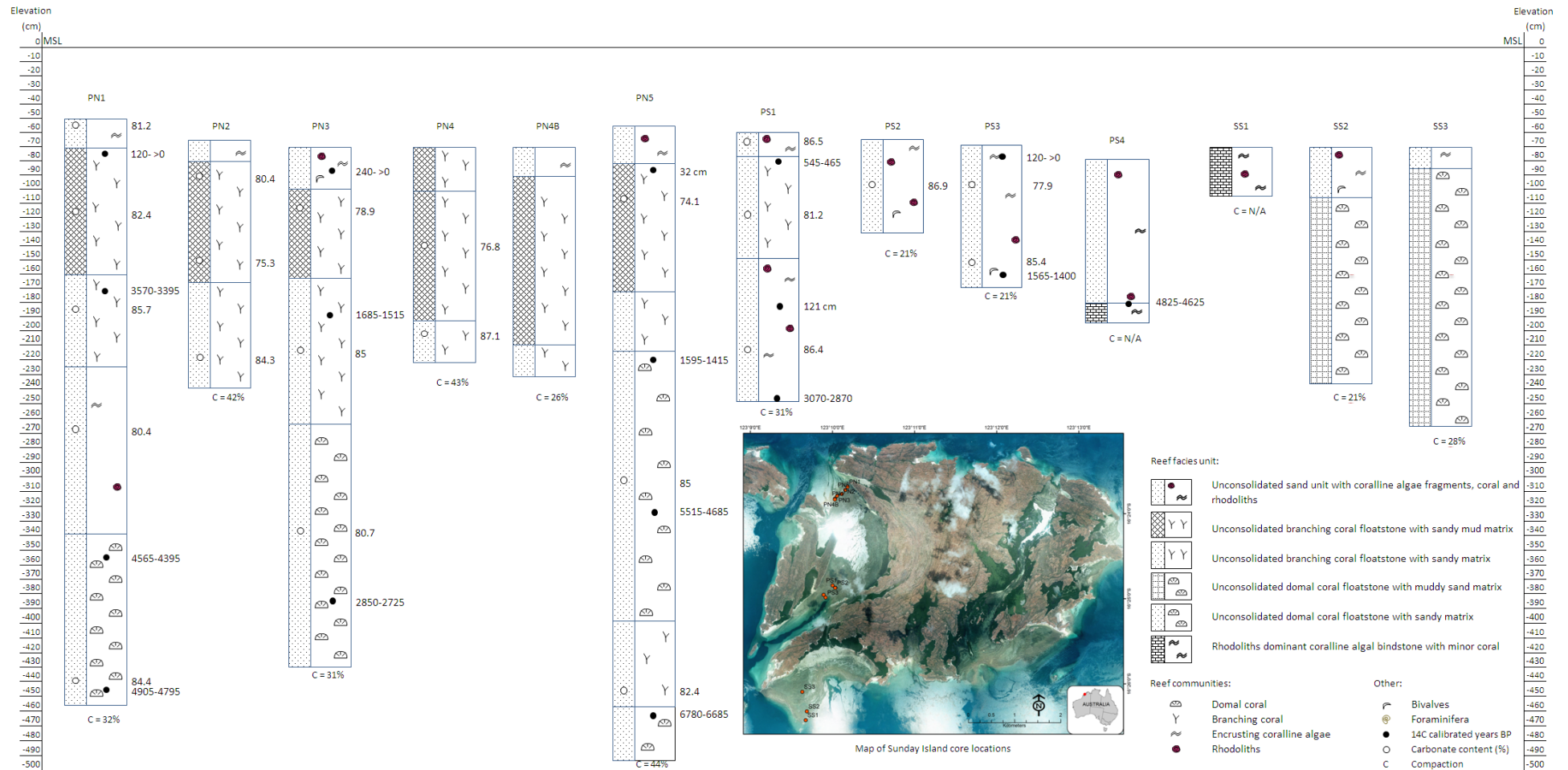
B = Bathurst and Irvine Island

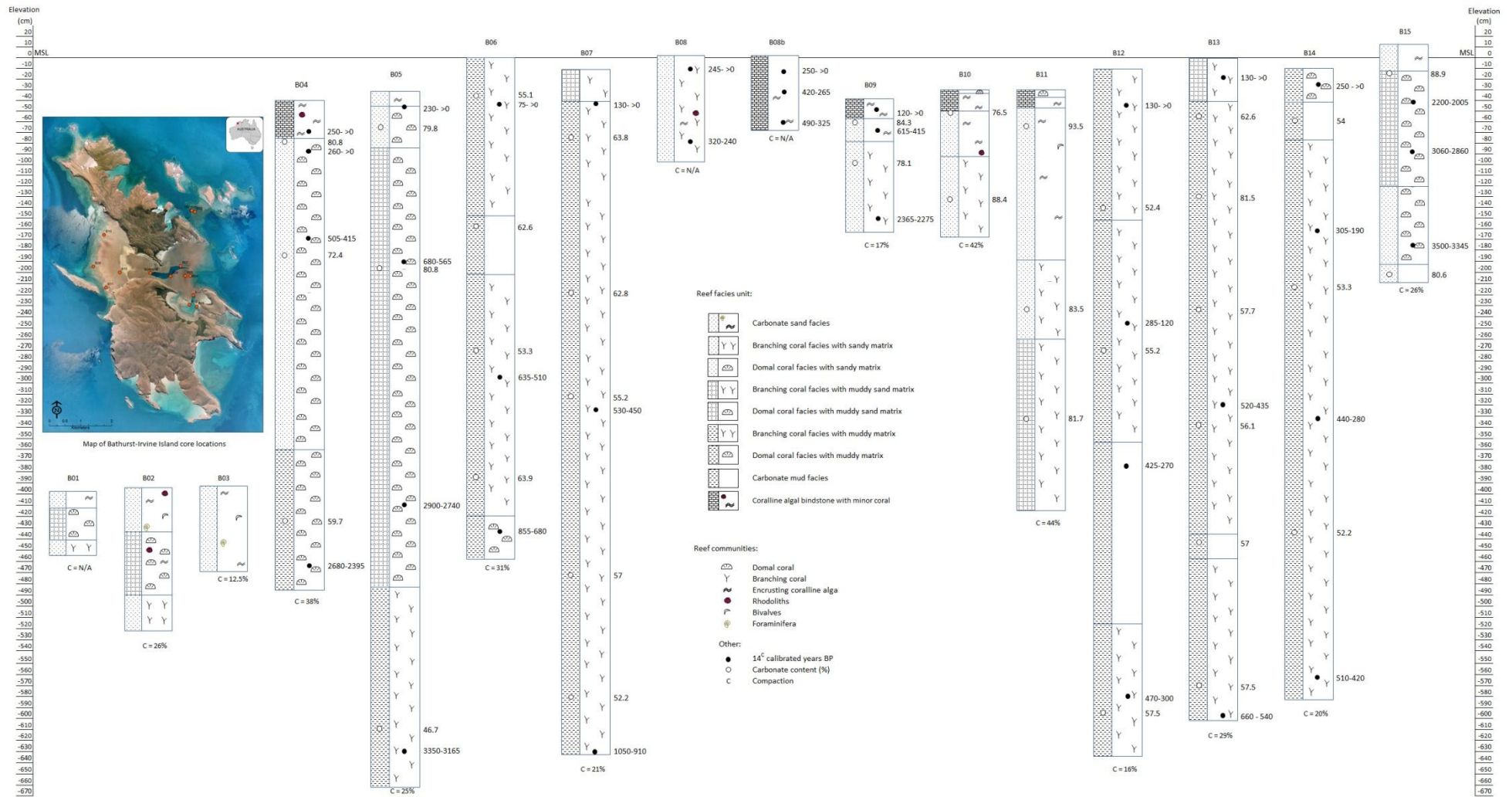
N/A = not available



Graphic Log	Description	Photo
	<p>1. Branching coral rubble more abundant at the top of the sequence mixed with domal coral. Matrix is muddy clay, greenish, shelly fragments. In some places, matrix is coarse sand at the top of the sequence (coarsening upward). Coralline algae is sparsely found, while bivalves and gastropods are abundant.</p> <p>Coral colonies: <i>Acropora</i>, <i>lobophyllia</i>, <i>acanthastrea</i>, <i>porites</i>, <i>goniastrea</i>, <i>goniopora</i>, <i>galaxea</i>, <i>fungia</i>, <i>turbinaria</i>, <i>favia</i>, <i>faviid</i>, <i>acanthastrea</i>, <i>Hydnopora</i>, <i>pavona</i>, <i>astrepore</i>, <i>montastrea</i>, <i>synphyllia</i>, <i>mosellya</i>, <i>lipophyllina</i>.</p> <p>2. Gravelly rock fragments mixed with rubbly branching corals overlain (unconformity?) calcrete</p> <p>3. Pleistocene calcrete (?), pale grey fine to coarse grained, angular – sub angular, shelly fragments, some fine to coarse grained coral gravel, foram shells and mollusc fragments, well lithified at the top but less compacted at the base, infilled by soil.</p> <p>4. Proterozoic hematitic sandstone, fine – medium grained, well sorted, rounded, compact, abundant mafic mineral (mica?)</p>	<p>Pit sea wall</p> <p>1</p> <p>2</p> <p>3</p> <p>4</p>









### Carbonate content on matrix sediment

Location	Sample code	Depth in core (m)	Sample weight (gr)	CO <sub>2</sub> Volume	CaCO <sub>3</sub> weight (gr)	CaCO <sub>3</sub> percentage in sample (%)	Average CaCO <sub>3</sub> percentage (%)
Tallon Reef	ET1-20	-0.2	0.25	50	0.2258	90.3101	89.4703
			0.5	97	0.4535	90.6977	
			0.75	141	0.6667	88.8889	
			1	185	0.8798	87.9845	
	ET1-84	-0.84	0.25	46	0.2064	82.5581	88.8647
			0.5	96	0.4486	89.7287	
			0.75	147	0.6957	92.7649	
			1	190	0.9041	90.407	
	ET7-12	-0.12	0.25	29	0.124	49.6124	55.3537
			0.5	62	0.2839	56.7829	
			0.75	94	0.439	58.5271	
			1	120	0.5649	56.4922	
	ET7-38	-0.38	0.25	39	0.1725	68.9922	74.249
			0.5	82	0.3808	76.1628	
			0.75	121	0.5698	75.969	
			1	160	0.7587	75.8721	
	ET7-210	-2.1	0.25	44	0.1967	78.6822	80.8705
			0.5	85	0.3953	79.0698	
			0.75	132	0.6231	83.0749	
			1	174	0.8266	82.655	
	ET7-358	-3.58	0.25	35	0.1531	61.2403	63.469
			0.5	69	0.3178	63.5659	
			0.75	103	0.4826	64.3411	
			1	137	0.6473	64.7287	
	ET12-5	-0.05	0.25	38	0.1676	67.0543	70.3731
			0.5	78	0.3614	72.2868	
			0.75	115	0.5407	72.093	
			1	148	0.7006	70.0581	
	ET12-93	-0.93	0.25	47	0.2112	84.4961	85.5943
			0.5	92	0.4293	85.8527	
			0.75	135	0.6376	85.0129	
			1	183	0.8702	87.0155	

Location	Sample code	Depth in core (m)	Sample weight (gr)	CO <sub>2</sub> Volume	CaCO <sub>3</sub> weight (gr)	CaCO <sub>3</sub> percentage in sample (%)	Average CaCO <sub>3</sub> percentage (%)
Sunday Reef	PN1-3	-0.03	0.25	46	0.2064	82.5581	81.1935
			0.5	88	0.4099	81.9767	
			0.75	128	0.6037	80.491	
			1	168	0.7975	79.7481	
	PN1-42	-0.42	0.25	45	0.2016	80.6202	82.4047
			0.5	89	0.4147	82.9457	
			0.75	131	0.6182	82.4289	
			1	176	0.8362	83.624	
	PN1-90	-0.9	0.25	46	0.2064	82.5581	85.6751
			0.5	93	0.4341	86.8217	
			0.75	137	0.6473	86.3049	
			1	183	0.8702	87.0155	
	PN1-150	-1.5	0.25	44	0.1967	78.6822	80.386
			0.5	87	0.405	81.0078	
			0.75	129	0.6085	81.137	
			1	170	0.8072	80.7171	
	PN1-270	-2.7	0.25	45	0.2016	80.6202	84.4234
			0.5	92	0.4293	85.8527	
			0.75	136	0.6424	85.6589	
			1	180	0.8556	85.562	
	PN2-14	-0.14	0.25	44	0.1967	78.6822	80.4264
			0.5	88	0.4099	81.9767	
			0.75	127	0.5988	79.845	
			1	171	0.812	81.2016	
	PN2-50	-0.5	0.25	40	0.1773	70.9302	75.2584
			0.5	81	0.376	75.1938	
			0.75	122	0.5746	76.615	
			1	165	0.7829	78.2946	
	PN2-90	-0.9	0.25	46	0.2064	82.5581	84.3427
			0.5	91	0.4244	84.8837	
			0.75	134	0.6328	84.3669	
			1	180	0.8556	85.562	
	PN3-30	-0.3	0.25	39	0.1725	68.9922	78.8921
			0.5	86	0.4002	80.0388	
			0.75	131	0.6182	82.4289	
			1	177	0.8411	84.1085	
	PN3-100	-1	0.25	46	0.2064	82.5581	84.9887
			0.5	91	0.4244	84.8837	
			0.75	138	0.6521	86.9509	
			1	180	0.8556	85.562	
	PN3-185	-1.85	0.25	45	0.2016	80.6202	80.7494
			0.5	87	0.505	81.0078	
			0.75	129	0.6085	81.137	
			1	169	0.8023	80.2326	
	PN4-40	-0.4	0.25	41	0.1822	72.8682	76.7926
			0.5	84	0.3905	78.1008	
			0.75	124	0.5843	77.907	
			1	165	0.7829	78.2946	
	PN4-76	-0.76	0.25	48	0.2161	86.4341	87.0882
			0.5	93	0.4341	86.8217	
			0.75	139	0.657	87.5969	
			1	184	0.875	87.5	
	PN5-30	-0.3	0.25	40	0.1773	70.9302	74.0875
			0.5	78	0.3614	72.2868	
			0.75	120	0.5649	75.323	
			1	164	0.7781	77.8101	
	PN5-140	-1.4	0.25	48	0.2161	86.4341	84.9887
			0.5	90	0.4196	83.9147	
			0.75	135	0.6376	85.0129	
			1	178	0.8459	84.593	
	PN5-220	-2.2	0.25	44	0.1967	78.6822	82.3643
			0.5	89	0.4147	82.9457	
			0.75	133	0.6279	83.7209	
			1	177	0.8411	84.1085	
	PS1-5	-0.05	0.25	47	0.2112	84.4961	86.4826
			0.5	94	0.439	87.7907	
			0.75	139	0.657	87.5969	
			1	181	0.8605	86.0465	
	PS1-40	-0.4	0.25	43	0.1919	76.7442	81.1531
			0.5	88	0.4099	81.9767	
			0.75	130	0.6134	81.7829	
			1	177	0.8411	84.1085	
	PS1-105	-1.05	0.25	47	0.2112	84.4961	86.3614
			0.5	92	0.4293	85.8527	
			0.75	139	0.657	87.5969	
			1	184	0.875	87.5	
	PS2-25	-0.25	0.25	48	0.2161	86.4341	86.8863
			0.5	94	0.439	87.7907	
			0.75	137	0.6473	86.3049	
			1	183	0.8702	87.0155	
	PS3-23	-0.23	0.25	42	0.187	74.8062	77.9231
			0.5	85	0.3953	79.0698	
			0.75	125	0.5891	78.553	
			1	167	0.7926	79.2636	
	PS3-70	-0.7	0.25	47	0.2112	86.4341	85.4328
			0.5	91	0.4244	84.8837	
			0.75	137	0.6473	86.3049	
			1	181	0.8605	86.0465	

Location	Sample code	Depth in core (m)	Sample weight (gr)	CO <sub>2</sub> Volume	CaCO <sub>3</sub> weight (gr)	CaCO <sub>3</sub> percentage in sample (%)	Average CaCO <sub>3</sub> percentage (%)
Bathurst/ Irvine Reef	B04-20	-0.2	0.25	44	0.1967	78.6822	80.7897
			0.5	87	0.405	81.0078	
			0.75	130	0.6134	81.7829	
			1	172	0.8169	81.686	
	B04-90	-0.9	0.25	44	0.2064	78.6822	72.4322
			0.5	77	0.3566	71.3178	
			0.75	112	0.5262	70.155	
			1	147	0.6957	69.5736	
	B04-240	-2.4	0.25	33	0.1434	57.3643	59.7141
			0.5	64	0.2936	58.7209	
			0.75	97	0.4535	60.4651	
			1	132	0.5231	62.3062	
	B05-25	-0.25	0.25	46	0.2064	82.5581	79.7804
			0.5	85	0.3953	79.0698	
			0.75	126	0.594	79.199	
			1	165	0.7829	78.2946	
	B05-125	-1.25	0.25	46	0.2064	82.5581	80.7897
			0.5	85	0.3953	79.0698	
			0.75	130	0.6134	81.7829	
			1	168	0.7975	79.7481	
	B05-435	-4.35	0.25	25	0.1047	41.8605	46.7135
			0.5	52	0.2355	47.093	
			0.75	78	0.3614	48.1912	
			1	106	0.4971	49.7093	
	B06-28	-0.28	0.25	30	0.1289	51.5504	55.1114
			0.5	61	0.2791	55.814	
			0.75	91	0.4244	56.5891	
			1	120	0.5649	56.4922	
	B06-110	-1.1	0.25	35	0.1531	61.2403	62.6615
			0.5	68	0.313	62.5969	
			0.75	101	0.4729	63.0491	
			1	135	0.6376	63.7597	
	B06-187	-1.87	0.25	28	0.1192	47.6744	53.3349
			0.5	59	0.2649	53.876	
			0.75	89	0.4147	55.2972	
			1	120	0.5649	56.4922	
	B06-266	-2.66	0.25	33	0.1434	57.3643	63.8727
			0.5	64	0.2936	58.7209	
			0.75	96	0.4486	59.8191	
			1	129	0.6085	60.6977	
	B07-50	-0.5	0.25	35	0.1531	61.2403	63.8727
			0.5	69	0.3178	63.5659	
			0.75	104	0.4874	64.8871	
			1	139	0.657	65.6977	
	B07-165	-1.65	0.25	33	0.1434	57.3643	62.823
			0.5	70	0.3227	64.5349	
			0.75	105	0.4922	65.6331	
			1	135	0.6376	63.7597	
	B07-240	-2.4	0.25	29	0.124	49.6124	55.2326
			0.5	63	0.2888	57.7519	
			0.75	91	0.4244	56.5891	
			1	121	0.5698	56.9767	
	B07-365	-3.65	0.25	31	0.1337	53.4884	57.009
			0.5	63	0.2888	57.7519	
			0.75	93	0.4341	57.8811	
			1	125	0.5891	58.9147	
	B07-450	-4.5	0.25	31	0.1337	53.4884	52.2852
			0.5	57	0.2597	51.938	
			0.75	84	0.3905	52.0672	
			1	110	0.5165	51.6473	
	B09-20	-0.2	0.25	43	0.1919	76.7442	84.262
			0.5	91	0.4244	84.8837	
			0.75	138	0.6521	86.9509	
			1	186	0.8847	88.469	
	B09-50	-0.5	0.25	42	0.187	74.8062	78.125
			0.5	84	0.3905	78.1008	
			0.75	127	0.5988	79.845	
			1	168	0.7975	79.7481	
	B10-10	-0.1	0.25	40	0.1773	70.5302	76.4696
			0.5	82	0.3808	76.1628	
			0.75	125	0.5891	78.553	
			1	169	0.8023	80.2326	
	B10-60	-0.6	0.25	50	0.2258	90.3101	88.4205
			0.5	94	0.439	87.7907	
			0.75	139	0.657	87.5869	
			1	185	0.8798	87.9845	
	B11-20	-0.2	0.25	52	0.2355	94.188	93.5078
			0.5	100	0.468	93.6047	
			0.75	148	0.7006	93.4109	
			1	195	0.9283	92.8295	
	B11-115	-1.1	0.25	48	0.2161	86.4341	83.6563
			0.5	89	0.4142	82.9457	
			0.75	132	0.6231	83.0749	
			1	173	0.8217	82.1705	
	B11-170	-1.7	0.25	46	0.2054	82.5581	81.7587
			0.5	88	0.4099	81.9767	
			0.75	130	0.6134	81.7829	
			1	170	0.8072	80.7171	
	B12-110	-1.1	0.25	31	0.1337	53.4884	52.4063
			0.5	57	0.2597	51.938	
			0.75	84	0.3905	52.0672	
			1	111	0.5213	52.1318	
	B12-220	-2.2	0.25	31	0.1337	53.4884	55.1922
			0.5	60	0.2742	54.845	
			0.75	90	0.4196	55.9432	
			1	120	0.5649	56.4922	
	B12-490	-4.9	0.25	32	0.1386	55.4264	57.4935
			0.5	62	0.2839	56.7829	
			0.75	93	0.4341	57.8821	
			1	127	0.5988	59.8837	
	B13-40	-0.4	0.25	33	0.1434	57.3643	62.6211
			0.5	69	0.3178	63.5659	
			0.75	103	0.4826	64.3411	
			1	138	0.6521	65.2132	
	B13-93	-0.93	0.25	45	0.2016	80.6202	81.5568
			0.5	87	0.405	81.0078	
			0.75	131	0.6182	82.4289	
			1	173	0.8217	82.1705	
	B13-167	-1.67	0.25	31	0.1337	53.4884	57.6954
			0.5	63	0.2888	57.7519	
			0.75	95	0.4438	59.1731	
			1	128	0.6037	60.3682	
	B13-242	-2.42	0.25	31	0.1337	53.4884	56.0804
			0.5	62	0.2839	56.7829	
			0.75	91	0.4244	56.5891	
			1	122	0.5746	57.4612	
	B13-315	-3.15	0.25	28	0.1192	47.6744	57.0494
			0.5	64	0.2936	58.7209	
			0.75	97	0.4535	60.4651	
			1	130	0.6134	61.3372	
	B13-405	-4.05	0.25	32	0.1386	55.4264	57.4935
			0.5	63	0.2888	57.7519	
			0.75	93	0.4341	57.8811	
			1	125	0.5891	58.9147	
	B14-40	-0.4	0.25	30	0.1289	51.5504	54.0213
			0.5	69	0.2694	53.876	
			0.75	88	0.4099	54.6512	
			1	119	0.5601	56.0078	
	B14-165	-1.65	0.25	30	0.1289	51.5504	53.3349
			0.5	60	0.2742	54.845	
			0.75	86	0.4002	53.3592	
			1	114	0.5359	53.5853	
	B14-340	-3.4	0.25	28	0.1192	47.6744	52.1641
			0.5	57	0.2597	51.938	
			0.75	87	0.405	54.0052	
			1	117	0.5504	55.0386	
	B15-20	-0.2	0.25	48	0.2161	86.4341	88.905
			0.5	95	0.4438	88.7597	
			0.75	142	0.6715	89.5349	
			1	191	0.908	90.8915	
	B15-160	-1.6	0.25	45	0.2016	80.6202	80.6282
			0.5	87	0.405	81.0078	
			0.75	129	0.6085	81.137	
			1	168	0.7975	79.7481	

Location	Sample code	Depth in core (m)	Sample weight (gr)	CO <sub>2</sub> Volume	CaCO <sub>3</sub> weight (gr)	CaCO <sub>3</sub> percentage in sample (%)	Average CaCO <sub>3</sub> percentage (%)
Adele Reef	A03-30	-0.3	0.25	50	0.2258	90.3101	84.8676
			0.5	90	0.4196	83.9147	
			0.75	132	0.6231	83.0749	
			1	173	0.8217	82.1705	
	A03-180	-1.8	0.25	45	0.2016	80.6202	78.6499
			0.5	84	0.3905	78.1008	
			0.75	125	0.5891	78.553	
			1	163	0.7733	77.3256	
	A03-340	-3.4	0.25	48	0.2161	86.4341	77.3175
			0.5	79	0.3663	73.2558	
			0.75	119	0.5601	74.677	
			1	158	0.745	74.9031	
	A04-35	-0.35	0.25	48	0.2161	86.4341	88.3802
			0.5	95	0.4438	88.7597	
			0.75	141	0.6667	88.8889	
			1	188	0.8944	89.438	
	A04-105	-1.05	0.25	50	0.2258	90.3101	89.228
			0.5	96	0.4486	89.7287	
			0.75	141	0.6667	88.8889	
			1	185	0.8798	87.9845	
	A04-212	-2.12	0.25	49	0.2209	88.3721	81.8798
			0.5	87	0.405	81.0078	
			0.75	127	0.5988	79.845	
			1	165	0.7829	78.2946	
	A05-20	-0.2	0.25	55	0.25	100	88.3398
			0.5	94	0.439	87.7907	
			0.75	134	0.6328	84.3669	
			1	171	0.812	81.2016	
	A05-140	-1.4	0.25	46	0.2064	82.5581	81.6376
			0.5	87	0.405	81.0078	
			0.75	130	0.6134	81.7829	
			1	171	0.812	81.2016	
	A06-10	-0.1	0.25	41	0.1822	72.8582	83.293
			0.5	90	0.4196	83.9147	
			0.75	138	0.6521	86.9509	
			1	188	0.8944	89.438	
	A06-150	-1.5	0.25	46	0.2064	82.5581	84.5042
			0.5	91	0.4244	84.8837	
			0.75	135	0.6376	85.0129	
			1	180	0.8556	85.562	
	A06-300	-3	0.25	41	0.1822	72.8682	79.2151
			0.5	86	0.4002	80.0388	
			0.75	130	0.6134	81.7829	
			1	173	0.8217	82.1705	
	A07-50	-0.5	0.25	53	0.2403	96.124	89.4703
			0.5	95	0.4438	88.7597	
			0.75	138	0.6521	86.9509	
			1	181	0.8605	86.0465	
	A07-155	-1.55	0.25	48	0.2161	86.4341	87.3304
			0.5	94	0.439	87.7907	
			0.75	139	0.657	87.5969	
			1	184	0.875	87.5	
	A07-245	-2.45	0.25	48	0.2161	86.4341	83.3737
			0.5	89	0.4147	82.9457	
			0.75	131	0.6182	82.4289	
			1	172	0.8169	81.686	
	A08-20	-0.2	0.25	35	0.1531	61.2403	75.6621
			0.5	84	0.3905	78.1008	
			0.75	126	0.594	79.199	
			1	177	0.8411	84.1085	
	A08-96	-0.96	0.25	44	0.1967	78.6822	79.3362
			0.5	85	0.3953	79.0698	
			0.75	127	0.5988	79.845	
			1	168	0.7975	79.7481	
	A09-20	-0.2	0.25	57	0.2597	103.876	91.2064
			0.5	98	0.4583	91.6667	
			0.75	136	0.6424	85.6589	
			1	176	0.8362	83.624	
	A09-127	-1.27	0.25	40	0.1773	70.9302	76.4695
			0.5	82	0.3808	76.1628	
			0.75	125	0.5891	78.553	
			1	169	0.8023	80.2326	
	A10-15	-0.95	0.25	45	0.2016	80.6202	85.1906
			0.5	92	0.4293	85.8527	
			0.75	137	0.6473	86.3049	
			1	185	0.8798	87.9845	
	A10-95	-0.95	0.25	48	0.2161	86.4341	87.0882
			0.5	93	0.4341	86.8217	
			0.75	139	0.657	87.5969	
			1	184	0.875	87.5	
	A10-180	-1.8	0.25	47	0.2112	84.4961	84.6657
			0.5	90	0.4196	83.9147	
			0.75	136	0.6424	85.6589	
			1	178	0.8459	84.593	



To whom it may concern:

I, **Michael J. O’Leary** have contributed as supervisor, technical advisor and through mentoring to three research papers as part of a PhD thesis prepared for Curtin University by Tubagus Solihuddin

I am also listed as co-author of the papers referred to below and did so in my capacity as PhD Supervisor.

List of articles:

Solihuddin T., Collins L. B., Blakeway D., **O’Leary M. J.**, 2015. Holocene coral reef growth and sea level in a macrotidal, high turbidity setting: Cockatoo Island, Kimberley Bioregion, northwest Australia. *Marine Geology* 359: 50–60.

Solihuddin T., **O’Leary M. J.**, Blakeway D., Kordi M., Parnum I., Collins L. B., 2016. Holocene reef evolution in a macrotidal setting: Buccaneer Archipelago, Kimberley Bioregion, Northwest Australia. *Coral Reefs* pp. 1-12 [DOI 10.1007/s00338-016-1424-1]

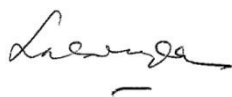
Solihuddin T., Bifarale G., **O’Leary M. J.**, Blakeway D., 2016. Geomorphology and Holocene accretion history of a mid-shelf platform reef: Adele Reef, Kimberley Bioregion, Northwest Australia. *Geo-Marine Letters* (in review).

The papers take part of the PhD thesis and first author Tubagus Solihuddin



(Supervisor and co-author signature)

**Michael J. O’Leary**



(Candidate signature)

**Tubagus Solihuddin**

To whom it may concern:

I, **David Blakeway** have participated in data collection, interpretation, and technical advisor to three research papers as part of a PhD thesis prepared for Curtin University by Tubagus Solihuddin

I am also listed as co-author of the papers referred to below and did so in my capacity as a research collaborator.

List of articles:

Solihuddin T., Collins L.B., **Blakeway D.**, O’Leary M.J., 2015. Holocene coral reef growth and sea level in a macrotidal, high turbidity setting: Cockatoo Island, Kimberley Bioregion, northwest Australia. *Marine Geology* 359: 50–60.

Solihuddin T., O’Leary M.J., **Blakeway D.**, Kordi M., Parnum I., Collins L.B., 2016. Holocene reef evolution in a macrotidal setting: Buccaneer Archipelago, Kimberley Bioregion, Northwest Australia. *Coral Reefs* pp. 1-12 [DOI 10.1007/s00338-016-1424-1]

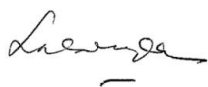
Solihuddin T., Bugarale G., O’Leary M.J., **Blakeway D.**, 2016. Geomorphology and Holocene accretion history of a mid-shelf platform reef: Adele Reef, Kimberley Bioregion, Northwest Australia. *Geo-Marine Letters* (in review).

The papers take part of the PhD thesis and first author Tubagus Solihuddin



(Co-author signature)

**David Blakeway**



(Candidate signature)

**Tubagus Solihuddin**

To whom it may concern:

I, **Moataz Kordi** have participated in coring data acquisition for the article:

Solihuddin T., O'Leary M.J., Blakeway D., **Kordi M.**, Parnum I., Collins L.B., 2016. Holocene reef evolution in a macrotidal setting: Buccaneer Archipelago, Kimberley Bioregion, Northwest Australia. Coral Reefs pp. 1-12 [DOI 10.1007/s00338-016-1424-1]

The paper takes part of the PhD thesis and first author is Tubagus Solihuddin



(Co-author signature)

**Moataz Kordi**



(Candidate signature)

**Tubagus Solihuddin**

To whom it may concern:

I, **Iain Parnum** have participated in bathymetry data acquisition and interpretation for the article:

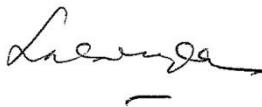
Solihuddin T., O’Leary M.J., Blakeway D., Kordi M., **Parnum I.**, Collins L.B., 2016. Holocene reef evolution in a macrotidal setting: Buccaneer Archipelago, Kimberley Bioregion, Northwest Australia. Coral Reefs pp. 1-12 [DOI 10.1007/s00338-016-1424-1]

The paper takes part of the PhD thesis and first author is Tubagus Solihuddin



(Co-author signature)

**Iain Parnum**



(Candidate signature)

**Tubagus Solihuddin**

To whom it may concern:

I, **Giada Bufarale** have participated in seismic data acquisition and interpretation for the article:

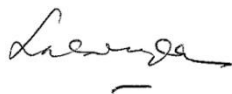
Solihuddin T., **Bufarale G.**, O’Leary M.J., Blakeway D., 2016. Geomorphology and Holocene accretion history of a mid-shelf platform reef: Adele Reef, Kimberley Bioregion, Northwest Australia. *Geo-Marine Letters* (in review).

The paper takes part of the PhD thesis and first author is Tubagus Solihuddin



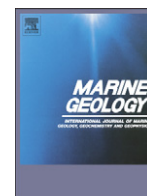
(Co-author signature)

**Giada Bufarale**



(Candidate signature)

**Tubagus Solihuddin**



# Holocene coral reef growth and sea level in a macrotidal, high turbidity setting: Cockatoo Island, Kimberley Bioregion, northwest Australia



Tubagus Solihuddin<sup>a,d,\*</sup>, Lindsay B. Collins<sup>a,d</sup>, David Blakeway<sup>b</sup>, Michael J. O' Leary<sup>c,d</sup>

<sup>a</sup> Department of Applied Geology, Curtin University, Bentley, WA 6102, Australia

<sup>b</sup> Fathom 5 Marine Research, 17 Staines Street, Lathlain, WA 6100, Australia

<sup>c</sup> Department of Environment and Agriculture, Curtin University, Bentley, WA 6102, Australia

<sup>d</sup> The Western Australian Marine Science Institution, Floreat 6014, Australia

## ARTICLE INFO

### Article history:

Received 9 September 2014

Received in revised form 6 November 2014

Accepted 18 November 2014

Available online 25 November 2014

### Keywords:

*Acropora*

*Porites*

Reef geomorphology

Holocene reef growth

Sea-level change

Accretion rate

## ABSTRACT

The inshore Kimberley Bioregion of northwest Australia is a macrotidal, low wave energy, frequent cyclones, and high turbidity setting with abundant fringing coral reefs. Here we describe the Holocene development of a sheltered fringing reef at Cockatoo Island in the Kimberley, using data from reef cross-sections subaerially exposed in an iron ore mining pit, seismic profiles across the adjacent contemporary reef, and GIS and ground truth mapping of contemporary reef habitats. Subsidence since the Last Interglacial has provided accommodation for ~13–20 m of Holocene reef accretion upon an older, probably Last Interglacial, reef. In the pit cross-sections, the reef initiated at ~9000 cal y BP and accreted in a catch-up mode, reaching sea level at ~3000 cal y BP, and reef accretion rates varied from 26.8 mm/year to 0.8 mm/year, averaging ~2 mm/year. The catch-up interpretation is supported by the predominance of branching *Acropora* throughout the Holocene section and the absence of contemporary intertidal indicators such as *Porites cylindrica* and *Millepora intricata*. This pattern differs from the otherwise similar mud-rich but mostly microtidal inshore fringing reefs of the Great Barrier Reef, which initiated in the late Holocene on shallow substrates under a stable sea level. The study provides the first Holocene reef growth history for an inshore Kimberley reef within a biodiversity “hotspot”.

© 2014 Elsevier B.V. All rights reserved.

## 1. Introduction

The Kimberley coast is a remote sparsely populated and poorly studied region located in the NW of Western Australia. However, the discovery of a major hydrocarbon province in the offshore Browse Basin, and an increase in petroleum exploration in the region, has led to a heightened awareness of the region's rich biodiversity (Collins, 2002; Chin et al., 2008; Collins et al., 2011). While the presence of coral reefs have been broadly documented, occurring as fringing reefs in coastal settings, platform reefs in mid-ramp settings and atoll-like reefs along the shelf margin (Wilson et al., 2011), there have been few investigations into their biogeography, diversity and developmental history.

Coral reefs are particularly ubiquitous to the complex drowned landscape of the Kimberley coast, which provides abundant Proterozoic deformed rocky substrate for fringing reef development. These inshore fringing reefs occur in sheltered and exposed settings and endure in seemingly extreme environment conditions including: high turbidity and sediment input, elevated water temperatures (av. 28.5 °C), a 10 m macrotidal range, significant subaerial exposure during low tides, and frequent cyclones. Despite these extreme conditions, the coral

biodiversity in the Kimberley is far richer than that of the inner GBR fringing reefs and a little richer than those of the Pilbara to the south (Wilson, 2013).

Critically, our understanding of the development of the Kimberley reefs still remains a gap in our knowledge. For example it is not known whether reefs are thin veneers over rock platforms or significant long-lived accretionary structures. Additionally, the linkages between present reef geomorphology, Holocene sea level rise, reef growth history, and coastal processes have been recognized (e.g. Wilson, 2013) but are yet to be explored in any detail. Despite this lack of knowledge, Kimberley reefs have been identified as having international significance and are in need of comprehensive study (Chin et al., 2008; Wilson, 2013).

This study will for the first time investigate the Holocene development and evolution of an inshore Kimberley coral reef located at Cockatoo Island (Fig. 1). Cockatoo is unique in that iron ore mining on the Island has exposed a complete vertical section of the inner part of a Holocene fringing reef. This has allowed for detailed stratigraphic, palaeoecological and geochronological analysis spanning the entire reef growth history, thus enabling an investigation into how these reefs were able to persist under extreme environmental conditions as well as respond to Holocene sea level change. The addition of seismic reconnaissance data has allowed for the broader reef architecture and structure to be assessed. Lastly this study develops a Holocene reef

\* Corresponding author at: Department of Applied Geology, Curtin University, Bentley, WA 6102, Australia. Tel.: +61 8 9266 3710.

E-mail address: [tubagus.solihuddin@postgrad.curtin.edu.au](mailto:tubagus.solihuddin@postgrad.curtin.edu.au) (T. Solihuddin).

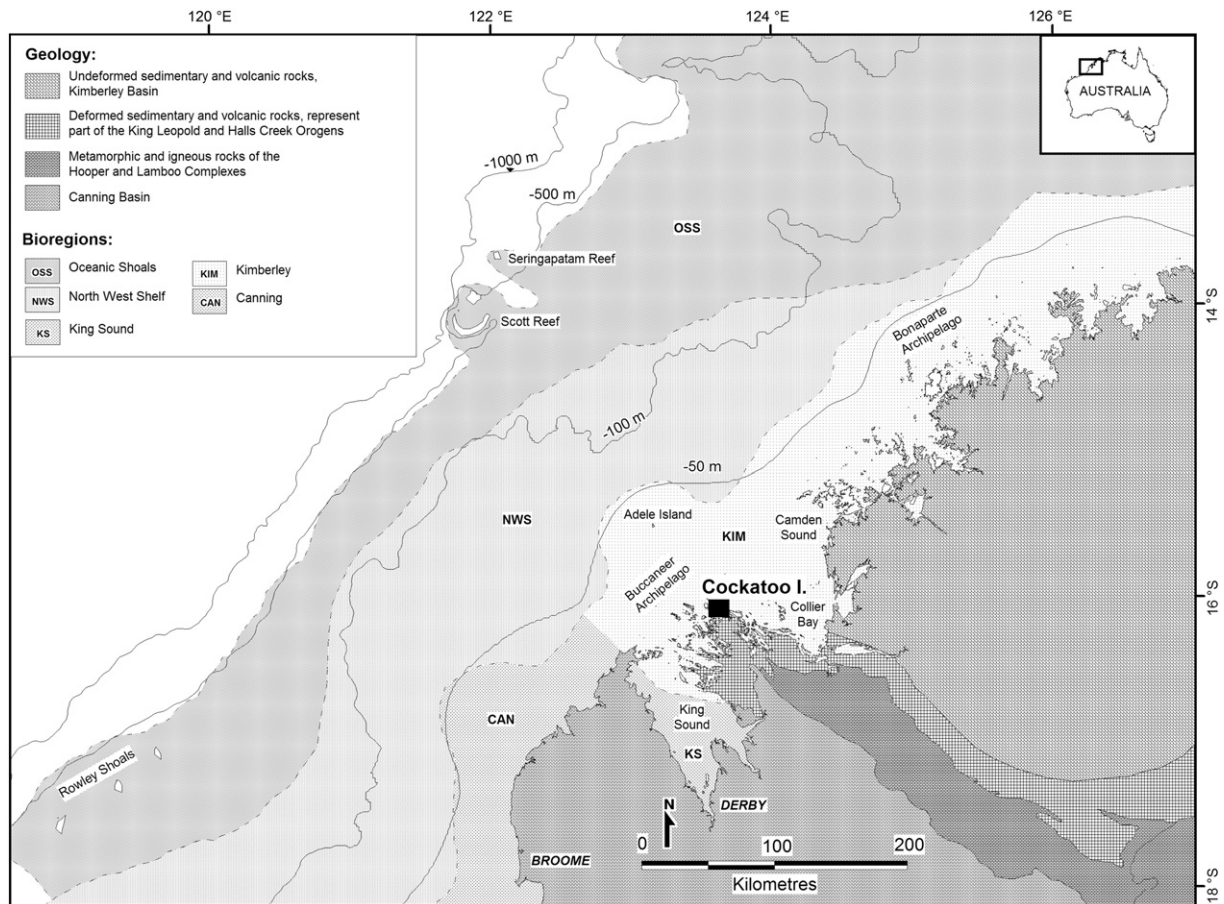


**Fig. 1.** Map showing Bioregions modified from the Integrated Marine and Coastal Regionalisation of Australia (IMCRA) and geology of the Kimberley Region. (Reproduced with permission from Griffin and Grey, 1990).

growth rate curve for the Kimberley, so that the shelf drowning history can be reconstructed. The initiative to protect these marine areas through the Kimberley Science and Conservation Strategy (Government of Western Australia, 2011) also requires a fundamental baseline understanding of how the environment formed for effective long term protection.

### 1.1. Oceanography of the Kimberley Region

The region is tidally dominated, with coastal mean spring range of 9.2 m in King Sound (see Fig. 1; Harris et al., 1991), the highest tide range in Australia (Short, 2011) and the second highest tide in the world after the Bay of Fundy in Canada (Purcell, 2002; Wolanski and Spagnol, 2003). This macro-tidal system generates an extensive intertidal zone and strong tidal currents, which in turn cause high turbidity in coastal waters (Brooke, 1997). The region lies in the monsoonal belt with prevailing westerly or northwesterly rain-bearing winds from November–March, and dry southeasterly or easterly trade winds from May to September. It is cyclone-influenced (average 3 per year, Lough, 1998) and has southwest prevailing swell.

The local oceanography of the inshore Kimberley Bioregion is influenced by the Holloway current, which is driven by the Indonesian Throughflow waters through a southward flow over the shallow Timor Shelf (DEWHA, 2008). This current flows seasonally from March to July and is closely associated with the northwest monsoon by which a south-westerly flow of surface water mass is released along the shelf margin. During the summer months (December to March), the Throughflow is deflected eastward, releasing a weak Holloway current along the inner shelf of the Kimberley. The upwelling generated by the Holloway current along with *in situ* planktonic

production are believed to be contributing to the reef development in this region due to their roles in delivering nutrients where measures of N (0.05/12.8  $\mu\text{M}$ ), P (0.11/0.85  $\mu\text{M}$ ) and carrying planktic biota including planktotrophic larvae and reef animals (Wilson, 2013). Nutrient concentrations in the nearshore coastal Kimberley waters are relatively high here, influenced by riverine inputs from the adjacent terrestrial, high runoff environment (Wilson, 2013).

## 2. Location and methodology

Cockatoo Island (Fig. 1) is located in the Buccaneer Archipelago (123.6°E; –16.1°S), approximately 7 km north of Yampi Peninsula. The geomorphology of the Buccaneer Archipelago and Yampi Peninsula are structurally controlled, reflecting the deformation geometry of the King Leopold Orogen (Wright, 1964). Cockatoo is an elongate island approximately 6 km long and 1.5 km wide and oriented along a NW/SE axis; with the NE side exposed to higher wave energies while the SW side is largely sheltered.

### 2.1. Geophysical surveys

Sub-bottom profiling was performed using an Applied Acoustics Boomer SBP system CSP-P300; with SBP Sound Source, AA201 Boomer Plate, mounted on a CAT100 surface tow catamaran. The receiver streamer had 8 element hydrophones, and A/D Interface Box from NI (National Instruments) Device Monitor V5.3.1. Data acquisition was made using Chesapeake Technology Inc SonarWiz 5 software. Position acquisition was made using a Fugro Seastar 8200XP/HP DGPS receiver. Survey lines were run across the modern reef flat up to a retaining seawall, which runs the length of the mining pit. Two survey lines were also



run along the length of the reef flat, parallel to the seawall and close to sections measured onshore.

## 2.2. Reef mapping

The distribution of living coral and associated substrates was based on aerial photography acquired on 5 May 2010. The image was corrected geometrically using a geographic coordinate system and WGS 84 ellipsoid reference. The three bands of aerial photography (RGB 123), along with ground truth information, were employed to extract reef facies information. Discrimination of substrates into distinct classes was recognized from reflectance spectra grouped using unsupervised classification digital processing in ArcMap's Image Analysis toolkit. The spectral signature of each pixel in the aerial photography was determined based on a grouping of the spectra of each individual band. The habitat classifications were ground truthed using towed camera transects over the reef flat and direct observations of the reef flat made on foot during spring low tides.

## 2.3. Ore pit mapping

Excavation of a 50 m deep, 750 m long open cut pit on Cockatoo Island has exposed a complete vertical section through the Holocene reef. Four stratigraphic sections were established along the face of the pit to log the reef exposures. At each site a vertical 0.7 m wide section from the base of the sequence to the top was logged, sampled and photographed. Information recorded includes: (i) the ratio of reef framework to matrix (following Embry and Klovan, 1971); (ii) sediment textural characteristics (using the Udden-Wentworth nomenclature, as well as a visual assessment of sediment composition); and (iii) coral generic identification. Overlapping photographs (0.7 m x 0.5 m) were also taken up each profile. Reef framework analysis and facies descriptions followed the terminology suggested by Montaggioni (2005), which highlights the growth forms of the dominant coral reef builders and environmental indicators. The carbonate content of matrix sediment was determined by carbonate bombe (weight % loss after treatment with 50% HCL) following guidelines from Müller and Gastner (1971). Position fixing was by DGPS tied to minesite datum. Elevations from each transect were plotted relative to the Australian Height Datum (AHD), which is 3.987 m below the Cockatoo mine grid datum (mine survey data).

## 2.4. Geochronology

*In situ* corals were collected from levels along each vertical section for accelerator mass spectrometry (AMS) radiocarbon dating in order to establish a geochronologic record of reef accretion. Radiocarbon dates were recalibrated using CALIB Version 5.0.2 and calibration curve Marine04 (<http://calib.qub.ac.uk/marine>; accessed November 2012). A weighted mean  $\Delta R$  value of  $+58$  (average calculation from 3 nearest points) was used as the best current estimate of variance in the local open water marine reservoir effect for Cockatoo Island and adjacent areas. Dates discussed in the text are calibrated in years Before Present (cal y BP) with the 68.2% ( $2\sigma$ ) probability range for all dated samples.

## 3. Results

### 3.1. Living coral community zonation

A map of reef habitats and substrates around Cockatoo Island, based on aerial photographic interpretation (Fig. 2) provides a broad characterisation of the reef flat and its coral and macroalgal cover. Aerial photographic mapping linked to on ground observations and video transects delineates four gradational intertidal habitat zones. From landward to seaward these are the (1) intertidal beach and boulder

rubble zone (2) inner sand flat and reef platform, (3) outer reef platform, and (4) forereef slope.

The upper intertidal zone consisting of steep sloping beaches of coarse, well-sorted siliciclastic sand is found in more embayed sections of the Island. Along sections of the Island consisting of steep plunging cliffs, hematite rich, sandstone boulder rubble deposits dominate the upper intertidal and supratidal zones.

The lower intertidal zone consists of sand flats of poorly sorted, predominantly calcareous, sand with a matrix of pale grey-green calcareous mud. This transitions into the inner reef platform that includes sparsely distributed small coral colonies, mainly *Porites* and faviids but including many other genera. Macroalgae, predominantly *Sargassum*, are seasonally abundant on coral rubble substrate in this zone. Small thickets of the branching hydroid *Millepora* and the branching coral *Porites cylindrica* are common on the mid reef flat about 50–150 m from shore, occurring within extensive shallow pools (Fig. 3A).

The outer reef platform zone occurs seaward of these pools where the reef flat rises slightly, and is emergent for several hours on extreme spring low tides. Corals here occur as numerous close-packed colonies. *Porites* predominates but an extensive range of other genera occur, including, in estimated order of abundance: *Turbinaria* (Fig. 3B), *Favia*, *Favites*, *Goniopora*, *Lobophyllia*, *Astreopora*, *Montipora*, *Merulina*, *Pectinia*, *Goniastrea*, *Cyphastrea*, *Galaxea* and *Acropora* (tabular and fine aborescent forms) *P. cylindrica* is the most common *Porites* but massive species are also common, usually as relatively small (<0.5 m) colonies, often with microatoll architecture due to low tide exposure.

The forereef slope is well defined and slopes seaward at approximately 30°, however, there is no raised reef crest along the reef edge. Video observations on the reef slope show a high cover (50–100%) of live branching *Acropora* (Fig. 3C) and, occasionally, *Seriatopora*, generally as large colonies, from the reef edge to approximately 10 m below AHD. Downslope, dead coral branches are sparsely colonised by encrusting *Montipora*, encrusting to plating pectiniid corals and small fine branching *Acropora* colonies to approximately 20 m below AHD. The lower slope consists of coral rubble, colonised by gorgonians and sponges, in a mud matrix. The base of the lower slope grades gently into burrowed mud at approximately 30 m below AHD.

### 3.2. Stratigraphy and palaeoecology

Stratigraphic and palaeoecological data from the Cockatoo Island fringing reef is shown in Fig. 4. Each of the four measured reef sections are located approximately 50 m seaward of the original steep rocky shoreline, and represent the inner reef platform environment.

The basement is the Proterozoic Elgee Siltstone. Overlying the Elgee Siltstone is a 1 to 2 m thick sedimentary talus breccia containing subangular haematite boulders. Above the breccia is a 3 to 5 m thick pale yellow coral-rich mudstone with occasional weakly-bedded sand horizons and a calcretised, iron-stained upper surface. Corals in this unit are mainly domal, with a few encrusting and branching forms. Colonies are generally small (<30 cm diameter) and invariably recrystallised. Faviids are predominant, including *Favia*, *Goniastrea*, *Cyphastrea* and *Platygyra*. Overlying this unit is a second 0.3 to 1 m thick haematite boulder breccia, followed by the Holocene reef, which is 8.4 to 12.7 m thick in the measured profiles. This is a minimum thickness because the upper contact is partly obscured by the rock overburden of the overlying seawall, and because there may have been some compaction of the Holocene by the seawall, a 13 m high structure comprising a clay core and rock armour.

All stratigraphic sections are dominated by single coral rudstone reef facies dominated by fragmented *Acropora* (typical diameter approximately 10–15 mm and length up to 150 mm) but also containing fragments and whole colonies of many other coral genera as well as abundant and diverse molluscan fauna. Additionally, the preservation of fine surface skeletal detail on most of the coral fragments indicates



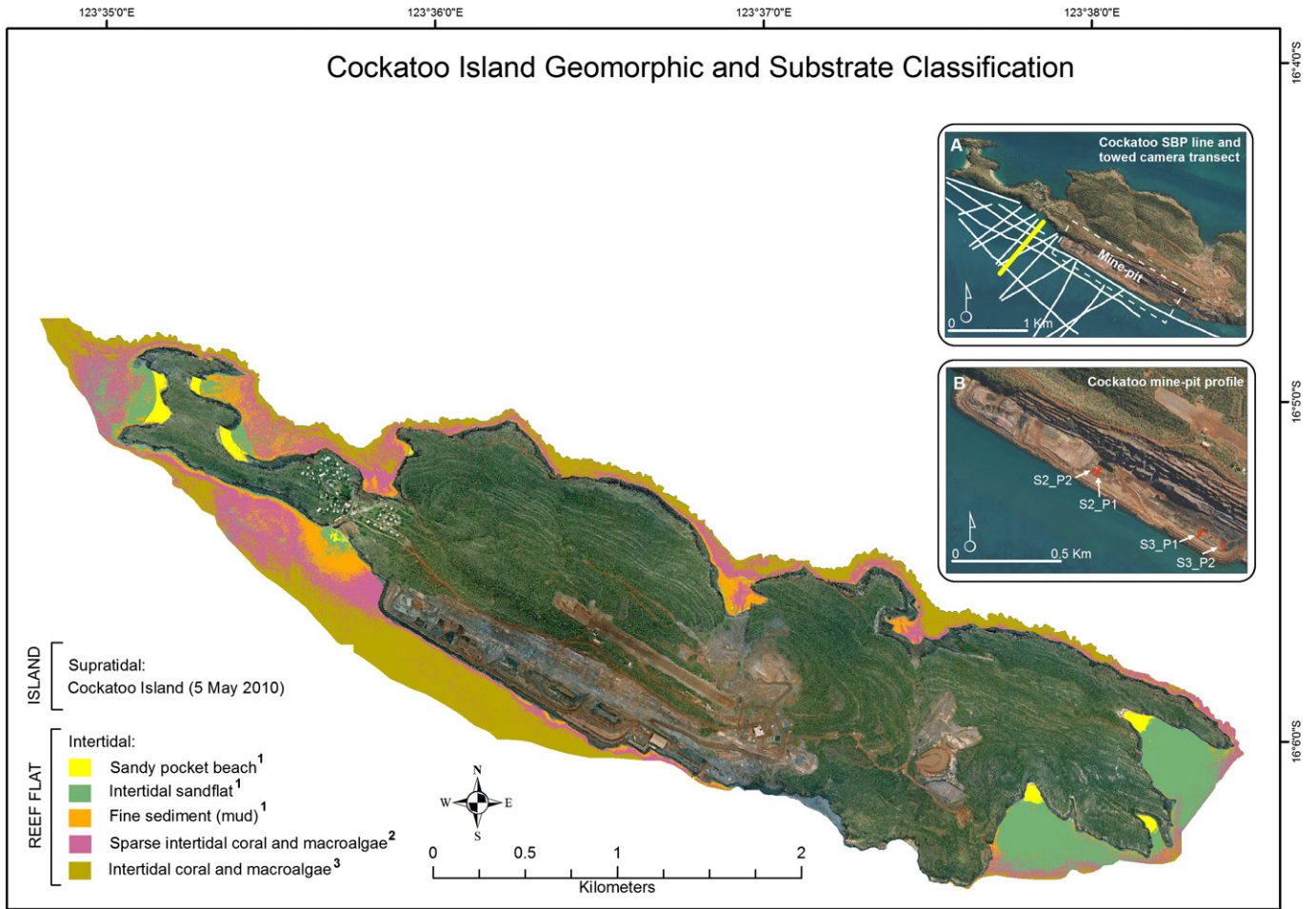


**Fig. 2.** Map showing Cockatoo Island geomorphic and substrate classification, based on aerial photography interpretation (RGB 123). Numbers in legend correlate with habitats identified by on ground and towed video observation: (1) intertidal beach and boulder rubble zone, (2) inner sand flat and reef platform, (3) outer reef platform. The narrow and steep forereef slope is not mappable here. The inset map (A) shows sub bottom profile (white line) and towed camera (yellow line) transects and (B) location of the mine-pit measured sections.

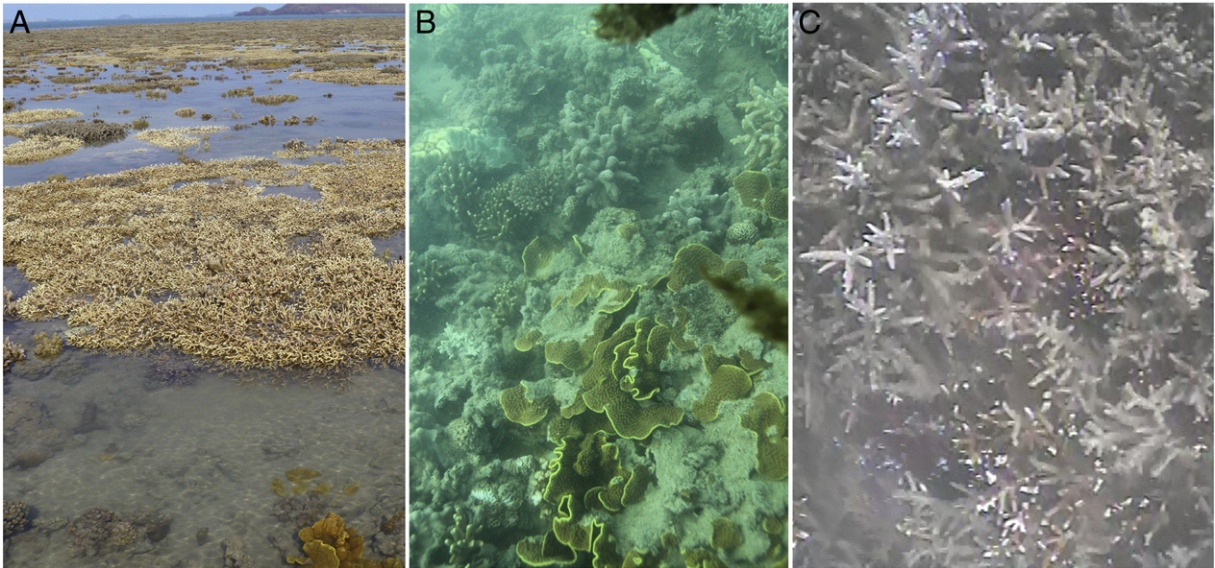


**Fig. 3.** Living coral communities on the SW Cockatoo Island fringing reefs. (A) The extensive shallow pools on reef flat at low tide showing small thickets of the branching hydroid *Millepora* and the branching coral *Porites cylindrica*. (B) *Turbinaria* and branching *Porites* in the outer reef flat. (C) High coral cover of branching *Acropora* on the forereef slope.

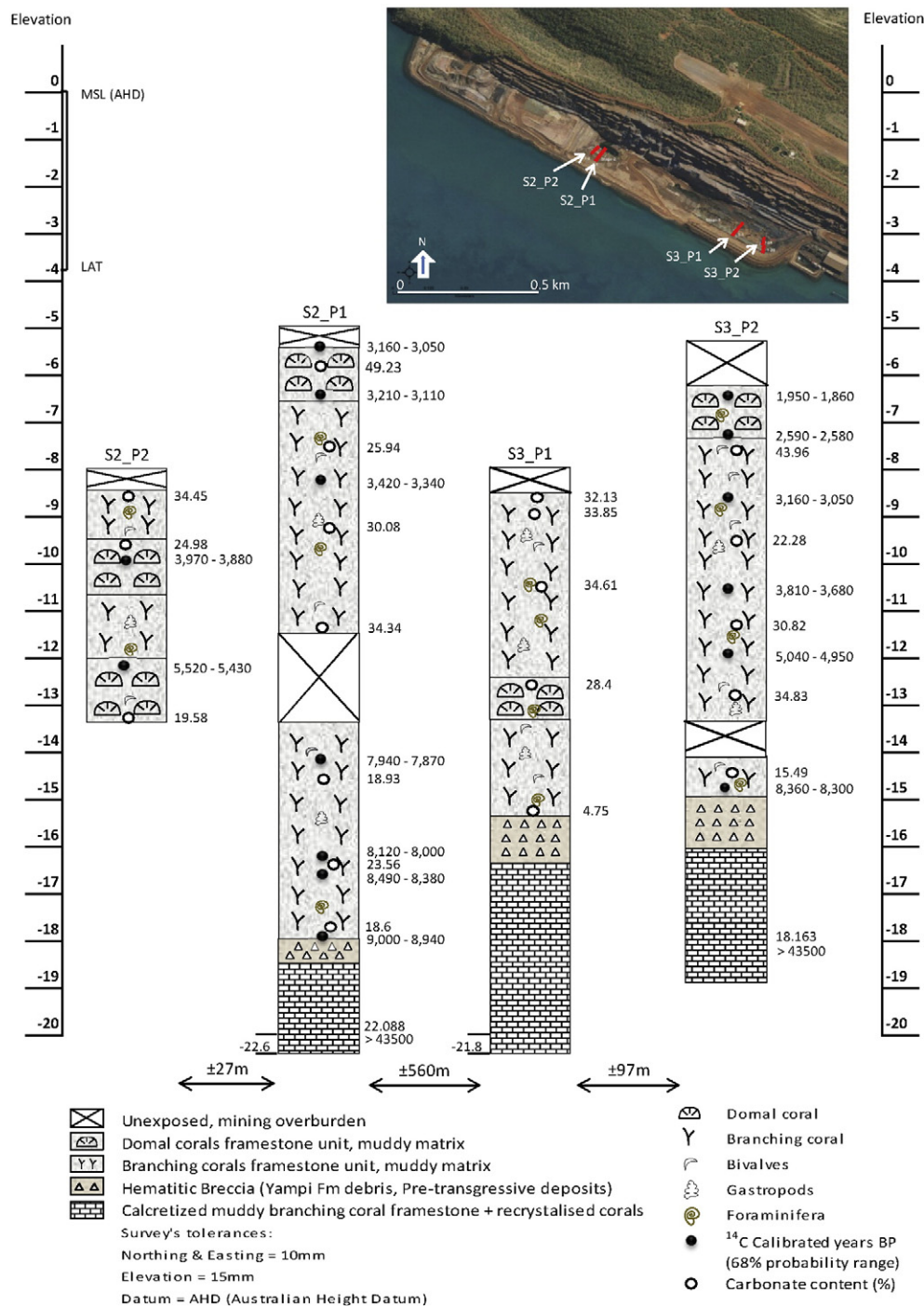


Fig. 4. Lithostratigraphic and chronostratigraphic summary of measured sections of Cockatoo mine-pit.

that they have undergone little transport; many appear to have collapsed where they grew. All interstices in the reef are completely filled with a poorly sorted grey-green calcareous mud containing sand to gravel-sized calcareous fragments and foraminifera tests. Coralline algae are rare throughout the sequence and there is virtually no inorganic cementation.

There are several non-acroporid dominant coral horizons in some sections but they do not appear to be laterally continuous. *Porites* is the most abundant genus but is not dominant to the extent that it is on the modern reef flat, and only occurs as massive forms, *P. cylindrica* is conspicuously absent from the Holocene. Additional taxonomic differences between the Holocene and the living reef are the absence of

branching *Millepora* from the Holocene and the relative scarcity of *Turbinaria* and tabular *Acropora* in the Holocene (Fig. 5).

Analysis of matrix sediments (Fig. 4) showed carbonate content increased up section from 4% to 18% carbonate in the basal 2–3 m of the measured sections to 43–49% for the uppermost 2 m of the sections. The non-carbonate components include terrigenous clays and minor organics.

### 3.3. Reef geochronology and growth history

Sixteen radiometric dates were made on coral clasts collected from reef sections (NW and SE) exposed along the seaward mine-pit wall.



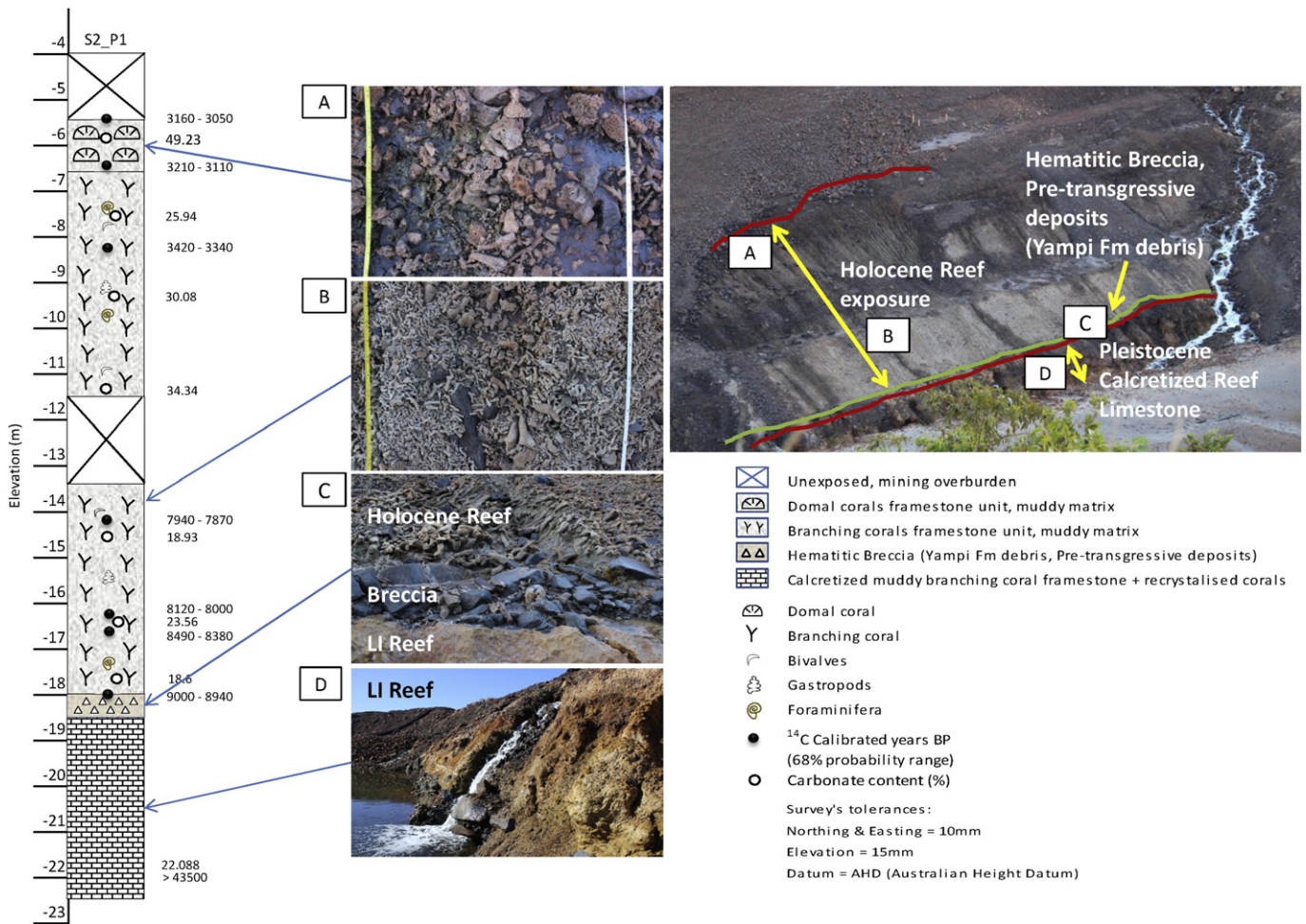


**Fig. 5.** Idealised stratigraphic column of Cockatoo mine-pit section (S2\_P1). Photo (A) showing the domal coral framestone with a muddy matrix, photo (B) showing the prevailing branching coral and coral rubble, photo (C) showing the contact between Holocene reef and Last Interglacial reef with a hematitic breccia as pre-transgressive deposits, and photo (D) showing the calcretized Last Interglacial reef exposure. Note  $^{14}\text{C}$  ages and % carbonate in matrix fraction are also shown.

All colonies were interpreted as *in situ* on taphonomic and orientation criteria. Results indicate earliest Holocene reef growth initiated directly on the underlying pre-transgressive hematitic breccias along the NW reef section (S2) at a depth of 18.1 m below AHD (MSL) by ~8970 cal y BP. While the upper 1 m of reef surface is obscured by the sea wall, it would appear the reef flat had reached the approximate level of mean low water (~5.5 m below present AHD) in the NW reef section (S2) as early as ~3105 cal y BP, while the SE reef section (S3) reached mean low water level at around ~1905 cal y BP. (Table 1).

Vertical accretion rates varied across NW and SW reef sites (Fig. 6). The NW section shows initial rapid vertical reef aggradation on the order of 3.8 mm/yr between 9 and 8 kyr BP, which occurred at some time post the initial flooding. There was an abrupt slowing after 7.9 kyr BP to around 1.2 mm/yr until around 5.5 kyr BP, where the reef showed gradual but sustained increase in accretion rates of up to 27 mm/yr as the reef flat reached near sea level with increasing light and energy. The SE section, unlike the NW section, did not show an initial rapid accretion but instead exhibited a more uniform accretion across its entire growth history. Unlike the NW section the SE section exhibited a slight reduction in vertical accretion after about 4 kyr BP from 3.6 mm/r to 2.0 mm/yr. The study was not able to establish the exact timing of when the SE section reached base level due to the top of the section being covered by mine waste.

Reef accretion records from the Abrolhos, Scott Reef, Middle Reef (GBR) and now Cockatoo Island are shown in Fig. 7. While the Abrolhos record exhibits a keep-up growth history closely following sea level, reef accretion data from Cockatoo suggest it grew in a catch-up phase for most of its growth history. A lack of subsidence since the LIG and

presence of a late Holocene highstand in SW Australian reefs (below 22 degrees south) contrasts with the Kimberley where no late Holocene highstand has been recorded to date, whilst there has been significant post-LIG subsidence at Cockatoo and Scott Reefs (Collins et al., 2011).

### 3.4. Reef architecture and seismic structure

Boomer profiles immediately seaward of the logged pit profiles show the modern reef flat surface terminating in a steep ( $\pm 30^\circ$ ) forereef slope with a 20 m thick-bedded sediment mound to seaward (Fig. 8). Three subsurface units are apparent, separated by reflectors at 37 m below sea level (bsl) and 40–45 m bsl.

Based on correlation with the logged sections, the seismic units correspond to the Holocene reef, the LIG reef and the Proterozoic bedrock. The Holocene reef is 15–20 m thick, with a flat upper surface at 8 m bsl, shallowing slightly to landward. The surface of the underlying LIG reef is irregular and has a distinct reef crest at 30–40 m (Fig. 9). A deeper unconformity with an average depth of 40–50 m marks the position of the Proterozoic rock foundation.

## 4. Discussion

### 4.1. Evidence of neotectonic subsidence along the Kimberley Coast and offshore shelf

As a trailing, intraplate continental margin, coastal WA should be relatively tectonically stable. However, recent studies have identified

**Table 1**  
Radiocarbon dates from selected samples across Cockatoo mine-pit transects.

SAMPLE NUMBER/ELEVATION (m)	LAB. CODE	MATERIAL	MEASURED AGE	$^{13}\text{C}/^{12}\text{C}$	CONVENTIONAL AGE	CALIBRATED (68% Probability) cal BP	CALIBRATED (95% Probability) cal BP
S3_P2-31/-14.794	Beta-364241	<i>Goniastrea</i>	7490 $\pm$ 30 BP	+1.3 o/oo	7920 $\pm$ 30 BP	8360–8300	8390–8270
S3_P2-28/-6.387	Beta-361585	<i>Galaxea</i>	1980 $\pm$ 30 BP	–1.7 o/oo	2360 $\pm$ 30 BP	1950–1860	1990–1820
S3_P2-27/-7.337	Beta-361584	<i>Porites</i>	2430 $\pm$ 30 BP	–0.6 o/oo	2830 $\pm$ 30 BP	2590–2580	2660–2340
S3_P2-26/-8.757	Beta-361583	<i>Porites</i>	2920 $\pm$ 30 BP	+0.2 o/oo	3330 $\pm$ 30 BP	3160–3050	3210–2980
S3_P225/-10.667	Beta-361582	<i>Porites</i>	3490 $\pm$ 30 BP	–2.4 o/oo	3860 $\pm$ 30 BP	3810–3680	3840–3630
S3_P2-24/-12.177	Beta-361581	<i>Porites</i>	4430 $\pm$ 30 BP	–1.5 o/oo	4820 $\pm$ 30 BP	5040–4950	5190–5140
S2_P1-13/-5.737	Beta-361580	<i>Porites</i>	2530 $\pm$ 30 BP	–0.7 o/oo	2930 $\pm$ 30 BP	2700–2640	2720–2510
S2_P1-12/-5.377	Beta-361579	<i>Porites</i>	2920 $\pm$ 30 BP	–0.1 o/oo	3330 $\pm$ 30 BP	3160–3050	3210–2980
S2_P1-11/-6.447	Beta-361578	<i>Montastrea</i>	2980 $\pm$ 30 BP	–1.2 o/oo	3370 $\pm$ 30 BP	3210–3110	3260–3050
S2_P1-10/-8.357	Beta-361577	<i>Cyphastrea</i>	3170 $\pm$ 30 BP	–1.4 o/oo	3560 $\pm$ 30 BP	3420–3340	3450–3310
S2_P2-09/-9.956	Beta-364239	<i>Porites</i>	4780 $\pm$ 30 BP	–1.0 o/oo	4010 $\pm$ 30 BP	3970–3880	4060–3830
S2_P2-08/-12.23	Beta-364238	<i>Porites</i>	3172 $\pm$ 30 BP	–1.9 o/oo	5160 $\pm$ 30 BP	5520–5430	5560–5320
S2_P1-07/-14.257	Beta-361576	<i>Porites</i>	7150 $\pm$ 30 BP	–3.1 o/oo	7510 $\pm$ 30 BP	7940–7870	7970–7830
S2_P1-06/-16.087	Beta-361575	<i>Porites</i>	7320 $\pm$ 30 BP	–3.4 o/oo	7670 $\pm$ 30 BP	8120–8000	8150–7970
S2_P1-05/-16.617	Beta-361574	<i>Lepastrea</i>	7650 $\pm$ 40 BP	–1.0 o/oo	8040 $\pm$ 40 BP	8490–8380	8540–8350
S2_P1-04/-18.087	Beta-361573	<i>Goniastrea</i>	8040 $\pm$ 50 BP	–1.1 o/oo	8430 $\pm$ 50 BP	9000–8940	9070–8840
S2_P1-03/-22.088	Beta-385986	Coral	>43,500 BP	–4.4 o/oo			
S3_P2-30/-18.163	Beta-385987	Coral	>43,500 BP	–4.9 o/oo			

All samples were dated at the Beta Analytic Inc. Miami, Florida USA.

seismic activity, and structural and geomorphological features consistent with ongoing crustal deformation (Sandiford, 2003; Quigley et al., 2006, 2007). On the continental scale Sandiford (2007) and DeCaprio et al. (2009) have identified tilting of the Australian plate driven by changes in mantle convection, whereby eastern and northwestern Australia is experiencing subsidence and southern and southwestern Australia is experiencing uplift.

Evidence supporting this theory can be found in the relative elevation of LIG shorelines along the WA coast. Presently LIG reefs outcrop intermittently above present sea level along a stretch of coast from Foul Bay (34°S) to Cape Keraudran (20° S) (Collins et al., 1996; O'Leary et al., 2008, 2013). North of this line the only occurrence of LIG reefs that has been observed is in bore holes from the shelf edge Scott Reef at an elevation of 36 to 60 m below AHD (Collins et al., 2011). Here we are able to provide the first evidence of a LIG reef from the Kimberley region, which outcrops at an elevation of 18 m below AHD. Although U-series analysis has not been carried out on this basal reef unit, the fact that corals exhibit a high degree of diagenetic alteration in contrast to the Holocene reef, and the Holocene and LIG reef are separated by a hematite breccia layer supports this interpretation.

Stratigraphic data from Cockatoo transects confirm that the LIG reef surface underlies the Holocene reef more broadly and exhibits reef terrace morphology. Assuming the LIG reef terrace reached base level the elevation would suggest a linear subsidence rate of around 0.1 m/ky since the LIG, this compares to a recent study which estimated subsidence rates at South and North Scott Reef on the Rowley Shelf margin

as 0.45 m/ka and 0.29 m/y respectively (Collins et al., 2011), where the shallowest LIG reef is at 36 m below AHD. Based on the proximal Cockatoo and distal Scott Reef subsidence data a subsidence with tilting offshore appears likely for the Kimberley coast and adjacent shelf.

#### 4.2. Holocene reef growth

Reef growth on Cockatoo Island initiated around 9 kyr BP at –18 m below AHD as evidenced from the radiocarbon ages from the basal Holocene corals. The timing of this event would suggest that corals became established not long after flooding of the antecedent substrate had occurred with sea level transgressing the –20 m elevation at around 10 kyr BP (Lambeck et al., 2010). Accretion curves plotted in Fig. 6 indicate the reef initially grew in a Keep-Up phase as shown by the high vertical accretion rates for this period. A reduction in reef accretion rate after 7.5 kyr BP and a shift from Keep-Up to Catch-Up growth phase likely resulted from the rapid deepening of the reef which became submerged to >10 m below AHD by ~7 kyr BP before eventually reaching MLW (~4 m below AHD) at ~3000 cal y BP.

Palaeoecological and sedimentological evidence for a Catch-Up reef growth includes the abundance of branching *Acropora* throughout the sequence and the predominance of a sandy mud matrix that becomes dominated by sand at the top, only becoming sandy at the top of the sequence. The absence of present-day intertidal indicators such as *P. cylindrica*, branching *Millepora*, tabular *Acropora* and coral micro atolls can also be considered to support a subtidal characterisation of the reef facies. However these indicators are also absent from the top of the logged profiles, when the reef had reached the intertidal zone. We conclude either that environmental or ecological conditions at the time did not suit the modern intertidal taxa, or that the modern coral community and zonation have only developed after prolonged intertidal exposure, and may therefore be restricted to a thin zone at the very top of the logged profiles which may not always show up in cross-section, or which we may have missed due to the seawall overburden.

As we currently lack any cross-reef age isochrons, we can only propose a reef growth style, based on field observations supported by seismic profiles. The interpretation outlined above—of the reef initiating as a blanket and growing upward—is one possibility; another is that the reef initiated close to shore and prograded seaward. These alternatives correspond to models A and B respectively in Kennedy and Woodroffe's (2002) review of fringing reef growth and morphology. We consider Kennedy and Woodroffe's more complex models C to F to be less likely analogs, due mainly to the apparently uniform internal structure of the Cockatoo reef in seismic profiles.

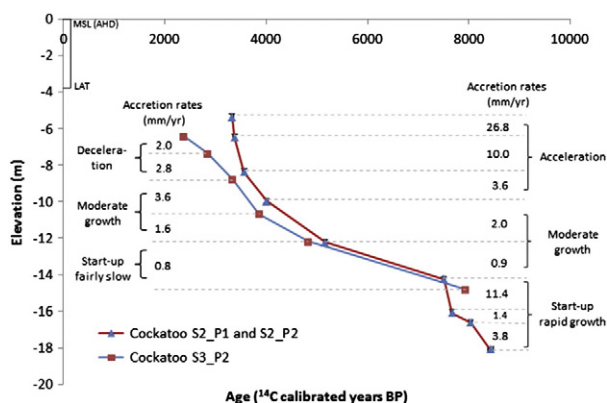


**Fig. 6.** Holocene vertical reef accretion and growth history curve for Cockatoo Island sections S2\_P1, S2\_P2, and S3\_P2.



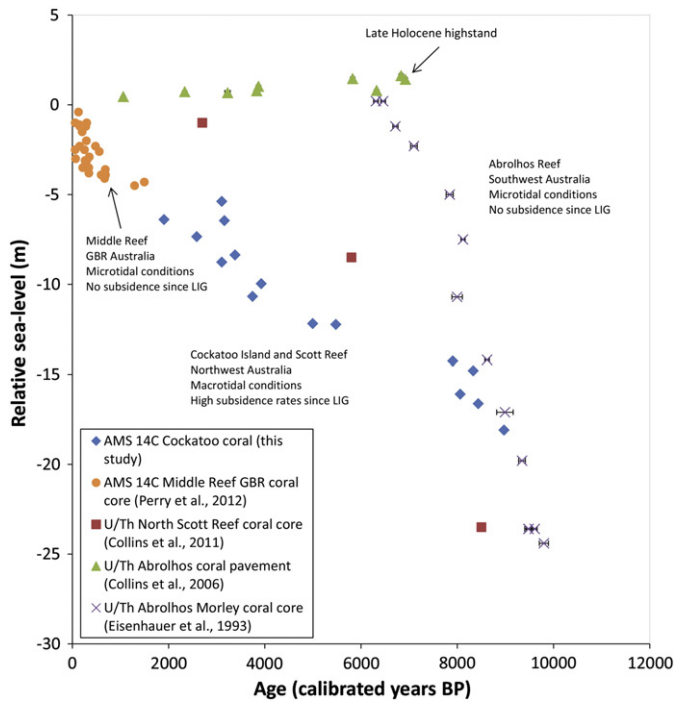


**Fig. 7.** Composite growth history records for Kimberley region and GBR derived from coral sections at Cockatoo Island (this study), coral in core from Middle Reef GBR (Perry et al., 2012), coral in core from North Scott Reef (Collins et al., 2011), cemented coral shingle pavement from Abrolhos reefs (Collins et al., 2006), and corals in core from Morley Island Abrolhos (Eisenhauer et al., 1993). Microtidal Abrolhos reefs from SW Australia lack subsidence since the LIG, in contrast with macrotidal Kimberley reefs with post-LIG subsidence. This is reflected in presence or absence of a Late Holocene highstand in the contrasting SL records. Abrolhos data for a keep up reef; Kimberley data for catch up reefs.

While we believe the vertical accretion model best represents our logged profiles, the reef further seaward may have become submerged too deeply to allow significant vertical accretion. On the modern reef, live coral cover is sharply reduced below about 10 m AHD and virtually absent below 20 m AHD, probably due to rapid light attenuation in the turbid water (Blakeway, 1997; Wilson et al., 2011). If this depth limit

applied throughout the Holocene, only those areas submerged to less than ~10–15 m AHD are likely to have accreted vertically to sea level, while deeper areas may have drowned before eventually being prograded over by the shallow reef (c.f. Hopley and Partain, 1986). Live coral cover on the shallow reef was probably relatively high throughout the vertical accretion phase. The baffling effect of the coral framework would have trapped suspended sediment, depositing the grey-green interstitial mud seen in cross-section. Tropical cyclones must have intermittently affected the reef, and are perhaps the main agent responsible for its detrital reef fabric (c.f. Braithwaite et al., 2000). When the reef reached sea level, which probably first occurred at or near the rocky shore, surface sediments would have become coarser due to wave winnowing, the zone of high coral density would have retracted seaward, and the characteristic community makeup of the current intertidal reef flat would have begun to develop. Eventually the reef attained its present state, with vertical accretion essentially ceased but progradation continuing through *in-situ* growth of branching *Acropora* colonies on the upper slope and deposition of *Acropora* fragments on the lower slope.

The typical sub-bottom profile of the reef shows a steep fore-reef slope unconformably overlying the LIG reef surface at 37 m. A further unconformity marks the boundaries between LIG reef and Proterozoic rock foundation underneath at a depth of 40–50 m. A 15–20 m Holocene reef build-up overlies consistently LIG reef at 37–40 m. This is in accordance with the stratigraphy examined at the adjacent minepit with the exception that the Holocene reef is thicker to seaward.

#### 4.3. Comparisons with other Holocene reef systems

The Cockatoo Island reef conforms reasonably well to the 'arborescent coral facies' description in Montaggioni's (2005) Indo-Pacific reef classification scheme. It differs from the typical arborescent coral reef in a couple of respects which probably reflect the reef's environmental setting, particularly the high turbidity and high terrigenous input. Firstly, the mud matrix is more pervasive at Cockatoo Island than in most arborescent coral reefs. As mentioned earlier we attribute this to high suspended sediment loads being baffled by the coral framework. Secondly, live branching coral (virtually all *Acropora*) on the modern Cockatoo Island reef occurs solely on the upper fore-reef between 4 and 10 m below AHD, whereas on other Indo-Pacific reefs it typically

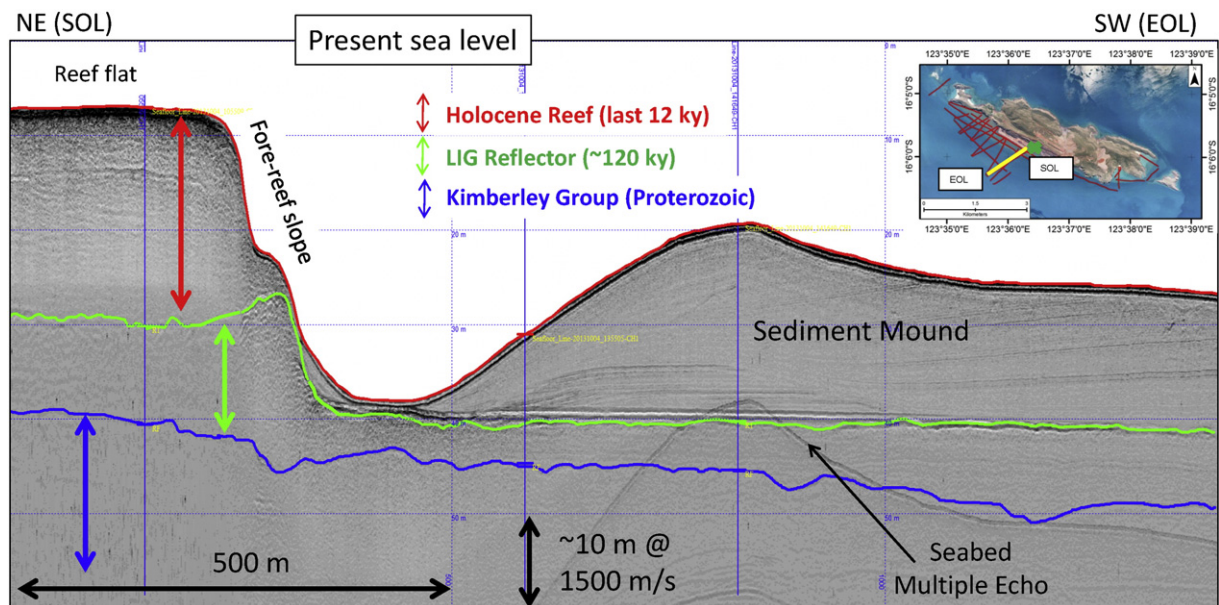


**Fig. 8.** Southwest Cockatoo Island SBP cross section showing two stages of reef development; Holocene and Last Interglacial, with a clear correlation to the measured island sections. Unconformities are coloured. (Blue = top Proterozoic; Green = top Last Interglacial Reflector).

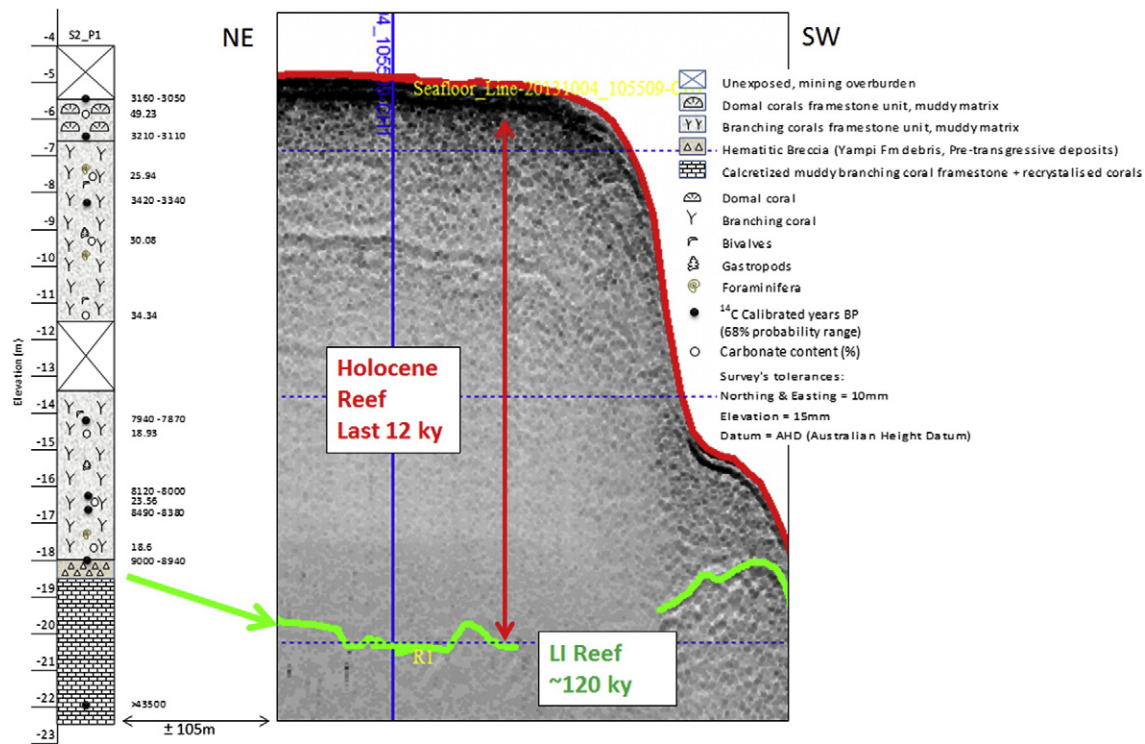


Fig. 9. SBP line with superimposed core log from adjacent mine pit, showing correlation between SBP units and lithological units in the subsurface.

occurs on mid and lower fore-reef slopes to approximately 20 m, and also on shallow inner reef flats and back-reef slopes (Montaggioni, 2005; Hopley et al., 2007). The compressed shallow subtidal distribution of branching *Acropora* at Cockatoo Island is probably a function of a) the low hydrodynamic energy, which allows it to grow undamaged in shallow water (at least during fair-weather conditions), b) the high turbidity, which sets the lower depth limit through light attenuation and possibly also sedimentation stress, and c) their low tolerance to subaerial exposure, which excludes them from the reef flat. Within their optimal 4 to 10 m depth range at Cockatoo Island, branching corals are prolific and seem able to competitively exclude (i.e. outgrow) all other coral types. The restriction of *Porites cylindrica* and branching *Millepora* to the intertidal zone may be a consequence of this competitive exclusion, as both would normally extend into subtidal habitat (Veron, 2000; Glynn and de Weerd, 1991).

The Cockatoo fringing reef shares several similarities with the near-shore turbid zone reefs of the GBR. Browne and Smithers (2012) describe reefs within 20 km of the Queensland coast influenced by episodic terrigenous sediment input, and fluctuating salinities (24–36 ppt). Table 2 compares the inshore GBR systems with the Cockatoo fringing reef. With the exception of the greater tidal range at Cockatoo, both have a similar oceanographic setting with significant sediment influx, sediment-tolerant corals, high coral cover, a significant proportion of *in situ* coral framework, and a mud-dominated matrix (coarsening at the top of the sequence). Differences include the hard foundation of the Cockatoo fringing reef versus the sand and gravel substrates of the GBR reefs, the greater age and thickness of the Cockatoo fringing reef, the higher proportion of detrital branching *Acropora* in the Cockatoo reef, and an apparently more sharply-defined coral depth zonation on the modern Cockatoo Island reef.

The overall mean accretion rate of the Cockatoo Island reef is ~2 mm/year, significantly lower than most turbid zone GBR reefs. However, the mean rate at Cockatoo Island includes approximately 2000 years of slow accretion when we infer the reef was deeply submerged. Accretion rates in the lowermost and uppermost few metres of the Cockatoo section, when the reef was probably submerged to the depth at which

the GBR reefs have developed ( $\leq 5$  m), are approximately equivalent to the mean rate of 8.4 mm/year recorded at Middle Reef, the fastest-growing of the cored turbid zone GBR reefs. These accretion rates are high in a global context and are only exceeded by a handful of reefs, generally within the aborescent or detrital categories (Montaggioni, 2005; Perry et al., 2012). Perry et al. (2012) attribute Middle Reef's rapid accretion to the deposition of fine-grained terrigenous sediments that are suspended from the surrounding seafloor or introduced during major floods. The fine-grained sediment infills the open reef fabric and inhibits post depositional skeletal destruction, thus aiding primary framework preservation and reef accretion. The Cockatoo fringing reef appears to have developed in a very similar way, with only a few deviations from Perry et al.'s model, including the predominance of detrital fabric instead of *in-situ* framework.

There are strong contrasts between the nearshore Cockatoo reef and the offshore reefs of the Oceanic Shoals Biozone located ~300 km to the Northwest including Scott Reef (Fig. 1) which rise from depths of 400 m, in cyclone and swell wave exposed and clear water settings. These reefs are atoll like, dominated by coral framework with sandy calcareous intercalations, with earlier Holocene reef onset ages (e.g. 11.5 ka for Scott Reef; Collins et al., 2011) and higher subsidence rates.

## 5. Conclusions

This study provides the first information on Holocene reef growth for a nearshore reef of the Kimberley Biozone.

- The Cockatoo fringing reef initiated on lithified Pleistocene substrates at approximately 9000 cal y BP and accreted in a catch-up mode, first reaching sea level at approximately 3000 cal y BP. The predominance of fast-growing branching *Acropora*, and the high rate of mud deposition, produced very rapid reef accretion in the upper and lower few metres of the sequence, when the reef surface was probably  $\leq 5$  m deep.
- A knowledge of the reef's foundations also leads to a calculated subsidence rate of the coastal Kimberley since Last Interglacial time of 0.11 m/ka.

**Table 2**

Summary of characteristics of turbid reefs from the GBR (after Browne and Smithers, 2012) and the Cockatoo fringing reef (this study).

Environmental controls	Inshore turbid reefs on the GBR (Browne et al., 2012)		Inshore turbid reefs at Cockatoo Island (this study)	
	Typical condition	Description	Typical condition	Description
Oceanography	Locally wind driven waves	Lack of coralline algae and robust <i>Acropora</i> communities, lack of oceanic swell	Strong tidal currents generated by high tidal range Low swell waves	Domal and robust-branching coral, coral rubble coralline algae exist on the contemporary reef surface
Fine-grained sediment load	High levels of sedimentation and turbidity	Sedimentation rate > 10 mg/cm <sup>2</sup> /day and turbidity levels from < 10 mg/L to > 50 mg/L	Intermittent high turbidity	Background turbidity is 1–2 NTU, and high turbidity is event-related
Reef initiation Substrate availability	Holocene mixed	6000–1000 yBP Sediment deposits on shallow coastal embayment are the most common substrates for reef growth	Holocene Lithified pre-existing reef, or Proterozoic metasediments are common substrates.	9000 yBP Most reefs develop on the LI reef with/without pre-transgressive deposits
Average rate of reef growth	Variable	2–7 mm/year	Variable	2.16–7.4 mm/year
Mode of growth	Mixed	Reefal foundations, terrigenous sand and rubble	Mixed	Reefal foundations, sand/silt matrix, coral rubble
Surrounding bathymetry	Shallow water (<15 m)	Reef growth restricted by shallow, turbid waters	Shallow water (<20–40 m)	Reefs occur down to 15 m depth with a sharp fore reef slope and sand/silt sediment mound to seaward
Sea level		Strongly influence high level wind driven suspended sediment, substrate availability and reef morphology	Rising Holocene sea levels have influenced reef growth	Plays a major role in reef development
Composition	Variable to low coral diversity	100–150 species Many inshore reefs have diverse coral communities, but many are also dominated by physiologically robust corals which may be more tolerant to change	Moderate biodiversity	17 coral genera are identified with the most common community and facies association being of branching corals (especially of the genera <i>Acropora</i> ) and domal corals including <i>Porites</i>
Community age structure	Low coralline algae cover Mixed to older Low recruitment and survival rates	<1% cover on the GBR Many inshore reef characterised by large, older coral colonies which are capable of tolerating high sediment loads Less suitable substrate availability due to high sediment cover and high level of algal competition. High sediment loads can affect the survival of coral juveniles	Low coralline algae cover	Specialised fauna capable of tolerating high sediment loads

- Like Scott Reef of the Oceanic Shoals Biozone to seaward, the Holocene reef at Cockatoo Island lacks evidence of the Late Holocene highstand that characterises coral reefs of the tectonically stable microtidal southwest Australian coast. Macrotidal conditions and coastal subsidence may have obscured such records, although further data from the Kimberley are needed to evaluate this conclusion.

Whilst growth rates of the Cockatoo reef fall into the Montaggioni (2005) “fast to moderate growing reef” category of Indo-Pacific reefs, a direct comparison with turbid reefs of the GBR is more appropriate given both systems are muddy in character, and similar growth rates are recorded for the two systems which contrast with the mainly clear water reefs studied by Montaggioni.

- Whilst the GBR and Cockatoo turbid reefs show broad similarities, one contrast is between palaeoecological and contemporary reef communities, which are similar in the GBR but distinctly different at Cockatoo Island. A likely explanation is that the modern Cockatoo community needs to adapt to manage the extreme conditions of currents, mud from slack water suspension fallout, and prolonged exposure due to macrotidal conditions, in contrast to more stable reef growth in catch up mode earlier in the Holocene.
- A potential analogue for the Holocene palaeoenvironment of muddy branching *Acropora* is provided by the contemporary shallow subtidal reef slope, which is the only habitat where live branching *Acropora* occur at present. The contemporary intertidal environment is

characterised by abundant *Porites cylindrica* and *Millepora intricata*, both absent from the Holocene.

- The muddy framework facies recorded at Cockatoo Island are in keeping with the turbid macrotidal conditions, whilst contrasting with the off shore sand Kimberley reefs.

The Cockatoo reef growth pattern suggests that the Kimberley near-shore reefs may be more resilient to periodic disturbance and the effects from terrestrial runoff than reefs elsewhere. Further, the study shows that reef response to climate is resilience through time. As such the information presented here should be taken into consideration when planning and siting Marine Parks.

### Acknowledgements

The Kimberley Reef Geomorphology Project 1.3.1 is funded by the Western Australian State Government and partners of the Western Australian Marine Science Institution. This research was assisted by the Dambimangari people through their advice and consent to access their traditional lands. Pluton Resources (particularly Jeremy Bower and Anson Griffith) are thanked for providing access to parts of their Cockatoo Island Mining Tenement and for logistic support during the study. The Cygnet Bay Marine Research Station provided vessel support for marine operations and access to research facilities at Cygnet Bay. James Brown assisted in the planning stage of the project, and Erin McGinty capably managed marine operations. MScience is thanked for




providing access to marine video of the reef. Giada Bufarale (seismic data acquisition), Moataz Kordi (remote sensing) and Alexandra Stevens (editing and improvement of drafts) at Curtin University were valued members of the research team. Finally, it must be noted that this research was completed in an area where the Traditional Owners have a rich cultural history of climate, land and environment based on thousands of years of habitation. It is important to consider that broad understanding alongside the modern science completed here.

## References

- Blakeway D., 1997. Scleractinian corals and reef development, part 9, in: Walker D. (Ed.), Marine biological survey of the central Kimberley coast, Western Australia. Perth: University of Western Australia. Unpublished report, W.A. Museum Library No. UR377; pp. 77–85.
- Braithwaite, C.J.R., Montaggioni, L.F., Camoin, G.F., Dalmaso, H., Dullo, W.C., Mangini, A., 2000. Origins and development of Holocene coral reefs: a revisited model based on reef boreholes in the Seychelles, Indian Ocean. *Int. J. Earth Sci.* 89, 431–445.
- Brooke, B., 1997. Geomorphology of the north Kimberley coast, in: Walker D. (Ed.), Marine biological survey of the central Kimberley coast. Western Australia. University of Western Australia, Perth, unpublished report, W.A. Museum Library No. UR377, pp. 13–39.
- Browne, N.K., Smithers, S.G., 2012. Coral reefs of the turbid inner-shelf of the Great Barrier Reef, Australia: An environmental and geomorphic perspective on their occurrence, composition and growth. *Earth-Sci. Rev.* 115 (1–2), 1–20.
- Chin, A., Sweatman, H., Forbes, S., Perks, H., Walker, R., Jones, G., Williamson, D., Evans, R., Hartley, F., Armstrong, S., Malcolm, H., Edgar, G., 2008. Status of the Coral Reefs in Australia and Papua New Guinea. In: Wilkinson, C. (Ed.), Status of Coral Reefs of the World. Global Coral Reef Monitoring Network, Reef and Rainforest Research Centre, pp. 159–176.
- Collins, L.B., 2002. Tertiary Foundation and Quaternary Evolution of Coral Reef Systems of Australia's North West Shelf. In: Keep, M., Moss, S.J. (Eds.), Proceeding of the Petroleum Exploration Society of Australia Symposium, pp. 129–152 (Perth, WA).
- Collins, L.B., Zhu, Z.R., Wyrwoll, K.H., 1996. The structure of the Easter Platform, Houtman Abrolhos reefs: Pleistocene foundations and Holocene reef growth. *Mar. Geol.* 135 (1–4), 1–13.
- Collins, L.B., Zhao, J.X., Freeman, H., 2006. A high-precision record of mid-late Holocene sea-level events from emergent coral pavements in the Houtman Abrolhos Islands, southwest Australia. *Quat. Int.* 145–146, 78–85.
- Collins, L.B., Testa, V., Zhao, J., Qu, D., 2011. Holocene growth history and evolution of the Scott Reef carbonate platform and coral reef. *J. R. Soc. West. Aust.* 94 (2), 239–250.
- DeCaprio, L., Gurnis, M., Mueller, R.D., 2009. Long-wavelength tilting of the Australian continent since the Late Cretaceous. *Earth Planet. Sci. Lett.* 278 (3–4), 175–185.
- Department of the Environment, Water, Heritage and the Arts (DEWHA), 2008. A Characterisation of the Marine Environment of the North-west Marine Region: Perth Workshop Report, A Summary of an Expert Workshop Convened in Perth, Western Australia, 5–6 September 2007. Commonwealth of Australia, Hobart.
- Eisenhauer, A., Wasserburg, G.J., Eisenhauer, A., Chen, J.H., Bonani, G., Collins, L.B., Zhu, Z.R., Wyrwoll, K.H., 1993. Holocene sea-level determination relative to the Australian continent: U/Th (TIMS) and <sup>14</sup>C (AMS) dating of coral cores from the Abrolhos Islands. *Earth Planet. Sci. Lett.* 114 (4), 529–547.
- Embry, A.F., Klován, J.E., 1971. A late Devonian reef tract on northeastern Banks Island, N.W.T. *Bull. Can. Petrol. Geol.* 19 (4), 730–781.
- Glynn, P., de Weerd, W.H., 1991. Elimination of two reef building hydrocorals following the 1982–83 El Niño warming event. *Science* 253, 69–71.
- Government of Western Australia, 2011. Kimberley Science and Conservation Strategy. Department of Environment and Conservation. Kensington, Perth.
- Griffin, T.J., Grey, K., 1990. Kimberley Basin. Memoir 3, Geology and Mineral Resources of Western Australia. Geological Survey of Western Australia, Perth, pp. 293–304.
- Harris, P.J., Baker, E.K., Cole, A.R., 1991. Physical sedimentology of the Australian continental shelf with emphasis on Late Quaternary deposits in major shipping channels, port approaches and choke points. University of Sydney, Ocean Sciences Institute (Report 51).
- Hopley, D., Partain, B., 1986. The structure and development of fringing reefs of the Great Barrier Reef Province. In: Baldwin, C.L. (Ed.), Fringing Reef Workshop: Science, Industry and Management. Great Barrier Reef Marine Park Authority, Townsville, pp. 13–33.
- Hopley, D., Smithers, S., Parnell, K., 2007. The Geomorphology of the Great Barrier Reef: Development, Diversity, Change. Cambridge University Press, Cambridge, UK.
- Kennedy, D.M., Woodroffe, C.D., 2002. Fringing reef growth and morphology: a review. *Earth Sci. Rev.* 57, 255–277.
- Lambeck, K., Woodroffe, C.D., Antonioli, F., Anzidei, M., Gehrels, W.R., Laborel, J., Wright, A.J., 2010. Palaeoenvironmental records, geophysical modelling, and reconstruction of sea-level trends and variability on centennial and longer timescales. In: Church, J.A., Woodworth, P.L., Aarup, T., Wilson, W.S. (Eds.), Understanding Sea-level Rise and Variability. Blackwell Publishing Ltd, pp. 61–121.
- Lough, J.M., 1998. Coastal climate of northwest Australia and comparisons with the Great Barrier Reef: 1960 to 1992. *Coral Reefs* 17 (4), 351–367.
- Montaggioni, L.F., 2005. History of Indo-Pacific coral reef systems since the last glaciation: development patterns and controlling factors. *Earth Sci. Rev.* 71 (1–2), 1–75.
- Müller, G., Gastner, M., 1971. The 'Karbonat-Bombe', a simple device for the determination of carbonate content in sediment, soils, and other materials. *Neues Jahrb. Mineral. Monatshefte* 10, 466–469.
- O'Leary, M.J., Hearty, P.J., McCulloch, M.T., 2008. U-series evidence for widespread reef development in Shark Bay during the last interglacial. *Palaeogeogr. Palaeoclimatol. Palaeoecol.* 259, 424.
- O'Leary, M., Hearty, P.J., Thompson, W.G., Raymo, M.E., Mitrovica, J.X., Webster, J.M., 2013. Ice sheet collapse following a prolonged period of stable sea level during the last interglacial. *Nat. Geosci.* 6 (9), 796–800.
- Perry, C.T., Smithers, S.G., Gulliver, P., Browne, N.K., 2012. Evidence of very rapid reef accretion and reef growth under high turbidity and terrigenous sedimentation. *Geology* 40 (8), 719–722.
- Purcell, S.P., 2002. Intertidal reefs under extreme tidal flux in Buccaneer Archipelago, Western Australia. *Coral Reefs* 21 (2), 191–192.
- Quigley, M.C., Cupper, M.L., Sandiford, M., 2006. Quaternary faults of south-central Australia: palaeoseismicity, slip rates and origin. *Aust. J. Earth Sci.* 53 (2), 285–301.
- Quigley, M.C., Sandiford, M., Cupper, M.L., 2007. Distinguishing tectonic from climatic controls on range-front sedimentation. *Basin Res.* 19 (4), 491–505.
- Sandiford, M., 2003. Neotectonics of southeastern Australia: linking the Quaternary faulting record with seismicity and in situ stress. In: Hillis, R.R., Muller, D. (Eds.), Evolution and Dynamics of the Australian Plate. vol. 22. Geological Society of Australia Special Publication, pp. 101–113.
- Sandiford, M., 2007. The tilting continent: a new constraint on the dynamic topographic field from Australia. *Earth Planet. Sci. Lett.* 261 (1–2), 152–163.
- Short, A.D., 2011. Kimberley beach and barrier systems: an overview. *J. R. Soc. West. Aust.* 94 (2), 121–132.
- Veron, J.E.N., 2000. Corals of the world. *Aust. Inst. Mar. Sci.* 1–3, 1,382.
- Wilson, B.R., 2013. The Biogeography of the Australian North West Shelf: Environmental Change and life's response. Elsevier, Burlington MA, USA.
- Wilson, B.R., Blake, S., Ryan, D., Hacker, J., 2011. Reconnaissance of species-rich coral reefs in a muddy, macro-tidal, enclosed embayment, - Talbot Bay, Kimberley, Western Australia. *J. R. Soc. West. Aust.* 94, 251–265.
- Wolanski, E., Spagnol, S., 2003. Dynamics of the turbidity maximum in King Sound, tropical Western Australia. *Estuar. Coast. Shelf Sci.* 56 (5–6), 877–890.
- Wright, R.L., 1964. Geomorphology of the west Kimberley area. *CSIRO Land Res. Ser.* 9, 103–118.



# Holocene reef evolution in a macrotidal setting: Buccaneer Archipelago, Kimberley Bioregion, Northwest Australia

Tubagus Solihuddin<sup>1,2</sup>  · Michael J. O’Leary<sup>2,3</sup> · David Blakeway<sup>4</sup> ·  
Iain Parum<sup>5</sup> · Moataz Kordi<sup>1,2</sup> · Lindsay B. Collins<sup>1,2</sup>

Received: 23 November 2015 / Accepted: 12 February 2016  
© Springer-Verlag Berlin Heidelberg 2016

**Abstract** This study uses information derived from cores to describe the Holocene accretion history of coral reefs in the macrotidal (up to 11 m tidal range) Buccaneer Archipelago of the southern Kimberley coast, Western Australia. The internal architecture of all cored reefs is broadly similar, constituting well-preserved detrital coral fragments, predominantly branching *Acropora*, in a poorly sorted sandy mud matrix. However, once the reefs reach sea level, they diverge into two types: low intertidal reefs that maintain their detrital character and develop relatively narrow, horizontal or gently sloping reef flats at approximately mean low water spring, and high intertidal reefs that develop broad coralline algal-dominated reef flats at elevations between mean low water neap and mean high water neap. The high intertidal reefs develop where strong, ebb-dominated, tidal asymmetry retains seawater over the low tide and allows continued accretion. Both reef types are ultimately constrained by sea level but differ in elevation by 3–4 m.

**Keywords** Reef geomorphology · Holocene reef growth · Sea level · Rhodoliths · Coralline algal reefs

## Introduction

Advances in our understanding of the post-glacial evolution of coral reefs throughout the Indo-Pacific and Caribbean regions have come mainly through knowledge gained by reef coring, beginning with Ladd et al. (1953) whose drilling on Eniwetok Atoll encountered basalt basement at a depth of 1.4 km, lending support to Darwin’s (1842) theory of atoll island evolution. A number of more recent review papers and books (e.g., Kennedy and Woodroffe 2002; Montaggioni 2005; Hopley et al. 2007) have described particular reef development patterns based on the timing of Holocene reef initiation, rates and modes of reef accretion and reef facies associations. These same reviews also highlighted a number of factors controlling reef accretion, including sea level, tectonics, antecedent topography, sea surface temperatures and salinities, nutrient, light and turbidity levels, aragonite saturation, hydrodynamic energy and substrate availability. Despite the number of factors controlling reef accretion, most reefs exist within a fairly narrow range of physiochemical parameters and can, therefore, be classified and categorised according to a small range of sedimentary facies, accretionary styles and geomorphic typologies. Here, we investigate reef development and evolution within a region where one environmental variable, tidal range, significantly exceeds that of typical reefs.

The Buccaneer Archipelago located on Western Australia’s Kimberley coast experiences a macrotidal tidal range of up to 11 m, which is the largest recorded in any tropical region. In addition to the extreme tidal range, the

---

Communicated by Geology Editor Prof. Chris Perry

---

✉ Tubagus Solihuddin  
tubagus.solihuddin@postgrad.curtin.edu.au

<sup>1</sup> Department of Applied Geology, Curtin University, Bentley, WA 6102, Australia

<sup>2</sup> The Western Australian Marine Science Institution, Floreat 6014, Australia

<sup>3</sup> Department of Environment and Agriculture, Curtin University, Bentley, WA 6102, Australia

<sup>4</sup> Fathom 5 Marine Research, 17 Staines Street, Lathlain, WA 6100, Australia

<sup>5</sup> Centre for Marine Science and Technology, Curtin University, Bentley, WA 6102, Australia

Buccaneer Archipelago is subject to strong currents, frequent cyclones and elevated turbidity. Despite these seemingly challenging environmental conditions, the region is known for its extensive and diverse coral reefs. Teichert and Fairbridge (1948) discuss the profusion of reefs in the Kimberley region, and Wilson et al. (2011) infer significant accumulations of coral framework in Talbot Bay. However, the true extent of reef framework development in the Kimberley was unknown until Solihuddin et al. (2015) described the Holocene development of a sheltered fringing reef at Cockatoo Island in the Kimberley. An open cut iron ore pit on the south-western side of the island has exposed a complete 15- to 20-m-thick Holocene reef sequence resting atop an older Pleistocene reef surface. Radiocarbon dating showed that reef initiation at Cockatoo Island occurred around 9000 calibrated years before present (cal yr BP), soon after the post-glacial flooding of the antecedent substrate, and accreted in catch-up mode (*sensu* Neumann and Macintyre 1985), reaching sea level by approximately 3000 cal yr BP.

The presence of a thick reef framework at Cockatoo Island raises broader questions around Holocene reef development in the Kimberley including: (1) what was the timing of reef ‘turn on’ (*sensu* Buddemeier and Hopley 1988) and does this vary regionally; (2) what was the accretionary style and how does this compare to other reef systems; and (3) how do coral reef facies reflect changing accretionary patterns or environmental stressors?

To address these questions, we conducted a systematic coring program from selected inshore reefs in the Buccaneer Archipelago, including Irvine/Bathurst Island, Sunday Island and Tallon Island, and performed sedimentary, palaeoecological and chronostratigraphic analyses on recovered cores.

## Materials and methods

### Regional setting

#### *Geology*

The Buccaneer Archipelago is located between latitudes 16.0°S and 16.4°S in the southern Kimberley region of north-western Australia. The archipelago is the seaward extension of the King Leopold Orogen, which consists of highly metamorphosed, strongly folded, faulted and eroded Proterozoic rocks of the Kimberley Group (Brunnschweiler 1957; Griffin and Grey 1990). A strong regional-scale north-west–south-east foliation has resulted in a deeply incised ria coast with more than 700 inshore islands, almost all of which are uninhabited and many unnamed. These islands represent the drowned remnants

of a broad, structurally controlled peneplain (Wilson 2013).

#### *Tides*

The Buccaneer Archipelago has a semi-diurnal macrotidal regime with spring tides ranging between 8 and 11 m. The complex bathymetry, embayed coast and numerous islands result in very strong and turbulent tidal flows, in some areas scouring the seabed and producing high levels of turbidity. Narrow passages between islands and inlets give rise to waterfall effects, whereby water piles up on one side of an inlet as the tide falls faster than the water can drain through the pass (e.g., Horizontal Falls, Talbot Bay). The rapidly falling tide also results in impounding of water on raised reef flats which then cascades over the forereef crest and slope (Richards and O’Leary 2015; Lowe and Falter 2015).

#### *Oceanography*

Sea surface temperatures reach 22–28 °C inshore and 17–27 °C offshore (Pearce and Griffiths 1991). The climate is semi-arid monsoonal, with pronounced ‘wet’ summers and ‘dry’ winters. Tropical monsoonal storms between November and April produce intense rainfall with an annual average from approximately 800 mm in the west to 1500 mm in the central and east Kimberley, whereas the dry season from May to September brings warm temperatures and low humidity (DEWHA 2008). Nutrient concentrations in the inshore Kimberley waters are relatively high, influenced by riverine inputs from the adjacent terrestrial, high run-off catchments (Wilson 2013). The region is prone to cyclones, experiencing approximately three per year (Lough 1998), and has a prevailing south-west swell (Pearce and Griffiths 1991).

### Multibeam

Reef elevation was measured through a multibeam echo sounder survey. The depth below the vessel was measured using an Odom ES3 multibeam echo sounder, which was combined with a Valeport sound velocimeter, a TSS 355B motion sensor and an iX Blue Octans gyro compass, and elevation was measured using Trimble Net R9 using RTX satellite subscription ( $\pm 2$  cm). Data were acquired and processed using QPS QINSy software (ver 8.10). Longitude and latitude were calculated relative to the Geocentric Datum of Australia 1994 (GDA 94) and elevation relative to the Australian Height Datum (AUSGeoid09). The processed data were gridded to either 0.5 or 1 m<sup>2</sup> and imported into MATLAB (ver 2013B) where a probability distribution was derived empirically for each site using the ‘ks-density’ function.

## Reef coring

A total of forty-two reef cores were collected from Tallon Island, Sunday Island and Irvine/Bathurst Islands (Fig. 1). Coring sites were selected to support the interpretation of previously surveyed subbottom profile survey data (Collins et al. 2015) and to ensure a spatially representative record of reef accretion. Cores were obtained by percussion coring and rotary drilling. Percussion coring was used where reef flats consisted of open framework and unconsolidated reef sediments. A 6.5-m-long, 80-mm-wide aluminium tube with 3-mm wall thickness was hammered into the reef using either a manual slide hammer or hydraulic powered post-driver. Coralline algal reef was sampled by rotary coring, using a handheld hydraulic core drill to drive a 50-cm-long and 80-mm-diameter diamond core with a 1-m extension rod. Core site positions were fixed by GPS, and elevations were derived from multibeam data, corrected to mean sea level (MSL).

## Core logging and sampling

Core logging and sampling documented characteristics including (1) the ratio of reef framework to matrix (after Embry and Klovan 1971); (2) sediment textural characteristics (using the Udden–Wentworth nomenclature, as well as a visual assessment of sediment composition); and (3) generic coral identification. Reef framework analysis and facies descriptions follow the terminology of Montaggioni (2005), highlighting the growth forms of the dominant reef builders and environmental indicators. All core log elevations were corrected and plotted relative to MSL.

## Radiocarbon dating

Coral specimens from distinct facies in each core were selected for accelerator mass spectrometry and radiometric carbon dating to establish a geochronological record of reef accretion. All specimens were in situ, based on orientation

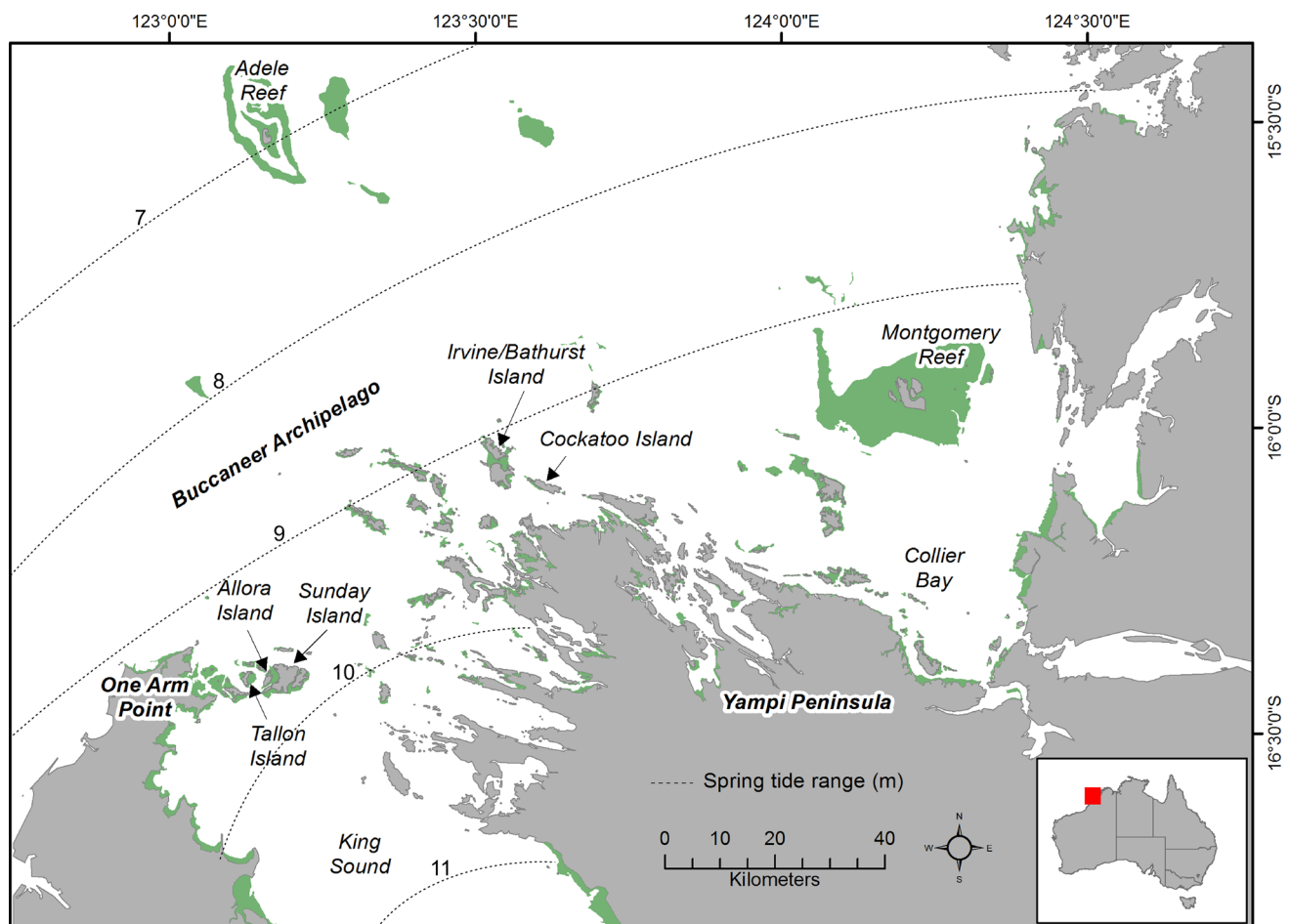


**Fig. 1** Map of the study area in the Buccaneer Archipelago. The green shading indicates reef habitat. Locations of the three study sites and surrounding islands are indicated by arrows

and skeletal condition, and free of boring, encrustation, and submarine cementation. Radiocarbon ages were recalibrated using CALIB version 7.0.4 and the Marine13 calibration curve (<http://calib.qub.ac.uk/marine>). A weighted mean  $\Delta R$  value of  $58 \pm 21$  (average calculation from three nearest points) was used as the best current estimate of variance in the local open water marine reservoir effect for the Buccaneer Archipelago and adjacent areas. Ages discussed in the text are in calibrated years before present (cal yr BP) with a 68.2 % ( $2\sigma$ ) probability range.

## Results

Below we summarise the geomorphology, contemporary benthic habitat, Holocene facies and accretion history of the three study sites. Due to the limitations of the coring equipment and the thickness of the Holocene reefs, the oldest/lowermost reef sections were not sampled. However, the position of the Holocene/pre-Holocene contact of several boreholes was inferred from earlier seismic records (Collins et al. 2015). The utility of these inferences is supported by work at Cockatoo Island (Solihuddin et al. 2015) where the inferred seismic boundary was traced directly to the Holocene/last interglacial reef contact in the mine pit cross section.

### Tallon Island

Tallon Island is an arc-shaped outcrop of Pre-cambrian quartzite, rising to a maximum elevation of 10 m above MSL based on shuttle radar topography mission (SRTM) data (<http://dds.cr.usgs.gov/srtm/>). The island is flanked to the west and east by Holocene fringing reefs. Reefs on the west and east sides of Tallon Island differ significantly in elevation, geomorphology and contemporary benthic habitats (Fig. 2). The western reef flat is 0.9 km wide and dips gently seaward with an inner elevation of 2.7 m below MSL dropping to 3.5 m below MSL at the reef flat edge. The modern reef flat habitats consist of sand and macroalgae-covered coral rubble with sparse live tabular *Acropora* and small colonies of *Goniastrea aspera* and other faviids. The eastern reef flat is 1.3 km wide and exhibits a near horizontal surface at an elevation of between 0.25 to 0.5 m above MSL. It shows zonation from nearshore mangroves to a shallow lagoon of seagrass and carbonate sand rimmed by a series of low-relief (10–20 cm) coralline algal terraces (Fig. 2).

Reef cores penetrated to a maximum depth of 6.3 m. The dominant facies was a delicate branching coral floatstone with mud to sand matrix, overlaid by a thin layer of unconsolidated carbonate sand. A series of anastomosing coralline algal terraces occur along the outer margin of the

eastern reef flat, coalescing into a 3-m high wall on the reef's north-east corner. Rotary coring of the wall recovered a coralline algal bindstone with a minimum vertical thickness of 1.1 m (the capacity of the equipment).

Nineteen radiometric ages were obtained from corals collected from eight cores (four percussions and four rotary) at Tallon Island. The oldest age, 7790–7645 cal yr BP, was obtained from the base of core WT1, 8.4 m below MSL on the west side of the island (Fig. 2). A similar age of 7305–7165 cal yr BP was recorded from the base of core ET7, 5.2 m below MSL on the east side of Tallon Island. The western core WT1 shows rapid vertical reef accretion until 6000 cal yr BP with a compressed section of 5000 yr in the upper 1.3 m. This is in contrast to core ET7, which shows continual rapid accretion and reached MSL elevation by 4000 cal yr BP. The coralline algal bindstone on the outer margin of the eastern reef flat accreted at approximately  $0.5 \text{ mm yr}^{-1}$  for at least 3000 years. Core from the coralline algal wall (ET 11) indicates that it is no longer accreting vertically, but continues to prograde laterally at  $0.6 \text{ mm yr}^{-1}$ .

### Sunday Island

The Sunday Island reef (also known as 'The Pool') is a 0.5- to 1-km-wide interisland reef platform between Sunday Island and Allora Island (Fig. 3). The reef surface is situated approximately 0.5 m below MSL but deepens to approximately 1.5 m below MSL at the core sites to the north and south. Modern habitats at these sites are composed of coarse carbonate sediments with abundant coralline algae-coated branching coral fragments and occasional small colonies of live massive coral. Low-relief rhodolith terraces, approximately 5–10 cm high, occur where seawater streams off the elevated reef at low tide. Immediately south-east of the southern core sites is a long (1.5 km), narrow (<100 m) and deep (30 m) channel flanked by a fringing reef (Fig. 3).

Reef cores penetrated to a maximum depth of 4.5 m below MSL at the northern side of the interisland reef platform and 2 m below MSL at the southern side. Facies in the northern side include a domal coral floatstone at the base of the cores and a branching coral floatstone at the top. The matrix is sand with abundant coralline algal and shell fragments, fining to sandy mud in the uppermost 1 m and overlaid by coarse carbonate sand containing abundant coralline algal fragments and rhodoliths. Facies in the southern side are medium- to coarse-grained carbonate sands with coralline algal fragments. A coralline algal bindstone was encountered at 1.8 m below MSL in core PS1.

Fifteen radiometric ages were obtained from six cores at Sunday Island (five percussions and one rotary). The oldest age, 6780–6625 cal yr BP, was from a *Porites* at 5.8 m

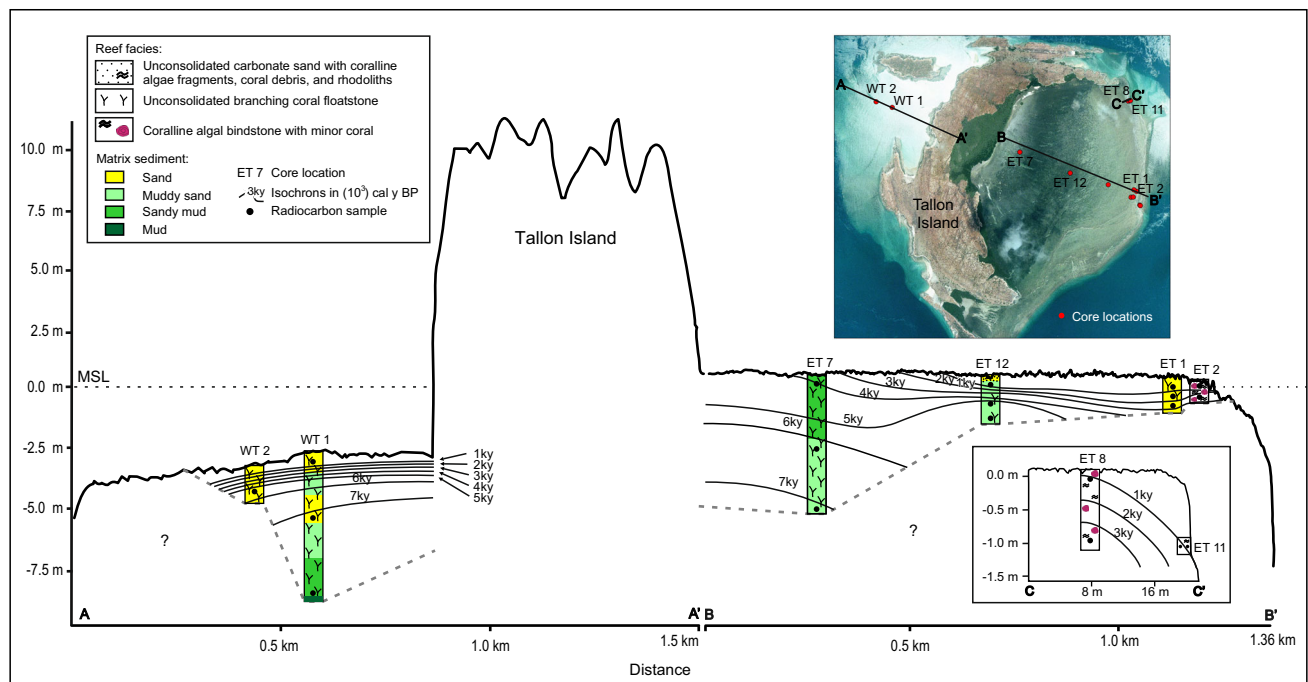


**Fig. 2** Cross section of the Tallon Island reefs with isochrons and summary of Holocene reef facies. The dominant facies was branching coral floatstone with mud to sand matrix, overlaid by a thin layer of unconsolidated carbonate sand

below MSL in core PN5 on the northern side of the interisland reef platform (Fig. 3). The transition from domal facies to branching *Acropora* upcore occurred at approximately 3 m below MSL and 2500–5000 cal yr BP. Shallow subsurface coral samples from cores PN1 and PN3 had modern ages of 240–0 cal yr BP and 120–0 cal yr BP, respectively. Reef accretion was relatively uniform throughout the recorded sequence, averaging approximately 1 mm yr<sup>-1</sup>. The coralline algal bindstone at the base of core PS1 had an age of 3070–2870 cal yr BP. Shallow subsurface samples throughout the interisland reef platform were modern or near-modern (Table 1).

### Irvine/Bathurst islands

Irvine/Bathurst islands are approximately 60 km north-east of Tallon and Sunday islands and 5 km north-west of Cockatoo Island (Fig. 1). Both islands consist of tightly folded Palaeoproterozoic sandstones. The islands are surrounded by fringing reefs that express a range of morphologies, with mangroves lining the more sheltered bays. An interisland fringing reef between the islands rises to a maximum height of approximately 0.25 m above MSL, comparable to the maximum elevation of the Tallon Island (~0.5 m above MSL) and Sunday Island (~0.5 m below MSL) reef flats but significantly higher than the neighbouring Cockatoo Island reef flat (~4.5 m below MSL; Solihuddin et al. 2015). Modern reef habitats include

patchy coral and sand within the deeper south- and east-facing bays of Irvine Island, extensive coralline pavement and rhodolith flats on the interisland reef platform, and steep-sided coral-lined pools within the reef flat. Coralline algal terraces occur on the seaward-sloping reef margins but are less developed than those of Tallon and Sunday islands.

Cores penetrated to a maximum depth of 6.3 m below MSL. The dominant facies at Irvine/Bathurst islands was a branching coral floatstone, which is especially abundant in the cores around the deep tidal pools. A domal coral floatstone was abundant in some sections, especially in the B04 and B05 cores (Fig. 4). Both coral units occurred in a muddy to sandy matrix. Surface facies were either coarse carbonate sand or coralline algal bindstone, both up to 30 cm thick.

Six cores were collected along an east–west transect between the islands (Fig. 4). The oldest reef encountered was ~3500–3345 cal yr BP at 2.7 m below MSL in core B15. This domal coral unit grew upward to 0.4 m below MSL at ~2000 cal yr BP before being covered by 0.3 m of carbonate sand. A similar domal coral unit occurs at ~5 m below MSL in cores B04 and B05 which dates to ~2395–2900 cal yr BP. In core B05, the domal coral unit is underlain by ~2 m of branching coral framestone with an age of ~3350–3165 cal yr BP. Thick sequences of branching *Acropora* framework were present in cores from the western margin of the reef flat and around the deep reef



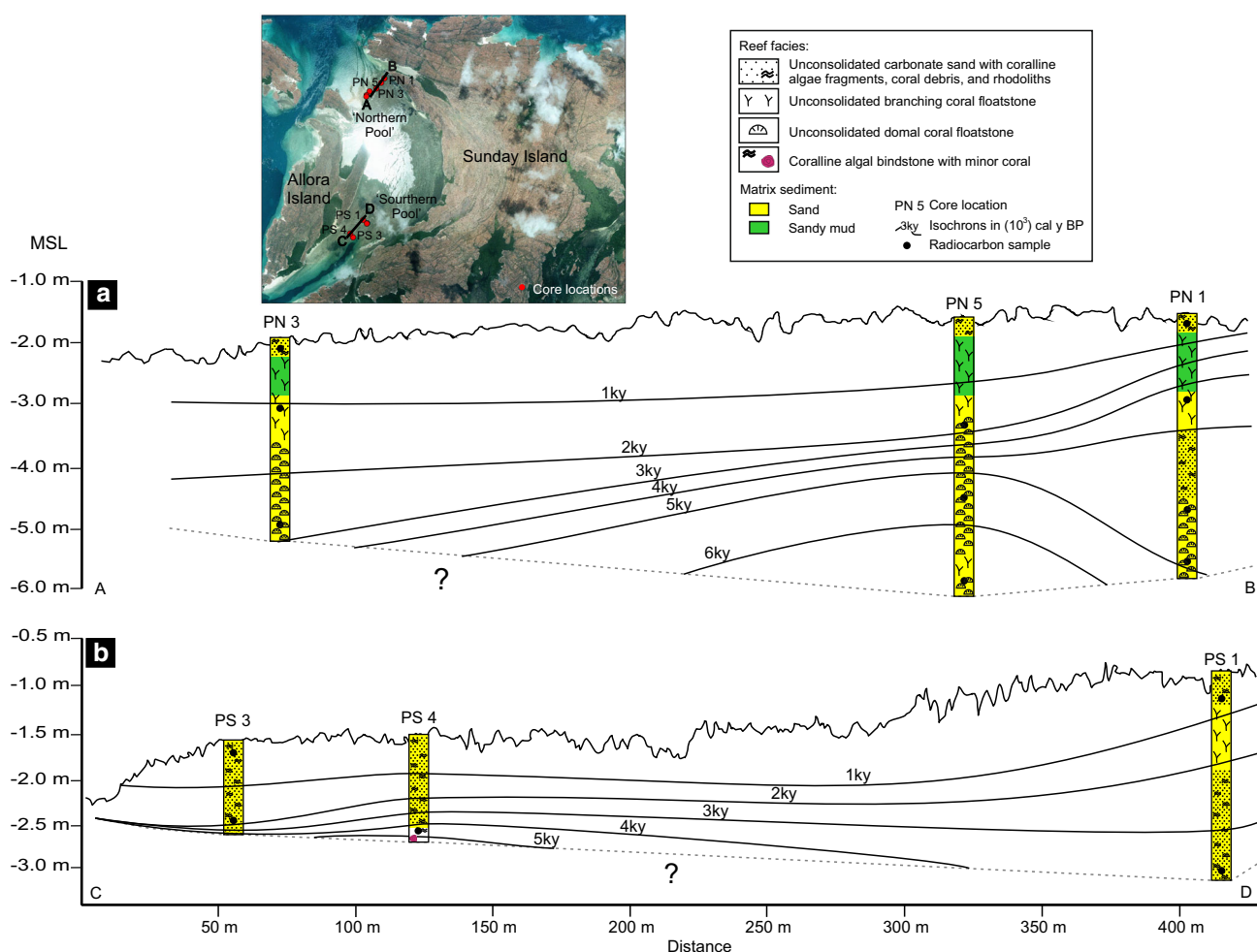


**Fig. 3** Cross section of the North (a) and South (b) Pool of Sunday Island with isochrons and summary of Holocene reef facies. Facies in the North Pool comprised a domal coral floatstone at the base of the

cores and a branching coral floatstone at the top. Facies in the South Pool are medium- to coarse-grained carbonate sands with coralline fragments

pool shown in Fig. 4. Near-surface samples from all cores except B15 returned modern or near-modern dates.

## Discussion

### Reef geomorphology

The surveyed fringing reefs can be classified into two geomorphic groups based on reef flat elevation: ‘low intertidal reefs’ (LIR) in which reef flat elevation is approximately mean low water spring (MLWS); and ‘high intertidal reefs’ (HIR) in which reef flat elevation clusters between mean low water neap (MLWN) and mean high water neap (MHWN) (Fig. 5). The two reef types can occur in close proximity as shown by the Tallon Island cross section (Fig. 2). While low intertidal elevations are typical of fringing reef flats worldwide, elevated reef flats are rare;

the only documented example we are aware of occurs at Atol das Rocas off Brazil, where Gherardi and Bosence (2001, 2005) reported reef elevations up to 1.5 m above MSL (see Fig. 2). Google Earth imagery indicates there may be several additional undocumented HIR—the platform reefs of Nova Viçosa, for example, 1500 km south of Atol das Rocas, appear morphologically similar to both Atol das Rocas and the Kimberley HIR. Like the Kimberley examples, the Brazilian HIR occur in a tide-dominated environment (defined by mean tidal range exceeding mean significant wave height; Lowe and Falter 2015). It is likely that many more HIR exist in tide-dominated environments worldwide, although the Kimberley probably holds the ultimate examples, given its extreme tidal range.

The apparent absence of reef flat elevations between MLWS and MLWN in the Kimberley (Fig. 5) suggests that both the HIR and LIR may be constrained at their present elevations. The question then arises as to how the HIR

**Table 1** Radiocarbon ages from selected samples across Tallon, Sunday and Irvine/Bathurst Reefs

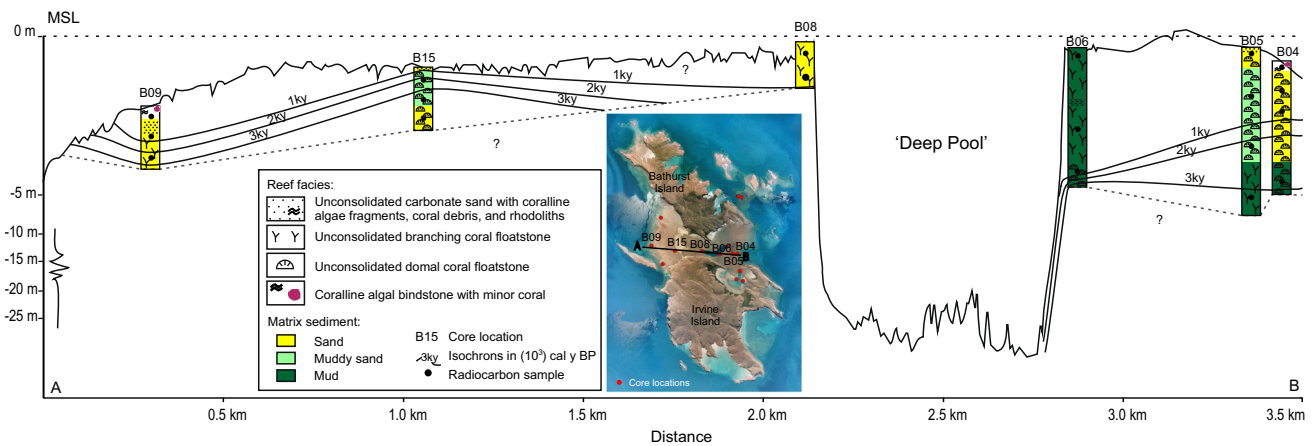
Location	Sample code	Depth (m)	Lab. code	Material	Method	Measured age	$^{13}\text{C}/^{12}\text{C}$ (‰)	Conventional age (BP)	Calibrated (68 % probability) cal yr BP	Accretion (mm/year)
Tallon Is.	ET7-30	-0.6	Beta-385991	<i>Acropora</i>	AMS	3610 ± 30	+0.4	4030 ± 30	4075–3870	
	ET7-313	-2.6	Beta-385992	<i>Seriatophora</i>	AMS	5730 ± 30	-0.3	6140 ± 30	6605–6410	0.8
	ET7-573	-5.2	Beta-385993	<i>Porites Cylindrica</i>	AMS	6360 ± 30	+0.0	6770 ± 30	7305–7165	3.6
	ET1-24.5	0.0	Beta-385988	<i>Acropora</i>	AMS	170 ± 30	+0.5	590 ± 30	265–55	
	ET1-74	-0.5	Beta-385989	<i>Porites Cylindrica</i>	AMS	1840 ± 30	-0.4	2240 ± 30	1865–1690	0.3
	ET1-123	-1.0	Beta-385990	Coralline algae	AMS	2630 ± 30	+1.0	3060 ± 30	2840–2715	0.5
	ET12-23	0.2	Beta-389407	Coral	AMS	370 ± 30	0.0	780 ± 30	450–285	
	ET12-132	-0.1	Beta-389408	Coral	AMS	4470 ± 30	+0.7	4890 ± 30	5265–5005	0.1
	ET12-202	-1.6	Beta-389409	Coral	AMS	4760 ± 30	-0.3	5170 ± 30	5570–5420	4.2
	ET2-8	0.2	Beta-391788	Coralline algae	AMS	650 ± 30	+1.8	1090 ± 30	660–540	
	ET2-100	-0.7	Beta-391789	Coral	AMS	2460 ± 30	-0.1	2870 ± 30	2690–2440	0.5
	WT1-30	-3.0	Beta-389404	<i>Acropora</i>	AMS	140 ± 30	-1.3	530 ± 30	230–post 0	
	WT1-294	-5.6	Beta-389405	Coral	AMS	6410 ± 30	+1.0	6840 ± 30	7395–7245	0.4
	WT1-573	-8.4	Beta-389406	Coral	AMS	6890 ± 30	+0.9	7310 ± 30	7790–7645	7.0
	WT2-87	-4.3	Beta-389469	<i>Porites Cylindrica</i>	Radiometric	4790 ± 30	+0.5	5210 ± 30	5805–5445	2.0
	ET8-12	-0.2	Beta-397764	Rhodoliths	AMS	1300 ± 30	-3.2	1660 ± 30	1250–1070	
	ET8-115	-1.2	Beta-397765	Coralline algae	AMS	2880 ± 30	+1.0	3310 ± 30	3175–2960	0.5
	ET11-10	-1.1	Beta-397766	Coralline algae	AMS	100.4 ± 0.4 pMC	+0.4	390 ± 30	Post 0	
	ET11-90	-1.9	Beta-397767	Coralline algae	AMS	1330 ± 30	+1.8	1770 ± 30	1320–1220	0.6
Sunday Is.	PN3-13	-2.0	Beta-389410	<i>Acropora</i>	AMS	130 ± 30	+0.3	540 ± 30	240–post 0	
	PN3-120	-3.1	Beta-385994	<i>Acropora</i>	AMS	1670 ± 30	+0.3	2080 ± 30	1685–1515	0.7
	PN3-319	-5.1	Beta-385995	<i>Platygra</i>	AMS	2710 ± 30	-3.0	3070 ± 30	2850–2725	1.7
	PN1-25	-1.8	Beta-389470	<i>Acropora</i>	Radiometric	90 ± 30	-1.2	480 ± 30	120–post 0	
	PN1-122	-2.8	Beta-389471	<i>Pavia</i>	Radiometric	3220 ± 30	+1.3	3650 ± 30	3570–3395	0.3
	PN1-308	-4.7	Beta-389472	Coral	Radiometric	4040 ± 30	-2.9	4400 ± 30	4565–4395	1.9
	PN1-388	-5.5	Beta-389473	Rhodoliths	Radiometric	4300 ± 30	-2.1	4680 ± 30	4905–4795	2.2
	PN5-169	-3.4	Beta-389474	<i>Porites</i>	Radiometric	1630 ± 30	-1.1	2020 ± 30	1595–1415	
	PN5-271	-4.5	Beta-389475	<i>Galaxea</i>	Radiometric	4420 ± 30	-1.2	4810 ± 30	5115–4865	0.3
	PN5-410	-5.8	Beta-389476	<i>Porites</i>	Radiometric	5900 ± 30	-0.2	6310 ± 30	6780–6625	0.8
	PS1-20	-1.2	Beta-385996	Coral	AMS	540 ± 30	-0.1	950 ± 30	545–465	
	PS1-184	-2.8	Beta-385997	Coralline algae	AMS	2800 ± 30	+1.7	3240 ± 30	3070–2870	0.6
	PS3-9	-1.8	Beta-389411	<i>Acropora</i>	AMS	80 ± 30	-0.7	480 ± 30	120–post 0	
	PS3-90	-2.6	Beta-391787	<i>Acropora</i>	AMS	1570 ± 30	+1.0	2000 ± 30	1565–1400	0.4
	PS4-100	-2.6	Beta-385998	Coral	AMS	4160 ± 30	+1.3	4590 ± 30	4825–4625	
	B04-30	-0.8	Beta-389477	Coralline algae	Radiometric	140 ± 30	+1.1	570 ± 30	255–post 0	
	B04-50	-1.0	Beta-389478	<i>Porites</i>	Radiometric	160 ± 30	+0.5	580 ± 30	260–post 0	80.0
	B04-130	-1.8	Beta-389479	<i>Favia</i>	Radiometric	490 ± 30	-1.0	880 ± 30	505–415	2.4
Irvine/Bathurst Is.										

Table 1 continued

Location	Sample code	Depth (m)	Lab. code	Material	Method	Measured age	$^{13}C/^{12}C$ (‰)	Conventional age (BP)	Calibrated (68 % probability) cal yr BP	Accretion (mm/year)
	B04-427	-4.8	Beta-389480	<i>Porites</i>	Radiometric	2370 ± 30	+4.4	2850 ± 30	2680–2395	1.4
	B05-16	-0.3	Beta-389413	<i>Galaxea</i>	AMS	160 ± 30	-2.2	530 ± 30	230–post 0	
	B05-160	-1.7	Beta-389414	<i>Galaxea</i>	AMS	740 ± 30	-1.0	1130 ± 30	680–565	2.8
	B05-385	-3.9	Beta-389415	<i>Galaxea</i>	AMS	2690 ± 30	+0.5	3110 ± 30	2900–2740	1.0
	B05-600	-6.1	Beta-389416	<i>Porites Cylindrica</i>	AMS	3070 ± 30	-1.7	3450 ± 30	3350–3165	5.0
	B08-12	-0.5	Beta-389417	<i>Acropora</i>	AMS	140 ± 30	-0.3	550 ± 30	245–post 0	
	B08-81	-1.2	Beta-389418	Coralline algae	AMS	270 ± 30	+0.5	690 ± 30	320–240	4.4
	B08b-35	-0.7	Beta-389481	Coralline algae	Radiometric	360 ± 30	-1.7	740 ± 30	420–265	
	B08b-64	-1.0	Beta-389482	Coralline algae	Radiometric	390 ± 30	+2.2	840 ± 30	490–325	4.6
	B09-12	-2.2	Beta-389483	<i>Porites</i>	Radiometric	70 ± 30	+0.3	480 ± 30	120–post 0	
	B09-30	-2.4	Beta-389484	Coralline algae	Radiometric	580 ± 30	+0.4	1000 ± 30	615–415	0.4
	B09-114	-3.2	Beta-389485	<i>Porites</i>	Radiometric	2270 ± 30	+0.4	2690 ± 30	2365–2275	0.4
	B12-35	-0.7	Beta-389419	<i>Acropora</i>	AMS	90 ± 30	-0.5	490 ± 30	130–post 0	
	B12-238	-2.8	Beta-389420	<i>Acropora</i>	AMS	220 ± 30	-0.2	630 ± 30	285–120	15.3
	B12-367	-4.1	Beta-389421	<i>Acropora</i>	AMS	360 ± 30	-1.0	750 ± 30	425–270	9.0
	B12-571	-6.1	Beta-389422	Coral	AMS	430 ± 30	-2.1	810 ± 30	470–300	53.3
	B14-16	-0.7	Beta-389423	<i>Favia</i>	AMS	110 ± 30	+2.6	560 ± 30	250–post 0	
	B14-154	-2.0	Beta-389424	Coral	AMS	280 ± 30	-1.0	670 ± 30	305–190	10.8
	B14-325	-3.7	Beta-389425	Coral	AMS	340 ± 30	+1.4	770 ± 30	440–280	14.8
	B14-554	-6.0	Beta-389426	Coral	AMS	500 ± 30	-1.1	890 ± 30	510–420	21.9
	B15-54	-1.3	Beta-391046	Coral	AMS	2060 ± 30	+3.3	2520 ± 30	2200–2005	0.6
	B15-101	-1.8	Beta-391047	Coral	AMS	2830 ± 30	-0.7	3230 ± 30	3060–2860	1.9
	B15-189	-2.7	Beta-391048	Coral	Radiometric	3190 ± 30	-0.4	3590 ± 30	3500–3345	
	B13-18	-0.7	Beta-391043	Coral	AMS	120 ± 30	-2.5	490 ± 30	130–post 0	
	B13-321	-3.6	Beta-391044	Coral	AMS	560 ± 30	-3.4	910 ± 30	520–435	7.0
	B13-597	-6.4	Beta-391045	Coral	AMS	700 ± 30	-1.5	1090 ± 30	660–540	22.9
	B07-32	-0.5	Beta-391040	Coral	AMS	110 ± 30	-1.8	490 ± 30	130–post 0	
	B07-316	-3.4	Beta-391041	Coral	AMS	520 ± 30	-0.2	930 ± 30	530–450	6.8
	B07-620	-6.4	Beta-391042	Coral	AMS	1100 ± 30	-1.1	1490 ± 30	1050–910	6.1
	B06-43	-0.7	Beta-391037	Coral	AMS	80 ± 30	-1.6	460 ± 30	75–post 0	
	B06-294	-3.2	Beta-391038	Coral	AMS	640 ± 30	-0.8	1040 ± 30	635–510	4.7
	B06-434	-4.6	Beta-391039	Coral	Radiometric	880 ± 30	-0.6	1280 ± 30	855–680	7.2

All samples were dated at Beta Analytic Inc, Miami, Florida, USA





**Fig. 4** Cross section of the interisland fringing reef of Irvine/Bathurst islands with isochrons and summary of Holocene reef facies. The dominant facies was a branching coral floatstone, especially in the

cores around the deep tidal pools. Note the exaggerated scale in the upper 5 m of the reef section

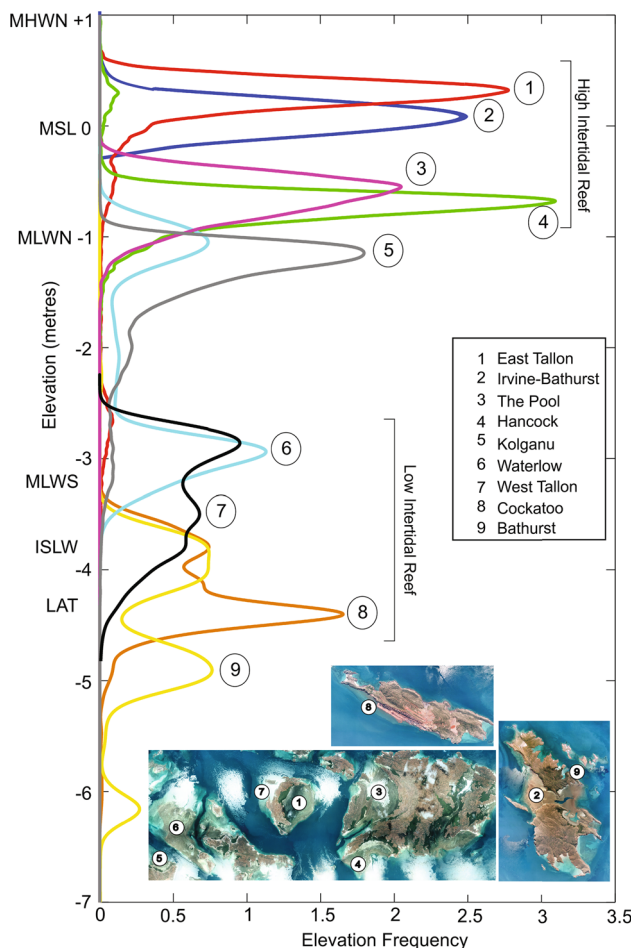


**Fig. 5** Probability density curves of reef elevations measured by multibeam echo sounder surveys

attain their elevation while LIR remain at the more typical MLWS level. The HIR versus LIR dichotomy is best represented at Tallon Island, where the western (LIR) and

eastern (HIR) reefs differ markedly in elevation (Fig. 2) despite occurring in similar, relatively sheltered settings. The main differences between these reefs, apart from their elevation, are the greater width of the HIR and the predominance of coralline algae on the HIR versus coral and sediment on the LIR. These features appear to be consistent throughout the Kimberley (e.g., Purcell 2002). Similarly, the Brazilian HIR are also characterised by extensive reef flats and coralline algal terraces (Gherardi and Bosence 2001; Fonseca et al. 2012). These consistencies suggest that some or all of the three factors of tidal range, reef flat width and coralline algae, interact to produce HIR. A recent hydrodynamic study of the Tallon Island HIR by Lowe et al. (2015) indicates how the process may occur. Lowe et al. (2015) recorded a dramatic tidal asymmetry, with the reef flat rapidly inundated over 2–3 h but draining very slowly over 9–10 h. Consequently, the reef flat never entirely dries, and reef flat organisms are able to survive and grow despite their elevation. Field measurements and modelling indicate that the ponding effect depends primarily on reef flat width and bottom friction; water residence times are greater on wide and ‘rough’ reefs, with roughness determined by benthic composition and biota (Lowe et al. 2015). This is perhaps the essential difference between the eastern HIR and the western LIR of Tallon Island. The wide and microtopographically complex eastern reef flat (Fig. 2) retains a film of seawater throughout the low tide cycle, effectively creating its own pseudo-accommodation space. Reef flat accretion here has an element of positive feedback, in that vertical reef accretion will pond seawater at a greater elevation, allowing further accretion. In contrast, the narrower, inclined and somewhat less complex (Fig. 2) western reef flat sheds seawater and therefore remains at MLWS. Based on Lowe et al.’s (2015) findings, we suggest that this division may apply

throughout the Kimberley: reef flats that are wide enough to retain seawater over the low tide cycle become HIR and those that do not remain as LIR at MLWS. We interpret the apparent absence of intermediate elevations to indicate that, during the Holocene highstand, all reefs with the potential to become HIR have done so, whereas other reefs have remained at MLWS.

In addition to reef flat width, several other factors may also influence water retention at low tide, but are perhaps secondary (e.g., reef aspect, reef flat slope, reef porosity, the presence or absence of tidal creeks and mangroves that may store and release seawater, and surrounding bathymetry that may restrict or enhance ebb tide run-off). Another factor that could promote water retention is a continuous marginal rim, i.e., a ‘bucket’ structure. However, our subsurface information suggests that raised rims have been absent or only very weakly developed through the Holocene and that the reefs have accreted more as ‘banks’ than ‘buckets’ (Fig. 2). Although coralline algal terraced margins are a consistent feature of Kimberley HIR (Purcell 2002; Wilson and Blake 2011; Lowe et al. 2015; Richards and O’Leary 2015), we interpret these as relatively late-stage surface features that develop as the reefs accrete beyond MLWS. The development of the terraced margins is likely flow-dependent, coralline algae thriving in the well-oxygenated seawater flowing off the reef flat at low tide.

We interpret the hydraulic analysis by Lowe et al. (2015) to indicate that the critical reef flat width initiating HIR development may be around 1 km for fringing reefs. The potential for any particular reef to attain this critical width may be determined largely by local factors, bathymetry perhaps being the most influential. Other factors being equal, wide reef flats are most likely to develop on broad shallow banks or where the fringing reefs of adjacent islands suture or coalesce together, whereas narrow reef flats are most likely to develop on narrow banks or against isolated steep-sided islands. At the sites we examined, the underlying structure appears to be a major determinant of bathymetry and hence of modern reef configuration. The HIR of Tallon Island are a possible example of structural control, because they appear to lie within a synclinal basin (Brunnschweiler 1957), which, when flooded by sea-level rise, may have become a sheltered, semi-enclosed habitat, perhaps more conducive to reef accretion than adjacent habitats outside the basin. Similarly, the relatively narrow (300 m) LIR at Cockatoo Island are limited primarily by the underlying structure. Because the bedrock there dips steeply seaward, the reef is prograding into relatively deep water (> 30 m; Solihuddin et al. 2015) and can only widen very slowly despite its high coral cover. The Cockatoo Island reef flat will therefore likely remain at its current MLWS elevation. This limitation may also apply to the

LIR reef on the western side of Tallon Island (Fig. 2). Such HIR apparently occur in macrotidal tropical environments worldwide but remain relatively understudied. Further research on HIR in the Kimberley and elsewhere would clarify the applicability and generality of our interpretations and may provide significant insights into Holocene reef growth and development in macrotidal settings.

### Chronology of Holocene reef build-up

Radiometric coral ages from reef cores suggest that reef accretion initiated soon after Holocene sea-level rise flooded the antecedent surface [based on the sea-level curve of Lambeck et al. (2014)]. The oldest dates recorded were 7305–7165 and 7790–7645 cal yr BP at 5.2 m below MSL from core ET7 on East Tallon Island and at 8.7 m below MSL in core WT1 on West Tallon Island, respectively. The latter age supports chronological data from Cockatoo Island in the Buccaneer Archipelago (Solihuddin et al. 2015), which showed reef initiation beginning at around 18 m below MSL as early as 9000–8940 cal yr BP, and more broadly suggests that the early Holocene environmental and oceanographic conditions in the southern Kimberley were favourable for the recruitment of corals and the development of coral reefs.

Isochrons for Tallon Island show that by 7000 cal yr BP, fringing reefs on both the eastern and western sides of the island had reached an elevation of ~5.0 m below MSL, which is ~1.8 m below present MLWS. Subsequently, the high intertidal fringing reef on the eastern side of Tallon continued to accrete vertically, reaching a maximum elevation of 0.5 m above MSL by around 4000 cal yr BP, whereas the low intertidal fringing reef on the western side of Tallon Island ceased vertical accretion at an elevation of 2.5 m below MSL (0.7 m above MLWS) at around 5000 cal yr BP (Fig. 2).

Reef cores were recovered from the northern and southern entrances of ‘The Pool’ which forms a high intertidal fringing reef between Sunday and Allora islands to capture the transition zone between the HIR and LIR reef morphologies (Fig. 3). The oldest coral collected from 5.8 m below MSL in core PN5 at the North Pool site returned a calibrated radiocarbon age of 6780–6675 cal yr BP, while the oldest coral collected from 2.6 m below MSL in core PS4 had an age of 4825–4625 cal yr BP at the South Pool site. The age isochrons in the North Pool indicate accretion in a quasi-progradational growth direction, which may indicate the reefs prograded seaward from the islands rather than having aggraded from depth. This may suggest that a deeper channel may have run the length of The Pool only to be sutured closed as the two prograding reefs from Allora and Sunday islands joined. A remnant of this passage is evident in the southern portion of The Pool

where age isochrons suggest it is ‘zipping’ closed in a north–south direction (Fig. 3).

A high intertidal interisland fringing reef joins Irvine/Bathurst islands and is characterised by a central 30-m-deep pool (Fig. 4) rather than a narrow channel opening to the sea, as is the case on the interisland reef joining Sunday and Allora islands. A 5-m-long core (B06) taken from the edge of the deep pool had a core top age of 75 to post 0 and a core bottom age of 855–680 cal yr BP. This suggests that accretion is dominantly progradational, and like the interisland reef joining Sunday and Allora islands, likely formed by the suturing of two fringing reefs prograding from each island (Fig. 4).

The oldest coral sample recovered at Irvine/Bathurst islands was 3500–3345 cal yr BP from core B15 at 2.7 m below MSL. The absence of older coral ages from Irvine/Bathurst islands is likely due to limited core penetration rather than late initiation, given that the neighbouring Cockatoo Island reef initiated at 9000 cal yr BP (Solihuddin et al. 2015).

Core top ages for the Irvine/Bathurst islands of less than 1000 cal yr BP suggests the reef flat has only recently reached its current elevation of 0.25 m above MSL, possibly indicating that the reef could still be aggrading and has not yet reached its maximum elevation. Low intertidal reefs are evident on the southern and south-eastern sides of Irvine Island, which are similar in elevation to the west Tallon LIR. However, no cores were retrieved at those locations so it is not possible to determine whether these low intertidal reefs are actively aggrading or have reached their maximum elevation, as interpreted for the west Tallon reef.

### Reef facies and accretionary style

The internal composition of the sampled reefs was largely comprised of coral fragments (predominantly delicate branching *Acropora*) in a poorly sorted sandy mud matrix. This suggests that relatively sheltered depositional environments have prevailed throughout the Holocene, in keeping with the low wave energy environment of the sample sites. Most of the coral fragments appear to be in situ based on skeletal preservation. Occasional horizons dominated by robust domal coral colonies are intercalated with the detrital units, and many of these colonies also appear to be in situ, based on orientation and preservation. We interpret the reefs to have been low-energy subtidal *Acropora*-dominated meadows that most likely had a relatively high live coral cover, and moderate diversity and structural complexity. The reef structure would have baffled the tidal currents and trapped fine sediment within the reef interstices similar to the nearby Cockatoo Island reef (Solihuddin et al. 2015). Based on these interpretations, the facies of the sampled Kimberley Reefs conform closely to those described by Perry et al. (2012) at Middle Reef, a

turbid nearshore reef within the mesotidal range (3.6 m) located in the central Great Barrier Reef. Both have high coral cover, sediment-tolerant corals and a mud-dominated matrix (Solihuddin et al. 2015).

The distribution of run-off from impounded seawater is probably responsible for the marked divergence between low and high intertidal reefs once they reach sea level (as discussed in ‘Reef geomorphology’). Low intertidal reefs usually maintain their general facies characteristics, which are composed of coral fragments and colonies in a muddy to sandy matrix, although the coral species often change (i.e., *Goniastrea aspera*, *Favia*, and *Montipora digitata* are observed to increase in abundance in some cores) and entirely different communities may arise in some localised areas (e.g., the inshore seagrass beds of East Tallon). In contrast, the HIR undergo a radical facies change and become dominated by coralline algae as they rise above MLWS and begin to form terraces.

**Acknowledgments** The Kimberley Reef Geomorphology Project 1.3.1 was funded by the Western Australian State Government and partners of the Western Australian Marine Science Institution. This research was assisted by the Bardi Jawi and Mayala people through their advice and consent to access their traditional lands. The Kimberley Marine Research Station at Cygnet Bay provided vessel support and access to research facilities. Thanks to Giada Bufarale for assistance with subsurface interpretations and to Alexandra Stevens for improvement of the manuscript.

### References

- Brunnschweiler RO (1957) The geology of Dampier Peninsula, Western Australia. Department of National Development, Bureau of Mineral Resources, Geology and Geophysics, Canberra
- Buddemeier RW, Hopley D (1988) Turn-ons and turn-offs: causes and mechanisms of the initiation and termination of coral reef growth. *Proc 6th Int Coral Reef Symp* 1: 253–261
- Collins LB, O’Leary MJ, Stevens AM, Bufarale G, Kordi M, Solihuddin T (2015) Geomorphic patterns, internal architecture and reef growth in a macrotidal, high-turbidity setting of coral reefs from the Kimberley Bioregion. *Australian Journal of Maritime and Ocean Affairs* 7:12–22
- Darwin CR (1842) The structure and distribution of coral reefs. Being the first part of the geology of the voyage of the ‘Beagle’. Smith, Elder and Co, London
- DEWHA (Department of the Environment, Water, Heritage and the Arts) (2008) A characterisation of the marine environment of the northwest marine region: Perth workshop report, a summary of an expert workshop convened in Perth, Western Australia, 5–6 September 2007. Commonwealth of Australia, Hobart
- Embry AF, Klován J (1971) A late Devonian reef tract on Northeastern Banks Island, NWT. *Bulletin of Canadian Petroleum Geology* 19:730–781
- Fonseca AC, Villaga R, Knoppers B (2012) Reef flat community structure of Atol das Rocas, northeast Brazil and southwest Atlantic. *J Mar Biol* 2012. [doi:10.1155/2012/179128]
- Gherardi DFM, Bosence DWJ (2001) Composition and community structure of the coralline-algal reefs from Atol das Rocas, South Atlantic, Brazil. *Coral Reefs* 19:205–219

- Gherardi DFM, Bosence DWJ (2005) Late Holocene reef growth and relative sea-level changes in Atol das Rocas, equatorial South Atlantic. *Coral Reefs* 24:264–272
- Griffin TJ, Grey K (1990) Kimberley Basin. In: Memoir 3, Geology and mineral resources of Western Australia. Geological Survey of Western Australia, Perth, pp 293–304
- Hopley D, Smithers SG, Parnell KE (2007) The geomorphology of the Great Barrier Reef: development, diversity and change. Cambridge University Press, New York
- Kennedy DM, Woodroffe CD (2002) Fringing reef growth and morphology: a review. *Earth Sci Rev* 57:255–277
- Ladd HS, Ingerson E, Townsend RC, Russell M, Stevenson HK (1953) Drilling on Eniwetok Atoll, Marshall Islands. *AAPG Bulletin* 37:2257–2280
- Lambeck K, Rouby H, Purcell A, Sun Y, Sambridge M (2014) Sea level and global ice volumes from the Last Glacial Maximum to the Holocene. *Proc Natl Acad Sci U S A* 111:15296–15303
- Lough JM (1998) Coastal climate of Northwest Australia and comparisons with the Great Barrier Reef: 1960 to 1992. *Coral Reefs* 17:351–367
- Lowe RJ, Falter JL (2015) Oceanic forcing of coral reefs. *Annu Rev Mar Sci* 7:43–66
- Lowe RJ, Leon AS, Symonds G, Falter JL, Gruber R (2015) The intertidal hydraulics of tide-dominated reef platforms. *J Geophys Res Oceans* 120:4845–4868
- Montaggioni LF (2005) History of Indo-Pacific coral reef systems since the last glaciation: development patterns and controlling factors. *Earth Sci Rev* 71:1–75
- Neumann AC, Macintyre IG (1985) Reef response to sea level rise: keep-up, catch-up or give-up. *Proc 5th Int Coral Reef Symp* 3:105–110
- Pearce AF, Griffiths RW (1991) The mesoscale structure of the Leeuwin Current: a comparison of laboratory models and satellite imagery. *J Geophys Res* 96:16739–16757
- Perry CT, Smithers SG, Gulliver P, Browne NK (2012) Evidence of very rapid reef accretion and reef growth under high turbidity and terrigenous sedimentation. *Geology* 40:719–722
- Purcell S (2002) Intertidal reefs under extreme tidal flux in Buccaneer Archipelago, Western Australia. *Coral Reefs* 21:191–192
- Richards ZT, O’Leary MJ (2015) The coralline algal cascades of Tallon Island (Jalan) fringing reef. NW Australia. *Coral Reefs* 34:595
- Solihuddin T, Collins LB, Blakeway D, O’Leary MJ (2015) Holocene coral reef growth and sea level in a macrotidal, high turbidity setting: Cockatoo Island, Kimberley Bioregion, northwest Australia. *Mar Geol* 359:50–60
- Teichert C, Fairbridge RW (1948) Some coral reefs of the Sahul Shelf. *Geogr Rev* 28:222–249
- Wilson BR (2013) The biogeography of the Australian North West Shelf: environmental change and life’s response. Elsevier, Burlington MA
- Wilson BR, Blake S (2011) Notes on the origin and biogeomorphology of Montgomery Reef, Kimberley, Western Australia. *J R Soc West Aust* 94:107–119
- Wilson BR, Blake S, Ryan D, Hacker J (2011) Reconnaissance of species-rich coral reefs in a muddy, macro-tidal, enclosed embayment, Talbot Bay, Kimberley, Western Australia. *J R Soc West Aust* 94:251–265

## PERMISSION LETTER

May 12, 2016

Springer reference**Coral Reefs**

pp 1-12

First online: 26 February 2016

**Holocene reef evolution in a macrotidal setting: Buccaneer Archipelago, Kimberley Bioregion, Northwest Australia**

Tubagus Solihuddin, Michael J. O'Leary, David Blakeway, Iain Parnum, Moataz Kordi, Lindsay B. Collins

© Springer-Verlag Berlin Heidelberg 2016

DOI 10.1007/s00338-016-1424-1

Print ISSN 0722-4028

Online ISSN 1432-0975

Journal No: 00338

Your project

**Requestor:** Tubagus Solihuddin  
tubagus.solihuddin@postgrad.curtin.edu.au

**University:** Curtin University

**Purpose:** Dissertation/Thesis

With reference to your request to reuse material in which Springer controls the copyright, our permission is granted free of charge under the following conditions:

Springer material

- represents original material which does not carry references to other sources (if material in question refers with a credit to another source, authorization from that source is required as well);
- requires full credit (Springer book/journal title, chapter/article title, volume, year of publication, page, name(s) of author(s), original copyright notice) to the publication in which the material was originally published by adding: "With permission of Springer";
- may not be altered in any manner. Abbreviations, additions, deletions and/or any other alterations shall be made only with prior written authorization of the author;
- Springer does not supply original artwork or content.

This permission

- is non-exclusive;
- is valid for one-time use only for the purpose of defending your thesis and with a maximum of 100 extra copies in paper. If the thesis is going to be published, permission needs to be reobtained.
- includes use in an electronic form, provided it is an author-created version of the thesis on his/her own website and his/her university's repository, including UMI (according to the definition on the Sherpa website: <http://www.sherpa.ac.uk/romeo/>);
- is subject to courtesy information to the co-author or corresponding author;
- is personal to you and may not be sublicensed, assigned, or transferred by you to any other person without Springer's written permission;
- is only valid if no personal rights, trademarks, or competitive products are infringed.

This license is valid only when the conditions noted above are met.

Permission free of charge does not prejudice any rights we might have to charge for reproduction of our copyrighted material in the future.

## PERMISSION LETTER

Rights and Permissions  
Springer  
Tiergartenstr. 17  
69121 Heidelberg  
Germany



## PERMISSION LETTER

November 8, 2016

Springer reference**Geo-Marine Letters**

December 2016, Volume 36, Issue 6, pp. 465-477

First online: 17 August 2016

***Geomorphology and late Holocene accretion history of Adele Reef: a northwest Australian mid-shelf platform reef***

Authors: Tubagus Solihuddin, Giada Bufarale, David Blakeway, Michael J. O'Leary

© Springer-Verlag Berlin Heidelberg 2016

**Material to be reused:** Excerpts

DOI 10.1007/s00367-016-0465-3

Print ISSN 0276-0460

Online ISSN 1432-1157

Journal no. 00367

Your project

**Requestor:** Tubagus Solihuddin  
tubagus.solihuddin@postgrad.curtin.edu.au

**University:** Curtin University

**Purpose:** Dissertation/Thesis

With reference to your request to reuse material in which Springer controls the copyright, our permission is granted free of charge under the following conditions:

Springer material

- represents original material which does not carry references to other sources (if material in question refers with a credit to another source, authorization from that source is required as well);
- requires full credit (Springer book/journal title, chapter/article title, volume, year of publication, page, name(s) of author(s), original copyright notice) to the publication in which the material was originally published by adding: "With permission of Springer";
- may not be altered in any manner. Abbreviations, additions, deletions and/or any other alterations shall be made only with prior written authorization of the author;
- Springer does not supply original artwork or content.

This permission

- is non-exclusive;
- is valid for one-time use only for the purpose of defending your thesis and with a maximum of 100 extra copies in paper. If the thesis is going to be published, permission needs to be reobtained.
- includes use in an electronic form, provided it is an author-created version of the thesis on his/her own website and his/her university's repository, including UMI (according to the definition on the Sherpa website: <http://www.sherpa.ac.uk/romeo/>);
- is subject to courtesy information to the co-author or corresponding author;
- is personal to you and may not be sublicensed, assigned, or transferred by you to any other person without Springer's written permission;
- is only valid if no personal rights, trademarks, or competitive products are infringed.

This license is valid only when the conditions noted above are met.

**PERMISSION LETTER**

Permission free of charge does not prejudice any rights we might have to charge for reproduction of our copyrighted material in the future.

Rights and Permissions

Springer

Tiergartenstr. 17

69121 Heidelberg

Germany